Non−Adiabatic R−Matrix Calculations For Proton−Hydrogen Scattering

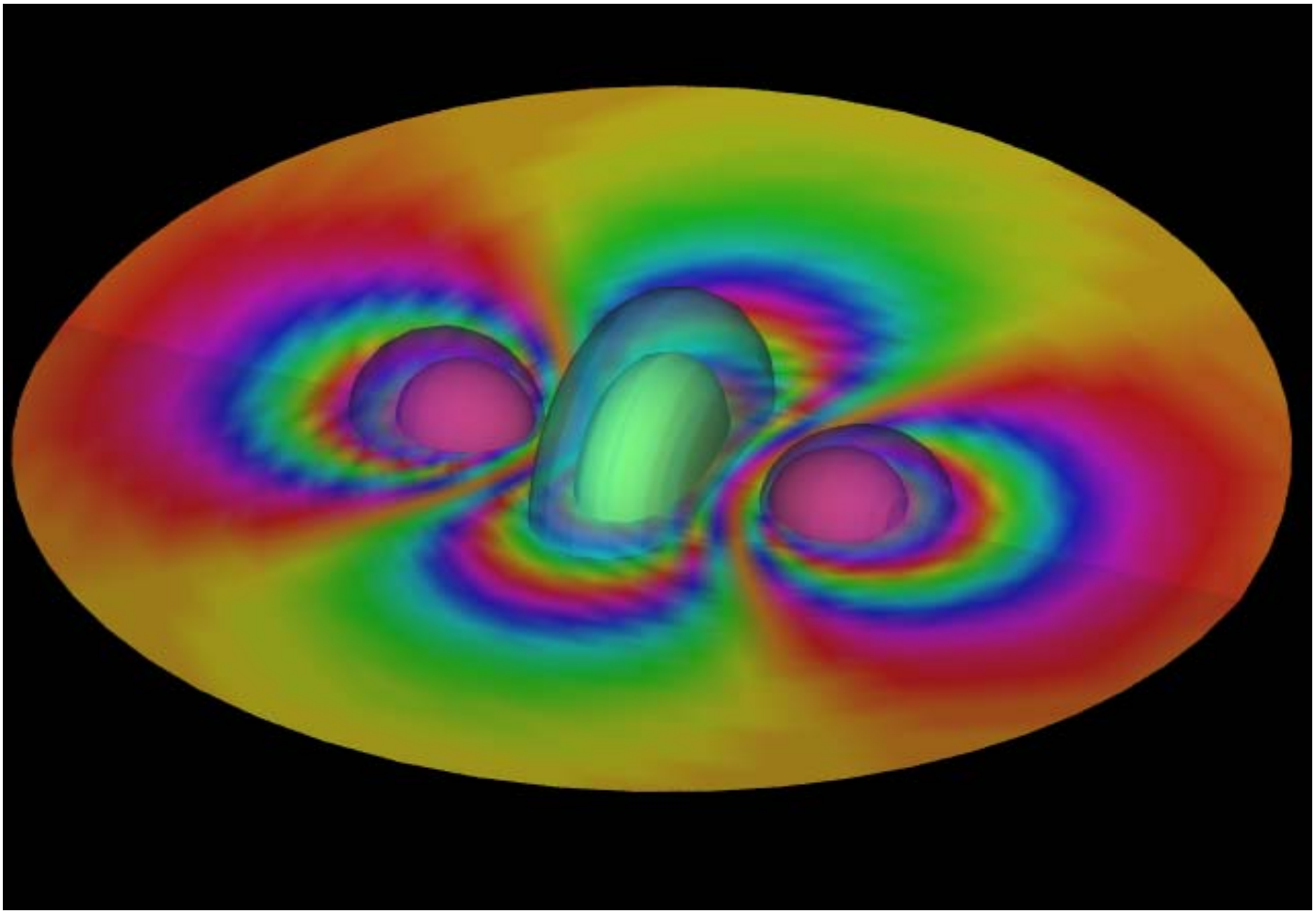

A study of the full quantum mechanical three body problem of H_2^+

by

Ken Museth

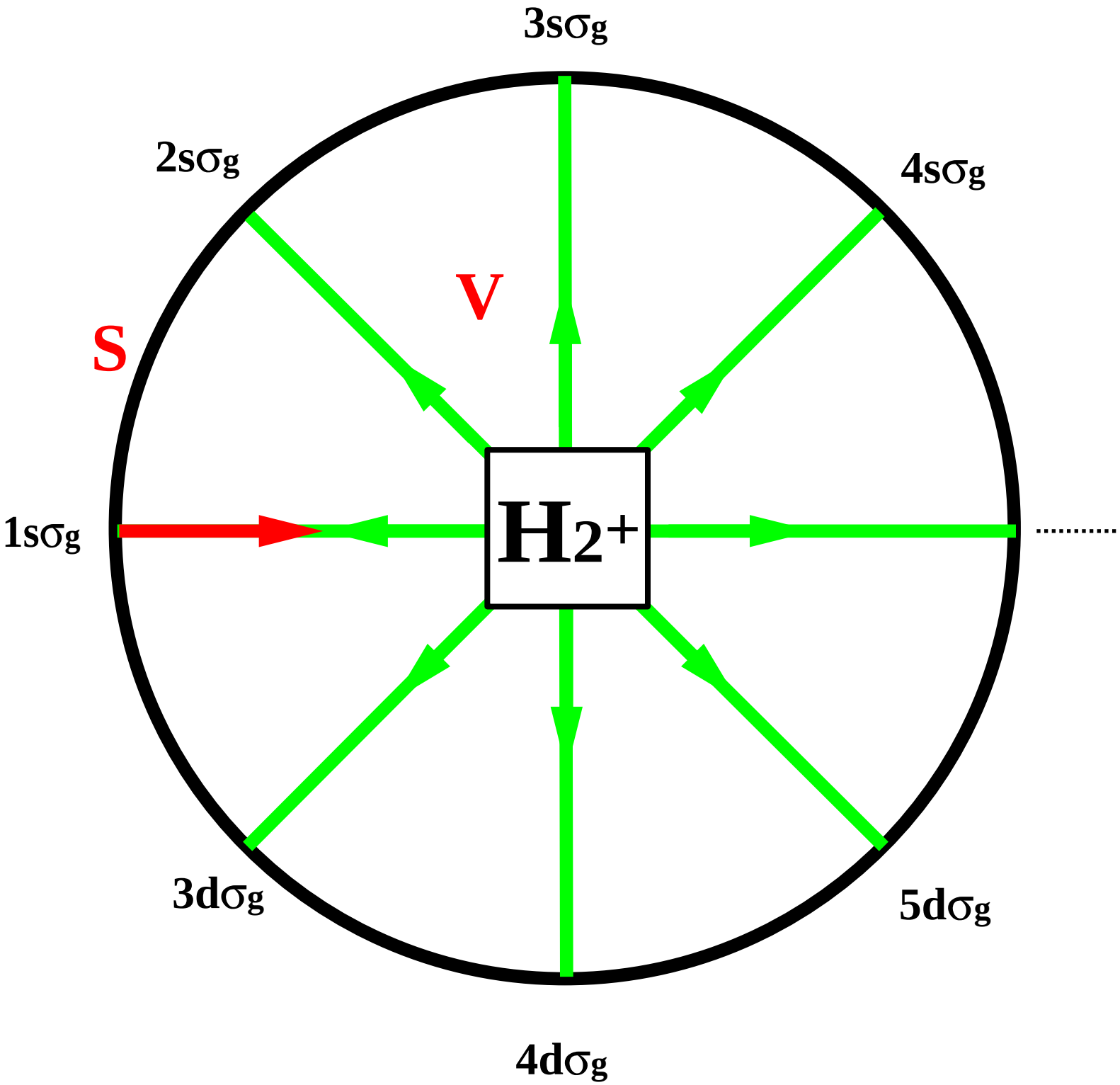
3sσg
2sσg
4sσg
V
S
1sσg
H2+
.....
3dσg
5dσg
4dσg

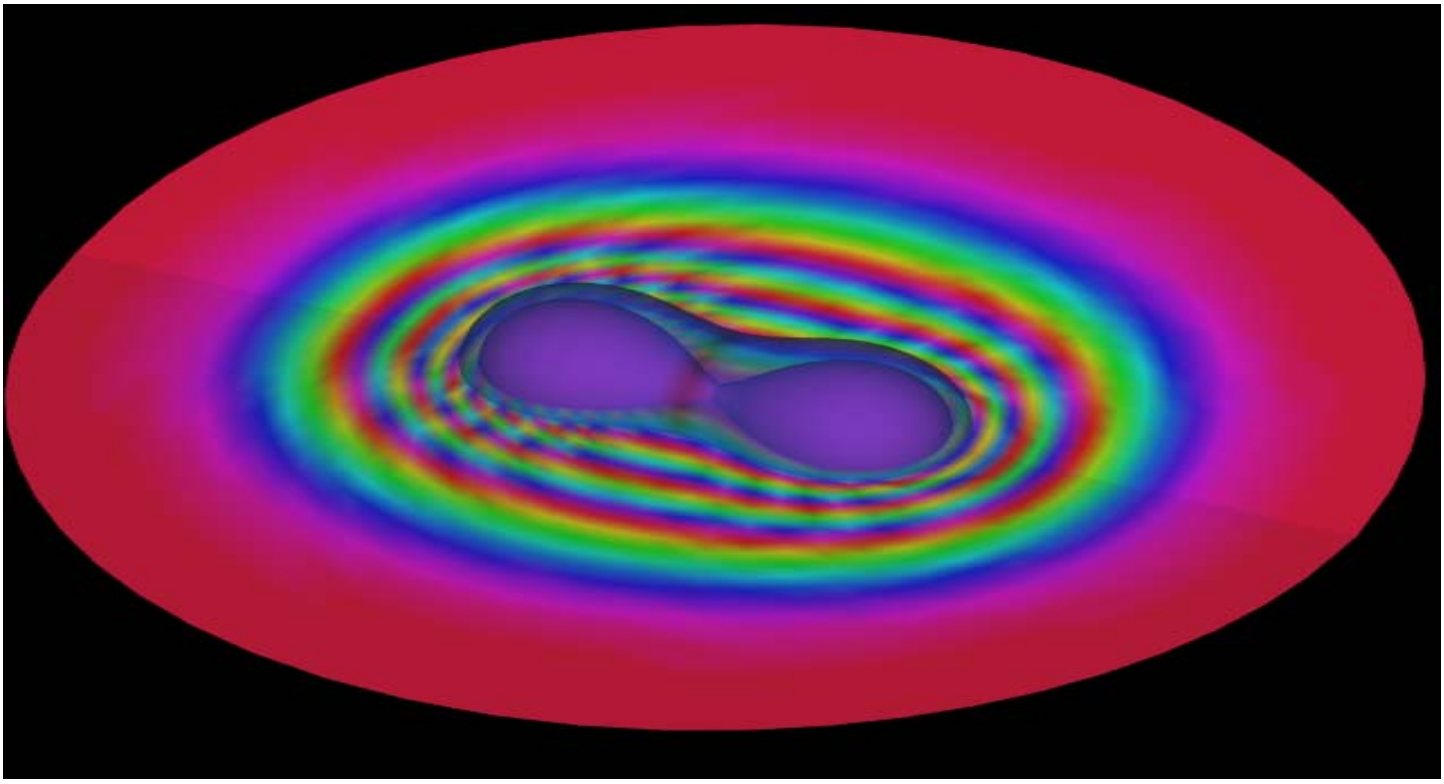

$1s\sigma_g$

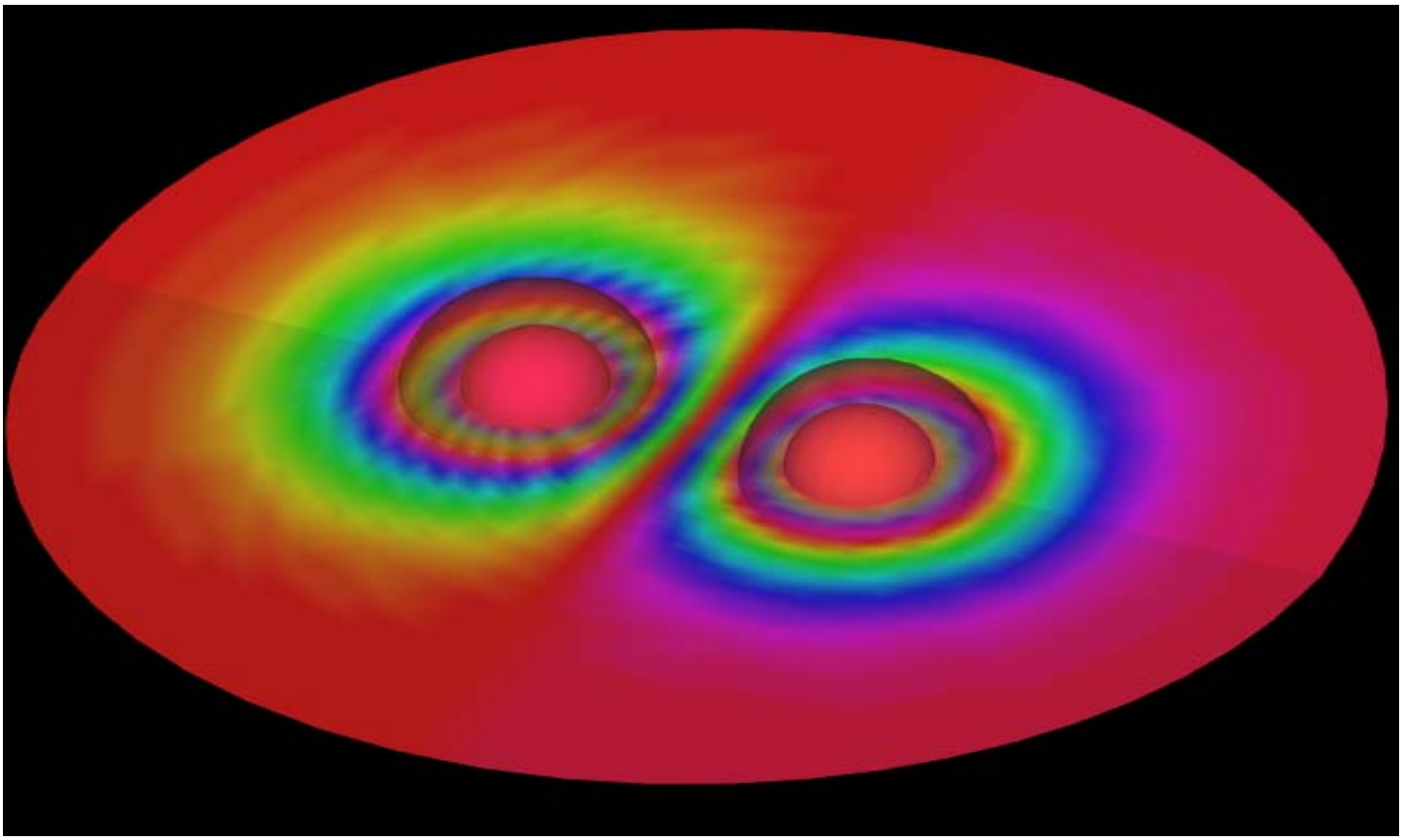

$2p\sigma_u$

COPENHAGEN UNIVERSITY

Non-Adiabatic R-Matrix Calculations For Proton-Hydrogen Scattering

A study of the full quantum mechanical three body problem of H_2^+

A THESIS

SUBMITTED TO THE UNIVERSITY OF COPENHAGEN
IN PARTIAL FULFILLMENT OF THE REQUIREMENTS

for the degree

CANDIDATA SCIENTIARUM
(CAND. SCIENT.)

Field of Theoretical Chemistry

By
Ken Museth

COPENHAGEN
February, 1994

The picture on the front-page shows a 3D-scalar plot with two iso-surfaces (of which one is transparent) and a one contour-surface of the total wave function for H_2^+, resulting from a scattering calculation where the incoming channel was a pure electronic $3d\sigma_g$ state. The inter-nuclear separation was fixed to 2 au in the plot. Note that the selected color-map is cyclic.

Abstract

We have performed *full quantum mechanical three body* (non-adiabatic) scattering calculations of the type:

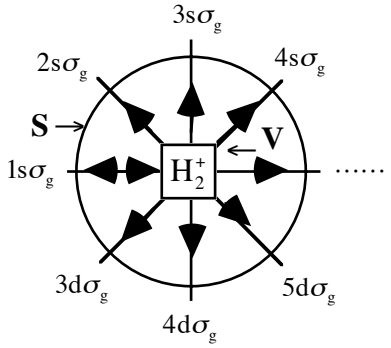

In the considered scattering calculations the incoming channels were respectively an electronic $1s\sigma_g$ (as in the above figure), $2p\sigma_u$ and $2p\pi_u$ state. Non-adiabatic radial coupling terms were included in the formulation, but angular coupling terms were neglected as a first approximation. Thus coupling between channels with different parity was neglected.

The impetus behind the study presented here is that the simple Born-Oppenheimer type approximation [1] (commonly known as the approximation of infinite nuclear masses) and semi-classical trajectory simulation methods do not form an optimal way towards the calculation of accurate scattering amplitudes for a three body system like the hydrogen molecular ion.

The work takes point of reference in the Wigner-Eisenbud [2] R-matrix theory where the configuration space is divided into two regions (see the above figure). A bounded internal interaction region V and an external region in which the interactions have vanished. The mapping of the internal scattering wave function onto the asymptotic states on the surface S enclosing V is expressed in terms of log-derivative boundary conditions represented by the R-matrix. The variational formulation of the Schrödinger equation and the associated scattering boundary conditions is conveniently expressed in the J-functional [3] which reads,

$$J(\psi,\phi) \equiv \int dv\left\{\left(E - W(x)\right)|\psi|^2 - |\nabla\psi|^2\right\} + \int ds\left\{\psi^*(x)\phi(x) + \phi^*(x)\psi(x)\right\} - \int ds\,ds'\left\{\phi^*(x)R_s(x,x')\phi(x')\right\}$$

where $\psi(x)$ denotes the scattering amplitude and $\phi(x)$ the asymptotic state. To reduce the full 3×3 dimensional problem of H_2^+ to just *three dimensions*, 3 translational and 3 rotational coordinates are separated out [4] to yield the following 3 body-fixed coordinates

$$\xi \equiv \left[|\vec{r} + R/2\vec{e}_3| + |\vec{r} - R/2\vec{e}_3|\right]/R \quad \text{, where} \quad 1 \le \xi \le \infty$$
$$\eta \equiv \left[|\vec{r} + R/2\vec{e}_3| - |\vec{r} - R/2\vec{e}_3|\right]/R \quad \text{, where} \quad -1 \le \eta \le 1$$
$$f \equiv R/2 \quad \text{, where} \quad 0 \le f \le \infty$$

where R denotes the inter-nuclear distance (in the direction $\vec{e}_3$) and $\vec{r} = (x,y,z)$ the vector from the nuclear center of mass to the electron.

The full scattering matrix for H_2^+ was then set up using some aspects of R-matrix theory that are derived from a *finite element method* (FEM, [5]) representation of $\psi(x)$ in the f coordinate. In the spheroidal coordinates (ξ,η) we used Born-Oppenheimer approximate Sturmian [6] basis functions, and a *discrete variable representation* scheme (DVR, [7]) to evaluate the J-functional in this basis-set.

To obtain absorption-coefficients for transitions of the type

$$H + H^+ \longrightarrow H_2^+\left[2p\sigma_u / 2p\pi_u\right] \longrightarrow H_2^+\left[1s\sigma_g\right] \longrightarrow H + H^+ + \nu$$

we next have to generate transition dipole moments between scattering wave functions initiated as respectively $1s\sigma_g$ and $2p\sigma_u / 2p\pi_u$ and subsequently apply a modified version of M. Baranger's "simplified quantum-mechanical theory of pressure broadening" [8]. The computed absorption spectra should then be compared with the absorption spectra recorded in hydrogen-rich white dwarf atmospheres [9, 10].

Acknowledgment

"If I have been able to see farther than others, it was because I stood on the shoulders of giants".

Sir Isaac Newton

This thesis entitled "Non-Adiabatic R-Matrix Calculations For Proton-Hydrogen Scattering" (subtitled "A study of the full quantum mechanical three body problem of H_2^+") is the result of my work towards the cand. scient. degree at the University of Copenhagen. The research and work on which this thesis is based was carried out partly at the Department of Theoretical Chemistry, Aarhus University, partly at the Chemical Laboratory III at University of Copenhagen and finally for a short time at the Department of Theoretical Chemistry at Université Paris-Sud, Orsay, France.

I wish to thank Professor Jan Linderberg, who acted as my supervisor during my study at Aarhus University, for the inspiration and support that he gave me during all stages of the work, and without whom this research project would never have been possible. I am equally grateful to my present supervisor Professor Gert Due Billing at the University of Copenhagen for all support, continuous interest and encouragement during faces of adversity, and for providing me with the opportunities to participate at the 4'th Topsøe Summer School meeting 91[1] , the MOLEC IX[2] and arranging for me to visit Professor Claude Leforestier [7] to whom I also wish to extend my thanks. Further I am also graceful to Peter Thejll [10] at the Niels Bohr Institute who originally motivated this research project from an astrophysics point of view, Dr. Kurt Mikkelsen for his strong coffee and my friend Ph.D. Matthew Dean Todd for many "useless" (in terms of the present work), but nevertheless very interesting and stimulating discussions. Last but by no means least I am very much indebted to my girlfriend Katrine Happe who constantly over the years have made me realize that there is more to life than just science and quantum mechanics. As she have put it; "in some ways the two-body problem is far more interesting than the three-body problem" - to be studied in this thesis.

---

1 Where I had the opportunity to meet both Professor William Miller and Professor Claude Leforestier in person, who both as it turned out later, should play a significant role in my present work [7, 11, 12].

2 Where I presented a poster on my work on non-adiabatic H_2^+ scattering, and was met with surprisingly great interest in especially my applications of the FEM and DVR schemes to the three body problem.

Preface

"We are not observers, we are participants in the making of what we call reality".

John A. Wheeler

The presented thesis is, in more than one respect, the result of a very *theoretical* study of the hydrogen molecular ion. Clearly it does not involve any experimental work whatsoever, and moreover it is based on a wide range of concepts, theorems and techniques used in the study of exact quantum mechanical treatments of small systems. It is my personal experience that one of the major obstacles faced by many students in learning quantum mechanics, at this level of exactness, is their unfamiliarity with many of these concepts and methods. Furthermore, since many of the required concepts and numerical techniques are not discussed in standard textbooks, I have dedicated the first part of this thesis (chapter 1-4) to an introduction to these methods that form the basis of the thesis. Also, as the presented approach to the three body problem of H_2^+ has never been attempted before, I feel a certain obligation towards the expert reader to make sure that he/she can follow the central ideas in the new non-adiabatic formulation discussed in chapter 5. Thus I have tried to make explanations clear and complete, and most of the derivations are hopefully given with enough detail to make them easy to follow. Resort to the frustrating phrase "it can be shown that" is avoided wherever possible, and some of the more involved derivations have been moved to appendixes. However, this representation of course entails the risk that what might appear relevant and complicated to me, might well be tiresome and trivial to the expert reader - in which case I hope that he/she can bear with my style. This last comment is especially directed towards chapter 5, where some readers perhaps will find the details long and tiresome, yet presumably not trivial.

As motivated above, the thesis consists of three distinct parts. The first four chapters serve as a general introduction to many of the required concepts, and a sort of mathematical toolbox for the whole study of the hydrogen molecular ion; in chapter 1 the methodology and some central techniques are introduces, then in chapter 2 the actual variational method is presented, next two very important numerical methods are discussed in chapter 3 and finally in chapter 4 some basic concepts, that will enable us to reduce the dimensionality of the three body system are presented. Then follows the next part of the thesis (chapter 5) where the explicit derivations of the working-formulas for the H_2^+ system are given, and the numerical schemes are explained. Finally, in chapter 6, an outline of the computer routines and the implemented algorithms are given, and the actual results form the scattering calculations are presented and subsequently discussed.

General motivation

"It is wrong to think that quantum physics is a picture of the natural world. It is rather a way to describe it. Thus there is no such thing as the quantum world. It is only an abstraction".

Niels Bohr

Introduction

The hydrogen molecular ion, H_2^+, comprising two protons and one electron, is the simplest molecule of all. It was first discovered in 1896 by J. J. Thomson at Cambridge in cathode rays, and one of the first treatments of H_2^+ was given in terms of the old quantum theory by Pauli [11] in 1922. If we neglect all effects coming from the spin of the particles and if in addition the motion of the protons is disregarded, we are faced with the problem of an electron moving in the presence of two fixed Coulomb centers of attraction - the so-called Born-Oppenheimer approximation [1]. In this from, the analysis of H_2^+ has attended considerable attention over the years; thus, Burrau [12] in 1927, Hylleraas [13] in 1931, Jaffé [14] in 1934, Sandman [15] in 1935 and many others have performed Born-Oppenheimer approximate calculations on both the ground state and some of the excited states. The separability of the electronic Schrödinger's equation in spheroidal coordinates enables solutions of almost unlimited accuracy to be computed. The full three-body problem of H_2^+ on the other hand, forms a much bigger theoretical as well as computational task - in fact it is well-known that there does not exist any analytical or even "exact" numerical solution to this problem. Further since the Born-Oppenheimer approximation in general terms is acknowledged as being a quite good approximation one could ask "*why bother to try and solve the full three-body problem of* H_2^+"?

Astrophysical motivation

Like atomic hydrogen, the molecular ion plays a fundamental role in the understanding and interpretation of light emitted from a large number of stars. H line absorption is proportional to the absorber density, but in the H_2^+-system the absorber density is proportional to the square of the H density, and hence a greater sensitivity to the pressure in the stellar atmosphere is found in the absorption features of H_2^+ than in H. In an atmosphere in equilibrium the pressure is given by the temperature and the gravity of the star so that it becomes possible to accurately study these parameters in stars that show H_2^+ absorption. The

stars in question are the hydrogen rich *white dwarfs* (WD). At a certain temperature (near 16000K) these WD's show UV absorption features from H_2^+ near 1400 Å on the wings of the Lyman α-line[3] [9]. The main interests in studying these WD's lies in the generally interesting role WD's have as end-products of nearly all stellar evolutions; 90% of all stars are believed to end up as WD's [10]. Of particular interest to some astrophysics (Peter Thejll [10]) is the presence of stellar oscillations in the so-called DA WD's in a temperature range that coincides with the range of temperature in which the H_2^+ features can be seen. Stellar oscillations can be used to study the stellar interior, and important insight into stellar evolution can be obtained if the most accurate information about the star can be gathered from analysis of the observed light-spectrum and collated with the information available from the analysis of the oscillations [16]. With the development of new observation techniques and in particular the launching of the *International Ultraviolet Explorer Satellite* (IUE) it is now possible to record very accurate absorption spectra from DA WD's, and correspondingly the need for more accurate theoretical calculations have emerged. The study of the absorption due to transitions among states of H_2^+, begins with the problem of obtaining a good representation of the transition dipole moment, which expresses the amplitude for the given transition. So far the study of transition dipole moments for H_2^+ have only been done in the adiabatic or Born-Oppenheimer approximation [1] using classical or semi-classical arguments. A good example of such an approach is the work by Bates [17, 18] which is based on the adiabatic potential energy curves for H_2^+. However, this and related models do not give the right absorption-coefficients, and it is believed that this is due to the neglect of non-adiabatic effects, i.e. the coupling of the nuclear and electronic motions. In other words we need to go beyond the simple Born-Oppenheimer approximation, and try to include non-adiabatic effects.

Quantum mechanical motivation

At the very heart of practically all ab initio quantum mechanical calculations for molecular systems lies either the Born-Oppenheimer [1] or the adiabatic approximation. The philosophy of these approaches are a separation (complete or partial) of the electronic and nuclear motions, taking point of reference in the large difference in the masses. Solving ab initio quantum mechanical calculations for many particle systems in this picture of a clamped nucleus Hamiltonian is difficult enough, and hence it is unlikely that calculations will be made at a higher level of approximation in the near future. There are, however, and this is of course the basis of this thesis, systems like H_2^+ (and its isotopes) for which this statement is definitely not true. These molecules contain so few particles that one need not make "any" approximations in the solving of Schrödinger's equation. Furthermore, since the nuclei are very light, the corrections to the Born-Oppenheimer or adiabatic results will be greater for

---

3 The spectral Lyman series refer to transitions, $|n_2, \ell_2, m_2\rangle \rightarrow |n_1, \ell_1, m_1\rangle + \lambda$, between states of the hydrogen atom where $n_1 = 1\,(\ell_1 = m_1 = 0)$ and $n_2 = \{2, 3, 4, ..\}$. The Lyman α-line is then the first allowed ($\Delta\ell = \pm 1$) spectral transition i.e. $|2, 1, \{0, \pm 1\}\rangle \rightarrow |1, 0, 0\rangle + \lambda_\alpha$ where $\lambda_\alpha \approx 1215.6\text{Å}$.

these molecules than for most others. Also as H_2^+ has only one electron, it has a status in the theory of molecules similar to that of the hydrogen atom in the theory of atoms; thus it serves as the natural starting point in a more general discussion of non-adiabatic effects for many-electron diatomic molecules.

Table of contents

List of figures and tables

1 Introduction to quantum mechanical scattering theory

1.1 Introduction

It is well recognized that quantum mechanical scattering theory provides the most complete and detailed description of atomic and molecular collisions, which is the fundamental microscopic event that underlies a chemical reaction. Such a desirable theory, able to describe the basic process for a chemical reaction from a knowledge of forces operating at the atomic and molecular levels, explains some of the large effort that has been and continues to be devoted to developing the theory to the practical stage that reliable calculations can be carried out for "real" chemical reactions. Another and equally large factor in the general motivation of theorists starting to think in terms of accurate reactive scattering calculations is definitely the experimental progress in this field. Thus, since the 1960's, when crossed molecular beam experiments had developed to such an extent that it was possible to study state-to-state dynamics of atom-diatom reactions such as

$$\mathrm{A} \;+\; \mathrm{BC}(v,\mathrm{j}) \xrightarrow{\text{Reactive}} \mathrm{AB}(v',\mathrm{j}') \;+\; \mathrm{C} \tag{1.1.1}$$

there has been intense interest and effort devoted to the application of quantum mechanical scattering theory to these reactions to give reliable values for the *differential cross section*

$$\frac{\mathrm{d}\sigma_{v,\mathrm{j}\to v',\mathrm{j}'}(\theta,\mathrm{E})}{\mathrm{d}\Omega} \tag{1.1.2}$$

This quantity, which gives a measure of the probability of producing the molecule AB in the vibrational-rotational state (v',j') from the reactant molecule BC in the vibrational-rotational state (v,j) with a solid scattering angle $\Omega = (\theta,\phi)$ and fixed collision energy E, provides the most detailed quantity that a reaction dynamical experiment can give. Crossed molecular beam experiments enable these differential cross sections to be fully resolved with respect to θ[4]. However, averaging over the scattering angle θ gives the *integral cross section*

$$\sigma_{v,\mathrm{j}\to v',\mathrm{j}'}(\mathrm{E}) = 2\pi\int_0^{\pi}\left\{\frac{\mathrm{d}\sigma_{v,\mathrm{j}\to v',\mathrm{j}'}(\theta,\mathrm{E})}{\mathrm{d}\Omega}\sin\theta\right\}\mathrm{d}\theta \tag{1.1.3}$$

which can, in principle, be measured in less sophisticated bulk experiments. *Thermal rate constants* to specified product states $\mathrm{AB}(v',\mathrm{j}')$ are then obtained by Boltzmann averaging these integral cross sections over the possible initial vibrational-rotational states (v,j) and collision energies E. This can be expressed as

---

4 For intermolecular (or isotopic) potentials which depend only on the separation of the two molecules, the scattering is cylindrically symmetric with respect to the axis of the incident beam of molecules in the relative-motion picture. Thus the scattering depends only on the deflection angle θ and not on the azimuthal angle ϕ.

$$\sigma_{v',j'}(T) = \sum_{v,j} \int f_{v,j}(E,T)\sigma_{v,j\to v',j'}(E)dE \tag{1.1.4}$$

where $f_{v,j}(E,T)$ is the Boltzmann distribution function which gives the probability of BC molecules to be in the state (v,j) with energy E at temperature T. These rate constants can then be summed over all possible product states (v',j') to give the *total reactive thermal rate coefficient* k(T).

$$k(T) = \sum_{v',j'} \sigma_{v',j'}(T) \tag{1.1.5}$$

This thermal rate coefficient, in turn, can be measured quite directly in a bulb. Thus, the theory of quantum mechanical scattering, which is the starting point in the derivation of an accurate theory of chemical reaction dynamics, provides a crucial link between the results obtained in detailed state selective molecular beam experiments and thermal average bulb measurements.

As implied by the title of this chapter, this short review is restricted to a rigorous accurate treatment of quantum calculations of reactive collisions. This is not meant to imply that it is necessary or even desirable to approach all applications in this manner. It is well recognized that if one is interested only in thermal reaction rate constants as the above k(T) in Eq. (1.1.5), then transition-state theory is often adequate. There are also many examples where classical trajectory simulation methods have been applied to describe more detailed state-to-state properties of reactions. Furthermore, there are a variety of approximate quantum mechanical and semi-classical methods (where only some of the degrees of freedom are treated quantum mechanically, the remaining classical) that are satisfactory and useful in various special situations. However, these models are, at least to some degree, empirical and often cannot give complete account for quantum mechanical phenomena such as tunneling or interference, and so only a rigorous quantum scattering calculation is guaranteed to be correct. Hence, it is very important to develop these capabilities to as great an extent as possible in order to be able, in some cases at least, to provide a "completely" reliable theoretical description. Such is the point of view of this thesis.

As pointed out above, there has been great activity and interest in the field of accurate quantum mechanical calculations of scattering problems for over 20 years. Quantum mechanical methods are now well established for solving elastic scattering (i.e. no energy transfer) problems,

$$A + BC(v,j) \xrightarrow{\text{Elastic}} A + BC(v,j) \tag{1.1.6}$$

and the more "interesting" inelastic (i.e. with energy transfer) problems,

$$A + BC(v,j) \xrightarrow{\text{Inelastic}} A + BC(v',j') \tag{1.1.7}$$

but it is only very recently that practical and general quantum mechanical methods for three dimensional reactive scattering problems like the ones in Eq. (1.1.1) have begun to emerge. This comparatively slow progress is closely related to the problems involved in the derivation of a set of coordinates that can most conveniently describe both the reactant and product states - the so-called "coordinate problem" that will be reviewed in the next section. Another and perhaps even larger factor than overcoming this coordinate problem is, simply, that in theoretical (and experimental) research one tends to gear the type of problem one addresses to the available resources at hand; ready access to super-computer facilities has stimulated many theorists to start thinking again about how to carry out accurate reaction scattering problems. In fact, this progress in computational hardware was strikingly evident during the evolution of algorithms and models for the presented problem. When I started out working with this H_2^+ problem at the University of Aarhus, I was "reduced" to working on an Alliant FX8/3 system which even at that time was considered a small computer. Now two years later I (and the theoretical group in Aarhus) have access to "real" super-computers that are more than 20-50 times as fast and have much bigger core memory than the Alliant FX8/3. In fact, now a days scientists can acquire desktop-computers or workstations that outperform the Alliant by a factor of 5-10, and only at a fraction the cost of the latter. So, in short, it was not until the recent advent of large memory super-computers that these technical difficulties in connection with three dimensional reactive scattering problems could "routinely" be overcome.

1.2 Coordinates

Before we move on to the real topic of this section, we briefly introduce the concept of channels as used in the general formulation of rearrangement scattering, since this term shall come in very handy in the following discussion of coordinates. Let us continue with the simple case of a three particle collision as illustrated in Eq. (1.1.1) and Eq. (1.1.6,7). It is quite deliberate that we have used the term particles, not in the classical sense, but simply to emphasize that the actual nature of the particles have no influence on this concept to be defined - so we could be referring to molecules, atoms, ions or even elementary particles as in the case of the H_2^+ system. With these three particles we assume that we can only form the following set of chemically distinct arrangements

$$\{B-C \quad + \quad A; \quad A-C \quad + \quad B; \quad A-B \quad + \quad C; \quad ABC\} \tag{1.2.1}$$

We shall further ignore any degeneracies that might arrive with the presence of identical particles, treating all the particles in the system as distinguishable particles[5]. Each of the arrangements corresponds to a special asymptotic form of the total wave function describing this three particle collision, and each of these so-called target wave functions can be

---

5 In practice, of course, these degeneracies are more expediently removed using permutation symmetry arguments that take proper account of the particle spin.

characterized by a set of quantum numbers, corresponding to an exhaustive set of mutually commuting operators of observable physical variables. In atomic and molecular collision theory each arrangement, and the set of quantum numbers which are needed to specify the target wave function, is called a *channel.* It is evident from Eq. (1.2.1) that we have assumed that configurations in which the three particles are far apart only occur with negligible probability, which physically corresponds to a scattering situation where the total energy lies well below the threshold energy for a complete dissociation. We now call these channels with an arrangement of three free particles closed channels, and all the other channels with arrangements as shown in Eq. (1.2.1) *open channels*. Each of the reactions depicted in Eq. (1.1.1) and Eq. (1.1.6,7) can now be viewed as reactions going from the same *reactant channel* ($A + BC(v, j)$) to three different *product channels.*

As indicated in the introduction to this chapter, one of the nasty problems with doing accurate quantum calculations on reactive collisions is the proper choice of coordinates. In short, the problem is that the coordinates which most conveniently describe the reactants of a chemical reaction are not particularly convenient for describing the products and vice versa. At first this might come as a surprise, since it is a well known fact that classical trajectory calculations on quite complicated reactions have been performed for some time, but the answer to this curiosity is actually quite obvious. Quantum mechanical calculations, by virtue of the uncertainty principle, describe all regions of the coordinate space at once[6], whereas classical trajectory calculations effectively access only a single point in this space at a time[7].

To keep the notation as simple as possible, we first look at the situation of the collinear (i.e. all particles move on a straight line) reaction as depicted in Eq. (1.1.1) - i.e. a two channel reactive scattering. In this simple case a convenient choice of coordinates would be the *natural collision coordinates*, as illustrated in figure 1. Here δu is the increment of the translational coordinate u, which asymptotically describes the mass-scaled separation between particle A or C and the pair BC or AB. In terms of scattering on a potential energy surface (to be defined in detail in the next section) this set of coordinates has the great advantage of a direct connection to the concept of the reaction path (illustrated as the thick line in figure 1). The u coordinate simply follows the reaction path from the entrance channel $A + BC$ with minus infinity ($u \rightarrow -\infty$) to the exit channel $AB + C$ with plus infinity ($u \rightarrow \infty$). Similarly, δv is an increment of the vibrational coordinate v, which asymptotically describes a mass-scaled separation of the two particles in the pair BC or AB. Obviously these natural collision coordinates are very convenient, and swing smoothly from the reactants to the products. However, the problem is how to generalize the coordinates to three dimensional and multi-channel scattering situations. In 3D, at each value of the conserved total angular momentum

---

6 Physical observables in the quantum theory correspond to operators that are “averaged” over the whole configuration space.

7 This intriguing, but fundamental relation between classical mechanics and quantum mechanics, is beautifully described in the Feynman Path Integral formulation of the latter. In this formulation of quantum mechanics the classical limit - the classical trajectory - is immediately visible.

number j, the vibrational coordinate v in figure 1 become a 2D (rotational-vibrational) surface which makes the idea of a vibrational coordinate somewhat more difficult to grasp, and in the case of more than two open channel the idea of a well defined reaction path u looses its meaning.

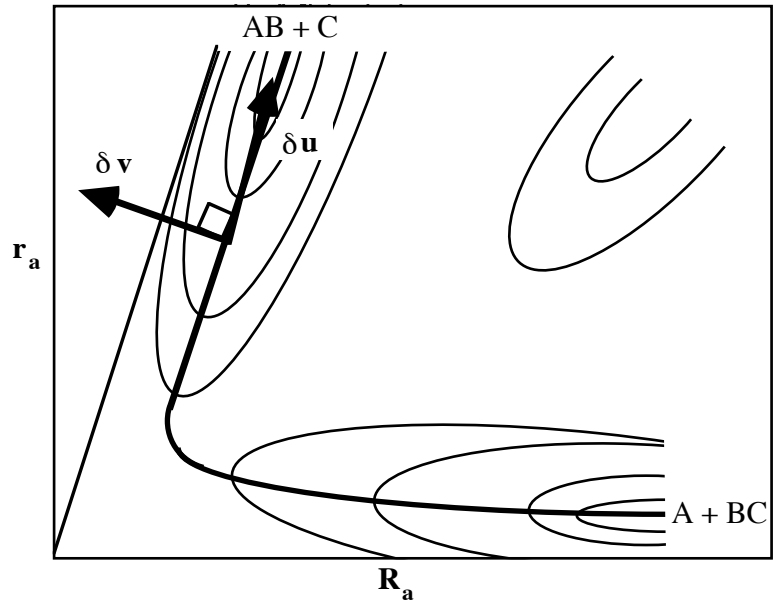

Figure 1 Natural collision coordinates

The *Jacobi-coordinates* are probably the most popular coordinates in terms of actual applications to be discussed in this section. Once again taking the simple collinear three particle reaction depicted in Eq. (1.1.1) as the working example, increments of the reactant and product mass-scaled Jacobi-coordinates (R_a, r_a) and (R_c, r_c) are shown in figure 2.

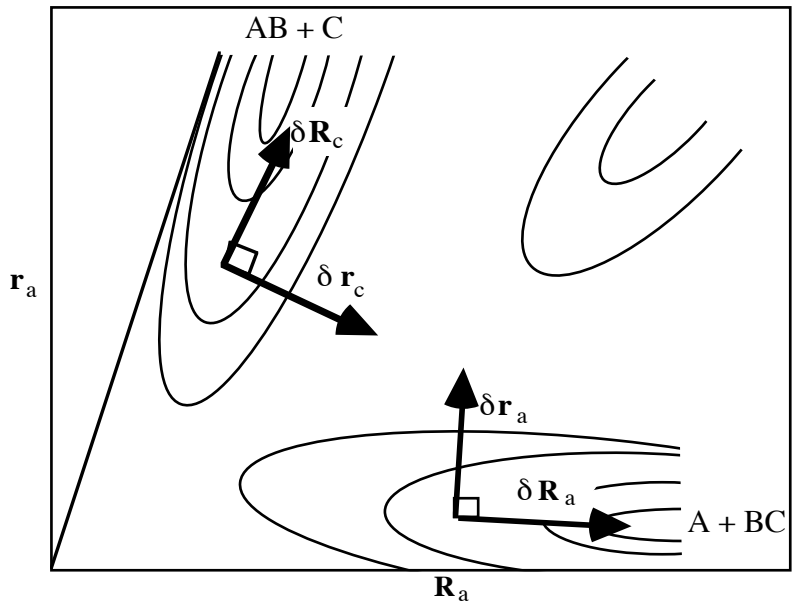

Figure 2 Mass-weighted Jacobi-coordinates

R_a is a mass-scaled distance between A and the center-of-mass of BC, and r_a is a mass-scaled distance between B and C. The mass-scaling factors are generally chosen so that the kinetic energy density contains only one mass-factor,

$$\mathbf{T}(\Psi) = \sum_j \frac{1}{2m_j}\left|-i\hbar\nabla_j\Psi\right|^2 \rightarrow \frac{1}{2M}\sum_j\left|-i\hbar\nabla_j\Psi\right|^2 \qquad (1.2.2)$$

where M can be chosen as the total mass. R_c and r_c are defined in a analogous way. It should be clear from figure 2 that either set of mass-scaled Jacobi-coordinates alone provides a complete description of the available collinear coordinate space. However, it should be equally clear that while R_a and r_a are better suited to describing translational and vibrational motions in the reactant channel, R_c and r_c are more appropriate for a corresponding description of the products. In spite of this coordinate problem, the Jacobi-coordinates are a very popular choice in collision scattering calculations, which is probably because these coordinates, and therefore also the formulations of quantum reactive scattering based on these coordinates, are quite easy to construct and generalize to different systems. In appendix A we present a scheme that can be used to construct the Jacobi-coordinates for a general N particle system. Further, there is a quite straightforward "solution" to this coordinate problem related to the Jacobi-coordinates, namely simply to retain both sets of coordinates at once, using each set for convenience as required. This simultaneous use of Jacobi-coordinates for the various arrangements is actually an approach that has been used for many years in electron structure quantum chemistry under the name linear combination of atomic orbitals (LCAO). The molecular orbitals for an electron are expanded in atomic orbital basis-functions utilizing the coordinates of the electron with respect to the different nuclear centers. In other words, the philosophy of this approach, similar[8] to that in the LCAO model, is a multi-center expansion. As a direct consequence of this natural and efficient way to represent a reactive scattering wave function, another complexity in introduced. The translational and vibrational motions in the reactant channel are coupled non-locally through the potential term in the Hamiltonian to those in the product channel. This non-local coupling between states in the reactant and product channels then appear as exchange integrals between basis-functions in different chemical arrangements. These exchange integrals are simply a mathematical manifestation of the interactions which cause the reaction to proceed, and they are quite analogous to electron exchange interactions in LCAO-like quantum chemistry that arise from matrix elements in which the electron coordinates have been exchanged.

The last approach to the coordinate problem that we shall discuss in this section is the use of the *hyper-spherical coordinates* [19] which, for the collinear case in Eq. (1.1.1), are simply polar coordinates as shown in figure 3 below.

---

8 It should be emphasized at this point that the analogy between multi-center expansions used in the Jacobi-coordinate approach and in the LCAO-model does indeed have it's limitations in the sense that the two cases refer to different physical situations, but nevertheless I find the analogy striking.

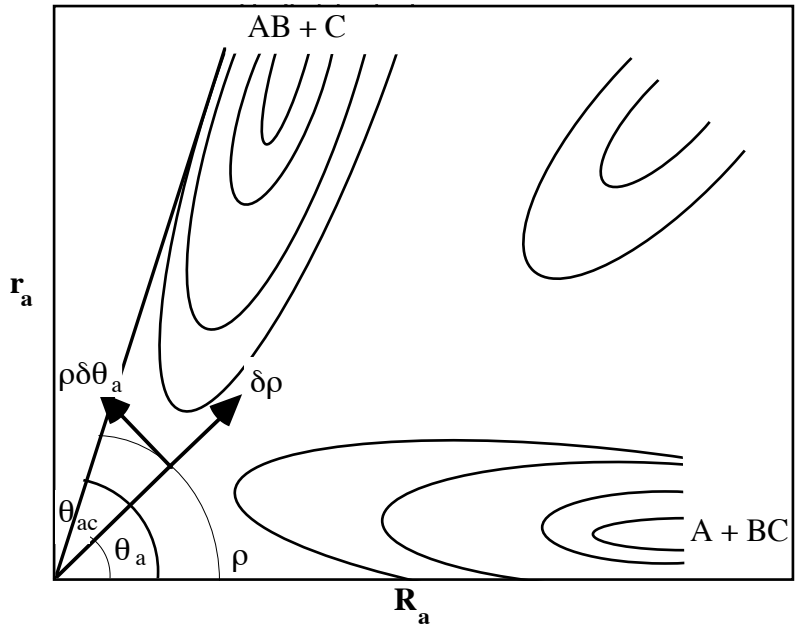

Figure 3 Hyper-spherical coordinates

Generally speaking, hyper-spherical coordinates are a set of translationally and rotationally invariant coordinates, where the characteristic hyper-spherical radius ρ serves as a reaction coordinate. The hyper-spherical radius for an N-particle system is defined as

$$\rho^2 = \sum_{J=1}^{N-1} \left|\vec{r}_j\right|^2 \tag{1.2.3}$$

where $\vec{r}_j$ are the mass-scaled Jacobi-coordinates, as defined in appendix A (recall $\vec{r}_N \equiv \vec{R}_G$ = center-of-mass vector). For the collinear example depicted in figure 3 the hyper-spherical coordinate simply reads as

$$\rho^2 = \left|\vec{r}_a\right|^2 + \left|\vec{R}_a\right|^2 \tag{1.2.4}$$

but it can equally well be defined in terms of the mass-scaled Jacobi vectors of the product arrangement $c(AB + C)$, and in this sense the hyper-spherical coordinate is "universal". The definition of the remaining set of invariants in the hyper-spherical coordinate set (θ_a in figure 3) is less straight-forward, which makes this choice of coordinate representation a little more difficult to derive than the Jacobi-coordinates. For the collinear case in figure 3 the "Delvers hyper-angle" [20, 21] , θ_a, is defined as

$$\theta_a = \tan^{-1}\left(r_a/R_a\right) \tag{1.2.5}$$

This coordinate is a function of the arrangement for which it is defined, and in fact the reactant hyper-angle θ_a and the product hyper-angle θ_c are related by $\theta_a + \theta_c = \theta_{ac}$, where

$$\theta_{ac} = \tan^{-1}\left(m_B/\mu\right) \tag{1.2.6}$$

with

$$\mu \equiv \sqrt{\frac{m_A m_B m_C}{m_A + m_B + m_C}} \tag{1.2.7}$$

is the skewing angle shown on the plot in figure 3. In the general three particle case a convenient choice would be the Mead's coordinates [22] where the invariants x and y are defined as

$$\begin{aligned} x &= \left(\left|\vec{R}_a\right|^2 - \left|\vec{r}_a\right|^2 \right) \Big/ \rho^2 \\ y &= 2\vec{R}_a \cdot \vec{r}_a \Big/ \rho^2 \end{aligned} \tag{1.2.8}$$

The big advantage of these hyper-spherical coordinates is that they describe the arrangement channels in an equivalent fashion, and the hyper-spherical radius ρ is a direct measure of the overall extent of the configuration space. This is illustrated below in figure 4 [23].

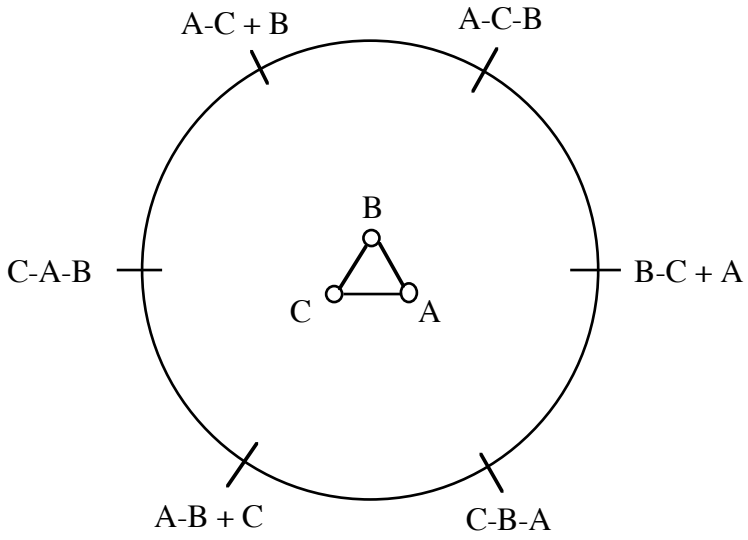

Figure 4 Arrangement-channels for 3 particles

Since $\left|\vec{R}_a \times \vec{r}_a\right|^2 = \rho^4\left(1 - x^2 - y^2\right)/4$, points on the unit circle in the (x,y)-plane correspond to collinear arrangements as depicted in figure 4, and points inside this circle refer to proper triangles. In other words, the collinear reaction that we have used as a working example throughout this section corresponds to a collision with the constraint $x^2 + y^2 = 1$. Hyper-spherical coordinates in four particle systems is discussed in reference [24]. Pursuing the (flimsy) analogy between multi-center expansions used in the Jacobi-coordinate approach and in the LCAO-model, hyper-spherical coordinates correspond to some sort of a single center expansion of the molecular orbital, and hence this approach does not introduce the tedious exchange integrals.

1.3 Beyond the Born-Oppenheimer approximation

At the very heart of practically all ab initio[9] quantum mechanical calculations for molecular systems lies either the Born-Oppenheimer or the adiabatic approximation. The philosophy of these approaches is a separation (complete or partial) of the electronic and nuclear motions, taking point of reference in the large difference in the masses (assumption of infinite nuclear masses). Solving ab initio quantum mechanical problems for many particle systems in this picture of a clamped nucleus Hamiltonian is difficult enough, and hence it is unlikely that calculations will be made at a higher level of approximation in the near future. There are, however, and this is of course the whole basis of this thesis, systems like H_2^+ (and its isotopes) for which this statement is definitely not true. These molecules contain so few particles that one need not make any approximations[10] in the solving of Schrödinger's equation. Furthermore, since the nuclei are very light, the corrections to the Born-Oppenheimer or adiabatic results will be greater for these molecules than for most others.

In order to give a more precise definition of these approximations and an enhancement of the methodology necessary for a detailed comparison of these and others approaches discussed in this thesis, we shall consider an N-particle system with g nuclei and N-g electrons. As a prelude to the separation of the nuclear and electronic motions, we introduce a partitioning of the particles in which the labels 1 through g refer to nuclei and the remainder to electrons. For this system the total non-relativistic Hamiltonian operator **H** reads as

$$\mathbf{H} = \mathbf{T}_{\mathrm{Nuc}} + \mathbf{T}_{\mathrm{Elec}} + \mathbf{W} \tag{1.3.1}$$

where the nuclear and electronic kinetic energy operators respectively are given as

$$\begin{aligned} \mathbf{T}_{\mathrm{Nuc}} &= -\sum_{j=1}^{g} \frac{\hbar^2}{2m_j} \nabla_j^2 \\ \mathbf{T}_{\mathrm{Elec}} &= -\sum_{j=g+1}^{N} \frac{\hbar^2}{2m_j} \nabla_j^2 \end{aligned} \tag{1.3.2}$$

and the potential energy operator for the case of Coulombic interaction is

$$\mathbf{W} = \sum_{\substack{j,k=1 \\ j<k}}^{N} \frac{e_j e_k}{4\pi\varepsilon_0} \mathbf{P}_{jk} \tag{1.3.3}$$

where the operator $\mathbf{P}_{jk}$ is defined through its action on the wave function

---

9 It is a fallacy to put the term ab initio equal to exact in general. Strictly speaking Ab initio means "from the beginning", and when used in the context of natural science, it means exact *within* the framework of a given (non-empirical) model or theory.

10 Except of course the approximation of representing the wave functions in a *finite* basis set (or grid) - due to the limited core memory on computers. However it should be emphasized that this is by no means a trivial approximation in the sense that a "bad" choice of the primitive basis functions can lead to very bad finite representations of the overall wave functions.

$$\mathbf{P}_{jk}\Psi\left(\vec{r}_1,\vec{r}_2,....,\vec{r}_N\right) = \left|\vec{r}_j - \vec{r}_k\right|^{-1}\Psi\left(\vec{r}_1,\vec{r}_2,....,\vec{r}_N\right) \tag{1.3.4}$$

The fundamental equation of motion for the system is now given through the well known time-independent Schrödinger equation

$$\mathbf{H}\left(\vec{r}_1,\vec{r}_2,....,\vec{r}_N\right)\Psi\left(\vec{r}_1,\vec{r}_2,....,\vec{r}_N\right) = E\Psi\left(\vec{r}_1,\vec{r}_2,....,\vec{r}_N\right) \tag{1.3.5}$$

where the eigenvalue E equals the total energy of the system. If we further define the electronic Hamiltonian $\mathbf{H}_{Elec}$ as the sum of $\mathbf{T}_{Elec}$ and $\mathbf{W}$ we get an additional eigenvalue equation

$$\mathbf{H}_{Elec}\left(\vec{r}_1,\vec{r}_2,....,\vec{r}_N\right)\Phi\left(\vec{r}_1,\vec{r}_2,....,\vec{r}_N\right) = \varepsilon\left(\vec{r}_1,\vec{r}_2,....,\vec{r}_g\right)\Phi\left(\vec{r}_1,\vec{r}_2,....,\vec{r}_N\right) \tag{1.3.6}$$

for fixed nuclear configuration $\left(\vec{r}_1,\vec{r}_2,....,\vec{r}_g\right)$. This equation is often referred to as the "clamped nucleus equation" where ε is the electronic energy for the nuclear configuration $\left(\vec{r}_1,\vec{r}_2,....,\vec{r}_g\right)$. Very generally speaking there now exist two distinct strategies to solve Eq. (1.3.5), both leading to coupled vibrational equations. To simplify the notation we will denote the nuclear coordinates $\left(\vec{r}_1,\vec{r}_2,....,\vec{r}_g\right)$ collectively by $\vec{R}$ and the electronic coordinates $\left(\vec{r}_{g+1},\vec{r}_{g+2},....,\vec{r}_N\right)$ collectively by $\vec{r}$.

One of the strategies involves the use of *diabatic states* $\Phi_m^o\left(\vec{r}\right)$, where the orthonormal electronic states $\Phi_m^o\left(\vec{r}\right)$ are defined as solutions to the clamped nucleus equation Eq. (1.3.6) at a chosen *reference* nuclear configuration $\vec{R}_0$:

$$\mathbf{H}_{Elec}\left(\vec{r},\vec{R}_0\right)\Phi_m^0\left(\vec{r}\right) = \varepsilon_m^0\Phi_m^0\left(\vec{r}\right) \tag{1.3.7}$$

In other words $\Phi_k^o\left(\vec{r}\right)$ does not depend explicitly on the nuclear coordinates. If we, as a first "ansatz", assume the basis-set $\left\{\Phi_m^o\left(\vec{r}\right)\right\}$ to be complete in the Hilbert space of the electronic domain $L^2\left(V_{Elec}\right)$ (which is not generally the case for a finite basis-set), the exact molecular wave function in Eq. (1.3.5) can be expanded as follows

$$\Psi\left(\vec{r},\vec{R}\right) = \sum_m \Phi_m^0\left(\vec{r}\right)\chi_m^0\left(\vec{R}\right) \tag{1.3.8}$$

Inserting this expansion into Eq. (1.3.5) results in

$$\sum_m\left\{\mathbf{T}_{Nuc}\left(\vec{R}\right) + \mathbf{H}_{Elec}\left(\vec{r},\vec{R}\right)\right\}\Phi_m^0\left(\vec{r}\right)\chi_m^0\left(\vec{R}\right) = E\sum_m \Phi_m^0\left(\vec{r}\right)\chi_m^0\left(\vec{R}\right) \tag{1.3.9}$$

To obtain an equation for the vibrational functions $\chi_m^0\left(\vec{R}\right)$, we now proceed with a technique that we will refer to as the "projection method", where we project the Schrödinger equation onto (in principle) all the diabatic states. This is done by multiplying Eq. (1.3.9) by all the states $\Phi_n^{0*}\left(\vec{r}\right)$ and integrating over the electronic domain, using the orthonormality relation

$$\int_{V_{Elec}} d\vec{r}\,\Phi_n^{0*}(\vec{r})\Phi_m^0(\vec{r}) = \delta_{nm} \tag{1.3.10}$$

We then obtain the coupled set of equations

$$\sum_m \left\{\left[\mathbf{T}_{Nuc}(\vec{R}) - E\right]\delta_{nm} + \overline{\overline{H}}_{nm}^{Elec}(\vec{R})\right\}\chi_m^0(\vec{R}) = 0 \tag{1.3.11}$$

where we have further defined the matrix elements

$$\overline{\overline{H}}_{nm}^{Elec}(\vec{R}) = \int_{V_{Elec}} d\vec{r}\,\Phi_n^{0*}(\vec{r})\mathbf{H}_{Elec}(\vec{r},\vec{R})\Phi_m^0(\vec{r}) \tag{1.3.12}$$

Note that *the nuclear kinetic energy is diagonal in the diabatic basis, whereas the electronic Hamiltonian, or more precisely the potential, couples the different diabatic states.*

An alternative strategy, which is the one that we shall use throughout this thesis, is to expand $\Psi(\vec{r},\vec{R})$ using a basis of adiabatic electronic states

$$\Psi(\vec{r},\vec{R}) = \sum_m \Phi_m(\vec{r},\vec{R})\chi_m(\vec{R}) \tag{1.3.13}$$

where the *adiabatic states* $\Phi_m(\vec{r},\vec{R})$ are solutions of the clamped nucleus equation

$$\mathbf{H}_{Elec}(\vec{r},\vec{R})\Phi_m(\vec{r},\vec{R}) = \varepsilon_m(\vec{R})\Phi_m(\vec{r},\vec{R}) \tag{1.3.14}$$

and depend *parametrically* on the nuclear coordinates $\vec{R}$. Again we have, as a first "ansatz", assumed the basis-set $\{\Phi_m(\vec{r},\vec{R})\}$ to be complete in the Hilbert space over the electronic domain $L^2(V_{Elec})$. The expansion in Eq. (1.3.13) is referred to as the Born-Huang series, and the electronic eigenvalues $\varepsilon_m(\vec{R})$ define the usual adiabatic potential energy surface shown in figures 1, 2 and 3 as contour plots. Inserting the adiabatic expansion Eq. (1.3.13) into the total Schrödinger equation Eq. (1.3.5) and multiplying by $\Phi_n^*(\vec{r},\vec{R})$ followed by an integration over the electronic domain, proceeding with the "projection method", results in

$$\left[\varepsilon_n(\vec{R}) - E\right]\chi_n(\vec{R}) + \sum_m \overline{\overline{T}}_{nm}^{Nuc}(\vec{R}) = 0 \tag{1.3.15}$$

where we have used the orthonormality relation

$$\int_{V_{Elec}} d\vec{r}\,\Phi_n^*(\vec{r},\vec{R})\Phi_m(\vec{r},\vec{R}) = \delta_{nm} \tag{1.3.16}$$

and defined the matrix elements

$$\overline{\overline{T}}_{nm}^{Nuc}(\vec{R}) = \int_{V_{Elec}} d\vec{r}\left\{\Phi_n^*(\vec{r},\vec{R})\mathbf{T}_{Nuc}\left[\Phi_m(\vec{r},\vec{R})\chi_m(\vec{R})\right]\right\} \tag{1.3.17}$$

We note that *the electronic Hamiltonian is diagonal in the adiabatic basis*, whereas the nuclear kinetic energy term couples the different adiabatic states $\Phi_m\left(\vec{r},\vec{R}\right)$.

The diabatic states are in some ways convenient for practical calculations because they refer to fixed nuclear configurations, but for a large nuclear domain, corresponding to the situation in reactive scattering with different arrangements, this approach is actually quite inefficient since one has to include many diabatic states in the expansion of the exact wave function $\Psi\left(\vec{r},\vec{R}\right)$. The adiabatic electronic states and the associated potential surfaces $\varepsilon\left(\vec{R}\right)$, on the other hand, emerge naturally from the theory of reactive scattering, and hence we shall restrict attention to this strategy of expansion in the rest of this thesis.

We now move on to a more detailed analysis of Schrödinger's equation Eq. (1.3.15) resulting from the adiabatic expansion and the use of the conventional "projection method". The nuclear kinetic energy matrix element $\overline{\overline{T}}_{nm}^{Nuc}\left(\vec{R}\right)$ has the explicit form, using Eq. (1.2.17)

$$\overline{\overline{T}}_{nm}^{Nuc}\left(\vec{R}\right) = -\sum_{j=1}^{g}\frac{\hbar^2}{2m_j}\int_{V_{Elec}} d\vec{r}\,\Phi_n^*\left(\vec{r},\vec{R}\right)\nabla_j^2\left[\Phi_m\left(\vec{r},\vec{R}\right)\chi_m\left(\vec{R}\right)\right] \tag{1.3.18}$$

and if we now switch to the convenient bra-ket notation[11], this is easily rewritten, using the rule for differentiation of a product-function twice, to

$$\overline{\overline{T}}_{nm}^{Nuc}\left(\vec{R}\right) = -\sum_{j=1}^{g}\frac{\hbar^2}{2m_j}\left[\delta_{nm}\nabla_j^2 + \left\langle\Phi_n\middle|\nabla_j^2\middle|\Phi_m\right\rangle + 2\left\langle\Phi_n\middle|\nabla_j\middle|\Phi_m\right\rangle\nabla_j\right]\chi_m\left(\vec{R}\right) \tag{1.3.19}$$

and inserting this result into Eq. (1.3.15) gives us

$$\sum_m\left[\sum_{j=1}^{g}-\frac{\hbar^2}{2m_j}\left\{\delta_{nm}\nabla_j^2 + \left\langle\Phi_n\middle|\nabla_j^2\middle|\Phi_m\right\rangle + 2\left\langle\Phi_n\middle|\nabla_j\middle|\Phi_m\right\rangle\nabla_j\right\} + \delta_{nm}\left\{\varepsilon_n\left(\vec{R}\right) - E\right\}\right]\chi_m\left(\vec{R}\right) = 0 \tag{1.3.20}$$

We are now about to realize one of the real disadvantages connected with the conventional "projection method" used in the adiabatic basis expansion: The orthonormality relation Eq. (1.3.16) in the bra-ket notation reads as

$$\left\langle\Phi_n\middle|\Phi_m\right\rangle = \delta_{nm} \tag{1.3.21}$$

Taking the gradient of this expression with respect to the nuclear coordinate j, and assuming that the differentiation simply goes inside the bra-ket notation, we have

---

11 The bra-ket notation is a short notation for integrals of the type:

$$\langle f|\mathbf{O}|g\rangle \equiv \left\langle f\middle|\mathbf{O}[g]\right\rangle \equiv \int_{-\infty}^{\infty}dx\left\{f^*(x)\mathbf{O}\left[g(x)\right]\right\} = \int_{-\infty}^{\infty}dx\left\{\mathbf{O}^*\left[g(x)\right]f(x)\right\}^* \equiv \left\langle\mathbf{O}[g]\middle|f\right\rangle^*$$

and we note that in the general definition operators always operate to the right, and only if the operator happens to be *Hermitian* can the operator in the above equation operate to the left - that is if

$$\int_{-\infty}^{\infty}dx\left\{f^*(x)\mathbf{O}\left[g(x)\right]\right\} = \int_{-\infty}^{\infty}dx\left\{\mathbf{O}^*\left[f(x)\right]g(x)\right\} \quad\Leftrightarrow\quad \langle f|\mathbf{O}|g\rangle \equiv \left\langle f\middle|\mathbf{O}[g]\right\rangle = \left\langle\mathbf{O}[f]\middle|g\right\rangle$$

$$\left\langle \nabla_j \Phi_n \middle| \Phi_m \right\rangle + \left\langle \Phi_n \middle| \nabla_j \Phi_m \right\rangle = \left\langle \Phi_m \middle| \nabla_j \Phi_n \right\rangle^* + \left\langle \Phi_n \middle| \nabla_j \Phi_m \right\rangle = 0 \tag{1.3.22}$$

which shows that these matrix elements are skew Hermitian ($\overline{\overline{A}}_{mn} = -\overline{\overline{A}}^*_{nm}$). If we take the gradient of Eq. (1.3.22) once more, we arrive at the following expression

$$\left\langle \nabla_j^2 \Phi_n \middle| \Phi_m \right\rangle + 2\left\langle \nabla_j \Phi_n \middle| \nabla_j \Phi_m \right\rangle + \left\langle \Phi_n \middle| \nabla_j^2 \Phi_m \right\rangle = 0 \tag{1.3.23}$$

This expression clearly shows that matrix elements of the type $\left\langle \Phi_n \middle| \nabla_j^2 \middle| \Phi_m \right\rangle$ are not generally Hermitian or even skew Hermitian. The term "generally" is used because only in a complete basis where we can write the resolution of unity[12] as

$$1 = \sum_k \left| \Phi_k \right\rangle \left\langle \Phi_k \right| \tag{1.3.24}$$

do we have

$$\left\langle \Phi_n \middle| \nabla_j \nabla_j \Phi_m \right\rangle = \sum_k \left\langle \Phi_n \middle| \nabla_j \Phi_k \right\rangle \left\langle \Phi_k \middle| \nabla_j \Phi_m \right\rangle \tag{1.3.25}$$

which is clearly (from Eq. (1.3.22)) Hermitian. These observations lead us to the following very important conclusion: Using the "projection method" in connection with the adiabatic basis expansion generally leads to non-Hermitian matrix expressions. As a direct consequence of this, the very important S-matrix derived within the framework of this approach is not guarantied to be unitary, and hence the condition that the number of particles should be conserved is not satisfied. This is guaranteed only in the limit of a complete adiabatic basis-set, which is of course practically unattainable. This is actually one of the main reasons why this approach is not very popular in terms of scattering calculations where the S-matrix is often the goal. Instead theoreticians often turn to other strategies, like the variational principles to be discussed in the next section, that do not suffer from this lack of symmetry. Further we can pinpoint the element in Eq. (1.3.20) that causes this non-Hermicity. Since for the vibrational functions $\chi_n\left(\ddot{\mathrm{R}}\right)$ and $\chi_m\left(\ddot{\mathrm{R}}\right)$ we have a set of expressions analogous to Eq. (1.3.21,22), and since the term ∇_j^2 is diagonal (and therefore does not cause any problems when Eq. (1.3.20) is projected onto $\chi_n^*\left(\ddot{\mathrm{R}}\right)$), we conclude that the term $\left\langle \Phi_n \middle| \nabla_j^2 \middle| \Phi_m \right\rangle$ alone causes the non-Hermicity.

One obvious, but very crude, way to overcome this problem of non-Hermicity is simply to neglect off diagonal matrix-elements of the type $\left\langle \Phi_m \middle| \nabla_j \middle| \Phi_n \right\rangle$ and $\left\langle \Phi_m \middle| \nabla_j^2 \middle| \Phi_n \right\rangle$ which correspond to using only one term in the expansion in Eq. (1.3.13). Eq. (1.3.20) then reduces to

---

12 The conventional notation for this completeness relation reads as

$$1 = \int_{-\infty}^{\infty} dx \left\{ \sum_k \phi_k^*(x)\phi_k(y) \right\} \quad \text{or} \quad \delta(y-x) = \sum_k \phi_k^*(x)\phi_k(y)$$

$$\left[-\sum_{j=1}^{g}\frac{\hbar^2}{2m_j}\left\{\nabla_j^2+\left\langle\Phi_m\middle|\nabla_j^2\middle|\Phi_m\right\rangle+2\left\langle\Phi_m\middle|\nabla_j\middle|\Phi_m\right\rangle\nabla_j\right\}+\varepsilon_m\left(\vec{R}\right)-E\right]\chi_m\left(\vec{R}\right)=0 \qquad (1.3.26)$$

This approach is referred to as the *adiabatic approximation* as opposed to the "exact" non-adiabatic[13] solution of Eq. (1.3.20). Clearly the original motivation for Born (1951) and Born and Huang (1956) to introduce this approximation, was not just to overcome the discussed problem of non-Hermicity, but rather to bring the expression Eq. (1.3.20) into a form that was easier to solve. If we further take the adiabatic states $\Phi_m\left(\vec{r},\vec{R}\right)$ to be real, the term $\left\langle\Phi_m\middle|\nabla_j\middle|\Phi_m\right\rangle$ vanishes[14]. In other words the adiabatic approximation neglects the terms $\left\langle\Phi_n\middle|\nabla_j\middle|\Phi_m\right\rangle$, but includes the term $\left\langle\Phi_m\middle|\nabla_j^2\middle|\Phi_m\right\rangle$. However, in the limit of a complete basis, these terms are related through Eq. (1.3.25), and as such it seems unjustifiable to keep $\left\langle\Phi_m\middle|\nabla_j^2\middle|\Phi_m\right\rangle$ but neglect $\left\langle\Phi_n\middle|\nabla_j\middle|\Phi_m\right\rangle$. This curiosity of the adiabatic approximation has led theoreticians to the opinion that for some systems[15] the result of neglecting the term $\left\langle\Phi_m\middle|\nabla_j^2\middle|\Phi_m\right\rangle$ as well as $\left\langle\Phi_m\middle|\nabla_j\middle|\Phi_m\right\rangle$ actually is a more "justifiable" approximation. This is the celebrated and well-known *Born-Oppenheimer approximation*. The corresponding equation for the vibrational functions $\chi_m\left(\vec{R}\right)$ reads as

$$\left[-\sum_{j=1}^{g}\frac{\hbar^2}{2m_j}\nabla_j^2+\varepsilon_m\left(\vec{R}\right)-E\right]\chi_m\left(\vec{R}\right)=0 \qquad (1.3.27)$$

It is widely believed that the decoupling of electronic and nuclear motions in such a way as to yield the above clamped nucleus Hamiltonian can be justified by reference to work presented in a paper [1] by Born and Oppenheimer published in 1927. Nowadays, however, it is more usual to attempt a justification in terms of an approach that was presented first by Born in 1951 and written up in a generally available form by Born and Huang [26] in 1954. It is also appropriate at this point to mention some work [27] by Brian T. Sutcliffe, whom I had the chance to meet during the "Advanced NATO Study Institute" held in Bad Windsheim, Germany 1991. He especially drew attention to the fact that the Born-Oppenheimer approximation (popularly known as the assumption of infinite nuclear masses) cannot be justified in any simple way in a completely non-classical theory. This then leads to the abandoning of molecular structures, and leaves us with what is known as non-adiabatic theory.

1.4 Variational methods in reactive scattering

In this section we will give a review of a very important technique used extensively in

---

13 The term non-adiabatic is clearly a double negative construction, but is *not* equivalent to diabatic.

14 $\overline{\overline{A}}_{mm}=-\overline{\overline{A}}_{mm}\Leftrightarrow\overline{\overline{A}}_{mm}=0$

15 Keld Bak, Aarhus University, concludes in his thesis [25] from 1982 that for the H_2 system with closely packed adiabatic states this adiabatic approximation is poor and the Born-Oppenheimer approximation actually gives better results.

the study of accurate inelastic and reactive scattering, namely the variational method. We start out with a short introduction to the course of history for these methods, and discuss some of them as we go along. However, no attempt is made here to give a comprehensive description of the various methods, but rather to summarize the basic ideas behind them and the problems associated with them. As we shall see there are several different variational principles for scattering problems, and although they are not all equivalent, many of them are special cases of the "Kohn variational principle" (KVP) originally introduced by Hulthén [28, 29] and by Kohn [30] in the late forties. However, this approach is well known to be plagued by the so-called "Kohn anomalies" [31], and hence most of these methods suffer from singularities and general problems with convergence. Instead of going into a thorough discussion of the KVP itself, we will give a fairly detailed description of a quite recent method [32] that, at least in principle, has overcome these problems of "Kohn anomalies". From this discussion it is then easy to derive the variational functional in the KVP, and we will finally comment on the explicit nature of the "Kohn anomalies".

Variational methods have actually been used in quantum chemistry successfully for more than 60 years, and as such there is really nothing curious about this approach. The earliest quantal applications of this method were made by Kellner [33] and by Hylleraas [34, 35] in the late twenties to the stationary state problem of the helium atom. These bound state calculations all take point of reference in the Rayleigh-Ritz variational principle, and they provide both an upper bound to an exact energy and a stationary property that determines free parameters (often the expansion coefficients) in the wave function. However, it was not until in the late forties that this method was applied to scattering problems. This comparatively slow progress is of course closely related to the different nature of the two problems. Bound states of an entire system are associated with wave functions that have vanishing amplitudes when the distance between any two particles tends to very large values[16], whereas in scattering problems the wave functions have boundary conditions corresponding to the different arrangements. Further, in scattering theory the energy is specified in advance. Generally, variational principles on these systems also determine the wave function, but not with the variational bounds that the bound state calculation provide. In other words, the parameters in the total wave function are determined so that a variational functional is made stationary, but the sign of the residual error (i.e. upper or lower bound) is not usually determined. This lack of a well-defined bounded quantity is a complicated aspect of variational calculations in scattering theory, since there is no simple absolute standard of comparison between different trial functions. As mentioned before there are several different variational principles for scattering problems, but the three most commonly used variational methods are due to Kohn and Hulthén (KVP) [28-30], Schwinger (SVP) [36] and Newton (NVP) [37]. Many attempts have been made to point out simple relations existing among the apparently independent variational methods, and some of the more elegant relations are given

16 $\Psi(\vec{\omega}) \in L^2(V)$

by Kato in his article from 1950 [38]. Simply by adjusting phase-constants, and rewriting the variational functional, he managed to derive the Kohn-, Hulthén- and the Schwinger-method from the same starting point. In the KVP, SVP and the NVP stationary estimates of the so-called reactance matrix, $\overline{\overline{K}}$, is computed using different variational functionals. The main difference in these three functionals is that the order of the error in the computed $\overline{\overline{K}}$ matrix, for a given number of steps in the successive generation of the exact wave function, increases[17]. The applied $\overline{\overline{K}}$ matrix is a real and symmetric matrix, that always will give a unitary scattering matrix, $\overline{\overline{S}}$, simply through its definition

$$\overline{\overline{S}} = \left(\overline{\overline{1}} + i\overline{\overline{K}}\right)\left(\overline{\overline{1}} - i\overline{\overline{K}}\right)^{-1} \tag{1.4.1}$$

In the simple case of a potential scattering (i.e. one-channel), the $\overline{\overline{K}}$ matrix is equal to the tangent of the phase-shift in the asymptotic wave function. However, as mentioned before, these variational methods have been somewhat unpopular in the past, due to the so-called "Kohn anomalies" [31]. Until recently, especially the KVP has not been generally used because of the spurious unphysical singularities that often result when it is used with standing wave boundary conditions. These anomalous singularities inherent in the KVP were first considered by Schwartz [39], who encountered the anomalies in variational calculations of electron hydrogen scattering. Also "Schwinger anomalies" have been observed by a number of people (e.g. [40]), but "Newton anomalies" have not yet been reported in the literature[18], though the NVP is a special case of the KVP and therefore would be expected to display anomalous singularities.

The problems of these anomalous (i.e. spurious, unphysical) singularities was really, at least formally, not overcome until in 1987 when Zhang and Miller published a paper [32] on what they refer to as "the S-matrix version of the Kohn variational principle". The philosophy behind this approach is actually quite simple and straightforward, and since it also deals in a more explicit way with the nature of the "Kohn anomalies", it deserves a little more attention than the variational methods mentioned above. Instead of first determining the real symmetric reactance matrix $\overline{\overline{K}}$, and then obtaining the S-matrix via Eq. (1.4.1), Zhang and Miller derived a variational functional, analogous to the one known from the Kohn variational principle, to give the $\overline{\overline{S}}$ matrix directly. The price for this simple direct approach, however, was that all the calculations, at least in the most general formulation, had to be done in the complex space, which, in terms of practical numerical implementations, is a high price to pay.

All of the relevant features and ideas of this method are illustrated by the simple case of a potential scattering (i.e. one channel) situation, where the Hamiltonian is given by

---

17 If $\delta f^{(0)}$ is the error in the trial wave function $f^{(0)}$, and $\delta f^{(1)}$ is the error in the first approximate wave function $f^{(1)}$ (which we expect to be a more accurate wave function than $f^{(0)}$) then the error term in the variational functionals are respectively $\delta f^{(0)}\delta f^{(0)}$ for KVP, $\delta f^{(0)}\delta f^{(1)}$ for SVP and $\delta f^{(1)}\delta f^{(1)}$ for NVP.

18 Truhlar, Kouri, and co.-workers have used the NVP expensively (e.g. [41]), but have not noted any of these anomalies in their applications.

$$\mathbf{H} = -\frac{\hbar^2}{2\mu}\frac{d^2}{dr^2} + W(r) \tag{1.4.2}$$

and where the potential satisfies $\lim_{r\to\infty}\left[W(r)\right] = 0$. Further, in order to keep the same notation as the one presented in the article [32], the convention is used throughout the rest of *this section* that wave functions in bra symbol, $\langle\ |$, in bra-ket matrix element notation are *not* complex conjugated - a somewhat odd convention. As mentioned above this method is characterized by a stationary estimate of the scattering matrix $\bar{\bar{S}}$ (as opposed to the K-matrix), where the functional to be extremized (denoted by ext) reads as

$$\bar{\bar{S}} = \text{ext}\left[\bar{\bar{S}}_t + \frac{i}{\hbar}\langle\Psi_t|\mathbf{H} - E|\Psi_t\rangle\right] \tag{1.4.3}$$

The label "t" refers to a trial state or matrix. The trial wave function, $\Psi_t(r)$, which is assumed to be regular at r=0, has an asymptotic form consisting of a superposition of an incoming[19] plane wave $\exp(-ikr)$ and an outgoing or scattered plane wave $\exp(ikr)$, where the component of the latter is given by definition as the S-matrix (here just a 1×1 complex matrix or number of unit modules). That is

$$\lim_{r\to\infty}\left[\Psi_t(r)\right] = -v^{-\frac{1}{2}}e^{-ikr} + v^{-\frac{1}{2}}e^{ikr}\bar{\bar{S}}_t \tag{1.4.4}$$

where the pre-exponential factor with $v = \hbar k/\mu$ corresponds to a simple flux normalization[20], and $k^2 = 2\mu E/\hbar^2$. In order to introduce the parameters c_m with which $\bar{\bar{S}}$ should be extremized with respect to, the strategy is now to write the trial function $\Psi_t(r)$ in the form

$$\Psi_t(r) = -u_0(R) + \sum_{m=1}^{N} c_m u_m(r) \tag{1.4.5}$$

where we have introduced the complex energy dependent basis functions

$$\begin{aligned} u_0(r) &= f(r)e^{-ikr}v^{-\frac{1}{2}} \\ u_1(r) &= u_0(r)^* \end{aligned} \tag{1.4.6}$$

---

19 The linear momentum of the plane waves read as

$$\mathbf{P}_z\left[\exp(\pm ikz)\right] = \frac{\hbar}{i}\frac{d}{dz}\left[\exp(\pm ikz)\right] = \pm k\hbar\exp(\pm ikz)$$

The terms incoming and outgoing are then used for respectively the plane wave $\exp(-ikz)$ and $\exp(ikz)$ keeping in mind that the domain of the reaction coordinate is $z \geq 0$ so that $z \to \infty$ corresponds to the asymptotic state.

20 The probability current $\vec{\mathbf{J}}$, i.e. the flow of probability across unit area in unit time, is generally defined as

$$\vec{\mathbf{J}} \equiv -\frac{i\hbar}{2\mu}\left(\Psi^*\vec{\nabla}\Psi - \Psi\vec{\nabla}\Psi^*\right)$$

Since the probability refers to the presence of one particle, it also represents the average flow or *flux* of particles across unit area pr. second. Hence we can also represent the flux as

$$\vec{J} = |\Psi|^2\vec{v}$$

where $|\Psi|^2$ is the density of particles and $\vec{v}$ the velocity. If multiplied by the charge of the particle we further have the electric current.

and a set of (unspecified) real square-integrable energy independent basis functions $\{u_m(r), m = 2,...N\}$. The function $f(r)$ in Eq. (1.4.6) is a so-called *cut-off function* with the property

$$\begin{aligned} \lim_{r\to 0}[f(r)] &= 0 \\ \lim_{r\to \infty}[f(r)] &= 1 \end{aligned} \tag{1.4.7}$$

such that, in agreement with the condition Eq. (1.4.4), we have the following asymptotic forms

$$\begin{aligned} &\lim_{r\to 0}[u_m(r)] = 0, \quad m \in \{0,1,...,N\} \\ &\lim_{r\to \infty}[u_0(r)] = v^{-½}e^{-ikr} \\ &\lim_{r\to \infty}[u_1(r)] = v^{-½}e^{ikr} \\ &\lim_{r\to \infty}[u_m(r)] = 0, \quad m \in \{2,3,...,N\} \end{aligned} \tag{1.4.8}$$

By comparison of Eq. (1.4.4-7) we further note that $\bar{\bar{S}} = c_1$. Integrating by parts twice

$$\langle u_i|\mathbf{H} - E|u_j\rangle = \langle u_j|\mathbf{H} - E|u_i\rangle - \frac{\hbar^2}{2\mu}\left[u_i\frac{du_j}{dr} - u_j\frac{du_i}{dr}\right]_0^\infty \tag{1.4.9}$$

we have the following commutation relations

$$\begin{aligned} &\left[\bar{\bar{M}}_0\right]_1 \equiv \langle u_0|\mathbf{H} - E|u_1\rangle = \langle u_1|\mathbf{H} - E|u_0\rangle - i\hbar \\ &\left[\bar{\bar{M}}_0\right]_m \equiv \langle u_0|\mathbf{H} - E|u_m\rangle = \langle u_m|\mathbf{H} - E|u_0\rangle, \quad m \in \{2,3,...,N\} \\ &\left[\bar{\bar{M}}\right]_{mn} \equiv \langle u_m|\mathbf{H} - E|u_n\rangle = \langle u_n|\mathbf{H} - E|u_m\rangle, \quad m,n \in \{1,2,...,N\} \\ &\bar{\bar{M}}_{00} \equiv \langle u_0|\mathbf{H} - E|u_0\rangle \end{aligned} \tag{1.4.10}$$

where we have defined the "almost" bound-bound $N \times N$ matrix $\bar{\bar{M}}$ (Hermitian), the free-bound $N \times 1$ matrix $\bar{\bar{M}}_0$ and the free-free 1×1 matrix $\bar{\bar{M}}_{00}$[21]. Substituting the expansion of $\Psi_t(r)$ in Eq. (1.4.5) into the variational expression Eq. (1.4.3), gives in terms of a matrix notation

$$\bar{\bar{S}} = \frac{i}{\hbar}\text{ext}\left[\bar{\bar{M}}_{00} + \bar{C}^T\bar{\bar{M}}\bar{C} - \bar{C}^T\bar{\bar{M}}_0 - \bar{\bar{M}}_0^T\bar{C}\right] \tag{1.4.11}$$

---

21 The unbound or free basis functions $u_0(r)$ and $u_1(r)$ are obviously not $L^2(V)$-functions, but nevertheless all the matrix elements involving these functions exist because

$$\lim_{r\to\infty}[(\mathbf{H} - E)u_m(r)] = \lim_{r\to\infty}\left[\left(-\frac{\hbar^2}{2\mu}\frac{d^2}{dr^2} - E\right)u_m(r)\right] = 0, \quad m \in \{0,1\}$$

An optimization of this equation with respect to the expansion coefficients $\overline{C}$ - that is

$$\frac{\partial}{\partial c_m}\left[\bar{\bar{S}}\right] = 0, \quad m \in \{0,1,...,N\} \tag{1.4.12}$$

leads to the condition

$$\overline{C} = \bar{\bar{M}}^{-1}\bar{\bar{M}}_0 \tag{1.4.13}$$

and back substituting this into Eq. (1.4.11) gives the working equation

$$\bar{\bar{S}} = \frac{i}{\hbar}\left[\bar{\bar{M}}_{00} - \bar{\bar{M}}_0^T\bar{\bar{M}}^{-1}\bar{\bar{M}}_0\right] \tag{1.4.14}$$

The "problem" connected with a direct numerical implementation of this S-matrix version of the Kohn variational principle is now evident; one has to invert a large $N \times N$ *complex matrix*, which in terms of allocation of core memory can be a problem if the dimension, N, is too large. The mathematical questions associated with the development of suitable numerically methods that can handle such large matrix-inversion-problems, have received considerable attention and a number of formal approaches have (and are being) developed. Especially Wyatt [42] has been very active in this field over the years. He, and co.-workers, have exploited a number of iterative methods that affords substantial savings in the actual memory used for matrix storage, without resorting to writing matrix elements to disk or other mass storage devices. In other words it is by no means impracticable to directly implement the S-matrix version of the Kohn variational principle, but still it is not numerically as "simple or uncomplicated" as most of the other variational methods discussed in this thesis. Zhang and Miller show that the "complex-inversion-problem" can, to some extent, be minimized by a partitioning of $\bar{\bar{M}}^{-1}$ into a real energy independent part and a complex energy dependent part, using the so-called Löwdin-Feshbach partitioning identity, but this means that the actual matrix inversion is now done in real algebra, such that singularities can in principle occur, though Zhang and Miller have not noted any of these anomalies in their applications.

At this point it is useful to compare the above procedure with the original K-matrix version of the Kohn variational principle, that we have discussed before. In this method the trial wave function $\Psi_t(r)$ is real with the asymptotic form

$$\lim_{r\to\infty}\left[\Psi_t(r)\right] = v^{-1/2}\sin(kr) + \bar{\bar{K}}_t v^{-1/2}\cos(kr) \tag{1.4.15}$$

We could now go through the same derivations as above, but this time with the real energy dependent free functions $u_0(r)$ and $u_1(r)$ as

$$u_0(r) = f(r)v^{-\frac{1}{2}}\sin(kr)$$
$$u_1(r) = f(r)v^{-\frac{1}{2}}\cos(kr) \tag{1.4.16}$$

to find the following final "working formula" for the K-matrix

$$\overline{\overline{K}} = -\frac{2}{\hbar}\left[\overline{\overline{M}}_{00} - \overline{\overline{M}}_0^T\,\overline{\overline{M}}^{-1}\,\overline{\overline{M}}_0\right] \tag{1.4.17}$$

where the matrix elements are defined in the same way as before, but note that all the elements are now *real*. The problem with "Kohn anomalies" in the Kohn variational principle and related methods now appears. In the present case the matrix representation of the Hamiltonian in the basis $\{u_m(r), m \in \{1,2,...N\}\}$ is real symmetric, and hence its eigenvalues are real. But every time that the energy E is equal to one of these eigenvalues, the matrix $\overline{\overline{M}}^{-1}$ is singular according to its definition Eq. (1.4.10). This may happen as the energy E is varied, or at fixed E if non-linear parameters in the basis-set $\{u_m(r), m \in \{1,2,...N\}\}$ are varied to cause one of the eigenvalues to pass through the value E. The problem is not so much when these eigenvalues are exactly equivalent to E, since this is very improbable to happen, as when they are close to E in terms of the machine precision on the used computer. Then $\overline{\overline{M}}^{-1}$ is close to singular, giving false large contributions to the K-matrix. This is exactly what Schwartz [39] discovered in 1961, when he reported that for certain values of E the phase shift (= K-matrix) did not converge. In the limit of a complete basis these so-called "false resonances" become infinitely narrow, and thus unobservable. In other words these "Kohn anomalies" are inevitable in variational approaches where the basis-set is real and finite, and hence they have been a serious problem in many practical calculations as mentioned before.

In contrast, the S-matrix version of the Kohn variational method has no anomalous singularities because the matrix of **H** is here *complex* symmetric. In fact the condition that $\overline{\overline{M}}^{-1}$ in Eq. (1.4.15) is singular is the secular equation for eigenvalues of Schrödinger's equation

$$[\mathbf{H} - E]\Psi(r) = 0 \tag{1.4.18}$$

where

$$\Psi(r) = \sum_{m=1}^{N} c_m u_m(r) \tag{1.4.19}$$

with the boundary conditions

$$\lim_{r\to\infty}[\Psi(r)] = \lim_{r\to\infty}[u_1(r)] \approx e^{ikr} \tag{1.4.20}$$

These complex energies are referred to as Siegert eigenvalues [43], and they are the physically correct complex poles of the S-matrix which characterize the positions and widths

of the scattering resonances. In other words Eq. (1.4.15) is only singular when it is supposed to be singular. However originally and other variational principle attracted our attention as a means by which one could avoid having to work in complex space and to introduce the arbitrary damping or cut-off functions, Eq. (1.4.7), that arise in Zhang and Miller's formulation, which I still believe to be somewhat awkward features of their approach. This "other variational principle" is the topic of the next chapter.

2 The variational R-matrix formulation of scattering

2.1 Introduction

R-matrix theory, introduced by Wigner and Eisenbud in 1947 [2], offers the most general approach to scattering problems in the adiabatic as well as the non-adiabatic pictures. What makes this theory particularly interesting to a chemist is that it is formulated in terms of states of the reactant and product arrangements, corresponding to the target wave functions in the different open channels. In other words, this theory has the boundary conditions on the solution wave function built into the Euler equations, and as such R-matrix theory can be viewed as a (time independent) propagation method[22], where the theory describes a way to propagate the scattering wave function from the known reactant wave function to the various known product target wave functions. Originally, R-matrix theory was derived for the study of nuclear resonance reactions, but since the theory is complete and rigorous it can be applied to reactions of any mechanism, within the limit of non relativistic quantum mechanics. These chemically desirable formal properties, together with the flexibility and the relatively stable numerical properties, would seem to place the R-matrix approach high among the candidates for future development as a practical approach to three-dimensional scattering.

No attempt is made in this chapter to give a comprehensive review of the R-matrix theory as it is presented in the original paper by Wigner and Eisenbud [2], since we shall simply not adopt this particular formulation of the theory. The origins and early development of R-matrix theory are well described in the exhaustive review by Lane and Thomas [44]. Instead, we will just point out the most important aspects of this model, and then move on to a more convenient and recent formulation of the theory , in terms of a variational principle of the R-matrix theory, much like the ones we described for the K- and S-matrix in the previous chapter, but still with some important differences.

One of the important differences between, for example, the S-matrix version of the Kohn variational principle and R-matrix theory is that in the latter approach the configuration space is “truncated”. In all the methods we discussed in chapter 1, at least in the formal presentation, all the matrix elements had to be evaluated over the entire configuration space. The basic technique of R-matrix theory, on the other hand, is to divide space into two regions: a bounded internal interaction region V within which all reactive and inelastic events take place, and an external region in which the interactions have vanished. Outside of V are certain configurations, arrangement channels, within which the particles are separated into one or other of the possible pairs “a”. In order to make this idea more precise, we shall consider a simple bimolecular reaction, and assume for simplicity that “for the rest of this paragraph the

---

22 When R-matrix theory is formulated in terms of a finite element basis (to be defined in chapter 3), this approach most resembles a propagation method as seen in time dependent quantum mechanics, except that here we propagate over space as opposed to time.

Born-Oppenheimer separation of nuclear an electronic motions holds", leaving a single electronic potential energy surface for the nuclear motion as discussed in the previous chapter. However, it should be emphasized that the R-matrix formulation is completely general, and is therefore equally capable of describing electronically *non-adiabatic* reactions (which is of course the central foundation or heart of this thesis). We further assume that in each arrangement channel "a" there is some finite radius, $r_a = s_a$, beyond which neither molecule experiences a significant polarizing potential field from the other. The interaction between the two molecules in arrangement "a" is then, for all $r_a \geq s_a$, simply a function of the intermolecular displacement coordinate r_a. With a total of g nuclei the equation $r_a = s_a$ defines a surface, S_a, in the $3g - 3$ dimensional coordinate space of center-of-mass frame of nuclear motion. From these "open-channel-surfaces" $\{S_a\}$ can be constructed a single closed surface, S, which is defined such that $r_a = s_a$ on that part of S which borders arrangement channel "a". This surface encloses the internal region, V, separating it from the arrangement channels. The point is now to evaluate the scattering wave function, $\Psi(\omega)$, in the internal region, $\omega \in V$, such that $\Psi(\omega \in S_a)$ equals the open-channel target wave functions corresponding to arrangement "a". This mapping of $\Psi(\omega)$ onto the target wave functions on S is exactly done via the R-matrix. In other words, each matrix element of $\overline{\overline{R}}$ represents the mapping of $\Psi(\omega)$ onto a given reactant and product state. At this point we also note that whereas the surface in Zhang and Miller's formulation is very diffuse because of the arbitrary cut-off functions, Eq. (1.4.7), the surface in the R-matrix theory acts more like a "hard sphere". The operator, or more correctly kernel, $\Re$ (corresponding to the continuous representation of $\overline{\overline{R}}$), relates or "propagates" one point on S to another. The R-matrix is real symmetric (as we shall see), which through the relation[23]

$$\overline{\overline{S}} = \overline{\overline{U}}\left(\overline{\overline{1}} + i\overline{\overline{R}}\right)\left(\overline{\overline{1}} - i\overline{\overline{R}}\right)^{-1}\overline{\overline{U}} \tag{2.1.1}$$

where $\overline{\overline{U}}$ is a unitary matrix, ensures that the S-matrix is unitary as desired. Comparing Eq. (2.1.1) with the corresponding relations for the reactant matrix $\overline{\overline{K}}$, Eq. (1.4.1), one might feel tempted to put $\overline{\overline{R}}$ equal to $\overline{\overline{K}}$ in the limit of an infinitely large surface S and interpret the presence of $\overline{\overline{U}}$ in Eq. (2.1.1) as a consequence of a finite S, but this is nevertheless fallacious[24]; $\overline{\overline{R}}$ and $\overline{\overline{K}}$ are not equal - as some text books (e.g. [45] p. 305) erroneously state.

---

23 This simple relation is only valid in the one dimensional case. In more dimensions the relation is more complicated, but it still ensures $\overline{\overline{S}}$ to be unitary for a real symmetric $\overline{\overline{R}}$.

24 In the simple one dimensional case, the S-, K- and R-matrix read as respectively

$$\overline{\overline{S}} \approx \exp(2i\delta_l)$$
$$\overline{\overline{K}} \approx \tan(\delta_l)$$
$$\overline{\overline{R}} \approx \tan(kr_s + \delta_l)$$

where δ_l is the phase shift and r_s defines the internal configuration space in the R-matrix theory. Note that δ_l is the quantum mechanical analog of the semiclassical phase shift η_l defined by

$$\Psi_l(r) \underset{r\to\infty}{\approx} \sin\left(kr - \tfrac{1}{2}l\pi + \eta_l\right)$$

Before we move on to an outline of the explicit form of the variational formulation of R-matrix theory that will be used in the description of H_2^+-scattering, we shall first stress a very important feature of this variational functional, namely that it is *Hermitian symmetric in a finite basis*, as opposed to the variational functionals and "conventional projection methods" described in chapter 1. To give a general proof of this we shall have to go through some tedious rewritings of the functional, but we will profit from some of the intermediate results later on.

In contrast to the methods that we have discussed previously, where we had to evaluate matrix elements over the Hamiltonian, the variational functional of R-matrix theory used in this thesis,

$$\int dr\left\{\mathbf{T}(\Psi)+\mathbf{W}(\Psi)\right\} \quad + \quad \textbf{\textit{Surface – term}} \tag{2.1.2}$$

consists of evaluating matrix elements over the kinetic energy density

$$\mathbf{T}(\Psi)=\sum_{j=1}^{N}\frac{1}{2m_j}\left|-i\hbar\nabla_j\Psi\right|^2 \tag{2.1.3}$$

and the potential energy density

$$\mathbf{W}(\Psi)=\sum_{j<k}\frac{e_j e_k}{4\pi\varepsilon_0\left|\vec{r}_j-\vec{r}_k\right|}\left|\Psi\right|^2 \tag{2.1.4}$$

plus an additional surface term containing the $\Re$-kernel, to be described in detail in the next section. Clearly the potential energy density is Hermitian in any basis-set, complete or not, and we therefore restrict our attention to the kinetic energy density in Eq. (2.1.3). The aim is now to bring $\mathbf{T}(\Psi)$ into a form analogous to the one listed in Eq. (1.3.20), and then show that, in a finite adiabatic basis-set, this expression is always Hermitian. As a prelude to this rewriting of Eq. (2.1.3), we first transform the coordinates from the laboratory-fixed frame of reference (with an arbitrary lab-fixed origin) to a space-fixed frame of reference whose origin is the nuclear center-of-mass. In order to aid the later separation of the nuclear and electronic motions we, further let the labels 1 through g refer to nuclei and the remainder to electrons. We now define the above transformation of the lab-fixed coordinates $\left\{\vec{r}_j'\right\}$ to the space-fixed coordinates $\left\{\vec{r}_j\right\}$ as

$$\vec{r}_j' \rightarrow \vec{r}_j=\vec{r}_j'-\vec{g}, \quad j=1,2,\ldots N \tag{2.1.5}$$

where the nuclear center-of-mass $\vec{g}$ is defined as

$$\vec{g}=\sum_{j=1}^{g}m_j\vec{r}_j'\Big/\sum_{j=1}^{g}m_j\equiv\sum_{j=1}^{N}\beta_j\vec{r}_j' \tag{2.1.6}$$

We have further introduced the constants β_j as

$$\begin{aligned} \beta_j &\equiv \tfrac{m_j}{M}, \quad j = 1,2....g \\ \beta_j &\equiv 0, \quad j = g+1, g+2....N \end{aligned} \tag{2.1.7}$$

where M denotes the total nuclear mass. As an additional set of coordinates, we use the total center-of-mass $\vec{G}$ defined as

$$\vec{G} = \sum_{j=1}^{N} m_j \vec{r}_j' \Big/ \sum_{j=1}^{N} m_j \equiv \sum_{j=1}^{N} \mu_j \vec{r}_j' \tag{2.1.8}$$

where $\mu_j \equiv \frac{m_j}{M_G}$ and M_G denotes the total mass of the system. This choice will allow us, as we shall see in chapter 4, to separate out this coordinate of the total wave function, corresponding to the translational invariant case of zero linear momentum where the energy of the system refers to the center-of-mass frame. Clearly this additional set of coordinates $\vec{G}$ makes one of the N sets of coordinates redundant and can therefore be removed from the wave function. We choose to eliminate $\vec{r}_g$ - that is

$$\vec{r}_g = \vec{k} \quad \Rightarrow \quad \vec{\nabla}_g \Psi = 0 \tag{2.1.9}$$

Under the now fully specified transformation, the kinetic energy density can be shown (see appendix B) to reduce to the form

$$\mathbf{T}(\Psi) = \mathbf{T}_N(\Psi) + \mathbf{T}_E(\Psi) + \mathbf{T}_G(\Psi) \tag{2.1.10}$$

where we have defined respectively the nuclear, electronic and center-of-mass kinetic energy densities

$$\begin{aligned} \mathbf{T}_N(\Psi) &= \sum_{j=1}^{g-1} \left\{ \frac{1}{2m_j} \left| -i\hbar \vec{\nabla}_j \Psi \right|^2 \right\} - \frac{1}{2M} \left| \sum_{j=1}^{g-1} \left\{ -i\hbar \vec{\nabla}_j \Psi \right\} \right|^2 \\ \mathbf{T}_E(\Psi) &= \sum_{j=g+1}^{N} \left\{ \frac{1}{2m_j} \left| -i\hbar \vec{\nabla}_j \Psi \right|^2 \right\} + \frac{1}{2M} \left| \sum_{j=g+1}^{N} \left\{ -i\hbar \vec{\nabla}_j \Psi \right\} \right|^2 \\ \mathbf{T}_G(\Psi) &= \frac{1}{2M_G} \left| -i\hbar \vec{\nabla}_G \Psi \right|^2 \end{aligned} \tag{2.1.11}$$

As will be argued in chapter 4, the center-of-mass kinetic energy density is a constant in this coordinate representation, and hence we restrict our attention to the two other terms. The last term in the electronic kinetic energy density is referred to as the mass polarization term, and is sometimes neglected due to large mass differences ($M >> m_j$, $j = g+1,...N$), but we shall not make this approximation since we seek an accurate solution to the H_2^+ scattering problem. To bring the nuclear kinetic energy density into a canonical form, we introduce the mass-weighted Jacobi-coordinates (denoted by J) for the nuclear coordinates as described in

appendix A (substitute $N \rightarrow g$). That is

$$\vec{r}_j \rightarrow \vec{r}_j^{\,J} = \sum_{i=1}^{g} \sqrt{\beta_i} C_{ij} \vec{r}_i \quad , j = 1,2...g \tag{2.1.12}$$

and, using the chain-rule on this transformation, Eq.(A.16), the orthonormality relation Eq. (A.11) we conclude (see Eq.(A.17))

$$\begin{aligned} \mathbf{T}_N(\Psi) &= \sum_{i=1}^{g} \left\{ \frac{1}{2m_i} \left| -i\hbar \vec{\nabla}_i \Psi \right|^2 \right\} - \frac{1}{2M} \left| \sum_{i=1}^{g} \left\{ -i\hbar \vec{\nabla}_i \Psi \right\} \right|^2 \\ &= \sum_{j=1}^{g} \sum_{i=1}^{g} \left\{ \frac{\beta_i}{2m_i} \left| -i\hbar C_{ij} \vec{\nabla}_j^J \Psi \right|^2 \right\} - \frac{1}{2M} \left| \sum_{j=1}^{g} \left\{ -i\hbar \vec{\nabla}_j^J \Psi \sum_{i=1}^{g} \sqrt{\beta_i} C_{ij} \right\} \right|^2 \\ &= \frac{1}{2M} \sum_{j=1}^{g-1} \left| -i\hbar \vec{\nabla}_j^J \Psi \right|^2 \end{aligned} \tag{2.1.13}$$

In other words, the orthogonality of the Jacobi-transformation ensures that the second term of the nuclear kinetic energy density vanishes. The next step is to expand $\Psi\left(\vec{r},\vec{R}\right)$ - where $\vec{r}$ collectively denotes $\left(\vec{r}_1^{\,J},....,\vec{r}_{g-1}^{\,J}\right)$ and $\vec{R}$ denotes $\left(\vec{r}_{g+1},...,\vec{r}_N\right)$ - in a set of orthonormal adiabatic states $\phi_n\left(\vec{r},\vec{R}\right)$, defined as solutions to the eigenvalue equation

$$\mathbf{T}_E\left[\phi\left(\vec{r},\vec{R}\right)\right] + \mathbf{W}\left[\phi\left(\vec{r},\vec{R}\right)\right] = \varepsilon_n\left(\vec{R}\right) \tag{2.1.14}$$

The part of the variational functional Eq. (2.1.2) that we have considered up till now then reads as

$$\begin{aligned} \int d\vec{r} \left\{ \mathbf{T}_N(\Psi) + \mathbf{T}_E(\Psi) + \mathbf{W}(\Psi) \right\} = \sum_{m,n} \Bigg\{ & \left(\varepsilon_n\left(\vec{R}\right) - E \right) \delta_{mn} - \frac{\hbar^2}{2M} \Big[\nabla \chi_m^* \nabla \chi_n \delta_{mn} + \\ & \left\langle \phi_m \middle| \nabla \middle| \phi_n \right\rangle \left(\nabla \chi_m^* \chi_n - \chi_m^* \nabla \chi_n \right) + \left\langle \nabla \phi_m \middle| \nabla \phi_n \right\rangle \chi_m^* \chi_n \Big] \Bigg\} \end{aligned} \tag{2.1.15}$$

where we have used the skew-Hermicity relation Eq. (1.4.43). This functional is clearly Hermitian symmetric[25], as opposed to Eq. (1.4.41) when integrated further over the nuclear domain, and we draw the important conclusion that, when using variational functionals of the type Eq. (2.1.15), Hermitian symmetry is guaranteed - also in the case of a non-complete basis. The complete variational functional is by definition stationary for an exact $\Psi(\vec{r},\vec{R})$ and hence the additional surface term in Eq. (2.1.2) is also Hermitian symmetric. In other words, the use of a variational functional of a form analogous to the one described in Eq. (2.1.2) ensures that the S-matrix is always unitary.

---

25 Note that we have an analogous skew-Hermitian relation to Eq. (1.3.22) for the matrix elements of the type

$$\int d\vec{R} \nabla \chi_m^* \chi_n = -\int d\vec{R} \chi_m^* \nabla \chi_n$$

2.2 Optimization of the J-functional

The variational formulation for Schrödinger's equation and the associated scattering boundary conditions expressed in terms of the Wigner Eisenbud R-matrix is conveniently expressed in the variational R-matrix functional [5, 46]

$$\begin{aligned} J(\Psi,\Phi) = &\int_V d\omega \left\{ \left[E - W(\omega) \right] |\Psi(\omega)|^2 - \mathbf{T}_E(\Psi) - \mathbf{T}_N(\Psi) \right\} \\ &+ \int_S d\omega \left\{ \Psi^*(\omega)\Phi(\omega) + \Phi^*(\omega)\Psi(\omega) \right\} \\ &- \int_S d\omega d\omega' \left\{ \Phi^*(\omega) \Re(\omega,\omega') \Phi(\omega') \right\} \end{aligned} \tag{2.2.1}$$

which we shall simply refer to as the *J-functional*. Note that ω is a compact notation for both nuclear and electronic coordinates. The idea is now first to take this J-functional as a postulate, and then to derive Schrödinger's equation as one of the Euler equations from the constraint of a stationary property of the J-functional in the limit of an exact $\Psi(\omega)$. This derivation will quickly demonstrate the idea behind the J-functional approach, and a definition of the wave function $\Phi(\omega)$ and the integral kernel $\Re(\omega,\omega')$ also follows. To give a general interpretation of the N-particle J-functional, we will have to make the assumption that the sum of the electronic and the nuclear kinetic energy density is of the form

$$\mathbf{T}_E(\Psi) + \mathbf{T}_N(\Psi) = \sum_{j=1}^{N} \frac{1}{2m_j} \left| -i\hbar \vec{\nabla}_j \Psi \right|^2 \tag{2.2.2}$$

This type of total kinetic energy density can either be obtained if one neglects the mass polarization term in Eq. (2.1.11) and puts $m_1 = m_2 = \ldots m_{g-1} = M$[26] in Eq. (2.2.2), or, quite generally for one electron systems such as the H_2^+-system, if we put $m_1 = m_2 = \ldots m_{g-1} = M$ and $m_{g+1} = 1/m_{g+1} + 1/M$ in Eq. (2.2.2). We shall further omit the $j = g$ in the summation of Eq. (2.2.2). We proceed by examining the first variation of the J-functional with respect to the functions $\Psi(\omega)$ and $\Phi(\omega)$.

$$\delta J = J(\Psi + \delta\Psi, \Phi + \delta\Phi) - J(\Psi,\Phi) - J(\delta\Psi, \delta\Phi) \tag{2.2.3}$$

Since the first term on the right hand side of Eq. (2.2.3) is simply given by

26 This is to obtain the canonical form in Eq. (2.1.13).

$$\begin{aligned}\delta J(\Psi+\delta\Psi,\Phi+\delta\Phi) = \int_V d\omega\Big\{&\big[E-W\big](\Psi+\delta\Psi)^*(\Psi+\delta\Psi)\\ &-\sum_{j=1}^{N}\frac{\hbar^2}{2m_j}\Big[\vec{\nabla}_j(\Psi+\delta\Psi)\Big]^*\vec{\nabla}_j(\Psi+\delta\Psi)\Big\}\\ &+\int_S d\omega\Big\{(\Psi+\delta\Psi)^*(\Phi+\delta\Phi)+(\Phi+\delta\Phi)^*(\Psi+\delta\Psi)\Big\}\\ &-\int_S d\omega d\omega'\Big\{(\Phi+\delta\Phi)^*\Re(\Phi+\delta\Phi)\Big\}\end{aligned} \tag{2.2.4}$$

where we have omitted the dependence upon ω in Ψ,Φ,W and $\Re$, it is easy to see that the overall variation of the J-functional reads as

$$\begin{aligned}\delta J = &\int_V d\omega\left\{\big[E-W\big]\delta\Psi^*\Psi-\sum_{j=1}^{N}\frac{\hbar^2}{2m_j}\Big[\vec{\nabla}_j\delta\Psi\Big]^*\vec{\nabla}_j\Psi\right\}+C.C\\ &+\int_S d\omega\Big\{\delta\Psi^*\Phi+\delta\Phi^*\Psi\Big\}+C.C.-\int_S d\omega d\omega'\Big\{\delta\Phi^*\Re\Phi\Big\}-C.C.\end{aligned} \tag{2.2.5}$$

where C.C. denotes the complex conjugation of the term in front. The second term in the volume integral of Eq. (2.2.5) can now be rewritten by applying the well-known Green's theorem

$$\int_V d\omega\Big\{\vec{\nabla}f(\omega)\vec{\nabla}g(\omega)\Big\}=\int_S d\omega\Big\{f(\omega)\vec{\nabla}g(\omega)\cdot\vec{n}(\omega)\Big\}-\int_V d\omega\Big\{f(\omega)\nabla^2 g(\omega)\Big\} \tag{2.2.6}$$

where $\vec{n}(\omega)$ is a unit vector on the closed surface S (i.e. $\omega\in S$) pointing away from the volume V which S encloses. Now substituting $g(\omega)\to\Psi(\omega)$ and $f(\omega)\to\delta\Psi^*(\omega)$ in Eq. (2.2.6), and noting that $\vec{\nabla}\Psi(\omega)\cdot\vec{n}(\omega)$, $\omega\in S$ is simply the definition of the normal derivative of $\Psi(\omega)$ on the surface S, here denoted by $\partial\Psi(\omega)/\partial n(\omega)$, we obtain the expression

$$\int_V d\omega\Big\{\vec{\nabla}_j\delta\Psi^*\vec{\nabla}_j\Psi(\omega)\Big\}=\int_S d\omega\left\{\delta\Psi^*\frac{\partial\Psi(\omega)}{\partial n_j(\omega)}\right\}-\int_V d\omega\Big\{\delta\Psi^*\nabla_j^2\Psi(\omega)\Big\} \tag{2.2.7}$$

Substituting Eq. (2.2.7) into Eq. (2.2.5) and collecting the terms according to the type of integration and variations with respect to $\Psi(\omega)$ and $\Phi(\omega)$, we finally obtain the expression

$$\begin{aligned}\delta J = &\int_V d\omega\left\{\Big[E-W(\omega)\Big]\Psi(\omega)+\sum_{j=1}^{N}\frac{\hbar^2}{2m_j}\nabla_j^2\Psi\right\}\delta\Psi^*(\omega)+C.C\\ &+\int_S d\omega\left\{\Phi(\omega)-\sum_{j=1}^{N}\frac{\hbar^2}{2m_j}\frac{\partial\Psi(\omega)}{\partial n_j(\omega)}\right\}\delta\Psi^*(\omega)+C.C.\\ &-\int_S d\omega\left\{\Psi(\omega)-\int_S d\omega'\Re(\omega,\omega')\Phi(\omega')\right\}\delta\Phi^*(\omega)+C.C.\end{aligned} \tag{2.2.8}$$

From Eq. (2.2.8) it is now easy to see that if we require the J-functional to be stationary with respect to variation of the functions $\Psi(\omega)$ and $\Phi(\omega)$ (i.e. $\delta J/\delta\Psi^* = \delta J/\delta\Phi^* = 0$), we obtain the desired set of Euler equations. The functional derivative $\delta J/\delta\Psi^*$ vanishes when

$$\left\{-\sum_{j=1}^{N}\frac{\hbar^2}{2m_j}\nabla_j^2 + W(\omega)\right\}\Psi(\omega) = E\Psi(\omega), \quad \omega \in V \tag{2.2.9}$$

which is simply the time-independent non-relativistic Schrödinger equation. $\delta J/\delta\Phi^*$ vanishes when

$$\Phi(\omega) = \sum_{j=1}^{N}\frac{\hbar^2}{2m_j}\frac{\partial\Psi(\omega)}{\partial n_j(\omega)}, \quad \omega \in S \tag{2.2.10}$$

and

$$\Psi(\omega) = \int_S d\omega' \Re(\omega,\omega')\Phi(\omega'), \quad \omega \in S \tag{2.2.11}$$

Substitution of Eq. (2.2.10) into Eq. (2.2.11) leads to the boundary condition

$$\Psi(\omega) = \sum_{j=1}^{N}\frac{\hbar^2}{2m_j}\int_S d\omega' \Re(\omega,\omega')\frac{\partial\Psi(\omega)}{\partial n_j(\omega)}, \quad \omega \in S \tag{2.2.12}$$

All in all we now have the very essence of the J-functional formulation of the R-matrix theory, and we are in the position to interpret $\Psi(\omega)$, $\Phi(\omega)$ and $\Re(\omega,\omega')$. For a stationary J-functional the function $\Phi(\omega), \omega \in S$ is equal to the mass weighted sum of the normal derivative of $\Psi(\omega)$ on different points (channels) on the surface S, and hence from Eq. (2.2.12) we conclude that the $\Re(\omega,\omega')$ operator (a continuous representation of the R-matrix) relates the normal derivative and amplitude of $\Psi(\omega)$ on the boundary S. We further note from Eq. (2.2.12) that if $\Re(\omega,\omega')$ is zero everywhere on S the wave function $\Psi(\omega)$ should have zero amplitude on the boundary, while it is required to have zero normal derivative everywhere if the reciprocal $\Re(\omega,\omega')$ vanishes. Although it may be a mere mathematical curiosity, we note that since the boundary condition Eq. (2.2.12) is expressed in terms of an integral equation, the $\Re(\omega,\omega')$ operator is some time referred to as the R-matrix kernel. The stationarity also requires that in the volume V $\Psi(\omega)$ is a solution to Schrödinger's equation Eq. (2.2.9). Summing up we conclude that *for a stationary J-functional, $\Psi(\omega)$ represents the solution to a scattering process described through the corresponding Schrödinger's Eq. (2.2.9) with the boundary condition Eq. (2.2.12).*

For an approximation of the R-matrix (and hence a numerical determination of the scattering amplitude), we now proceed with a finite basis expansion of the wave function $\Psi(\omega)$. To keep the notation as general as possible, in order to leave the specific choice of basis functions to the next chapter, we simply choose a set of functions $\{u_j(\omega), j = 1,..K\}$ in

the Sobolev space $H^{(1)}(V)$, which implies that integrals of the form

$$\int_V d\omega \left\{ \left[\vec{\nabla} u_m(\omega) \right]^* \vec{\nabla} u_n(\omega) + u_m^*(\omega) u_n(\omega) \right\} \tag{2.2.13}$$

exist i.e. converge. It is important to note that $H^{(1)}(V)$ is a subspace of the corresponding Hilbert space $L^2(V)$, which is the space to which all the basis functions we described in chapter 1 belong. We write $\Psi(\omega)$ as

$$\Psi(\omega) = \sum_{j=1}^{K} c_j u_j(\omega) \tag{2.2.14}$$

and, inserting this expansion into Eq. (2.2.1), and defining the matrix elements A_{ij} as

$$A_{ij} = \int_V d\omega \left\{ \left[E - W(\omega) \right] u_i^*(\omega) u_j(\omega) - \sum_{k=1}^{N} \frac{\hbar^2}{2m_k} \nabla_k u_i^*(\omega) \nabla_k u_j(\omega) \right\} \tag{2.2.15}$$

the J-functional reduces to

$$\begin{aligned} J(\Psi, \Phi) = & \sum_{i,j=1}^{K} c_i^* c_j A_{ij} + \sum_{j=1}^{K} c_i^* \int_S d\omega' \left\{ u_j^*(\omega') \Phi(\omega') \right\} \\ & + C.C. - \int_S d\omega d\omega' \left\{ \Phi^*(\omega) \Re(\omega, \omega') \Phi(\omega') \right\} \end{aligned} \tag{2.2.16}$$

Since the solutions to Schrödinger's equation with the associated scattering boundary conditions are found for a stationary J-functional, we proceed with a variation of Eq. (2.2.16) with respect to c_i^*

$$\frac{\partial J}{\partial c_i^*} = \sum_{j=1}^{K} c_j A_{ij} + \int_S d\omega' \left\{ u_i^*(\omega') \Phi(\omega') \right\} = 0, \quad i = 1, 2, \ldots K \tag{2.2.17}$$

From the variation of J with respect to $\Phi(\omega)$ we found the integral equation Eq. (2.2.11), and inserting the finite basis expansion Eq. (2.2.14) in to this equation simply gives us the boundary condition

$$\sum_{j=1}^{K} c_j u_j(\omega) - \int_S d\omega' \left\{ \Re(\omega, \omega') \Phi(\omega') \right\} = 0, \quad \omega \in S \tag{2.2.18}$$

Expressing Eq. (2.2.17,18) in a matrix notation gives

$$\overline{\overline{D}}(\omega)\begin{bmatrix} c_1 \\ c_2 \\ \vdots \\ c_K \\ 1 \end{bmatrix} \equiv \begin{bmatrix} A_{11} & A_{12} & \cdots & A_{1K} & \int_S d\omega' \left\{ u_1^*(\omega')\Phi(\omega') \right\} \\ A_{21} & A_{22} & \cdots & A_{2K} & \int_S d\omega' \left\{ u_2^*(\omega')\Phi(\omega') \right\} \\ \vdots & \vdots & \ddots & \vdots & \vdots \\ A_{1K} & A_{K2} & \cdots & A_{KK} & \int_S d\omega' \left\{ u_K^*(\omega')\Phi(\omega') \right\} \\ u_1(\omega) & u_2(\omega) & \cdots & u_K(\omega) & -\int_S d\omega' \left\{ \Re(\omega,\omega')\Phi(\omega') \right\} \end{bmatrix} \begin{bmatrix} c_1 \\ c_2 \\ \vdots \\ c_K \\ 1 \end{bmatrix} = \overline{0} \qquad (2.2.19)$$

A solution of this matrix equation is obtainable when the determinant of the $(K+1)\times(K+1)$ matrix, $\overline{\overline{D}}(\omega)$, vanishes, that is if

$$\det\left[\overline{\overline{D}}(\omega)\right] = \int_S d\omega \left\{ \det\left[\overline{\overline{E}}(\omega,\omega')\right]\Phi(\omega') \right\} = 0 \qquad (2.2.20)$$

where we have defined the matrix

$$\overline{\overline{E}}(\omega,\omega') \equiv \begin{bmatrix} A_{11} & A_{12} & \cdots & A_{1K} & u_1^*(\omega') \\ A_{21} & A_{22} & \cdots & A_{2K} & u_2^*(\omega') \\ \vdots & \vdots & \ddots & \vdots & \vdots \\ A_{1K} & A_{K2} & \cdots & A_{KK} & u_K^*(\omega') \\ u_1(\omega) & u_2(\omega) & \cdots & u_K(\omega) & -\Re(\omega,\omega') \end{bmatrix} \qquad (2.2.21)$$

This can only be so for an arbitrary surface function $\Phi(\omega')$ if

$$\det\left[\overline{\overline{E}}(\omega,\omega')\right] = -\Re(\omega,\omega')\det\left[\overline{\overline{A}}\right] + \det\left[\overline{\overline{B}}(\omega,\omega')\right] = 0 \qquad (2.2.22)$$

where we have defined the matrix $\overline{\overline{B}}(\omega,\omega')$

$$\overline{\overline{B}}(\omega,\omega') \equiv \begin{bmatrix} A_{11} & A_{12} & \cdots & A_{1K} & u_1^*(\omega') \\ A_{21} & A_{22} & \cdots & A_{2K} & u_2^*(\omega') \\ \vdots & \vdots & \ddots & \vdots & \vdots \\ A_{1K} & A_{K2} & \cdots & A_{KK} & u_K^*(\omega') \\ u_1(\omega) & u_2(\omega) & \cdots & u_K(\omega) & 0 \end{bmatrix} \qquad (2.2.23)$$

and hence we obtain the following general expression for the R-matrix kernel

$$\Re(\omega,\omega') = \det\left[\overline{\overline{B}}(\omega,\omega')\right] \Big/ \det\left[\overline{\overline{A}}\right] \qquad (2.2.24)$$

Clearly, from Eq. (2.2.24), $\Re(\omega,\omega')$ will exhibit poles if the matrix $\overline{\overline{A}}$ is singular, just as we found that the KVP displays poles when the matrix $\overline{\overline{M}}$ in Eq. (1.4.17) is singular. In other words this variational R-matrix approach is also "potentially plagued" by singularities analogous to the "Kohn anomalies" we discussed in the previous chapter, but, as we shall see

soon, these poles are not as troublesome as the poles in the Kohn variational principle in the sense that we still obtain converges for the total wave function $\Psi(\omega)$ - one could say that the "poles are integrable". For a singular A-matrix it is evident from Eq. (2.2.11) that a stationary solution exists for $\Phi(\omega) = 0$ on S. As an interesting special case we choose a orthonormal basis $\{u_j(\omega),\ j = 1,2,..K\}$ on V to give a diagonal matrix $\overline{\overline{A}}$, since this will allow us to derive an explicit expression for $\Re(\omega,\omega')$. Eq. (2.2.22) then reduces to

$$\begin{vmatrix} E-E_1 & 0 & \cdots & 0 & u_1^*(\omega') \\ 0 & E-E_2 & \cdots & 0 & u_2^*(\omega') \\ \vdots & \vdots & \ddots & \vdots & \vdots \\ 0 & 0 & \cdots & E-E_K & u_K^*(\omega') \\ u_1(\omega) & u_2(\omega) & \cdots & u_K(\omega) & -\Re(\omega,\omega') \end{vmatrix} = \tag{2.2.25}$$

$$-\Re(\omega,\omega')\prod_{i=1}^{K}\{E-E_i\} - \sum_{i=1}^{K}\left\{u_i^*(\omega')u_i(\omega)\prod_{\substack{j=1\\ j\neq i}}^{K}\{E-E_j\}\right\} = 0$$

which gives the so-called *standard spectral form* of the R-matrix kernel known from the original paper by Wigner and Eisenbud [2]

$$\Re(\omega,\omega') = \sum_{i=1}^{K}\frac{u_i(\omega)u_i^*(\omega')}{E_i - E} \tag{2.2.26}$$

From this expression it is clear that the R-matrix kernel exhibits poles if one or more of the basis functions $u_i(\omega)$ happens to have an eigenvalue $E_i = E$, and this situation is again analogous to the one we discussed in chapter 1 section 4 for the matrix $\overline{\overline{M}}$ in the Kohn variational principle. We conclude this chapter by noting that for an arbitrary surface function $\Phi(\omega')$, Eq. (2.2.19) reduces to the central matrix equation,

$$\begin{bmatrix} A_{11} & A_{12} & \cdots & A_{1K} & u_1^*(\omega') \\ A_{21} & A_{22} & \cdots & A_{2K} & u_2^*(\omega') \\ \vdots & \vdots & \ddots & \vdots & \vdots \\ A_{1K} & A_{K2} & \cdots & A_{KK} & u_K^*(\omega') \\ u_1(\omega) & u_2(\omega) & \cdots & u_K(\omega) & -\Re(\omega,\omega') \end{bmatrix}\begin{bmatrix} c_1 \\ c_2 \\ \vdots \\ c_K \\ 1 \end{bmatrix} = \vec{0}, \quad \omega,\omega' \in S \tag{2.2.27}$$

3 Numerical implementation of reactive scattering

3.1 Introduction

Accurate methods for the estimation of the numerical predictions of quantum mechanics have been sought since its inception. Generally, there exist three different types of approaches in quantum mechanics to obtain a numerical solution of the Euler equations describing the system at hand. The first approach represent the states of the system as ket vectors in the "somewhat abstract" occupation number space, as it is done in the *second quantization method*. These ket vectors do not contain a reference to any particular basis-set, as is the case in the conventional "first quantization". The reference to a particular basis-set is instead built into the second quantization operators in such a way that there exist a correlation principle[27] between the first and second quantization. Another characteristic feature of this method is that the statistics, which the particles of the system obey, is built into the formulation itself[28]. The second quantization formulation is an approach that has been successfully applied in many fields such as quantum electrodynamics[29] and electronic structure problems[30]. Although the mathematical questions associated with the development of this method have received considerable attention and a number of formal approaches have (and are being) developed [49], their presentation in this chapter will be limited to the above comment for several reasons. First, they lie outside my personal experience in terms of actual applications, and second and most importantly they have not provided the formalism within which most accurate quantal approaches to calculations of reactive scattering have been developed.

The second type of approach we have already become acquainted with in chapter 1; namely a *state expansion* of the wave function, in, for example, diabatic or adiabatic states. Strictly speaking this would imply that one does know an analytical expression for the eigensolutions $\phi_n(x)$ of some zero-order Hamiltonian, and this is unfortunately seldom the case for most scattering problems, including the H_2^+-system. Instead it is more likely that one does only know a numerical expression of $\phi_n(x)$ in terms of some convenient finite basis-set. This *finite basis representation* (FBR) of a wave function is an approach that is widely used in scattering problems. One can subdivide the FBR approach into two different types. We shall refer to the first as a *global element method* (GEM[31]), where the basis elements are defined

---

27 For the fermions this correlation is given by the well-known Condon-Slater rules [47].

28 The so-called occupation number operator in the second quantization formulation obeys either Bose-Einstein statistics (for bosons) or Fermi-Dirac statistics (for fermions).

29 A good example of the application of the second quantization method in quantum electrodynamics is given in reference [48] p. 35, where the Hamiltonian for the free field is written as a sum of one-dimensional harmonic oscillator Hamiltonians, which are in turn represented in second quantization annihilation and creation operators obeying Bose-Einstein statistics.

30 The second quantization formulation offers a very convenient way to obtain the Hartree-Fock equations.

31 It is acknowledged that this is not a standard textbook notation, but we shall use it anyway for convenience. At this point I would like to quote a theorist that once stated that "the problem with understanding modern quantum

over the entire electronic or nuclear domain of interest. For instance the $u_i(x)$ basis functions mentioned in Miller's one channel S-matrix version of Kohn's variational principle are elements of this type. The other type of basis elements are only defined (or more correctly have non-zero amplitude) in a local part of the space defining the coordinate domain of interest. This approach is called a *finite element method* (FEM), and after giving a short introduction below we shall apply this method on the results for the R-matrix formulation obtained in the previous chapter.

This technique of splitting the space into a number of small domains directly lead us to the last approach where the space is discretized on a grid or set of points. One of these *grid methods,* the discrete variable representation (DVR), is quite popular in time independent as well as time dependent scattering theory, and since it will play a central role in the numerical calculations presented in this thesis we shall give an introduction to this method. As we shall see this method is actually closely related to the FBR (or GEM), since there exists an isomorphism - in terms of a unitary transformation - between the DVR and an orthonormal FBR.

3.2 The finite element method

Originally the FEM was developed in the forties by the mathematician Richard Courant. Soon it was used in engineering science, in order to calculate static and dynamic stresses of complicated constructions, and as such it is a well known and mathematically thoroughly prepared technique. Nevertheless, it is only recently (in the eighties) that this method has proven useful for quantum mechanical problems. The FEM can be formulated in more than one dimension, but we will first restrict our attention to the one-dimensional case, and then later comment on multi-dimensional FEM as compared to multi dimensional DVR. The first step in the FEM is to choose the grid on which the elements of the scheme should be defined. Here we already encounter one of the great advantages of this method: the size and shape of the underlying grid in the FEM can be defined very freely so that physical properties can be taken into account, e.g. one can use small grid spacing in regions of physical importance and large grid spacing in regions of lesser weight. Thus the point distribution can be adapted to a given problem. The next step is to choose the functions that span each element; these are typically polynomials of some given type and order. In the following we present a very easy way to generate the N+1 "linearly independent"[32] polynomials of degree N in the element from a to b. We start by defining the linear functions $B_0^1(x)$ and $B_1^1(x)$[33] through the relations

---

chemistry really boils down to how one should manage to recollect the meaning of all the different abbreviations used in the literature."

32 i.e., the basis set in each element is complete for any function that can be expressed as a polynomial of degree $\leq N$. That is the determinant of the matrix consisting of the N+1 coefficients of N+1 polynomials is required not to vanish.

33 I have chosen to use an other notation for the basis functions, $B_k^N(x)$, than the one presented in reference [50]. In my opinion this leads to simpler notations, and the reader is not confused by the "Dirac-like" notation, which strictly

[50]

$$B_0^1(x) + B_1^1(x) = 1, \quad aB_0^1(x) + bB_1^1(x) = x \tag{3.2.1}$$

which give the explicit expressions

$$B_0^1(x) = \frac{b - x}{b - a}, \quad B_1^1(x) = \frac{x - a}{b - a} \tag{3.2.2}$$

that are clearly linearly independent, and as in figure 5.

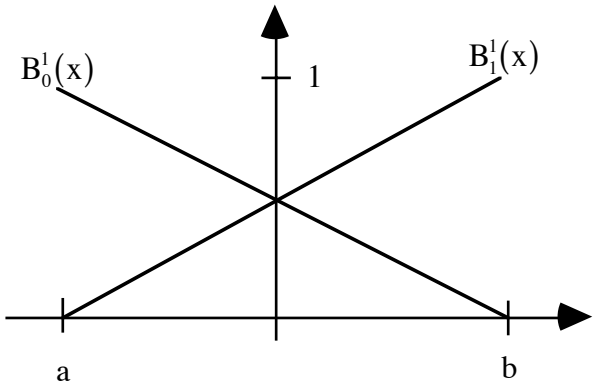

Figure 5 Bézier functions of degree 1

The higher degree functions are now defined from these functions in the following way

$$B_k^N(x) \equiv \left[B_0^1(x)\right]^{N-k}\left[B_1^1\right]^k, \quad k = 0,1,\ldots N \tag{3.2.3}$$

and they are referred to as the Bézier functions of degree N. Clearly, these basis functions are not orthogonal, but their overlap integrals are easily determined from the relation

$$\int_a^b dx\left\{\left[B_0^1(x)\right]^{n_1}\left[B_1^1(x)\right]^{n_2}\right\} = \int_a^b dx\left\{\left[\frac{x - a}{b - a}\right]^{n_1}\left[\frac{b - x}{b - a}\right]^{n_2}\right\} = (b - a)\frac{n_1!n_2!}{(n_1 + n_2 + 1)!} \tag{3.2.4}$$

Matrix elements of the Bézier functions, over a general polynomial function $f(x)$, are easily obtained if $f(x)$ is first resolved in Bézier polynomials using Eq. (3.2.1), and the resulting integral evaluated using Eq. (3.2.4). The x-derivative, $\frac{d}{dx}B_i^N(x)$, of the Bézier basis functions of degree N, $\{B_i^N(x), i = 0,1,\ldots N\}$, are easily expressed in the same Bézier basis using Eq. (3.2.1), and, in general we write

$$\frac{d}{dx}B_i^N(x) = \langle x|\mathbf{P}|B_i^N\rangle = \langle x|\left\{\sum_{j=0}^N |B_j^N\rangle\langle B_j^N|\right\}\mathbf{P}|B_i^N\rangle = \sum_{j=0}^N \langle B_j^N|\mathbf{P}|B_j^N\rangle\langle x|B_i^N\rangle \tag{3.2.5}$$

---

speaking has nothing to do with a Dirac notation.

where we have used the Dirac notation[34] $\langle x|f\rangle$ for a general function $f(x)$. Further we have introduced the functions $\langle x|\tilde{\alpha}\rangle$, which are biorthogonal[35] to $\langle x|\alpha\rangle$, used the associated closure relation[36], and replaced d/dx by the symbol $\mathbf{P}$ to remind us of the relation to the linear momentum operator. For the first- and third-degree polynomials the matrices $\left[\overline{\overline{\langle\tilde{\alpha}|\mathbf{P}|\beta\rangle}}\right]$ are easily shown to be

$$\left[\overline{\overline{\left\langle \tilde{B}_i^1 \middle| \mathbf{P} \middle| B_j^1 \right\rangle}}\right] = \begin{array}{c} \\ \tilde{B}_0^1 \\ \tilde{B}_1^1 \end{array} \begin{array}{c} \begin{array}{cc} \mathbf{P} & \\ B_0^1 & B_1^1 \end{array} \\ \begin{bmatrix} -\frac{1}{h} & \frac{1}{h} \\ -\frac{1}{h} & \frac{1}{h} \end{bmatrix} \end{array}, \qquad \left[\overline{\overline{\left\langle \tilde{B}_i^3 \middle| \mathbf{P} \middle| B_j^3 \right\rangle}}\right] = \begin{array}{c} \\ \tilde{B}_0^3 \\ \tilde{B}_1^3 \\ \tilde{B}_2^3 \\ \tilde{B}_3^3 \end{array} \begin{array}{c} \begin{array}{cccc} \mathbf{P} & B_0^3 & B_1^3 & B_2^3 & B_3^3 \end{array} \\ \begin{bmatrix} -\frac{3}{h} & \frac{1}{h} & 0 & 0 \\ -\frac{3}{h} & -\frac{1}{h} & \frac{2}{h} & 0 \\ 0 & -\frac{2}{h} & \frac{1}{h} & \frac{3}{h} \\ 0 & 0 & -\frac{1}{h} & \frac{3}{h} \end{bmatrix} \end{array} \tag{3.2.6}$$

where $h \equiv b - a$. We can now write the simple matrix equation (arriving from successive use of Eq. (3.2.5)) for the x-derivative of any order

$$\left[\overline{\overline{\langle\tilde{\alpha}|d^k/dx^k|\beta\rangle}}\right] = \left[\overline{\overline{\langle\tilde{\alpha}|\mathbf{P}|\beta\rangle}}\right]^k \tag{3.2.7}$$

We now move on to defining the overall elements $F_j(x)$ of the FEM scheme, using the discussed Bézier polynomials as "generators" for the basis-set. According to the theory of finite element methods it is sufficient for the present problem to consider function spaces in C^0 since only first derivatives are present in the J-functional presented in the previous

---

34 The Dirac notation is closely related to the so-called Dirac function $\delta(x - x_0)$. This function is actually the eigensolution, $\Psi(x)$, to the eigenvalue equation $\mathbf{x}\Psi(x) = x_0\Psi(x)$ of the coordinate "operator" $\mathbf{x}$, and has the property

$$\int_{-\infty}^{\infty} dx f(x)\delta(x - x_0) = f(x_0)$$

Hence the Dirac notation can be viewed as a standard bra-ket notation if we put

$$\langle x|f\rangle = \int_{-\infty}^{\infty} dx' f(x')\delta(x' - x) = f(x)$$

For this reason the Dirac notation is sometimes referred to as the "coordinate representation of $f(x)$" ($f(x)$ is projected onto the eigenfunction of x).

35 $\langle x|\tilde{\alpha}\rangle \equiv \sum_\gamma \Delta^{-1}_{\gamma\alpha}\langle x|\gamma\rangle$ where $\Delta_{\gamma\alpha} \equiv \langle\gamma|\alpha\rangle$ so that $\langle\beta|\tilde{\alpha}\rangle = \sum_\gamma \Delta^{-1}_{\gamma\alpha}\langle\beta|\gamma\rangle = \sum_\gamma \Delta^{-1}_{\gamma\alpha}\Delta_{\beta\gamma} = \left[\overline{\overline{\Delta\Delta}}^{-1}\right]_{\alpha\beta} = \delta_{\alpha\beta}$

36 Since the Bézier basis set $\left\{B_k^N(x),\ k = 0,..,N\right\}$ by definition spans the space of polynomials of degree $\le N$ any polynomial $f(x)$ of degree $\le N$ can be expanded as

$$\langle x|f\rangle = \sum_{i=0}^{N} C_i\langle x|B_i^N\rangle$$

and multiplying this expression by the biorthogonal Bézier function $\tilde{B}_j^N(x)$ (see the previous footnote) followed by an integration over x leads to the desired closure relation

$$\left\langle \tilde{B}_j^N \middle| f \right\rangle = \sum_{i=0}^{N} C_i\left\langle \tilde{B}_j^N \middle| B_i^N \right\rangle = \sum_{i=0}^{N} C_i\delta_{ij} = C_j$$

$$\Rightarrow \quad \left\langle \tilde{B}_j^N \middle| f \right\rangle = \sum_{i=0}^{N}\left\langle \tilde{B}_i^N \middle| f \right\rangle\left\langle \tilde{B}_j^N \middle| B_i^N \right\rangle = \left\langle \tilde{B}_j^N \middle| \left\{\sum_{i=0}^{N} |B_i^N\rangle\langle\tilde{B}_i^N|\right\} \middle| f \right\rangle \quad \Rightarrow \quad \sum_{i=0}^{N} |B_i^N\rangle\langle\tilde{B}_i^N| = 1$$

chapter. Another example is considered in appendix C with C^1 space which give wave functions with continuous gradients. In order to fulfill the continuity criterion $F_j(x) \in C^0$ of the solution from one element to the next, the basis functions in the FEM are constructed in a special way. For the simple linear case we define the elements $F_j(x)$, generated from the Bézier functions of degree 1, in the following way

$$F_j(x) = \begin{cases} \left(x - x_{j-1}\right) \Big/ \left(x_j - x_{j-1}\right) & \text{for} \quad x_{j-1} \le x < x_j \\ \left(x_{j+1} - x\right) \Big/ \left(x_{j+1} - x_j\right) & \text{for} \quad x_j \le x < x_{j+1} \\ 0 & \text{otherwise} \end{cases} \tag{3.2.8}$$

so that we obtain a situation as depicted in figure 6.

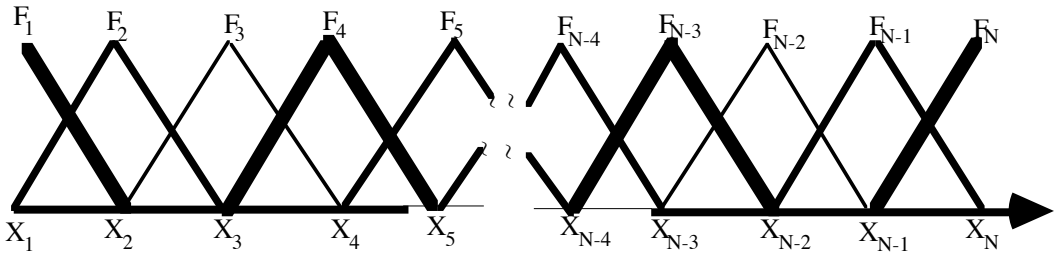

Figure 6 Linear FEM functions

Clearly from figure 6 the basis function $F_j(x)$ only has an overlap with the neighboring functions $F_{j-1}(x)$ (that is if $j \ge 2$) and $F_{j+1}(x)$ (if $j \le N-1$), and we further note that we have as many basis functions $F_j(x)$ as we have grid points. In other words, any general matrix written in this basis-set will be tridiagonal. In appendix C we give an example of another convenient choice of C^1 FEM basis functions, the so-called third degree Hermite type functions, where we have 2 functions per grid-point which effects another but still very simple block structure of general matrices in this basis (see figure C.1). Besides the sparseness of the matrices this is yet another advantage of the FEM; namely, that one can "force" the matrices to have a desired block structure.

As an application of this feature of the FEM we shall now derive a recursive procedure to solve the matrix equation Eq. (2.2.27) derived in the previous chapter. We start by defining the basis functions $u_i(\omega)$ in the expansion Eq. (2.2.14) as a real product basis with the coefficients C_i absorbed into the functions. That is,

$$\Psi(\omega) = \sum_{i=1}^{N} u_i(\omega), \qquad u_i(\omega) = F_i(q) \sum_{j=1}^{M} C_j^i \psi_j^i\left(\omega_q\right) \tag{3.2.9}$$

where $F_i(q)$ are the linear FEM functions defined in Eq. (3.2.8), q is often chosen as the hyper-spherical radius, and $\psi_j^i(\omega_q)$ are *channel wave functions* of the remaining coordinates collectively denoted by ω_q. In this basis-set $\left\{u_i(\omega),\ i = 1,..,N\right\}$, it is evident from the above discussion, and from the fact that only $u_N(\omega)$ has non-zero amplitude on the surface S, that

the matrix equation Eq. (2.2.27) now reduces to

$$\begin{bmatrix} \overline{\overline{A}}_{11} & \overline{\overline{A}}_{12} & \overline{\overline{0}} & \cdots & \overline{0} \\ \overline{\overline{A}}_{21} & \overline{\overline{A}}_{22} & \overline{\overline{A}}_{23} & \overline{\overline{0}} & \overline{0} \\ \overline{\overline{0}} & \overline{\overline{A}}_{32} & \ddots & \overline{\overline{A}}_{N-1N} & \vdots \\ \vdots & \overline{\overline{0}} & \overline{\overline{A}}_{NN-1} & \overline{\overline{A}}_{NN} & \overline{u}_N^*(\omega') \\ \overline{0}^T & \overline{0}^T & \cdots & \overline{u}_N^T(\omega) & -R(\omega,\omega') \end{bmatrix} \begin{bmatrix} \overline{C}_1 \\ \overline{C}_2 \\ \vdots \\ \overline{C}_N \\ 1 \end{bmatrix} = \overline{0}, \quad \omega,\omega' \in S \tag{3.2.10}$$

so that

$$\begin{aligned} &\overline{\overline{A}}_{11}\overline{C}_1 + \overline{\overline{A}}_{12}\overline{C}_2 = \overline{0} \\ &\overline{\overline{A}}_{jj-1}\overline{C}_{j-1} + \overline{\overline{A}}_{jj}\overline{C}_j + \overline{\overline{A}}_{jj+1}\overline{C}_{j+1} = \overline{0}, \quad j = 2,3,..,N-1 \\ &\overline{\overline{A}}_{NN-1}\overline{C}_{N-1} + \overline{\overline{A}}_{NN}\overline{C}_N + \overline{u}_N(\omega') = \overline{0}, \quad \omega' \in S \\ &\overline{u}_N^T(\omega')\overline{C}_N - R(\omega,\omega'), \quad \omega,\omega' \in S \end{aligned} \tag{3.2.11}$$

In the above equations $\overline{\overline{A}}_{ij}$ is a square $M \times M$ matrix, $\overline{u}_N$ and $\overline{C}_i$ are column vector of dimension M and $R(\omega,\omega')$ (from now on denoted R) is a real number (or a one-dimensional matrix). The idea is now to apply a recursive procedure that successively computes $R(\omega,\omega')$ starting at the boundary q_N, and then going inwards to q_1, in such a way that it allow us to judge the possible convergence as more and more functions are included in the domain of small q. From Eq. (3.2.11), we have

$$\begin{aligned} R &= \overline{D}_N^T\overline{C}_N \\ \overline{C}_N &= \overline{\overline{R}}_N\overline{D}_N + \overline{\overline{B}}_{N-1}\overline{C}_{N-1} \end{aligned} \tag{3.2.12}$$

where we have defined

$$\begin{aligned} \overline{D}_N &\equiv \overline{u}_N \\ \overline{\overline{R}}_N &\equiv -\overline{\overline{A}}_{NN}^{-1} \\ \overline{\overline{B}}_{N-1} &\equiv \overline{\overline{R}}_N\overline{\overline{A}}_{NN-1} \end{aligned} \tag{3.2.13}$$

and combining the two expressions in Eq. (3.2.12), we find

$$R = \overline{D}_N^T\overline{\overline{R}}_N\overline{D}_N + \overline{D}_{N-1}^T\overline{C}_{N-1} \tag{3.2.14}$$

where we have defined

$$\overline{D}_{N-1} = \overline{\overline{B}}_{N-1}^T\overline{D}_N \tag{3.2.15}$$

Solving Eq. (3.2.11) for $\overline{C}_{N-1}$ we find

$$\overline{C}_{N-1} = \overline{\overline{R}}_{N-1}\overline{D}_{N-1} + \overline{\overline{B}}_{N-2}\overline{C}_{N-2} \tag{3.2.16}$$

I we define

$$\overline{\overline{R}}_{N-1} = -\left[\overline{\overline{A}}_{N-1N-1} + \overline{\overline{A}}_{N-1N}\overline{\overline{B}}_{N-1}\right]^{-1} \tag{3.2.17}$$

and combining Eq. (3.2.16) and Eq. (3.2.14) we have

$$R = \overline{D}_N^T\overline{\overline{R}}_N\overline{D}_N + \overline{D}_{N-1}^T\overline{\overline{R}}_{N-1}\overline{D}_{N-1} + \overline{D}_{N-2}^T\overline{D}_{N-2} \tag{3.2.18}$$

where

$$\overline{D}_{N-2} = \overline{\overline{B}}_{N-2}^T\overline{D}_{N-1} \tag{3.2.19}$$

We finally conclude with the recursive formula

$$R = \sum_{k=0}^{N-1}\overline{D}_{N-k}^T\overline{\overline{R}}_{N-k}\overline{D}_{N-k} \tag{3.2.20}$$

where

$$\left.\begin{aligned}\overline{D}_k &= \overline{\overline{B}}_k^T\overline{D}_{k+1}\\ \overline{\overline{R}}_k &= -\left[\overline{\overline{A}}_{kk} + \overline{\overline{A}}_{k+1k}^T\overline{\overline{B}}_k\right]^{-1}\\ \overline{\overline{B}}_k &= \overline{\overline{R}}_{k+1}\overline{\overline{A}}_{k+1k}\end{aligned}\right\}, \quad 1 \le k \le N-1 \tag{3.2.21}$$

with the initial expressions for $\overline{\overline{R}}_N$ and $\overline{\overline{D}}_N$ given in Eq. (3.2.13). The amplitudes now read as

$$\begin{aligned}\overline{C}_1 &= \overline{\overline{R}}_1\overline{D}_1\\ \overline{C}_k &= \overline{\overline{R}}_k\overline{D}_k + \overline{\overline{B}}_{k-1}\overline{C}_{k-1}, \quad 2 \le k \le N\end{aligned} \tag{3.2.22}$$

This recursive formula causes the amplitude of the scattering wave function to be *propagated* from q_1 to the boundary q_N .

3.3 The discrete variable representation

Grid methods have been applied to quantum mechanical problems for many years, but the discrete variable representation (DVR) method is actually relatively new, and has proven to be a powerful (and sophisticated) approach to the solution of numerical problems, in terms of obtaining accurate matrix elements within a minimal basis-set. To put this method into an appropriate historical perspective, we will briefly examine some of the more important stages in its development.

Pointwise representations were first introduced by Hartree [51] and Hylleraas [35] in the late twenties under the name finite difference methods (FD). Here the Euler equation (i.e., the Schrödinger equation or a variational functional) is discretized on a grid. In this representation

$$\left[\overline{\overline{T}} + \overline{\overline{W}}^{G} - E\overline{\overline{I}}\right]\overline{\Psi} = \overline{0} \tag{3.3.1}$$

$\overline{\Psi}$ is a vector of the amplitudes on the grid, the potential is represented by a diagonal matrix with elements corresponding to the values of $\mathbf{W}$ in the grid points (denoted by the label G) and the kinetic energy term $\overline{\overline{T}}$ is a sparse matrix obtained from a Taylor series expansion of the derivative on the grid (see appendix D[37]). Before the emerge of real super computers in the eighties and massively parallel computers in the nineties the FD method had not really proved advantageous in more than two dimensions since a very large number of grid points was necessary to obtain an accurate representation of the kinetic energy term through the FD scheme. This problem of representing $\mathbf{T}$ in an accurate way (with the limited core memory available) was more or less overcome with the introduction of the *collocation* or *Pseudo-Spectral methods* in the early eighties. This method takes point of reference in a finite basis representation (FBR) $\{u_i(x)\}$, generally chosen as eigenstates (or close to) of the kinetic energy operator, such that matrix elements $\langle u_m|\mathbf{T}|u_n\rangle$ in the equation

$$\mathbf{T}u_n(x) = \sum_m \langle u_m|\mathbf{T}|u_n\rangle u_m(x) \tag{3.3.2}$$

(assuming an orthonormal basis) are known. As in the FD method, the Euler equation is discretized on a grid $\{x_p, \quad p = 1,...,N\}$ to give a very easy handling of the local potential term (as opposed to the non-local $\mathbf{T}$).

$$\sum_n C_n \left[\sum_m \left\{\langle u_m|\mathbf{T}|u_n\rangle u_m(x_p)\right\} + \left\{W(x_p) - E\right\}u_n(x_p)\right] = 0, \quad p = 1,...,N \tag{3.3.3}$$

If we now define the collocation matrix $\overline{\overline{R}}_{pn} \equiv u_n(x_p)$, Eq. (3.3.3), can be written in the matrix notation

$$\left[\overline{\overline{R}}\,\overline{\overline{T}} + \left(\overline{\overline{W}}^{G} - E\overline{\overline{I}}\right)\overline{\overline{R}}\right]\overline{C} = \overline{0} \tag{3.3.4}$$

Inserting the unit matrix $\overline{\overline{R}}^{-1}\overline{\overline{R}}$ between the square bracket and $\overline{C}$, and noting that $\overline{\Psi} \equiv \left[\Psi(x_p)\right] = \overline{\overline{R}}\,\overline{C}$, we obtain the relation between the FD and the collocation method

$$\left[\overline{\overline{R}}\,\overline{\overline{T}}\,\overline{\overline{R}}^{-1} + \overline{\overline{W}}^{G} - E\overline{\overline{I}}\right]\overline{\Psi} = \overline{0} \tag{3.3.5}$$

Multiplying Eq. (3.3.4) by $\overline{\overline{R}}^{-1}$ from the left we arrive at the expression

$$\left[\overline{\overline{T}} + \overline{\overline{R}}^{-1}\overline{\overline{W}}^{G}\overline{\overline{R}} - E\overline{\overline{I}}\right]\overline{C} = \overline{0} \tag{3.3.6}$$

---

37 This appendix D is really only included since I found some errors in the original lecture notes by Claude Leforestier handed out during the 4'th Topsøe Summer School. In other words, we shall not use this method on the H_2^+ problem.

which shows that in the FBR associated with the collocation method the potential term reads as

$$\langle u_n | \mathbf{W} | u_m \rangle = \left[\overline{\overline{R}}^{-1} \overline{\overline{W}}^{G} \overline{\overline{R}} \right]_{nm} \tag{3.3.7}$$

and hence, for an ill-conditioned collocation matrix (i.e. $\overline{\overline{R}}$ close to singular), corresponding to a poor choice of basis-set and grid, the potential is not accurately represented. To overcome this problem "routinely" we have to switch to DVR where the *Gauss quadrature theorem* prescribes a way to obtain an optimum choice of grid points and basis-set. So as a prelude to the introduction of DVR we will briefly present this Gauss quadrature theorem.

The idea of Gauss quadrature is to discretize an integral through the approximation

$$\int_a^b dx W(x) f(x) \approx \sum_{i=1}^{N} \omega_i f(x_i) \tag{3.3.8}$$

where $f(x)$ is an arbitrary function, $W(x)$ is a known weighting function, ω_i are the weights of the quadrature scheme, and x_i are referred to as the abscissas. The fundamental theorem of Gauss quadrature now reads: if we choose the abscissas in the N-point quadrature formula Eq. (3.3.8) as the N roots $\{x_i, i = 1,...,N\}$ of the polynomial $P_N(x)$ of degree N orthogonal over the interval $[a;b]$ with the weighting function $W(x)$, meaning $P_N(x) \in \{P_m(x), 0 \le m \le \infty\}$ where

$$\int_a^b dx P_n(x) W(x) P_m = N_n \delta_{nm} \tag{3.3.9}$$

and where N_n is a normalization constant, and if we choose the N weights ω_i as solutions to the set of linear equations[38]

$$\begin{bmatrix} P_0(x_1) & P_0(x_2) & \cdots & P_0(x_N) \\ P_1(x_1) & P_1(x_2) & \cdots & P_1(x_N) \\ \vdots & \vdots & \ddots & \vdots \\ P_{N-1}(x_1) & P_{N-1}(x_2) & \cdots & P_{N-1}(x_N) \end{bmatrix} \begin{bmatrix} \omega_1 \\ \omega_2 \\ \vdots \\ \omega_N \end{bmatrix} = \begin{bmatrix} N_0/P_0 \\ 0 \\ \vdots \\ 0 \end{bmatrix} \tag{3.3.10}$$

then *the Gauss quadrature formula Eq. (3.3.8) is exact if the function $f(x)$ can be expressed as a polynomial of degree $\le 2N - 1$.* In order to use this result in the DVR method, we define a set of *orthonormal* functions[39]

---

38 This set of linear equations simply ensures that Eq. (3.3.8) is correct if the function $f(x)$ can be expressed as a polynomial of degree $\le N - 1$, since Eq. (3.3.9) with a polynomial of degree zero (i.e. a constant) gives

$$\int_a^b dx P_n(x) W(x) P_0(x) = P_0 \int_a^b dx P_n(x) W(x) = P_0 \sum_{i=1}^{N} \omega_i P_n(x_i) = N_0 \delta_{no}, \quad n = 0,1,...N-1$$

39 Note that these functions $u_n(x)$ are not generally polynomials due to the weighting function $W(x)$ in Eq. (3.3.11).

$$\begin{aligned} u_n(x) &\equiv \sqrt{W(x)}\,\overline{P}_n(x) \\ \overline{P}_n(x) &\equiv P_n(x)\ \sqrt{N_n} \end{aligned} \tag{3.3.11}$$

so that for an arbitrary function $g(x)$ can be approximated as

$$\langle u_n|g|u_m\rangle = \int_a^b dx\, u_n(x)g(x)u_m(x) \approx \sum_{i=1}^{N} \omega_i \overline{P}_n(x_i)g(x_i)\overline{P}_m(x_i) \tag{3.3.12}$$

where we have used Eq. (3.3.8) with $f(x) = \overline{P}_n(x)g(x)\overline{P}_m(x)$ and ignored any error-terms[40]. We now introduce the new weights Ω_i defined as

$$\Omega_i \equiv \omega_i / W(x_i) \tag{3.3.13}$$

such that Eq. (3.3.12) has the convenient form

$$\langle u_n|g|u_m\rangle \approx \sum_{i=1}^{N} \Omega_i u_n(x_i)g(x_i)u_m(x_i) \tag{3.3.14}$$

Setting $g(x) = 1$ in Eq. (3.3.14) and introducing the collocation matrix $\overline{\overline{R}}_{in} \equiv u_n(x_i)$ gives the matrix relation[41]

$$\overline{\overline{R}}^{+}\,\overline{\overline{\Omega}}\,\overline{\overline{R}} = \overline{\overline{1}} \tag{3.3.15}$$

where $\overline{\overline{\Omega}}$ is defined as a diagonal matrix with the values given in Eq. (3.3.13). From Eq. (3.3.15) it now follows that[42]

$$\langle u_n|g|u_m\rangle = \left[\overline{\overline{R}}^{+}\,\overline{\overline{\Omega}}\,\overline{\overline{g}}^{G}\,\overline{\overline{R}}\right]_{nm} = \left[\overline{\overline{R}}^{-1}\,\overline{\overline{g}}^{G}\,\overline{\overline{R}}\right]_{nm} \tag{3.3.16}$$

---

40 For a N-point gaussian-like quadrature scheme we generally have [52]

$$\int_a^b dx\{f(x)\} = A\sum_{p=1}^{N} \omega_p f(x_p) + B\frac{d^{2N}}{dx^{2N}}[f(x)], \quad a < x < b$$

where A and B are constants. When applying this integration formula to Eq. (3.3.12) and Eq. (3.3.14), where $f(x) = u_n(x)g(x)u_m(x)$, we would expect the largest error to enter the N-point DVR scheme when the degree of $f(x)$ reaches a maximum value, i.e. when $n = m = N-1$. Hence the leading error-term, R, is given by

$$\begin{aligned} R \propto \frac{d^{2N}}{dx^{2N}}\left[u_{N-1}^2(x)g(x)\right] &= g(x)\frac{d^{2N}}{dx^{2N}}\left[u_{N-1}^2(x)\right] + g'(x)\frac{d^{2N-1}}{dx^{2N-1}}\left[u_{N-1}^2(x)\right] \\ + g''(x)\frac{d^{2N-2}}{dx^{2N-2}}\left[u_{N-1}^2(x)\right] + \ldots\ldots &\propto g''(x) + \ldots\ldots, \quad a < x < b \end{aligned}$$

After this somewhat shallow analysis we conclude that *the leading error-term in a N-point DVR scheme is proportional to the second derivative of the function.*

41 $$\delta_{nm} = \sum_{i=1}^{N} \overline{\overline{R}}_{in}\Omega_i\overline{\overline{R}}_{im} = \sum_{i,j=1}^{N} \overline{\overline{R}}^{+}_{ni}\Omega_i\delta_{ij}\overline{\overline{R}}_{jm} \equiv \left[\overline{\overline{R}}^{+}\,\overline{\overline{\Omega}}\,\overline{\overline{R}}\right]_{nm}$$

42 As noted before the label "G" added to a matrix representation of a function, $f(x)$, indicates that the matrix is diagonal with the elements equal to values of $f(x)$ in the discrete grid points - that is

$$\left[\overline{\overline{f}}^{G}\right]_{pq} \equiv \delta_{pq} f(x_p)$$

which does not depend explicitly on the weights ω_i. However, we will have to invert the collocation matrix $\overline{\overline{R}}$ in this formulation and so instead we define the *unitary* matrix $\overline{\overline{U}}$ as

$$\overline{\overline{U}}_{in} \equiv \sqrt{\Omega_i}\,\overline{\overline{R}}_{in} \quad \Rightarrow \quad \overline{\overline{U}} = \overline{\overline{\Omega}}^{1/2}\overline{\overline{R}} \tag{3.3.17}$$

such that Eq. (3.3.15) simply reads as

$$\overline{\overline{U}}^{+}\overline{\overline{U}} = \bar{\bar{1}} \tag{3.3.18}$$

Eq. (3.3.16) now reduces to the very important relation

$$\langle u_n|g|u_m\rangle = \left[\overline{\overline{U}}^{+}\overline{\overline{g}}^{G}\overline{\overline{U}}\right]_{nm} = \sum_p U^*_{pn}U_{pm}g(x_p) \tag{3.3.19}$$

From the orthonormal basis-set $\{u_n(x)\}$ we can now define another *orthonormal* basis-set $\{X_p(x)\}$ by the unitary transformation

$$X_p(x) \equiv \sum_{n=1}^{N}\overline{\overline{U}}^{*}_{pn}u_n(x) \quad \Leftrightarrow \quad u_n(x) = \sum_{p=1}^{N}\overline{\overline{U}}_{pn}X_p(x) \tag{3.3.20}$$

such that

$$\langle X_p|g|X_q\rangle = \left[\overline{\overline{U}}\,\overline{\overline{U}}^{+}\overline{\overline{g}}^{G}\overline{\overline{U}}\,\overline{\overline{U}}^{+}\right]_{pq} = \left[\overline{\overline{g}}^{G}\right]_{pq} = g(x_p)\delta_{pq} \tag{3.3.21}$$

Now we are finally in the position to define the overall DVR scheme. First we choose the orthonormal basis-set $\{u_n(x),\, n = 1,..,N\}$ (see Eq. (3.3.11)) either as eigenstates of the kinetic energy operator, or at least as a set of basis functions that enables us to determine the matrix elements $\langle u_n|\mathbf{T}|u_m\rangle$. In chapter 5 we shall see how this is done in practice using the characteristic recurrence relations for the derivative of the orthogonal polynomials. This set of N functions then determines a Gauss quadrature scheme as discussed above, defining the weights ω_i and the collocation matrix $\overline{\overline{R}}$. We then use the definition in Eq. (3.3.17) to give us the unitary matrix $\overline{\overline{U}}$, which in turn defines the orthonormal basis-set $\{X_p(x),\, p = 1,..,N\}$. The wave function in the FBR $\{u_n(x),\, n = 1,..,N\}$ reads as

$$\Psi(x) = \sum_{n=1}^{N}C_n u_n(x) \tag{3.3.22}$$

and, inserting Eq. (3.3.20) and Eq. (3.3.17) into Eq. (3.3.22) we obtain the expression for $\Psi(x)$ in the $\{X_p(x),\, p = 1,..,N\}$ basis-set[43]

---

43 $$\Psi(x) = \sum_{n=1}^{N}C_n\sum_{p=1}^{N}\overline{\overline{U}}_{pn}X_p(x) = \sum_{p=1}^{N}\sqrt{\Omega_p}\left\{\sum_{n=1}^{N}C_n\overline{\overline{R}}_{pn}\right\}X_p(x) = \sum_{p=1}^{N}\sqrt{\Omega_p}\left\{\sum_{n=1}^{N}C_n u_n(x_p)\right\}X_p(x) = \sum_{p=1}^{N}\sqrt{\Omega_p}\Psi(x_p)X_p(x)$$

$$\Psi(x) = \sum_{p=1}^{N} \sqrt{\Omega_p}\,\Psi(x_p)X_p(x) \tag{3.3.23}$$

This is clearly a *discrete variable representation* of the function $\Psi(x)$. In other words, there exists an isomorphism (due to the unitary matrix $\overline{\overline{U}}$) between the finite basis representation (FBR) of $\Psi(x)$ in $\{u_n(x),\ n = 1,..,N\}$ and a discrete variable representation (DVR) of $\Psi(x)$ in $\{X_p(x),\ p = 1,..,N\}$. Setting the variable x equal to one of the N grid points (abscissas) x_q in Eq. (3.3.23) results in

$$\Psi(x_q) = \sum_{p=1}^{N} \sqrt{\Omega_p}\,\Psi(x_p)X_p(x_q) \tag{3.3.24}$$

Now noting that the expansion coefficients $\Psi(x_p)$ in Eq. (3.3.23) are linearly independent, we arrive at the important result

$$X_p(x_q) = \Omega_p^{-1/2}\delta_{pq} \tag{3.3.25}$$

which simply tells that the basis function $X_p(x)$ in the set $\{X_p(x),\ p = 1,..,N\}$, defining the DVR scheme, has the property of being zero at every grid point different from x_p. It can further be shown that

$$X_p(x) << \Omega_p^{-1/2}\delta_{pq} \quad \text{for} \quad x \in [x_1; x_{p-1}] \cup [x_{p+1}; x_N] \tag{3.3.26}$$

such that these basis functions $X_p(x)$ have a "delta-function-like" property at the quadrature points. In other words, the underlying DVR basis discretizes the coordinate space in "much the same way" as the FEM does. Because of this oscillatory behavior of the basis functions $X_p(x)$, with nodes at the grid points, the DVR scheme can give very poor results if the function represented through the DVR, Eq. (3.3.23), has an oscillatory behavior close to that of the basis-set $\{X_p(x),\ p = 1,..,N\}$[44] . With this in mind, we should stress that adding more grid points (i.e. enlarging the basis-set) is strictly speaking not always tantamount to obtaining greater accuracy in the DVR scheme[45] - although this may be a mere mathematical curiosity, as such situations, according to my own experience, are extremely rare in practice.

Although the one dimensional DVR just discussed is useful, the use of direct product DVR for multi-dimensional problems is much more advantageous. There are four possible

---

44 As a sample "worst-case example", consider the function

$$\Psi(x) \propto \prod_{p=1}^{N} (x - x_p)$$

having nodes exactly at the grid points. A discrete variable representation of this function will be very poor since using Eq. (3.3.24) simply give us a zero-function.

45 Press *et al*. [53], in the introduction to quadrature methods, make the same point, provocatively, by asserting that "it can not be overemphasized that high order is not the same as high accuracy. High order translates to high accuracy only when the integrand is very smooth, in the sense of being well-approximated by a polynomial."

reasons for this. First, the Hamiltonian matrix in the multi-dimensional DVR is very easy to construct as we shall see in chapter 5. Second, for a DVR in an orthonormal coordinate system, the Hamiltonian is sparse. Third, the DVR handles singular terms (e.g. $1/\vec{r}$ in the potential) in a very efficient way (i.e. analytical) by choosing the ad hoc FBR, as opposed to the FEM where one has to be more careful (i.e. put certain elements to zero). Fourth, the multi-dimensional DVR scheme easily allows for *preconditioning* and hence truncation of the product basis in the different dimensions to give a very compact overall basis-set. To illustrate this preconditioning, consider a two-dimensional Hamiltonian

$$\mathbf{H}(\xi,\eta) = \mathbf{H}_0(\xi,\eta) + \mathbf{W}(\xi,\eta) \tag{3.3.27}$$

where $\mathbf{H}_0(\xi,\eta)$ is the zero order Hamiltonian, assumed at first not to be separable in the two variables. Let there be given two ad hoc FBR basis-sets $\{L_i(\xi)\}$ and $\{P_i(\eta)\}$ and the associated sets of DVR grid points $\{\xi_i\}$ and $\{\eta_i\}$. Now fix the variable η, in the zero order Hamiltonian, one by one to the different grid points η_p and solve the corresponding eigenvalue equation

$$\mathbf{H}_0(\xi,\eta_p)Y_q^p(\xi) = \varepsilon_q^p Y_q^p(\xi) \tag{3.3.28}$$

followed by a truncation of the expansion

$$Y_q^p(\xi) = \sum_i C_{iq}^p L_i(\xi) \tag{3.3.29}$$

In an analogous way we can construct the truncated zero order basis functions $N_p^q(\eta)$ in the basis $\{P_i(\eta)\}$. The full two-dimensional problem now reads as

$$\mathbf{H}(\xi,\eta)\Psi(\xi,\eta) = E\Psi(\xi,\eta) \tag{3.3.30}$$

where

$$\Psi(\xi,\eta) = \sum_{pq} C_{pq} Y_q^p(\xi) N_p^q(\eta) \tag{3.3.31}$$

The resulting product basis-set $\{N_p^q(\eta)Y_q^p(\eta)\}$, in which the zero order Hamiltonian is close to diagonal, is compact as compared to the direct product basis-set $\{L_i(\xi)P_j(\eta)\}$ used in the expansion

$$\Psi(\xi,\eta) = \sum_{ij} C'_{ij} L_i(\xi) P_j(\eta) \tag{3.3.32}$$

The price for this convenient compact basis-set on the other hand is the time consuming truncations in every grid point, a step that is inevitable unless the zero order Hamiltonian is separable in the different coordinates, which, as we shall see in chapter 5, is the case for the zero order Hamiltonian for H_2^+. Then the zero order compact basis-set is simply constructed

as the truncated eigenfunctions of the different components of the zero order Hamiltonian, giving a product basis-set in which $\mathbf{H}_0(\xi,\eta)$ is diagonal. Nevertheless, we stress this feature of the DVR scheme, and note that, in multi-dimensional finite element methods, we do not have this type of preconditioning to obtain a compact basis-set.

4 Translation and rotation in quantum mechanics

4.1 Introduction

In this chapter we are going to present some important results from the theory of translations and rotations in quantum mechanics, that will enable us to reduce the nine dimensional scattering problem, of the three particle system H_2^+, in the laboratory-fixed frame of reference to a three dimensional problem in a body-fixed frame of reference. This separation of 3 translational and 3 rotational coordinates from the wave function, is described in the standard way [4], and the results and methods outlined will then be applied to the variational R-matrix functional in chapter 5. Further we shall mention some coupling relations for the so-called rotational matrix elements, to be defined, that will help us to derive the expression for the dipole transition moment for H_2^+ in the body-fixed frame of reference, chapter 5 section 9.

As a prelude to the separation of the translational and rotational coordinates we will briefly discuss the constants of motion that will be used to label, and hence characterize, the wave function. These quantum numbers describe the eigenstates of a set of observables which constitute a complete set of commuting observables for the physical system. The latter concept is defined as a set of physical observables which all commute with one another and for which there is only one simultaneous eigenstate belonging to any set of eigenvalues. From the homogeneity and isotropy assumed for space, one induces the symmetries of spatial displacements (translations) and rotations; that is, one assumes that space is Euclidean and three-dimensional, having the isometry group, E(3), of rotations and translations. As we will demonstrate in section two and three, the generators of translations and rotations are respectively the linear momentum operator and angular momentum operator. Noting that a symmetry operator, by definition, is an operator that commutes with the Hamiltonian operator, we then conclude that in the absence of external fields a complete set of commuting observables consists of the operators

$$\left\{\mathbf{H}, \mathbf{J}^2, \mathbf{J}_3, \vec{\mathbf{P}}\right\} \tag{4.1.1}$$

where $\mathbf{H}$ is the usual total non relativistic Hamiltonian, $\mathbf{J}^2$ is the square of the total angular momentum (excluding spin), $\mathbf{J}_3$ is the third component of $\vec{\mathbf{J}}$ and $\vec{\mathbf{P}}$ collectively denotes the three components of the total linear momentum. Correspondingly we have a set of six real quantum numbers

$$\left\{E, J, m, \vec{k}\right\} \tag{4.1.2}$$

so that we can label the wave function as

$$\Psi_{Jm\vec{k}}(\omega) \tag{4.1.3}$$

where

$$\begin{aligned}
\mathbf{J}^2\Psi_{Jm\vec{k}}(\omega) &= \hbar^2 J(J+1)\Psi_{Jm\vec{k}}(\omega) \\
\mathbf{J}_3\Psi_{Jm\vec{k}}(\omega) &= \hbar m\Psi_{Jm\vec{k}}(\omega) \\
\vec{\mathbf{P}}\Psi_{Jm\vec{k}}(\omega) &= \vec{k}\Psi_{Jm\vec{k}}(\omega)
\end{aligned} \tag{4.1.4}$$

ignoring the total energy E as a constant of motion, since it will be fixed in our scattering calculations. The first step is now to separate out the label $\vec{k}$.

4.2 Translational invariance

The description of the action of translational operators on wave functions in quantum mechanic is actually quite easy, as compared to the problem of characterizing rotations. The reason for this is that three dimensional translations, by virtue of the homogeneity of space, form an abelian[46] group. For physics, the translation generator is the (Hermitian) linear momentum operator $\vec{\mathbf{P}}$, and the associated operator $\boldsymbol{P}(\vec{a})$ generating finite displacements is realized by

$$\boldsymbol{P}(\vec{a}) = \exp\left(-i\vec{a}\cdot\vec{\mathbf{P}}/\hbar\right) \tag{4.2.1}$$

This operator can be shown to displace the system be the vector $\vec{a}$. Consider the action of $\boldsymbol{P}(\vec{a})$ on the function $\varphi(\vec{r})$. Using the power series for the exponential and assuming that the derivatives of $\varphi(\vec{r})$ exist we find

$$\begin{aligned}
\boldsymbol{P}(\vec{a})\varphi(\vec{r}) &= \sum_{n=0}^{\infty}\frac{1}{n!}\left(-\frac{i}{\hbar}\vec{a}\cdot\vec{\mathbf{P}}\right)^n\varphi(\vec{r}) \\
&= \sum_{n=0}^{\infty}\frac{1}{n!}\left(-\vec{a}\cdot\vec{\nabla}\right)^n\varphi(\vec{r}) = \varphi(\vec{r}-\vec{a})
\end{aligned} \tag{4.2.2}$$

where we have used $\vec{\mathbf{P}} \equiv -i\hbar\vec{\nabla}$ and the Taylor series for $\varphi(\vec{r}-\vec{a})$. The commutativity of translations ($\boldsymbol{P}(\vec{a})\boldsymbol{P}(\vec{b}) = \boldsymbol{P}(\vec{b})\boldsymbol{P}(\vec{a}) = \boldsymbol{P}(\vec{a}+\vec{b})$) is vectorially realized as the well known parallelogram law. Further we note that if $\varphi_{\vec{k}}(\vec{r})$ is assumed to be an eigenstate of the linear momentum $\vec{\mathbf{P}}$, we can insert Eq. (4.1.4) into Eq. (4.2.2) to give

$$\boldsymbol{P}(\vec{a})\varphi_{\vec{k}}(\vec{r}) = \exp\left(-i\vec{a}\cdot\vec{k}/\hbar\right)\varphi_{\vec{k}}(\vec{r}) = \varphi_{\vec{k}}(\vec{r}-\vec{a}) \tag{4.2.3}$$

and setting $\vec{k} = \vec{0}$ we find the elementary, but fundamental relation

---

46 A group where all elements commute with one another.

$$\varphi_{\vec{0}}(\vec{r}-\vec{a}) = \varphi_{\vec{0}}(\vec{r}) \tag{4.2.4}$$

which simply tells that an eigenstate of $\vec{\mathbf{P}}$ with zero linear momentum is translationally invariant. Clearly $\exp(i\vec{k}\cdot\vec{r}/\hbar)$ is an eigenstate of $\vec{\mathbf{P}}$, with linear momentum $\vec{k}$, and hence we can factor an arbitrary eigenstate of $\vec{\mathbf{P}}$ into a product of the latter times a translational invariant function.

$$\varphi_{\vec{k}}(\vec{r}) = \exp\left(i\vec{k}\cdot\vec{r}/\hbar\right)\varphi_{\vec{0}}(\vec{r}) \tag{4.2.5}$$

We now return to the problem of an N particle system, where $\vec{\mathbf{P}}$ reads as

$$\vec{\mathbf{P}} = -i\hbar\sum_{i=1}^{N}\vec{\nabla}_i \tag{4.2.6}$$

and where an eigenstate of $\vec{\mathbf{P}}$ is a function of the coordinate set $\left\{\vec{R}_1,\vec{R}_2,.....,\vec{R}_N\right\}$

$$\Psi_{\vec{k}}\left(\vec{R}_1,\vec{R}_2,.....,\vec{R}_N\right) \tag{4.2.7}$$

In order to separate out a set of translational coordinates, we perform a linear transformation on the laboratory-fixed coordinates to a set of coordinates, $\{\vec{r}_1,\vec{r}_2,.....,\vec{r}_N\}$, that we shall refer to as the space-fixed coordinates. This linear transformation of the N-dimensional vector space (R^{3N}) into itself, is represented by the $N\times N$ matrix $\overline{\overline{V}}$

$$\left[\vec{r}_1,\vec{r}_2,....,\vec{r}_N\right] = \left[\vec{R}_1,\vec{R}_2,.....,\vec{R}_N\right]\overline{\overline{V}} \tag{4.2.8}$$

where $\det\overline{\overline{V}} \neq 0$ ($\overline{\overline{V}}^{-1}$ should exist), and where the i'th column in $\overline{\overline{V}}$ contains the coefficients for the linear combination of the space-fixed vector $\vec{r}_i$ in the set of laboratory-fixed vectors $\{\vec{R}_1,\vec{R}_2,.....,\vec{R}_N\}$. We now seek a matrix $\overline{\overline{V}}$ that will construct as many translational invariant space-fixed vectors (hence the name) as possible, i.e. *as many as possible of the columns of* $\overline{\overline{V}}$ *should have vanishing sum*. Clearly if all the vectors $\{\vec{r}_1,\vec{r}_2,.....,\vec{r}_N\}$ are translational invariant, the determinant of $\overline{\overline{V}}$ vanishes[47] and hence we do not have a linear transformation. In other words this choice of $\overline{\overline{V}}$ results in a set of linearly dependent vectors, which is not desirable. If we instead construct $\overline{\overline{V}}$ such that the sum of the elements in only the first N-1 columns vanish, corresponding to the set $\{\vec{r}_1,\vec{r}_2,.....,\vec{r}_{N-1}\}$ being translational invariant, then $\det\overline{\overline{V}} \neq 0$. The translational vector $\vec{r}_N$ is now denoted $\vec{R}_0$. The point is now that in these coordinates the total linear momentum in Eq. (4.2.6) takes the simple form

$$\vec{\mathbf{P}} = -i\hbar\sum_{i=1}^{N}\sum_{j=1}^{N}\frac{\partial\vec{r}_i}{\partial\vec{R}_j}\frac{\partial}{\partial\vec{r}_i} = -i\hbar\sum_{i=1}^{N}\frac{\partial}{\partial\vec{r}_i}\sum_{j=1}^{N}\overline{\overline{V}}_{ij} = -i\hbar\frac{\partial}{\partial\vec{r}_N} \equiv -i\hbar\vec{\nabla}_{R_0} \tag{4.2.9}$$

where we have used the chain rule and the fact that $\left\{\vec{r}_1,\vec{r}_2,.....,\vec{r}_{N-1}\right\}$ is chosen to be

---

47 By N-1 simple row additions we can bring $\overline{\overline{V}}$ into a matrix with a zero-row (i.e. $\det\left(\overline{\overline{V}}\right) = 0$)

translationally invariant[48]. Hence an eigenstate of $\vec{\mathbf{P}}$ as given in Eq. (4.2.7) can be expressed as $\exp(i\vec{k}\cdot\vec{R}_0/\hbar)$ times an eigenstate of $\vec{\mathbf{P}}$ with $\vec{k}=\vec{0}$ only depending on the translational invariant coordinates (in agreement with Eq. (4.2.4)).

$$\Psi'_{\vec{k}}\left(\vec{R}_1,\vec{R}_2,....,\vec{R}_N\right)=\Psi_{\vec{k}}\left(\vec{r}_1,\vec{r}_2,....,\vec{r}_{N-1},\vec{R}_0\right)=\exp\left(-i\vec{k}\cdot\vec{R}_0/\hbar\right)\Psi_{\vec{0}}\left(\vec{r}_1,\vec{r}_2,....,\vec{r}_{N-1}\right) \qquad (4.2.10)$$

The kinetic energy term depending on the coordinate $\vec{R}_0$ in the Hamiltonian gives a constant when acting on Eq. (4.2.10), and hence this term is insignificant. Consequently we simply eliminate the translational coordinate $\vec{R}_0$ corresponding to the invariant case $\vec{k}=\vec{0}$ where the energy of the system refers to a space-fixed frame of reference ($\vec{R}_0=\vec{0}$).

The explicit linear transformation from laboratory-fixed to space-fixed coordinates can be performed in a number of different ways as discussed in chapter 1, and in the next chapter we will give an example for the H_2^+-system. In appendix A we have presented a very convenient choice of the $N\times N$ matrix $\overline{\overline{V}}$, where the first N-1 coordinates are defined as mass-weighted Jacobi coordinates and $\vec{R}_0$ is defined as the center-of-mass coordinates. This matrix $\overline{\overline{V}}$ further has the nice property that $|\det\overline{\overline{V}}|=1$ (by virtue of the "orthogonal construction"), and hence this transformation does not introduce any additional factors in the volume element (see appendix E) in the variational functional. In this case we simply eliminate the center-of-mass coordinates to obtain the translational invariant formulation. Since $\vec{k}$ is now fixed to $\vec{0}$ we shall not use this quantum number in the labeling of the wave function any more.

4.3 Rotational invariance

The results obtained in the previous section for translations were all "thoroughly familiar", but when it comes to rotations we lack a primitive model - the rotational analogous to vectors - capable of making the rotational structure intuitive obvious. The theory of rotations in quantum physics is closely related to the theory of angular momentum, just as the linear momentum was central in the discussion of translations, but in contrast to the latter the characterization of rotations is less simple and involves an extensive use of group theoretical arguments. Hence we shall just outline some of the most important aspects of this theory, and present a number of relations that will be useful in the description of the H_2^+ system in a body-fixed frame of reference.

We start with the relatively simple matrix representation of the group of three-dimensional pure rotations R(3) by 3×3 real, proper, orthogonal matrices $\overline{\overline{R}}\in SO(3)$, but before we do this we shall first parametrize the group of rotations. The "simplest" parametrization of a rotation is of course through a vector and an angle characterizing the direction and angle of the rotation, but throughout this thesis we are going to use the more practical Euler angles α,β and γ. Geometrically, the Euler angles are described by a

48 The coordinates $\left\{\vec{r}_1,\vec{r}_2,.....,\vec{r}_{N-1}\right\}$ are chosen as translationally invariant i.e. $\sum_{i=1}^{N}\overline{\overline{V}}_{ij}=0$ for $1\le j\le N-1$.

sequence of three rotations of vectors, which we now describe in terms of a fixed frame $(\vec{e}_1,\vec{e}_2,\vec{e}_3)$ (the space-fixed frame) and a frame $(\vec{f}_1,\vec{f}_2,\vec{f}_3)$ (the body-fixed frame) resulting from the rotation, see figure 7 [54].

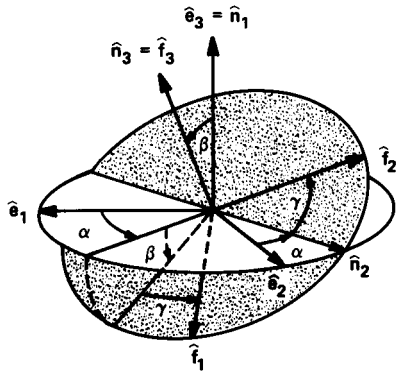

Figure 7 Definition of Euler angles

First we rotate the angle α about $\vec{e}_3$, then β about the *new* y-axis $\vec{n}_2 = (-\sin\alpha, \cos\alpha, 0)$ and finally we rotate the angle γ about the *new* z-axis $\vec{n}_3 = \vec{f}_3 = (\cos\alpha\sin\beta, \sin\alpha\sin\beta, \cos\beta)$. Alternatively we can describe the three Euler angles in terms of a sequence of three other rotations, where we first rotate the angle γ about $\vec{e}_3$, then β about $\vec{e}_2$ and finally α about $\vec{e}_3$. The two definitions are equal as they describe the same overall rotation. In terms of a column-vector notation, a matrix representation of the overall rotation now reads as

$$\vec{x} \rightarrow \vec{x}' = \overline{\overline{R}}(\alpha,\beta,\gamma)\cdot\vec{x} \tag{4.3.1}$$

or equally

$$x_i' \equiv \sum_{j=1}^{3} \overline{\overline{R}}_{ij}(\alpha,\beta,\gamma)x_j \tag{4.3.2}$$

where

$$\overline{\overline{R}}(\alpha,\beta,\gamma) = \begin{bmatrix} \cos\alpha & -\sin\alpha & 0 \\ \sin\alpha & \cos\alpha & 0 \\ 0 & 0 & 1 \end{bmatrix} \cdot \begin{bmatrix} \cos\beta & 0 & \sin\beta \\ 0 & 1 & 0 \\ -\sin\beta & 0 & \cos\beta \end{bmatrix} \cdot \begin{bmatrix} \cos\gamma & -\sin\gamma & 0 \\ \sin\gamma & \cos\gamma & 0 \\ 0 & 0 & 1 \end{bmatrix} \tag{4.3.3}$$

which in the domain of definition for the Euler angles

$$0 \le \alpha < 2\pi \quad 0 \le \beta \le \pi \quad 0 \le \gamma < 2\pi \tag{4.3.4}$$

enumerate all elements of SO(3) exactly[49] once. We further note that

---

49 This is not strictly true (for $\beta = 0$ or $\beta = \pi$), but in order to use a convenient notation we shall ignore this. Actually

$$\overline{\overline{R}}(2\pi-\gamma,\pi-\beta,2\pi-\alpha)=\overline{\overline{R}}^{T}(\alpha,\beta,\gamma)=\overline{\overline{R}}^{-1}(\alpha,\beta,\gamma) \tag{4.3.5}$$

where the last identity follows from the fact that $\overline{\overline{R}}(\alpha,\beta,\gamma)\in SO(3)$ i.e. $\overline{\overline{R}}(\alpha,\beta,\gamma)$ is orthogonal.

One can now show, via the so-called Cartan mapping [54], that there exist a two-fold homomorphism[50] between the group SU(2) of 2×2 unitary unimodular matrices $\overline{u}$ (i.e. $\overline{u}^{+}\overline{u}=\overline{\overline{I}}$ and $\det\overline{u}=1$) and the group SO(3), that we have just "shown" to form a representation of the group R(3) of three-dimensional rotations. In Euler angles $\overline{u}(\alpha,\beta,\gamma)$ reads as

$$\overline{u}(\alpha,\beta,\gamma)=\exp\left[-i\alpha\overline{\overline{J}}_3^{(\frac{1}{2})}\right]\exp\left[-i\beta\overline{\overline{J}}_2^{(\frac{1}{2})}\right]\exp\left[-i\gamma\overline{\overline{J}}_3^{(\frac{1}{2})}\right] \tag{4.3.6}$$

where $\overline{\overline{J}}_i^{(\frac{1}{2})}$ are the 2×2 angular momentum matrices. It can now be shown, and this is far from trivial, that the $(2J+1)\times(2J+1)$ unitary matrices

$$\overline{\overline{D}}^{J}(\alpha,\beta,\gamma)=\exp\left[-i\alpha\overline{\overline{J}}_3^{(J)}\right]\exp\left[-i\beta\overline{\overline{J}}_2^{(J)}\right]\exp\left[-i\gamma\overline{\overline{J}}_3^{(J)}\right] \tag{4.3.7}$$

where $\overline{\overline{J}}_i^{(J)}$ are the general angular momentum matrices[51], form all the distinct irreducible unitary representations of the group SU(2) as J in Eq. (4.3.7) takes on all integral and half-integral values. Having pointed out the homomorphism between the rotation group R(3), represented by $\{\overline{\overline{R}}(\alpha,\beta,\gamma)\in SO(3)\}$, and the unitary group $\{\overline{u}(\alpha,\beta,\gamma)\in SU(2)\}$, and the complete set of irreducible representations of the latter $\{\overline{\overline{D}}^{J}(\alpha,\beta,\gamma)\in U(2J+1)\}$ we can now write the irreducible representations of the rotation group directly. As special cases of Eq. (4.3.7) we note that for J=0, J=$\frac{1}{2}$ and J=1 respectively the rotation matrices reads as

$$\begin{aligned}
&\overline{\overline{D}}^{0}(\alpha,\beta,\gamma)=1\\
&\overline{\overline{D}}^{\frac{1}{2}}(\alpha,\beta,\gamma)=\overline{u}(\alpha,\beta,\gamma)\\
&\overline{\overline{D}}^{1}(\alpha,\beta,\gamma)=\overline{\overline{A}}^{+}\overline{\overline{R}}(\alpha,\beta,\gamma)\overline{\overline{A}}
\end{aligned} \tag{4.3.8}$$

---

this also means that the first identity of Eq. (4.3.5) [54] (and Eq. (4.3.15) is not rigorously exact. The more "correct" way would be to use the four real Euler-Rodrigues parameters $(\alpha_0,\alpha_1,\alpha_2,\alpha_3)$, which define the surface of a unit sphere, S^3, in four space (i.e. $\alpha_0^2+\alpha_1^2+\alpha_2^2+\alpha_3^2=1$), but since this parametrization is less easy to visualize, and hence grasp, we shall not do so.

50 The two matrices $\overline{u}(\alpha,\beta,\gamma)$ and $-\overline{u}(\alpha,\beta,\gamma)$ are associated with the same matrix $\overline{\overline{R}}(\alpha,\beta,\gamma)$, and the Cartan mapping formula [54] establishes the relation. Actually this mapping was originally established between *isotopic vectors* (a vector of zero length) in three-dimensional Euclidean space and *spinors* (elements in two-dimensional complex space).

51 Generally $\overline{\overline{J}}_i^{(J)}$ is the $(2J+1)\times(2J+1)$ matrix representation of the i'th component of the angular momentum in a complete basis of eigenstates with total angular momentum j - that is

$$\overline{\overline{J}}_i^{(J)}\equiv\left[\langle Jm|\mathbf{J}_i|Jm'\rangle \quad m,m'\in\{-J,-J+1,\ldots,J\}\right]$$

For $J=\frac{1}{2}$ as in Eq. (4.3.5) $\overline{\overline{J}}_i^{(\frac{1}{2})}=\frac{1}{2}\overline{\overline{\sigma}}_i$, where the latter are the familiar Pauli matrices, known from the theory of spin.

where the matrix $\overline{\overline{\mathrm{A}}}$ transforms $(\vec{e}_1,\vec{e}_2,\vec{e}_3)$ to the so-called *spherical basis* $(\vec{e}_{+1},\vec{e}_0,\vec{e}_{-1})$ given as

$$\begin{aligned}\vec{e}_{+1} &= -(\vec{e}_1 + i\vec{e}_2)/\sqrt{2}\\ \vec{e}_0 &= \vec{e}_3\\ \vec{e}_{-1} &= (\vec{e}_1 - i\vec{e}_2)/\sqrt{2}\end{aligned} \tag{4.3.9}$$

We now define the *unitary operator* $\mathbf{U}(\alpha,\beta,\gamma)$ as

$$\mathbf{U}(\alpha,\beta,\gamma) = \exp[-i\alpha\mathbf{J}_3]\exp[-i\beta\mathbf{J}_2]\exp[-i\gamma\mathbf{J}_3] \tag{4.3.10}$$

where $\mathbf{J}_i$ is the i'th component of the total angular momentum operator. The rotation matrix in Eq. (4.3.7) can then be expressed in the form

$$\overline{\overline{\mathrm{D}}}^{\mathrm{J}}_{\mathrm{m'm}}(\alpha,\beta,\gamma) = \langle \mathrm{Jm'}|\mathbf{U}(\alpha,\beta,\gamma)|\mathrm{Jm}\rangle = \exp(-\mathrm{im'}\alpha)\mathrm{d}^{\mathrm{J}}_{\mathrm{m'm}}(\beta)\exp(-\mathrm{im}\gamma) \tag{4.3.11}$$

where we have used that $|\mathrm{Jm}\rangle$ is an eigenket of $\mathbf{J}_3$, and defined the reduced rotation matrix

$$\mathrm{d}^{\mathrm{J}}_{\mathrm{m'm}}(\beta) \equiv \langle \mathrm{Jm'}|\exp[-i\beta\mathbf{J}_2]|\mathrm{Jm}\rangle \tag{4.3.12}$$

The action of $\mathbf{U}(\alpha,\beta,\gamma)$ on a given eigenket $|\mathrm{Jm}\rangle$ then reads as

$$|\mathrm{Jm}\rangle' \equiv \mathbf{U}(\alpha,\beta,\gamma)|\mathrm{Jm}\rangle = \sum_{\mathrm{m'}=-\mathrm{J}}^{\mathrm{J}} \overline{\overline{\mathrm{D}}}^{\mathrm{J}}_{\mathrm{m'm}}(\alpha,\beta,\gamma)|\mathrm{Jm'}\rangle \tag{4.3.13}$$

To interpret the physical significance of the unitary operator $\mathbf{U}(\alpha,\beta,\gamma)$, we consider the transformation of the angular momentum $\vec{\mathbf{J}} = (\mathbf{J}_1,\mathbf{J}_2,\mathbf{J}_3)$ corresponding to the change of basis described above in Eq. (4.3.13). That is

$$\begin{aligned}\mathbf{J}_{\mathrm{i}}'|\mathrm{Jm}\rangle' &\equiv \mathbf{U}(\alpha,\beta,\gamma)\mathbf{J}_{\mathrm{i}}|\mathrm{Jm}\rangle\\ &= \mathbf{U}(\alpha,\beta,\gamma)\mathbf{J}_{\mathrm{i}}\mathbf{U}^{-1}(\alpha,\beta,\gamma)\mathbf{U}(\alpha,\beta,\gamma)|\mathrm{Jm}\rangle\\ &= \mathbf{U}(\alpha,\beta,\gamma)\mathbf{J}_{\mathrm{i}}\mathbf{U}^{-1}(\alpha,\beta,\gamma)|\mathrm{Jm}\rangle'\\ \Downarrow\quad \mathbf{J}_{\mathrm{i}}' &= \mathbf{U}(\alpha,\beta,\gamma)\mathbf{J}_{\mathrm{i}}\mathbf{U}^{-1}(\alpha,\beta,\gamma)\end{aligned} \tag{4.3.14}$$

The point is now that one can show[52] that when $\mathbf{U}(\alpha,\beta,\gamma)$ acts on the vector *operator* $\mathbf{J}_{\mathrm{i}} \rightarrow \mathbf{J}_{\mathrm{i}}'$, corresponding to the unitary change of *basis* $|\mathrm{Jm}\rangle \rightarrow |\mathrm{Jm}\rangle'$, given in Eq. (4.3.13), $\mathbf{J}_i$ is transformed according to a sequence of three rotations by the Euler angles $2\pi-\gamma,\pi-\beta,2\pi-\alpha$ - that is

---

52 Using the Baker-Campbell-Hausdorff relation together with the commutation relations $\vec{\mathbf{J}}\times\vec{\mathbf{J}} = i\vec{\mathbf{J}}$ and $[\,\vec{a}\cdot\vec{\mathbf{J}},\vec{\mathbf{J}}\,] = -i\vec{a}\times\vec{\mathbf{J}}$ where $[\,a_i,\mathbf{J}_j\,] = 0$ [54].

$$\mathbf{J}_i' = \sum_{j=1}^{3} \overline{\overline{R}}_{ij}(2\pi-\gamma,\pi-\beta,2\pi-\alpha)\mathbf{J}_j = \sum_{j=1}^{3} \overline{\overline{R}}_{ij}^{-1}(\alpha,\beta,\gamma)\mathbf{J}_j = \sum_{j=1}^{3} \overline{\overline{R}}_{ji}(\alpha,\beta,\gamma)\mathbf{J}_j \qquad (4.3.15)$$

where we have used Eq. (4.3.5). In other words the rotation $\overline{\overline{R}}(\alpha,\beta,\gamma)$ of a *coordinate* vector $\vec{x} \in R^3$, Eq. (4.3.1), corresponds to the inverse rotation $\overline{\overline{R}}^{-1}(\alpha,\beta,\gamma)$ of a vector *operator*, Eq. (4.3.14). In terms of spherical components Eq. (4.3.2) and Eq. (4.3.15) take the following interesting forms

$$\left.\begin{aligned} x_i' &= \sum_{j=-1}^{1} \overline{\overline{D}}_{ij}^{1*}(\alpha,\beta,\gamma)x_j \\ \mathbf{J}_i' &= \sum_{j=-1}^{1} \overline{\overline{D}}_{ji}^{1}(\alpha,\beta,\gamma)\mathbf{J}_j \end{aligned}\right\} \quad i = -1,0,1 \qquad (4.3.16)$$

where we have used Eq. (4.3.8,9). This difference by $\overline{\overline{R}}(\alpha,\beta,\gamma)$ (or $\overline{\overline{D}}^{1*}(\alpha,\beta,\gamma)$) versus $\overline{\overline{R}}^{-1}(\alpha,\beta,\gamma)$ (or $\overline{\overline{D}}^{1}(\alpha,\beta,\gamma)$) it not an error, but a consequence of an important distinction in the meaning of the two transformations[53]. The duality arrives from the fact that one can choose to work with either the *passive* or the active formulation of the effect of a group element on a set of coordinates. In the passive formulation the set of coordinates denotes the same point kept fixed in the space, and the coordinate system and symmetry elements are changed under the operation. On the other hand, in the *active* formulation the coordinate system and the symmetry elements are kept fixed, while the coordinate set is moved during the symmetry operation. These two possible interpretations of a rotation are, to repeat, dual to each other, and this duality accounts for the fact that $\overline{\overline{R}}(\alpha,\beta,\gamma)$ appears in the active transformation, Eq. (4.3.2), and $\overline{\overline{R}}^{-1}(\alpha,\beta,\gamma)$ in the passive transformation, Eq. (4.3.15). This duality in viewpoint of a transformation can be very confusing, especially to an inexperienced reader that tries to gain information form different textbooks using different conventions. I found that most books on this subject either take the active view [54-56] or are not fully consistent [57, 58] throughout. In the book by Rose [57] the passive view is taken in the Cartesian representation, $\overline{\overline{R}}(\alpha,\beta,\gamma)$, of a rotation, but it fails to take the passive functional convention and gets $\overline{\overline{D}}^{j}(\alpha,\beta,\gamma)$ functions that really represent the inverse of $\overline{\overline{R}}(\alpha,\beta,\gamma)$. The book by Tinkham [58] also lack a consistent definition; it intends to take the active view, but actually uses the passive convention when defining the Cartesian representation. A good reference where the passive view is taken consistently throughout is the paper [59] by Pack and Parker. However I found the book by Biedenharn and Louck [54] to be very useful. It

---

53 This difference, to repeat, is not an error, but - in the final analysis - the result of conventions made in the definition of a so-called irreducible tensor operator. The irreducible tensor operators are the operator analoges of the basic ket vectors in the multiplicity $\{|Jm\rangle: \quad m = J,\ldots,-J\}$, and, like these multiplets, physical tensor operators usually carry additional lables that specify the physical properties of the operator. Let us next note that the tensor operator concept involves *two distinct spaces* on which transformations occur: The first is the Hilbert space which undergoes the transformation $|\Psi\rangle \rightarrow \mathbf{U}|\Psi\rangle$; and the second is the index space $\{(J,m)\}$, which lables the operators. The tensor operator concept links these two spaces by requiring that the induced transformation $\mathbf{T}_m^J \rightarrow \mathbf{U}\mathbf{T}_m^J\mathbf{U}^{-1}$, Eq. (4.3.14), be the same as the index transformation $|Jm\rangle \rightarrow \sum \overline{\overline{D}}_{m'm}^{J}(\alpha,\beta,\gamma)|Jm'\rangle$, Eq. (4.3.13).

takes the active view, and hence throughout this thesis we will restrict ourselves to use the *active convention*, which is also what we have done so far in the definitions discussed above. The present remark is intended to clarify this situation.

In order to be explicit let us the notation[54] that $\mathfrak{R}$ represent an abstract rotation of the axes and let $\overline{\overline{\mathrm{R}}}(\mathfrak{R})$ be the matrix which represents its action on Cartesian coordinates and $\overline{\overline{\mathrm{D}}}^{\mathrm{j}}(\mathfrak{R})$ be the rotation matrix that represents its action on functions transforming as the j'th irreducible representation of the rotation group in three dimensions. It is imperative, as discussed above, that $\overline{\overline{\mathrm{R}}}(\mathfrak{R})$ and $\overline{\overline{\mathrm{D}}}^{\mathrm{j}}(\mathfrak{R})$ be homomorphic representations of the group; that is, if $\mathfrak{R}_{\mathrm{ij}}$ is the rotation that carries frame j into frame i, so that

$$\mathfrak{R}_{31} = \mathfrak{R}_{32}\mathfrak{R}_{21} \tag{4.3.17}$$

then we must have

$$\overline{\overline{\mathrm{R}}}\left(\mathfrak{R}_{31}\right) = \overline{\overline{\mathrm{R}}}\left(\mathfrak{R}_{32}\right)\overline{\overline{\mathrm{R}}}\left(\mathfrak{R}_{21}\right) \tag{4.3.18}$$

and

$$\overline{\overline{\mathrm{D}}}^{\mathrm{j}}\left(\mathfrak{R}_{31}\right) = \overline{\overline{\mathrm{D}}}^{\mathrm{j}}\left(\mathfrak{R}_{32}\right)\overline{\overline{\mathrm{D}}}^{\mathrm{j}}\left(\mathfrak{R}_{21}\right) \tag{4.3.19}$$

The rotation matrices $\overline{\overline{\mathrm{R}}}(\alpha,\beta,\gamma)$ of Eq. (4.3.3) and $\overline{\overline{\mathrm{D}}}^{\mathrm{j}}(\alpha,\beta,\gamma)$ of Eq. (4.3.7) does satisfy Eq. (4.3.18,19) respectively. In considering the action of rotations on functions of coordinates, we use the *functional convention*

$$\left[\mathfrak{R}\Psi\right](\vec{\mathrm{x}}) \equiv \Psi\left(\overline{\overline{\mathrm{R}}}^{-1}\cdot\vec{\mathrm{x}}\right) \tag{4.3.20}$$

The functional analog to Eq. (4.3.13) then reads as

$$\left[\mathfrak{R}\Psi^{\mathrm{J}}_{\mathrm{m}}\right](\vec{\mathrm{x}}) = \sum_{\mathrm{m}'=-\mathrm{J}}^{\mathrm{J}} \overline{\overline{\mathrm{D}}}^{\mathrm{J}}_{\mathrm{m}'\mathrm{m}}(\mathrm{R})\Psi^{\mathrm{J}}_{\mathrm{m}'}(\vec{\mathrm{x}}) \tag{4.3.21}$$

Combining Eq. (4.3.20,21), we obtain the important (active) relation

$$\begin{aligned}\Psi^{\mathrm{J}}_{\mathrm{m}}(\vec{\mathrm{x}}') &= \left[\mathfrak{R}^{-1}\mathfrak{R}\Psi^{\mathrm{J}}_{\mathrm{m}}\right](\vec{\mathrm{x}}') = \left[\mathfrak{R}^{-1}\Psi^{\mathrm{J}}_{\mathrm{m}}\right]\left(\overline{\overline{\mathrm{R}}}^{-1}\cdot\vec{\mathrm{x}}'\right)\\ &= \sum_{\mathrm{m}'=-\mathrm{J}}^{\mathrm{J}} \overline{\overline{\mathrm{D}}}^{\mathrm{J}}_{\mathrm{m}'\mathrm{m}}\left(\mathrm{R}^{-1}\right)\Psi^{\mathrm{J}}_{\mathrm{m}'}\left(\overline{\overline{\mathrm{R}}}^{-1}\cdot\vec{\mathrm{x}}'\right) = \sum_{\mathrm{m}'=-\mathrm{J}}^{\mathrm{J}} \overline{\overline{\mathrm{D}}}^{\mathrm{J}*}_{\mathrm{mm}'}(\mathrm{R})\Psi^{\mathrm{J}}_{\mathrm{m}'}\left(\overline{\overline{\mathrm{R}}}^{-1}\cdot\vec{\mathrm{x}}'\right)\\ &= \sum_{\mathrm{m}'=-\mathrm{J}}^{\mathrm{J}} \overline{\overline{\mathrm{D}}}^{\mathrm{J}*}_{\mathrm{mm}'}(\mathrm{R})\Psi^{\mathrm{J}}_{\mathrm{m}'}(\vec{\mathrm{x}})\end{aligned} \tag{4.3.22}$$

where we have used the used the unitary property of the rotation matrices

---

54 In this notation for an abstract rotation $\mathfrak{R}$ we do not use a parametrization in Euler angles, simply to keep the notation short.

$$\overline{\overline{D}}^{J}\left(\Re^{-1}\right)=\left[\overline{\overline{D}}^{J}\left(\Re\right)\right]^{-1}=\left[\overline{\overline{D}}^{J}\left(\Re\right)\right]^{+} \tag{4.3.23}$$

in the second line of Eq (4.3.22), and the inverse of Eq. (4.3.1) in the last line. The relation in Eq. (4.3.22) is very important in the discussion of body-fixed frames (to be introduced later), and the use of complex conjugated rotation matrices is not a "perverse convention", but a necessity for overall consistency. The functions $\overline{\overline{D}}^{J*}_{m',m}(\alpha,\beta,\gamma)$ - as opposed to the $\overline{\overline{D}}^{J}_{m',m}(\alpha,\beta,\gamma)$ themselves - transform properly as state vectors carrying angular momentum labels (J, m). In fact it is not that difficult to show[55] that the function $\overline{\overline{D}}^{J*}_{m',m}(\alpha,\beta,\gamma)$ is actually the wave function for a rotating symmetric top (a solid body with center-of-mass fixed in space) with a total angular momentum J, a z-component m' of the angular momentum referred to space-fixed axis and a z-component m of the angular momentum referred to body-fixed axis. For now we will just note that a wave function with sharp angular momentum (J, m) can be expanded as a series of $2J+1$ wave functions that are functions of rotated coordinates and with total angular momentum J, each weighted by a symmetric top wave function also with total angular momentum J.

Before we move on to apply the results presented above on the H_2^+ system, we will state two important relations involving the rotation matrices $\overline{\overline{D}}^{J}_{m',m}(\alpha,\beta,\gamma)$, since they will be needed later on. The reader who wishes derivations can get them from Biedenharn and Louck [54] p. 68 and p. 86. The rotation matrices satisfy the fundamental orthogonality relations

$$\int_0^{2\pi}d\alpha\int_0^{\pi}d\beta\sin\beta\int_0^{2\pi}d\gamma\left\{\overline{\overline{D}}^{J*}_{m'm}\left(\alpha,\beta,\gamma\right)\overline{\overline{D}}^{J'}_{\mu'\mu}\left(\alpha,\beta,\gamma\right)\right\}=\frac{8\pi^2}{2J+1}\delta_{JJ'}\delta_{m'\mu'}\delta_{m\mu} \tag{4.3.24}$$

and

$$\int_0^{2\pi}d\alpha\int_0^{\pi}d\beta\sin\beta\int_0^{2\pi}d\gamma\left\{\overline{\overline{D}}^{J*}_{m'm}\left(\alpha,\beta,\gamma\right)\overline{\overline{D}}^{J_1}_{m_1'm_1}\left(\alpha,\beta,\gamma\right)\overline{\overline{D}}^{J_2}_{m_2'm_2}\left(\alpha,\beta,\gamma\right)\right\}=\frac{2\pi^2}{2J+1}C^{J_1J_2J}_{m_1'm_2'm'}C^{J_1J_2J}_{m_1m_2m} \tag{4.3.25}$$

where $C^{J_1J_2J}_{m_1m_2m}$ and $C^{J_1J_2J}_{m_1'm_2'm'}$ in the latter orthogonality relation are Wigner coefficients; also known as Clebsch-Gordan, Wigner and vector-coupling coefficients. There exist a large number of relations for these coupling coefficients (symmetry and orthogonality relations and the so-called triangle conditions), but we will not take up space with the many tiresome relations here, as that would clearly be to go too far in the present context of this thesis. Instead we will just refer to the excellent text book by Biedenharn and Louck [54] , where these relations are discussed and where tables with explicit expressions for many of the Wigner coefficients are presented.

---

55 See Biedenharn and Louck [54] p. 57-66. The proof is quite easy, but we will not take up space with the long tiresome details here, as that would clearly be to go too far in the present context of this thesis.

5 Numerical implementation of proton hydrogen scattering

5.1 Introduction

With the completion of the introduction to the required quantum mechanical methodology, we are now finally in the position to treat the problem of proton hydrogen scattering using the variational R-matrix formulation described in chapter 2. As a prelude to the implementation of the scheme derived in chapter 3 (see Eq. (3.2.21-22)) we will derive an explicit expression for the H_2^+ J-functional, that allows the usage of several numerical methods - with reference to the ones already discussed in chapter 3 section 2 and 3. In doing so we will use the notation throughout this chapter that the "A-term of the J-functional" refers to the J-functional, Eq. (2.2.1), *excluding the surface term*, corresponding to the operator representation of the matrix $\overline{\overline{A}}$ defined in Eq. (2.2.15) - that is

$$A(\Psi) \equiv \int_V d\omega \left\{ \left[E - W(\omega) \right] |\Psi(\omega)|^2 - \mathbf{T}_E(\Psi) - \mathbf{T}_N(\Psi) \right\} \tag{5.1.1}$$

where the nuclear and electronic kinetic energy densities are given in Eq. (2.2.2). In the following five sections of this chapter (5.2-6) we are going to rewrite this A-term of the J-functional, in order to obtain a convenient form in which the zero order term, referred to as the adiabatic term, is separable in three coordinates. Next we discuss the Born-Oppenheimer approximate and the full three body treatment of H_2^+ in section 5.7 and 5.8 respectively. The outcome of the derivations in these sections forms the heart of the numerical calculations to be discussed in chapter 6. Finally in section 5.9 we shall derive a numerical scheme for the full three body transition dipole moment of H_2^+ as this will be needed in a future study of H_2^+ absorption in white dwarfs.

5.2 The J-functional in the Lab.-fixed frame of reference

In the laboratory-fixed frame of reference with an arbitrary origin the H_2^+ system is described in terms of the position-vectors of the three particles as depicted in figure 8. The two protons are denoted respectively a and b, and the electron is denoted e. The laboratory-fixed frame of reference is described in terms of the three unit vectors $\vec{e}'_x, \vec{e}'_y$ and $\vec{e}'_z$. Expressed in the laboratory-fixed frame of reference, the A-term of the J-functional, Eq. (5.1.1), reads as

$$A(\Psi) = \int_V d\vec{r}_a d\vec{r}_b d\vec{r}_e \left\{ \left[E - W \right] |\Psi|^2 - \frac{\hbar^2}{2m_a} \left| \vec{\nabla}_a \Psi \right|^2 - \frac{\hbar^2}{2m_b} \left| \vec{\nabla}_b \Psi \right|^2 - \frac{\hbar^2}{2m_e} \left| \vec{\nabla}_e \Psi \right|^2 \right\} \tag{5.2.1}$$

where the potential energy density term, W, will be defined later. This is clearly a 9-dimensional integral, but as argued in chapter 4 section 2 it is sufficient to treat the translationally invariant case where the linear momentum of the system is fixed to $\vec{0}$,

corresponding to the elimination of the center-of-mass coordinates, such that Eq. (5.2.1) effectively reduces to a 6-dimensional integral. In other words we need to introduce a new set of coordinates which explicitly includes the center-of-mass coordinates, and this leads us to what we shall refer to as the space-fixed coordinates.Laboratory-fixed coordinates

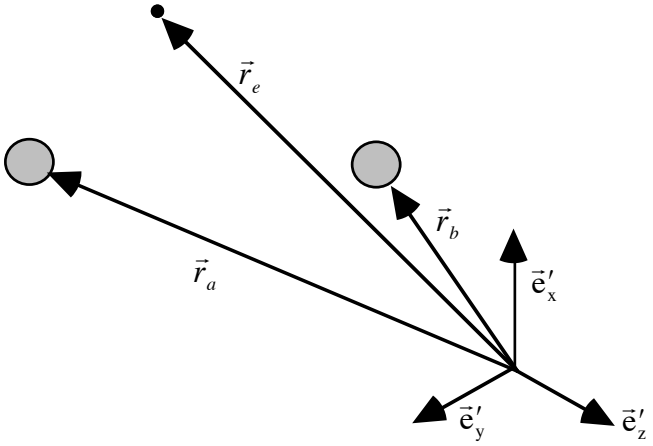

Figure 8 Laboratory-fixed frame of reference

5.3 The J-functional in the space-fixed frame of reference

As mentioned in chapter 1 section 2, and outlined in appendix A, the mass-weighted Jacobi coordinates, Eq. (A.14), provide a convenient set of translational invariant coordinates that transform the kinetic energy density into a canonical form with only one mass-factor (see Eq. (A.17)). Nevertheless this is not exactly the type of space-fixed coordinates that we are going to apply on the H_2^+ system. The reason for this is purely a matter of convenience since the direct approach using the mass-weighted Jacobi-coordinates introduces the mass scaling-factors listed in Eq. (A.14), which in turn prevents an easy physical interpretation of the coordinates. In stead we choose to ignore the mass scaling-factors in the mass-weighted Jacobi coordinates, and define what we could call the "non-mass-weighted Jacobi coordinates" or simply *Jacobi-coordinates* $\vec{r}', \vec{R}'$ and $\vec{R}'_G$ for a "heavy-heavy-light" particle-system as H_2^+. We define

$$\begin{aligned}
\vec{r}' &\equiv \vec{r}_e - \frac{m_a\vec{r}_a + m_b\vec{r}_b}{m_a + m_b} \\
\vec{R}' &\equiv \vec{r}_a - \vec{r}_b \\
\vec{R}'_G &\equiv \frac{1}{M}\left(m_a\vec{r}_a + m_b\vec{r}_b + m_e\vec{r}_e\right)
\end{aligned} \tag{5.3.1}$$

where $M \equiv m_a + m_b + m_e$ is the total mass of the system. The matrix-representation for this change of coordinates then reads as

$$\left[\vec{r}\,',\vec{R}\,',\vec{R}\,'_G\right]=\left[\vec{r}_a,\vec{r}_b,\vec{r}_e\right]\overline{\overline{V}}=\left[\vec{r}_a,\vec{r}_b,\vec{r}_e\right]\begin{bmatrix}-\dfrac{m_a}{m_a+m_b} & 1 & \dfrac{m_a}{M}\\ -\dfrac{m_b}{m_a+m_b} & -1 & \dfrac{m_b}{M}\\ 1 & 0 & \dfrac{m_e}{M}\end{bmatrix} \tag{5.3.2}$$

which should be compared to the transformation matrix $\overline{\overline{V}}$, entering Eq. (A.13), for the corresponding mass-weighted Jacobi coordinates for a three-particle system (N=3). From the above matrix-representation of the change of coordinates, Eq. (5.3.2), we can draw some conclusions, much like the ones discussed for the mass-weighted Jacobi coordinates in appendix A. First it is easy to show that the transformation matrix, $\overline{\overline{V}}$, is unimodular, see Eq. (E.7), but since the columns and rows are clearly not orthonormal we conclude that the coordinate transformation is not equal to a real unitary transformation. Further since the sum of the elements in the first two columns is zero, we have, as expected, that both $\vec{r}\,'$ and $\vec{R}\,'$ are *translationally invariant*. The physical significance and interpretation of this special choice of space-fixed coordinates, see figure 9, is as follows; $\vec{R}\,'$ is the inter-nuclear coordinate vector, $\vec{R}\,'_G$ is the center-of-mass coordinate vector and $\vec{r}\,'$ is the coordinate vector from the *nuclear*-center-of-mass to the electron, and is therefore referred to as the *space-fixed electronic coordinate vector*.

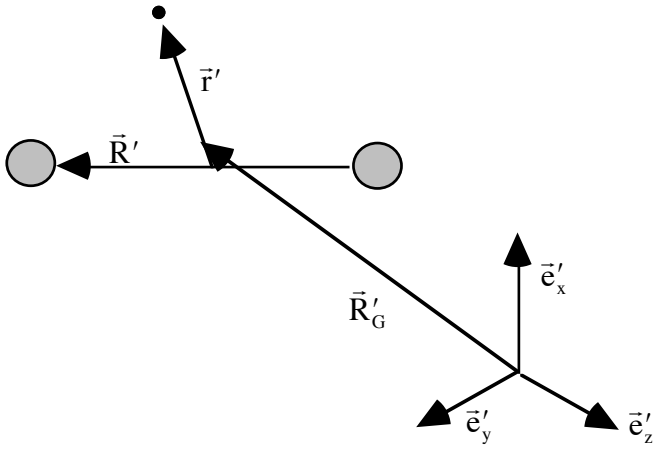

Figure 9 Space-fixed frame of reference

In order to transform the A-term of the J-functional, Eq. (5.2.1), from the laboratory-fixed coordinates into the space-fixed coordinates, we express the gradients with respect to the old coordinates, $\vec{r}_a,\vec{r}_b$ and $\vec{r}_e$, in terms of the gradients with respect to the new coordinates, $\vec{r}\,',\vec{R}\,'$ and $\vec{R}\,'_G$, using the chain-rule.

$$\begin{aligned}
\vec{\nabla}_e\Psi &= \frac{\delta\vec{r}'}{\delta\vec{r}_e}\vec{\nabla}_{r'}\Psi + \frac{\delta\vec{R}'}{\delta\vec{r}_e}\vec{\nabla}_{R'}\Psi + \frac{\delta\vec{R}'_G}{\delta\vec{r}_e}\vec{\nabla}_{R'_G}\Psi = \vec{\nabla}_{r'}\Psi + \frac{m_e}{M}\vec{\nabla}_{R'_G}\Psi \\
\vec{\nabla}_a\Psi &= -\frac{m_a}{m_a+m_b}\vec{\nabla}_{r'}\Psi + \vec{\nabla}_{R'}\Psi + \frac{m_a}{M}\vec{\nabla}_{R'_G}\Psi \\
\vec{\nabla}_b\Psi &= -\frac{m_b}{m_a+m_b}\vec{\nabla}_{r'}\Psi - \vec{\nabla}_{R'}\Psi + \frac{m_b}{M}\vec{\nabla}_{R'_G}\Psi
\end{aligned} \tag{5.3.3}$$

We are now in the position to transform the kinetic energy density terms in Eq. (5.2.1) into the new coordinates.

$$\begin{aligned}
-\frac{\hbar^2}{2m_e}\left|\vec{\nabla}_e\Psi\right|^2 - \frac{\hbar^2}{2m_a}\left|\vec{\nabla}_a\Psi\right|^2 - \frac{\hbar^2}{2m_b}\left|\vec{\nabla}_b\Psi\right|^2 &= -\frac{\hbar^2}{2m_e}\left|\vec{\nabla}_{r'}\Psi + \frac{m_e}{M}\vec{\nabla}_{R'_G}\Psi\right|^2 \\
&\quad -\frac{\hbar^2}{2m_a}\left|-\frac{m_a}{m_a+m_b}\vec{\nabla}_{r'}\Psi + \vec{\nabla}_{R'}\Psi + \frac{m_a}{M}\vec{\nabla}_{R'_G}\Psi\right|^2 \\
&\quad -\frac{\hbar^2}{2m_b}\left|-\frac{m_b}{m_a+m_b}\vec{\nabla}_{r'}\Psi - \vec{\nabla}_{R'}\Psi + \frac{m_b}{M}\vec{\nabla}_{R'_G}\Psi\right|^2 \\
&= -\frac{\hbar^2}{2\mu_e}\left|\vec{\nabla}_{r'}\Psi\right|^2 - \frac{\hbar^2}{2\mu}\left|\vec{\nabla}_{R'}\Psi\right|^2 - \frac{\hbar^2}{2M}\left|\vec{\nabla}_{R'_G}\Psi\right|^2
\end{aligned} \tag{5.3.4}$$

where we have defined the mass-factors

$$\begin{aligned}
\mu &\equiv \left[1/m_a + 1/m_b\right]^{-1} = 918.07576000 \\
\mu_e &\equiv \left[1/\left(m_a+m_b\right) + 1/m_e\right]^{-1} = 0.99972776545
\end{aligned} \tag{5.3.5}$$

and listed the values [60] for the H_2^+ system in atomic units[56]. As Eq. (5.3.4) indicates it turns out that when expressing the kinetic energy density in terms of the new space-fixed coordinates all the cross-terms cancel out, and we are left with three terms each weighted by a different mass-factor. This is a direct consequence of the fact that we have chosen to neglect the mass-factors included in the mass-weighted Jacobi coordinates, Eq. (A.14), when we defined the space-fixed coordinates, Eq (5.2.1). We also note that the two mass-factors, μ and μ_e, defined in Eq. (5.3.5), are actually equal to respectively the two- and three-particle reduced masses, μ_{12} and $\mu_{12,3}$, defined in the paragraphs following Eq. (A.9,10) (when particle 3 equals the electron). From the fact that the transformation matrix, $\overline{\overline{V}}$, is found to be unimodular, we further conclude (see Eq. (E.6-8)) that the volume element in Eq. (5.2.1) simply transforms as

$$\int_V d\vec{r}_a d\vec{r}_b d\vec{r}_e = \int_V d\vec{R}' d\vec{R}'_G d\vec{r}' \tag{5.3.6}$$

---

56 In the system of atomic units the following set of constants $\left\{\hbar, m_e, e, 4\pi\varepsilon_0, a_0\right\}$ have a numerical value of 1.

The A-term of the J-functional expressed in terms of the space-fixed coordinates then reads as

$$A(\Psi) = \int_V d\vec{R}' d\vec{R}'_G d\vec{r}' \left\{ \left[E - W \right] |\Psi|^2 - \frac{\hbar^2}{2\mu} \left| \vec{\nabla}_{R'} \Psi \right|^2 - \frac{\hbar^2}{2\mu_e} \left| \vec{\nabla}_{r'} \Psi \right|^2 - \frac{\hbar^2}{2M} \left| \vec{\nabla}_{R'_G} \Psi \right|^2 \right\} \tag{5.3.7}$$

where the kinetic energy density is split into three terms with the following physical significance; the first term describes the relative *nuclear* motion, the next the *electronic* motion relative to the nuclear center-of-mass and the last term is a kinetic energy density term related to the motion of the *center-of-mass of the total system*. As discussed in chapter 4 section 2 it is sufficient to treat the translationally invariant case where the linear momentum of the system is fixed to $\vec{0}$, corresponding to the elimination of the center-of-mass coordinates, such that the A-term of the J-functional reduces to

$$A(\Psi) = \int_V d\vec{R}' d\vec{r}' \left\{ \left[E - W \right] |\Psi|^2 - \frac{\hbar^2}{2\mu} \left| \vec{\nabla}_{R'} \Psi \right|^2 - \frac{\hbar^2}{2\mu_e} \left| \vec{\nabla}_{r'} \Psi \right|^2 \right\} \tag{5.3.8}$$

5.4 The J-functional in the body-fixed frame of reference

The next step is now to introduce a frame of reference, $\vec{e}_x, \vec{e}_y$ and $\vec{e}_z$, that is fixed to the two-body system of the protons, and hence follow the motion of the protons. Such a frame is referred to as a body-fixed frame of reference. An important property of all body-fixed frames, in contrast to arbitrary moving frames, is that the translationally invariant coordinates of the particles relative to the body-fixed frame are invariants under all rotations-inversions of the particles. Another important property of a body-fixed frame is that the generator of rotation of the frame is the total orbital angular momentum of the particles. In other words (with reference to the discussion in section 4.3) the introduction of such a frame into the description of the motion of the H_2^+ system serves partially to define a transformation from Cartesian coordinates to new coordinates in such a way that we are assured of being able to construct states of the system having sharp total orbital angular momentum (i.e. good quantum labels (J,m)). Corresponding to the space-fixed coordinates $\vec{r}', \vec{R}'$ and $\vec{R}'_G$, expressed in terms of the unit-vectors $\vec{e}'_x, \vec{e}'_y$ and $\vec{e}'_z$, we define a set of coordinates in the body fixed unit-vectors $\vec{e}_x, \vec{e}_y$ and $\vec{e}_z$, and denote then $\vec{r}, \vec{R}$ and $\vec{R}_G$. In these body-fixed coordinates Eq. (5.3.8) then reads as

$$A(\Psi) = \int_V d\vec{R} d\vec{r} \left\{ \left[E - W \right] |\Psi|^2 - \frac{\hbar^2}{2\mu} \left| \vec{\nabla}_R \Psi \right|^2 - \frac{\hbar^2}{2\mu_e} \left| \vec{\nabla}_r \Psi \right|^2 \right\} \tag{5.4.1}$$

The transformation from the space fixed frame of reference to the body fixed frame of reference is chosen so that the new z-axis ($\vec{e}_z$) will point in the direction of the inter-nuclear vector, such that the inter-nuclear separation, $\vec{R} = (0,0,R)$, will appear explicitly in the expression for the corresponding A-term of the J-functional - see figure 10.

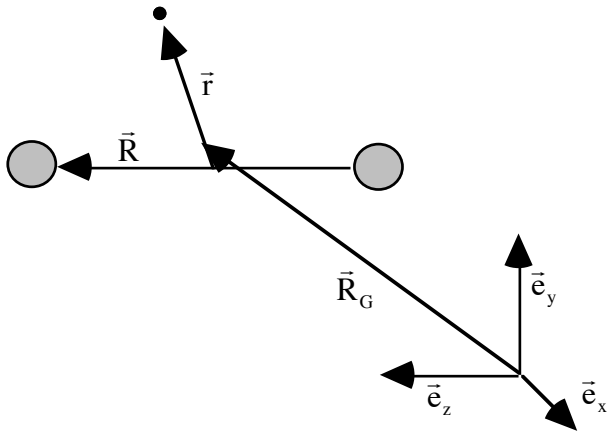

Figure 10 Body-fixed frame of reference

The rotation operation is represented by the real unitary $\bar{\bar{R}}(\alpha,\beta,0)$-matrix, Eq. (4.3.3), where α and β are the two Euler angles necessary to parametrize the rotation described above. The definition of α and β as the angles that rotate the space-fixed unit-vectors into the body-fixed unit-vectors is illustrated in figure 11.

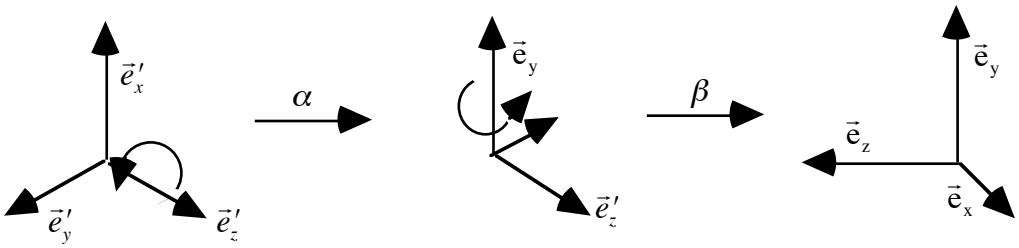

Figure 11 Rotation from the space-fixed to body-fixed frame

With the introduction of body-fixed coordinates as described above the inter-nuclear coordinate vector $\vec{R}$, can now be parametrized in terms of the two Euler angles α and β, needed to rotate the space-fixed frame of reference into the body-fixed frame of reference, and the inter-nuclear separation R. In other words the new coordinates are defined in such a way as to give a simple description of the inter-nuclear vector, but the body fixed electronic coordinate vector, $\vec{r}$, does not enter the definition of $\vec{e}_x, \vec{e}_y$ and $\vec{e}_z$, and in the following we will denote the three Cartesian components of $\vec{r}$ by x, y and z. To express the nuclear kinetic energy density, entering Eq. (5.4.1), in terms of the body fixed variables x, y, z, R, α and β, we first have to derive an expression for the gradient with respect to $\vec{R}$ in terms of these variables. To obtain such an expression we have to go through some long and tedious derivations, but as I have never seen these derivations presented in the literature before, and since the results obtained from these efforts form the very heart of this thesis, we shall not retain going into a somewhat detailed discussion. The derivation takes of course point of reference in the explicit definition of the rotation of the space-fixed unit vectors $\vec{e}'_x, \vec{e}'_y$ and $\vec{e}'_z$ into the body-fixed axis $\vec{e}_x, \vec{e}_y$ and $\vec{e}_z$.

$$\left[\vec{e}_x,\vec{e}_y,\vec{e}_z\right]=\left[\vec{e}'_x,\vec{e}'_y,\vec{e}'_z\right]\overline{\overline{R}}(\alpha,\beta,0) \tag{5.4.2}$$

where $\overline{\overline{R}}(\alpha,\beta,0)$ is the matrix representation of the rotation given in Eq. (4.3.3) - that is

$$\overline{\overline{R}}(\alpha,\beta,0)=\begin{bmatrix}\cos\alpha\cos\beta & -\sin\alpha & \cos\alpha\sin\beta\\ \sin\alpha\cos\beta & \cos\alpha & \sin\alpha\sin\beta\\ -\sin\beta & 0 & \cos\beta\end{bmatrix} \tag{5.4.3}$$

The body-fixed coordinates expressed in terms of the space-fixed frame of reference then reads as

$$\left[\vec{r},\vec{R}\right]\equiv\left[\vec{e}_x,\vec{e}_y,\vec{e}_z\right]\begin{bmatrix}x & 0\\ y & 0\\ z & R\end{bmatrix}=\left[\vec{e}'_x,\vec{e}'_y,\vec{e}'_z\right]\overline{\overline{R}}(\alpha,\beta,0)\begin{bmatrix}x & 0\\ y & 0\\ z & R\end{bmatrix} \tag{5.4.4}$$

An infinitesimal variation of $\vec{r}$ and $\vec{R}$, with fixed axis $\vec{e}'_x,\vec{e}'_y$ and $\vec{e}'_z$, then reads as

$$\left[\delta\vec{r},\delta\vec{R}\right]=\left[\vec{e}'_x,\vec{e}'_y,\vec{e}'_z\right]\delta\overline{\overline{R}}(\alpha,\beta,0)\begin{bmatrix}x & 0\\ y & 0\\ z & R\end{bmatrix}+\left[\vec{e}'_x,\vec{e}'_y,\vec{e}'_z\right]\overline{\overline{R}}(\alpha,\beta,0)\begin{bmatrix}\delta x & 0\\ \delta y & 0\\ \delta z & \delta R\end{bmatrix} \tag{5.4.5}$$

Next we project the above equation onto the axis of the body-fixed frame of reference, by multiplying Eq. (5.4.5) by the column vector $\begin{bmatrix}\vec{e}_x\\ \vec{e}_y\\ \vec{e}_z\end{bmatrix}$.

$$\begin{aligned}\begin{bmatrix}\vec{e}_x\\ \vec{e}_y\\ \vec{e}_z\end{bmatrix}\left[\delta\vec{r},\delta\vec{R}\right]&=\overline{\overline{R}}^{T}(\alpha,\beta,0)\begin{bmatrix}\vec{e}'_x\\ \vec{e}'_y\\ \vec{e}'_z\end{bmatrix}\left[\vec{e}'_x,\vec{e}'_y,\vec{e}'_z\right]\delta\overline{\overline{R}}(\alpha,\beta,0)\begin{bmatrix}x & 0\\ y & 0\\ z & R\end{bmatrix}\\ &+\overline{\overline{R}}^{T}(\alpha,\beta,0)\begin{bmatrix}\vec{e}'_x\\ \vec{e}'_y\\ \vec{e}'_z\end{bmatrix}\left[\vec{e}'_x,\vec{e}'_y,\vec{e}'_z\right]\overline{\overline{R}}(\alpha,\beta,0)\begin{bmatrix}\delta x & 0\\ \delta y & 0\\ \delta z & \delta R\end{bmatrix}\\ &=\overline{\overline{R}}^{T}(\alpha,\beta,0)\delta\overline{\overline{R}}(\alpha,\beta,0)\begin{bmatrix}x & 0\\ y & 0\\ z & R\end{bmatrix}+\begin{bmatrix}\delta x & 0\\ \delta y & 0\\ \delta z & \delta R\end{bmatrix}\end{aligned} \tag{5.4.6}$$

where we have used the fact that $\overline{\overline{R}}(\alpha,\beta,0)$ is real unitary. The variation, $\delta\overline{\overline{R}}(\alpha,\beta,0)$, with respect to the Euler angles reads as

$$\delta\overline{\overline{\mathrm{R}}}(\alpha,\beta,0) = \delta\begin{bmatrix}\cos\alpha\cos\beta & -\sin\alpha & \cos\alpha\sin\beta\\ \sin\alpha\cos\beta & \cos\alpha & \sin\alpha\sin\beta\\ -\sin\beta & 0 & \cos\beta\end{bmatrix}$$
$$= \begin{bmatrix}-\sin\alpha\cos\beta & -\cos\alpha & -\sin\alpha\sin\beta\\ \cos\alpha\cos\beta & -\sin\alpha & \cos\alpha\sin\beta\\ 0 & 0 & 0\end{bmatrix}\delta\alpha + \begin{bmatrix}-\cos\alpha\sin\beta & 0 & \cos\alpha\cos\beta\\ -\sin\alpha\sin\beta & 0 & \sin\alpha\cos\beta\\ -\cos\beta & 0 & -\sin\beta\end{bmatrix}\delta\beta \tag{5.4.7}$$

and multiplying Eq. (5.4.7) with $\overline{\overline{\mathrm{R}}}^{\mathrm{T}}(\alpha,\beta,0)$ gives, after some rewriting

$$\overline{\overline{\mathrm{R}}}^{\mathrm{T}}(\alpha,\beta,0)\delta\overline{\overline{\mathrm{R}}}(\alpha,\beta,0) = \begin{bmatrix}0 & -\cos\beta & 0\\ \cos\beta & 0 & \sin\beta\\ 0 & -\sin\beta & 0\end{bmatrix}\delta\alpha + \begin{bmatrix}0 & 0 & 1\\ 0 & 0 & 0\\ -1 & 0 & 0\end{bmatrix}\delta\beta \tag{5.4.8}$$

Now substituting Eq. (5.4.8) into Eq. (5.4.6) gives

$$\begin{bmatrix}\vec{\mathrm{e}}_{\mathrm{x}}\\ \vec{\mathrm{e}}_{\mathrm{y}}\\ \vec{\mathrm{e}}_{\mathrm{z}}\end{bmatrix}\left[\delta\vec{\mathrm{r}},\delta\vec{\mathrm{R}}\right] = \begin{bmatrix}0 & -\cos\beta\delta\alpha & \delta\beta\\ \cos\beta\delta\alpha & 0 & \sin\beta\delta\alpha\\ -\delta\beta & -\sin\beta\delta\alpha & 0\end{bmatrix}\begin{bmatrix}\mathrm{x} & 0\\ \mathrm{y} & 0\\ \mathrm{z} & \mathrm{R}\end{bmatrix} + \begin{bmatrix}\delta\mathrm{x} & 0\\ \delta\mathrm{y} & 0\\ \delta\mathrm{z} & \delta\mathrm{R}\end{bmatrix} \tag{5.4.9}$$

which reduces to

$$\begin{bmatrix}\delta\vec{\mathrm{r}}\cdot\vec{\mathrm{e}}_{\mathrm{x}} & \delta\vec{\mathrm{R}}\cdot\vec{\mathrm{e}}_{\mathrm{x}}\\ \delta\vec{\mathrm{r}}\cdot\vec{\mathrm{e}}_{\mathrm{y}} & \delta\vec{\mathrm{R}}\cdot\vec{\mathrm{e}}_{\mathrm{y}}\\ \delta\vec{\mathrm{r}}\cdot\vec{\mathrm{e}}_{\mathrm{z}} & \delta\vec{\mathrm{R}}\cdot\vec{\mathrm{e}}_{\mathrm{z}}\end{bmatrix} = \begin{bmatrix}\delta\mathrm{x} + \mathrm{z}\delta\beta - \mathrm{y}\cos\beta\delta\alpha & \mathrm{R}\delta\beta\\ \delta\mathrm{y} + \mathrm{x}\cos\beta\delta\alpha + \mathrm{z}\sin\beta\delta\alpha & \mathrm{R}\sin\beta\delta\alpha\\ \delta\mathrm{z} - \mathrm{y}\sin\beta\delta\alpha - \mathrm{x}\delta\beta & \delta\mathrm{R}\end{bmatrix} \tag{5.4.10}$$

Using this matrix identity we can first express the variations of α, β and R by equating the second columns.

$$\begin{aligned}\delta\alpha &= \delta\vec{\mathrm{R}}\cdot\vec{\mathrm{e}}_{\mathrm{y}}/(\mathrm{R}\sin\beta)\\ \delta\beta &= \delta\vec{\mathrm{R}}\cdot\vec{\mathrm{e}}_{\mathrm{x}}/\mathrm{R}\\ \delta\mathrm{R} &= \delta\vec{\mathrm{R}}\cdot\vec{\mathrm{e}}_{\mathrm{z}}\end{aligned} \tag{5.4.11}$$

Substituting these expressions into the identities obtained by equating the first columns in Eq. (5.4.10) then gives the variations in the electronic coordinates.

$$\begin{aligned}\delta\mathrm{x} &= \delta\vec{\mathrm{r}}\cdot\vec{\mathrm{e}}_{\mathrm{x}} + \delta\vec{\mathrm{R}}\cdot\left(\vec{\mathrm{e}}_{\mathrm{y}}\frac{\mathrm{y}}{\mathrm{R}}\cot\beta - \vec{\mathrm{e}}_{\mathrm{x}}\frac{\mathrm{z}}{\mathrm{R}}\right)\\ \delta\mathrm{y} &= \delta\vec{\mathrm{r}}\cdot\vec{\mathrm{e}}_{\mathrm{y}} - \delta\vec{\mathrm{R}}\cdot\left(\vec{\mathrm{e}}_{\mathrm{y}}\frac{\mathrm{x}}{\mathrm{R}}\cot\beta + \vec{\mathrm{e}}_{\mathrm{y}}\frac{\mathrm{z}}{\mathrm{R}}\right)\\ \delta\mathrm{z} &= \delta\vec{\mathrm{r}}\cdot\vec{\mathrm{e}}_{\mathrm{z}} + \delta\vec{\mathrm{R}}\cdot\left(\vec{\mathrm{e}}_{\mathrm{y}}\frac{\mathrm{y}}{\mathrm{R}} - \vec{\mathrm{e}}_{\mathrm{x}}\frac{\mathrm{x}}{\mathrm{R}}\right)\end{aligned} \tag{5.4.12}$$

The variation of the total wave function caused by infinitesimal variations of x, y, z, R,

α and β or $\vec{r}$ and $\vec{R}$ is given by the chain-rule.

$$\begin{aligned}\delta\Psi &= \delta x\frac{\partial\Psi}{\partial x} + \delta y\frac{\partial\Psi}{\partial y} + \delta z\frac{\partial\Psi}{\partial z} + \delta R\frac{\partial\Psi}{\partial R} + \delta\alpha\frac{\partial\Psi}{\partial\alpha} + \delta\beta\frac{\partial\Psi}{\partial\beta} \\ &= \delta\vec{r}\cdot\vec{\nabla}_r\Psi + \delta\vec{R}\cdot\vec{\nabla}_R\Psi\end{aligned} \tag{5.4.13}$$

and substituting Eq. (5.4.11,12) into this expression give us

$$\begin{aligned}\delta\Psi = \delta\vec{r}\cdot\left(\vec{e}_x\frac{\partial}{\partial x} + \vec{e}_y\frac{\partial}{\partial y} + \vec{e}_z\frac{\partial}{\partial z}\right)\Psi + \frac{1}{R}\delta\vec{R}\cdot\left\{\vec{e}_y\left(y\frac{\partial}{\partial z} - z\frac{\partial}{\partial y}\right) - \vec{e}_x\left(z\frac{\partial}{\partial x} - x\frac{\partial}{\partial z}\right)\right. \\ \left. -\vec{e}_y\cot\beta\left(x\frac{\partial}{\partial y} - y\frac{\partial}{\partial x}\right) + \vec{e}_x\frac{\partial}{\partial\beta} + \frac{\vec{e}_y}{\sin\beta}\frac{\partial}{\partial\alpha} + \vec{e}_z R\frac{\partial}{\partial R}\right\}\Psi\end{aligned} \tag{5.4.14}$$

We now introduce what we will refer to as the *body-fixed Cartesian electronic*[57] *angular momentum operators*

$$\mathbf{L}_x \equiv -i\hbar\left(y\frac{\partial}{\partial z} - z\frac{\partial}{\partial y}\right), \quad \mathbf{L}_y \equiv -i\hbar\left(z\frac{\partial}{\partial x} - x\frac{\partial}{\partial z}\right), \quad \mathbf{L}_z \equiv -i\hbar\left(x\frac{\partial}{\partial y} - y\frac{\partial}{\partial x}\right) \tag{5.4.15}$$

Comparing Eq. (5.4.13,14) and substituting Eq. (5.4.15) into the result give us

$$\vec{\nabla}_R\Psi = \frac{1}{\hbar R}\left\{i\vec{e}_y\mathbf{L}_x - i\vec{e}_x\mathbf{L}_y - i\vec{e}_y\cot\beta\mathbf{L}_z + \vec{e}_x\hbar\frac{\partial}{\partial\beta} + \vec{e}_y\frac{\hbar}{\sin\beta}\frac{\partial}{\partial\alpha} + \vec{e}_z\hbar R\frac{\partial}{\partial R}\right\}\Psi \tag{5.4.16}$$

To write this expression in terms of the well-known step-up and step-down angular-momentum operators $\mathbf{L}_+$ and $\mathbf{L}_-$, defined as

$$\mathbf{L}_+ \equiv \mathbf{L}_x + i\mathbf{L}_y, \quad \mathbf{L}_- \equiv \mathbf{L}_x - i\mathbf{L}_y \tag{5.4.17}$$

we next introduce the *spherical basis* mentioned in chapter 4 section 3, such that the real basis $\vec{e}_x,\vec{e}_y,\vec{e}_z$ are now expressed the complex basis-vectors (see Eq. (4.3.9))

$$\begin{aligned}\vec{e}_x &= \frac{1}{\sqrt{2}}\left(\vec{e}_{+1} + \vec{e}_{-1}\right) \\ \vec{e}_y &= \frac{1}{i\sqrt{2}}\left(\vec{e}_{+1} - \vec{e}_{-1}\right) \\ \vec{e}_z &= \vec{e}_0\end{aligned} \tag{5.4.18}$$

Now substituting Eq. (5.4.18) into Eq. (5.4.16) and using the definition in Eq. (5.4.17) give us

---

57 Note that in the body-fixed frame of reference, the nuclear do not contribute to the total orbital angular momentum, "$\vec{R}\|\vec{v}_{nuc} \Rightarrow \vec{L}_{nuc} \equiv \vec{R}\times\vec{P}_{nuc} = \vec{0}$", and the term "electronic" is then actually redundant.

$$\begin{aligned}\vec{\nabla}_R\Psi = &\frac{\vec{e}_-}{\sqrt{2}\hbar R}\left(\cot\beta \mathbf{L}_z - \mathbf{L}_+ + \frac{i\hbar}{\sin\beta}\frac{\partial}{\partial\alpha} + \hbar\frac{\partial}{\partial\beta}\right)\Psi \\ &-\frac{\vec{e}_+}{\sqrt{2}\hbar R}\left(\cot\beta \mathbf{L}_z - \mathbf{L}_- + \frac{i\hbar}{\sin\beta}\frac{\partial}{\partial\alpha} - \hbar\frac{\partial}{\partial\beta}\right)\Psi + \vec{e}_0\frac{\partial\Psi}{\partial R}\end{aligned} \tag{5.4.19}$$

From the orthogonality of the of the spherical basis-vectors we finally conclude

$$\begin{aligned}\left|\vec{\nabla}_R\Psi\right|^2 = &\frac{1}{2\hbar^2R^2}\left|\cot\beta \mathbf{L}_z\Psi - \mathbf{L}_+\Psi + \frac{i\hbar}{\sin\beta}\frac{\partial\Psi}{\partial\alpha} + \hbar\frac{\partial\Psi}{\partial\beta}\right|^2 \\ &+\frac{1}{2\hbar^2R^2}\left|\cot\beta \mathbf{L}_z\Psi - \mathbf{L}_-\Psi + \frac{i\hbar}{\sin\beta}\frac{\partial\Psi}{\partial\alpha} - \hbar\frac{\partial\Psi}{\partial\beta}\right|^2 + \left|\frac{\partial\Psi}{\partial R}\right|^2\end{aligned} \tag{5.4.20}$$

Before we can write down the complete expression for the A-term of the J-functional in the body-fixed coordinates we have to consider the corresponding change of the volume element in the integral. In appendix E this change of basis is discussed in details, and we just conclude (see Eq. (E.15)

$$\int_V d\vec{R}'d\vec{r}' = \int_V d\vec{R}d\vec{r} = \int_{V_{elec}} d\vec{r}\int_0^\infty R^2dR\int_0^{2\pi}d\alpha\int_0^\pi \sin\beta d\beta \tag{5.4.21}$$

Finally substituting Eq. (5.4.20,21) into Eq. (5.4.1) result in the following expression for the overall change of coordinates for the A-term of the J-functional.

$$\begin{aligned}A(\Psi) = &\int_{V_{elec}} d\vec{r}\int_0^\infty R^2dR\int_0^{2\pi}d\alpha\int_0^\pi \sin\beta d\beta\left\{(E-W)|\Psi|^2 - \frac{\hbar^2}{2\mu_e}\left|\vec{\nabla}_r\Psi\right|^2\right. \\ &-\frac{\hbar^2}{2\mu}\left|\frac{\partial\Psi}{\partial R}\right|^2 - \frac{1}{4R^2\mu}\left|\cot\beta \mathbf{L}_z\Psi - \mathbf{L}_+\Psi + \frac{i\hbar}{\sin\beta}\frac{\partial\Psi}{\partial\alpha} + \hbar\frac{\partial\Psi}{\partial\beta}\right|^2 \\ &\left.-\frac{1}{4R^2\mu}\left|\cot\beta \mathbf{L}_z\Psi - \mathbf{L}_-\Psi + \frac{i\hbar}{\sin\beta}\frac{\partial\Psi}{\partial\alpha} - \hbar\frac{\partial\Psi}{\partial\beta}\right|^2\right\}\end{aligned} \tag{5.4.22}$$

5.5 Introduction of spheroidal coordinates

For any three-dimensional Schrödinger equation, whether exact solutions can be obtained or not depends almost exclusively on the existence of certain coordinate systems in which the Schrödinger equation can be reduced to a set of ordinary differential equations by method of separation of variables. However, since the birth of quantum mechanics in 1926, only a small number of physically useful separable Schrödinger equations have been discovered. Even if the Born-Oppenheimer approximation is used there is still only one molecule for which the electronic Schrödinger equation can be solved exactly. This is precisely the hydrogen molecular ion. As it has only one electron, it has the status in the

theory of molecules similar to that of the hydrogen atom in the theory of atoms. Whereas the equation for the atom is separable in spherical polar coordinates, Burrau [12] showed in 1927 that the electronic equation for the molecular ion is separable in *spheroidal coordinates*.

The spheroidal (i.e. confocal ellipsoidal) coordinate scheme is the natural one to use for a two-center system like H_2^+. Although these coordinates are discussed in many textbooks [61], it seems appropriate to at least summarize their properties here. If the point "e" is separated r_a and r_b from the two centers "a" and "b" respectively, we define two of the three spheroidal coordinates (ξ, η, ϕ) as

$$\xi \equiv (r_a + r_b)/R, \quad \eta \equiv (r_a - r_b)/R \tag{5.5.1}$$

where R is the separation between the two centers, see figure 12[58]. The third spheroidal coordinate ϕ defines the angle between the plane "abe" and a fixed plane through "a" and "b". It should be noted that this coordinate ϕ is actually equal to the third Euler angle γ describing the angle of rotation about the z-axis. Lines of constants $(\xi, \eta), (\xi, \phi)$ and (η, ϕ) are circles (in the xy-plane), ellipses, and hyperbolas respectively.

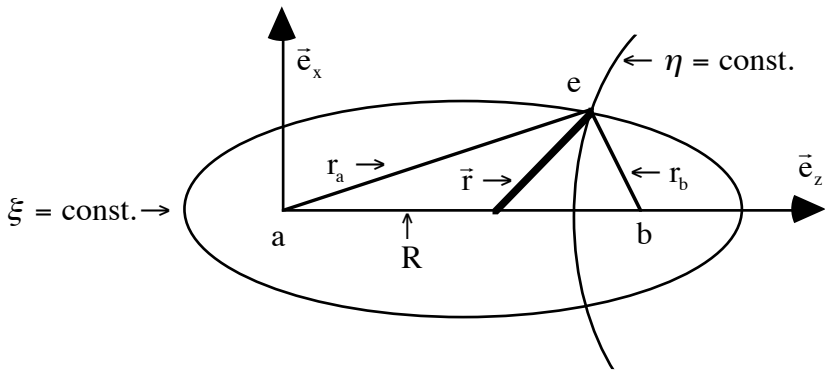

Figure 12 Spheroidal coordinates

Next we note that for the two center problem of H_2^+, described in the Cartesian body-fixed frame of reference introduced in the previous section, r_a and r_b respectively reads as

$$r_a = |\vec{r} + \vec{e}_3 R/2|, \quad r_b = |\vec{r} - \vec{e}_3 R/2| \tag{5.5.2}$$

The overall transformation from the body-fixed coordinates $\vec{r}$ and R to the spheroidal coordinates ξ, η and ϕ plus the coordinate f (defined as the half nuclear separation) then reads as

---

58 To simplify the figure, the point "e" has been drawn for the special case for which $\phi = 0$, corresponding to the coincidence of the xz plane and the plane "abe".

$$\begin{aligned}
\xi &= \left[\left|\vec{r} + \vec{e}_3 R/2\right| + \left|\vec{r} - \vec{e}_3 R/2\right|\right]/R \quad ,1 \le \xi \le \infty \\
\eta &= \left[\left|\vec{r} + \vec{e}_3 R/2\right| - \left|\vec{r} - \vec{e}_3 R/2\right|\right]/R \quad ,-1 \le \eta \le 1 \\
\phi &= \tan^{-1}\left(\frac{y}{x}\right) \quad ,0 \le \phi \le 2\pi \\
f &= R/2 \quad ,0 \le f \le \infty
\end{aligned} \tag{5.5.3}$$

where we have also listed the domain of definition for the new coordinates. The reverse relations for the connection between ξ, η, ϕ and f and the Cartesian coordinate scheme x, y, z and R is

$$\begin{aligned}
x &= f\sqrt{\left(\xi^2 - 1\right)\left(1 - \eta^2\right)}\cos\phi \\
y &= f\sqrt{\left(\xi^2 - 1\right)\left(1 - \eta^2\right)}\sin\phi \\
z &= f\xi\eta \\
R &= 2f
\end{aligned} \tag{5.5.4}$$

An additional set of useful relations when working in the spheroidal coordinates are

$$r_a = \left|\vec{r} + \vec{e}_3 R/2\right| = f\left(\xi + \eta\right), \quad r_b = \left|\vec{r} - \vec{e}_3 R/2\right| = f\left(\xi - \eta\right) \tag{5.5.5}$$

In order to express the A-term of the J-functional, Eq. (5.4.22), in terms of the new coordinates defined above we will have to go through some derivations much like the ones discussed in the previous section for the body-fixed coordinates. Again these derivations might seem long and tiresome to the reader, but as I have not yet seen them detailed in the literature and since the results obtained through the effort, forms the heart of this thesis, I find it appropriate to at least to some detail present them here. We use the chain-rule on Eq.(5.5.4) to find the variations of x, y, z and R in terms of ξ, η, ϕ and f.

$$\begin{aligned}
\delta x &= \delta\xi\frac{\partial x}{\partial \xi} + \delta\eta\frac{\partial x}{\partial \eta} + \delta\phi\frac{\partial x}{\partial \phi} + \delta f\frac{\partial x}{\partial f} \\
&= \xi f\sqrt{\frac{1-\eta^2}{\xi^2-1}}\cos\phi\delta\xi - f\eta\sqrt{\frac{\xi^2-1}{1-\eta^2}}\cos\phi\delta\eta - \sqrt{\left(\xi^2-1\right)\left(1-\eta^2\right)}\left(f\sin\phi\delta\phi - \cos\phi\delta f\right) \\
&= \frac{x\xi}{\xi^2-1}\delta\xi - \frac{x\eta}{1-\eta^2}\delta\eta - y\delta\phi + \frac{x}{f}\delta f \\
\delta y &= \frac{y\xi}{\xi^2-1}\delta\xi - \frac{y\eta}{1-\eta^2}\delta\eta + x\delta\phi + \frac{y}{f}\delta f \\
\delta z &= f\eta\delta\xi + f\xi\delta\eta + \xi\eta\delta f \\
\delta R &= 2\delta f
\end{aligned} \tag{5.5.6}$$

Writing this in terms of a matrix equation give us the inverse Jacobi-matrix $\overline{\overline{J}}^{-1}$ (see appendix E) for the transformation from the body-fixed Cartesian coordinates to the new coordinates.

$$\begin{bmatrix} \delta x \\ \delta y \\ \delta z \\ \delta R \end{bmatrix} \equiv \overline{\overline{J}}^{-1} \cdot \begin{bmatrix} \delta\xi \\ \delta\eta \\ \delta\phi \\ \delta f \end{bmatrix} = \begin{bmatrix} \frac{x\zeta}{\xi^2-1} & -\frac{x\eta}{1-\eta^2} & -y & \frac{x}{f} \\ \frac{y\xi}{\xi^2-1} & -\frac{y\eta}{1-\eta^2} & x & \frac{y}{f} \\ f\eta & f\xi & 0 & \xi\eta \\ 0 & 0 & 0 & 2 \end{bmatrix} \cdot \begin{bmatrix} \delta\xi \\ \delta\eta \\ \delta\phi \\ \delta f \end{bmatrix} \tag{5.5.7}$$

As outlined in appendix E, Eq. (E.2), the change of volume associated with this change of coordinates is now given by $|\det \overline{\overline{J}}^{-1}| = 2f^3(\xi^2 - \eta^2)$, and so all in all we have the following transformation of the volume element entering Eq. (5.4.22)

$$R^2 dR d\vec{r} = 4f^2 dR dx dy dz = 4f^2 \left|\det \overline{\overline{J}}^{-1}\right| d\xi d\eta d\phi df = 8f^5\left(\xi^2 - \eta^2\right) d\xi d\eta d\phi df \tag{5.5.8}$$

In order to express the kinetic energy densities, in Eq. (5.4.22), in the new coordinates we need to know the variations of ξ, η, ϕ and f in terms of infinitesimal variations of x, y, z and R. In other words we have to determine[59] the Jacobi matrix explicitly. The inverse of the matrix-equation Eq. (5.5.7) reads as

$$\begin{bmatrix} \delta\xi \\ \delta\eta \\ \delta\phi \\ \delta f \end{bmatrix} = \begin{bmatrix} \frac{x\xi}{f^2\left(\xi^2-\eta^2\right)} & \frac{y\xi}{f^2\left(\xi^2-\eta^2\right)} & \frac{\eta\left(\xi^2-1\right)}{f\left(\xi^2-\eta^2\right)} & -\frac{\xi\left(\xi^2-1\right)}{2f\left(\xi^2-\eta^2\right)} \\ -\frac{x\eta}{f^2\left(\xi^2-\eta^2\right)} & -\frac{y\eta}{f^2\left(\xi^2-\eta^2\right)} & \frac{\xi\left(1-\eta^2\right)}{f\left(\xi^2-\eta^2\right)} & -\frac{\eta\left(1-\eta^2\right)}{2f\left(\xi^2-\eta^2\right)} \\ -\frac{y}{f^2\left(\xi^2-1\right)\left(1-\eta^2\right)} & \frac{x}{f^2\left(\xi^2-1\right)\left(1-\eta^2\right)} & 0 & 0 \\ 0 & 0 & 0 & \frac{1}{2} \end{bmatrix} \cdot \begin{bmatrix} \delta x \\ \delta y \\ \delta z \\ \delta R \end{bmatrix} \tag{5.5.9}$$

The chain-rule in combination with Eq. (5.5.9) now gives

---

59 The matrix inversion is most easily done using a mathematical algebra program like “Mathematica” from Wolfram Research, Inc.

$$
\begin{aligned}
\delta\Psi &= \frac{\partial\Psi}{\partial\xi}\delta\xi + \frac{\partial\Psi}{\partial\eta}\delta\eta + \frac{\partial\Psi}{\partial\phi}\delta\phi + \frac{\partial\Psi}{\partial \mathrm{f}}\delta \mathrm{f} \\
&= \frac{1}{\mathrm{f}^2\left(\xi^2-\eta^2\right)}\left\{\left(\mathrm{x}\xi\frac{\partial\Psi}{\partial\xi} - \mathrm{x}\eta\frac{\partial\Psi}{\partial\eta} - \frac{\mathrm{y}\left(\xi^2-\eta^2\right)}{\left(\xi^2-1\right)\left(1-\eta^2\right)}\frac{\partial\Psi}{\partial\phi}\right)\delta\mathrm{x}\right. \\
&\quad + \left(\mathrm{y}\xi\frac{\partial\Psi}{\partial\xi} - \mathrm{y}\eta\frac{\partial\Psi}{\partial\eta} + \frac{\mathrm{x}\left(\xi^2-\eta^2\right)}{\left(\xi^2-1\right)\left(1-\eta^2\right)}\frac{\partial\Psi}{\partial\phi}\right)\delta\mathrm{y} \\
&\quad + \mathrm{f}\left(\eta\left(\xi^2-1\right)\frac{\partial\Psi}{\partial\xi} + \xi\left(1-\eta^2\right)\frac{\partial\Psi}{\partial\eta}\right)\delta\mathrm{z} \\
&\quad \left. - \frac{\mathrm{f}}{2}\left(\eta\left(\xi^2-1\right)\frac{\partial\Psi}{\partial\xi} + \xi\left(1-\eta^2\right)\frac{\partial\Psi}{\partial\eta} - \mathrm{f}\left(\xi^2-\eta^2\right)\frac{\partial\Psi}{\partial \mathrm{f}}\right)\delta\mathrm{R}\right\} \\
&= \frac{\partial\Psi}{\partial \mathrm{x}}\delta\mathrm{x} + \frac{\partial\Psi}{\partial \mathrm{y}}\delta\mathrm{y} + \frac{\partial\Psi}{\partial \mathrm{z}}\delta\mathrm{z} + \frac{\partial\Psi}{\partial \mathrm{R}}\delta\mathrm{R}
\end{aligned}
\tag{5.5.10}
$$

such that

$$
\left|\frac{\partial\Psi}{\partial \mathrm{R}}\right|^2 = \frac{1}{4\mathrm{f}^2\left(\xi^2-\eta^2\right)^2}\left|\left(\xi^2-1\right)\left(\mathrm{f}\frac{\partial\Psi}{\partial \mathrm{f}} - \xi\frac{\partial\Psi}{\partial\xi}\right) + \left(1-\eta^2\right)\left(\mathrm{f}\frac{\partial\Psi}{\partial \mathrm{f}} - \eta\frac{\partial\Psi}{\partial\eta}\right)\right|^2 \tag{5.5.11}
$$

Next we derive $|\vec{\nabla}_{\mathrm{r}}\Psi|^2$ in terms of the new coordinates ξ, η, ϕ and f. The straight-forward way would be to use

$$
\left|\vec{\nabla}_{\mathrm{r}}\Psi\right|^2 = \left|\frac{\partial\Psi}{\partial \mathrm{x}}\right|^2 + \left|\frac{\partial\Psi}{\partial \mathrm{y}}\right|^2 + \left|\frac{\partial\Psi}{\partial \mathrm{z}}\right|^2 \tag{5.5.12}
$$

in combination with Eq. (5.5.10), but we will use a somewhat more cleaver approach. In a, strictly speaking incorrect, but nevertheless useful mathematical notation, we can write

$$
\vec{\nabla}_{\mathrm{r}}\Psi = \vec{\nabla}_{\mathrm{r}}\xi\frac{\partial\Psi}{\partial\xi} + \vec{\nabla}_{\mathrm{r}}\eta\frac{\partial\Psi}{\partial\eta} + \vec{\nabla}_{\mathrm{r}}\phi\frac{\partial\Psi}{\partial\phi} = \frac{\partial\Psi}{\partial\vec{\mathrm{r}}} = \frac{\partial\xi}{\partial\vec{\mathrm{r}}}\frac{\partial\Psi}{\partial\xi} + \frac{\partial\eta}{\partial\vec{\mathrm{r}}}\frac{\partial\Psi}{\partial\eta} + \frac{\partial\phi}{\partial\vec{\mathrm{r}}}\frac{\partial\Psi}{\partial\phi} \tag{5.5.12}
$$

and a "plain differentiation" of the relations in Eq. (5.5.3), then leads to the following expressions for the gradient of the spheroidal coordinates with respect to $\vec{\mathrm{r}}$

$$
\begin{aligned}
\vec{\nabla}_{\mathrm{r}}\xi &= \frac{1}{\mathrm{R}}\left(\frac{\vec{\mathrm{r}}+\vec{\mathrm{e}}_{\mathrm{z}}\mathrm{R}/2}{\left|\vec{\mathrm{r}}+\vec{\mathrm{e}}_{\mathrm{z}}\mathrm{R}/2\right|} + \frac{\vec{\mathrm{r}}-\vec{\mathrm{e}}_{\mathrm{z}}\mathrm{R}/2}{\left|\vec{\mathrm{r}}-\vec{\mathrm{e}}_{\mathrm{z}}\mathrm{R}/2\right|}\right) \\
\vec{\nabla}_{\mathrm{r}}\eta &= \frac{1}{\mathrm{R}}\left(\frac{\vec{\mathrm{r}}+\vec{\mathrm{e}}_{\mathrm{z}}\mathrm{R}/2}{\left|\vec{\mathrm{r}}+\vec{\mathrm{e}}_{\mathrm{z}}\mathrm{R}/2\right|} - \frac{\vec{\mathrm{r}}-\vec{\mathrm{e}}_{\mathrm{z}}\mathrm{R}/2}{\left|\vec{\mathrm{r}}-\vec{\mathrm{e}}_{\mathrm{z}}\mathrm{R}/2\right|}\right) \\
\vec{\nabla}_{\mathrm{r}}\phi &= \frac{\vec{\mathrm{e}}_{\mathrm{y}}/\mathrm{x} - \vec{\mathrm{e}}_{\mathrm{x}}\mathrm{y}/\mathrm{x}^2}{1+\left(\mathrm{y}/\mathrm{x}\right)^2} = \frac{\mathrm{x}\vec{\mathrm{e}}_{\mathrm{y}} - \mathrm{y}\vec{\mathrm{e}}_{\mathrm{x}}}{\mathrm{x}^2+\mathrm{y}^2} = \frac{\vec{\mathrm{e}}_{\mathrm{z}}\times\vec{\mathrm{r}}}{\left|\vec{\mathrm{e}}_{\mathrm{z}}\times\vec{\mathrm{r}}\right|^2}
\end{aligned}
\tag{5.5.13}
$$

From these expressions it is easy to show the orthogonality relations

$$\vec{\nabla}_r\xi\cdot\vec{\nabla}_r\eta=\vec{\nabla}_r\xi\cdot\vec{\nabla}_r\varphi=\vec{\nabla}_r\eta\cdot\vec{\nabla}_r\phi=0 \tag{5.5.14}$$

It is then evident that when taking the norm square of Eq. (5.5.12), to give $|\vec{\nabla}_r\Psi|^2$, we do not get any cross-terms - that is

$$\left|\vec{\nabla}_r\Psi\right|^2=\left|\vec{\nabla}_r\xi\right|^2\left|\frac{\partial\Psi}{\partial\xi}\right|^2+\left|\vec{\nabla}_r\eta\right|^2\left|\frac{\partial\Psi}{\partial\eta}\right|^2+\left|\vec{\nabla}_r\phi\right|^2\left|\frac{\partial\Psi}{\partial\phi}\right|^2 \tag{5.5.15}$$

The above three norm squares of the gradients with respect to $\vec{r}$ are now obtained as the sum of the square of the first three elements in the corresponding first three rows of the Jacobi matrix $\bar{\bar{J}}$, in Eq. (5.5.9) - recalling that for instance $\vec{\nabla}_r\xi\equiv\left[\frac{\partial\xi}{\partial x},\frac{\partial\xi}{\partial y},\frac{\partial\xi}{\partial z}\right]=\left[\bar{\bar{J}}_{11},\bar{\bar{J}}_{12},\bar{\bar{J}}_{13}\right]$. We then write

$$\begin{aligned}\left|\vec{\nabla}_r\Psi\right|^2&=\frac{1}{f^4\left(\xi^2-\eta^2\right)^2}\left\{x^2\xi^2+y^2\xi^2+f^2\eta^2\left(\xi^2-1\right)^2\right\}\left|\frac{\partial\Psi}{\partial\xi}\right|^2\\&+\frac{1}{f^4\left(\xi^2-\eta^2\right)^2}\left\{x^2\xi^2+y^2\xi^2+f^2\xi^2\left(1-\eta^2\right)^2\right\}\left|\frac{\partial\Psi}{\partial\eta}\right|^2\\&+\frac{y^2+x^2}{f^4\left(\xi^2-1\right)^2\left(1-\eta^2\right)^2}\left|\frac{\partial\Psi}{\partial\phi}\right|^2\\&=\frac{\xi^2-1}{f^2\left(\xi^2-\eta^2\right)}\left|\frac{\partial\Psi}{\partial\zeta}\right|^2+\frac{1-\eta^2}{f^2\left(\xi^2-\eta^2\right)}\left|\frac{\partial\Psi}{\partial\eta}\right|^2+\frac{1}{f^2\left(\xi^2-1\right)\left(1-\eta^2\right)}\left|\frac{\partial\Psi}{\partial\phi}\right|^2\\&=\frac{1}{f^2\left(\xi^2-\eta^2\right)}\left\{\left(\xi^2-1\right)\left|\frac{\partial\Psi}{\partial\xi}\right|^2+\left(1-\eta^2\right)\left|\frac{\partial\Psi}{\partial\eta}\right|^2+\left(\frac{1}{\xi^2-1}+\frac{1}{1-\eta^2}\right)\left|\frac{\partial\Psi}{\partial\phi}\right|^2\right\}\end{aligned} \tag{5.5.16}$$

where we have used Eq. (5.5.4) in the intermediate step.

To express the body-fixed angular-momentum operators $\mathbf{L}_z,\mathbf{L}_+$ and $\mathbf{L}_-$ in terms of the spheroidal coordinates, we use Eq. (5.5.4) and Eq. (5.5.10), and obtain

$$\mathbf{L}_z\equiv-i\hbar\left(x\frac{\partial}{\partial y}-y\frac{\partial}{\partial x}\right)=-\frac{i\hbar}{f^2\left(\xi^2-\eta^2\right)}\frac{\left(x^2+y^2\right)\left(\xi^2-\eta^2\right)}{\left(\xi^2-1\right)\left(1-\eta^2\right)}\frac{\partial}{\partial\phi}=-i\hbar\frac{\partial}{\partial\phi} \tag{5.5.17}$$

and[60]

60 In the last step of Eq. (5.5.18) we have used the relations

$$\left(ix\mp y\right)=i\left(x\pm iy\right)=\pm i\left(iy\pm x\right)\quad\text{and}\quad\left(iy\pm x\right)=\pm\left(x\pm iy\right)=\pm f\sqrt{\left(\xi^2-1\right)\left(1-\eta^2\right)}\exp\left(\pm i\varphi\right)$$

$$\begin{aligned}
\mathbf{L}_{\pm} \equiv \mathbf{L}_x \pm i\mathbf{L}_y &= -i\hbar\left(y\frac{\partial}{\partial z} - z\frac{\partial}{\partial y}\right) \pm i(-i)\hbar\left(z\frac{\partial}{\partial x} - x\frac{\partial}{\partial z}\right) = z\hbar\left(i\frac{\partial}{\partial y} \pm \frac{\partial}{\partial x}\right) - \hbar\frac{\partial}{\partial z}(iy \pm x) \\
&= \frac{\hbar(iy \pm x)}{f^2(\xi^2 - \eta^2)}\left\{\left(z\xi - f\eta(\xi^2 - 1)\right)\frac{\partial}{\partial \xi} - \left(z\eta - f\xi(1 - \eta^2)\right)\frac{\partial}{\partial \eta} \pm \frac{iz(\xi^2 - \eta^2)}{(\xi^2 - 1)(1 - \eta^2)}\frac{\partial}{\partial \phi}\right\} \\
&= \frac{\hbar z(iy \pm x)}{f^2(\xi^2 - \eta^2)}\left\{\frac{1}{\xi}\frac{\partial}{\partial \xi} - \frac{1}{\eta}\frac{\partial}{\partial \eta} \pm \frac{i(\xi^2 - \eta^2)}{(\xi^2 - 1)(1 - \eta^2)}\frac{\partial}{\partial \phi}\right\} \\
&= \frac{\hbar\exp(\pm i\phi)\sqrt{(\xi^2 - 1)(1 - \eta^2)}}{\xi^2 - \eta^2}\left\{\pm\eta\frac{\partial}{\partial \xi} \mp \xi\frac{\partial}{\partial \eta} + \frac{i\xi\eta(\xi^2 - \eta^2)}{(\xi^2 - 1)(1 - \eta^2)}\frac{\partial}{\partial \phi}\right\}
\end{aligned} \tag{5.5.18}$$

To complete the derivation of the A-term of the J-functional in terms of spheroidal coordinates we need to define the potential term W. As the potential for the isolated H_2^+ system is just a three-particle electrostatic coulomb potential we have

$$\begin{aligned}
W &= \frac{e^2}{4\pi\varepsilon_0}\left(\frac{1}{|\vec{r}_a - \vec{r}_b|} - \frac{1}{|\vec{r}_e - \vec{r}_a|} - \frac{1}{|\vec{r}_e - \vec{r}_b|}\right) \\
&= \frac{e^2}{4\pi\varepsilon_0}\left(\frac{1}{|\vec{R}'|} - \frac{1}{|\vec{r}' + \vec{R}'/2|} - \frac{1}{|\vec{r}' - \vec{R}'/2|}\right) \\
&= \frac{e^2}{4\pi\varepsilon_0}\left(\frac{1}{|\vec{R}|} - \frac{1}{|\vec{r} + \vec{e}_3 R/2|} - \frac{1}{|\vec{r} - \vec{e}_3 R/2|}\right) \\
&= \frac{e^2}{4\pi\varepsilon_0}\left(\frac{1}{2f} - \frac{1}{f(\xi + \eta)} - \frac{1}{f(\xi - \eta)}\right) = \frac{e^2}{8\pi\varepsilon_0 f}\left(1 - \frac{4\xi}{\xi^2 - \eta^2}\right)
\end{aligned} \tag{5.5.19}$$

where we have used the fact that the transformation from the space-fixed frame to the body-fixed frame is unitary (i.e. norm conserving) in the second step, and used Eq. (5.5.5) in the last step. Now finally substituting Eq. (5.5.8), Eq. (5.5.11) and Eq. (5.5.16-19) into Eq. (5.4.22) we conclude

$$A(\Psi) = \int_0^\infty df 8f^5 \int_1^\infty d\xi \int_{-1}^1 d\eta \int_0^{2\pi} d\phi \int_0^{2\pi} d\alpha \int_0^\pi d\beta \sin\beta \left\{A_{elec}(\Psi) + A_{radi}(\Psi) + A_{ang}(\Psi) + A'_{ang}(\Psi)\right\} \tag{5.5.20}$$

where we have defined four terms; the *electronic* term

$$\begin{aligned}
A_{elec}(\Psi) = &\left[E - \frac{e^2}{8\pi\varepsilon_0 f}\left(1 - \frac{4\xi}{\xi^2 - \eta^2}\right)\right](\xi^2 - \eta^2)|\Psi|^2 \\
&- \frac{\hbar^2}{2\mu_e f^2}\left[(\xi^2 - 1)\left|\frac{\partial\Psi}{\partial\xi}\right|^2 + (1 - \eta^2)\left|\frac{\partial\Psi}{\partial\eta}\right|^2 + \left(\frac{1}{\xi^2 - 1} + \frac{1}{1 - \eta^2}\right)\left|\frac{\partial\Psi}{\partial\phi}\right|^2\right]
\end{aligned} \tag{5.5.21}$$

the nuclear kinetic or *radial* term

$$A_{radi}(\Psi) = -\frac{\hbar^2}{8\mu f^2\left(\xi^2-\eta^2\right)}\left|\left(\xi^2-1\right)\left(f\frac{\partial\Psi}{\partial f}-\xi\frac{\partial\Psi}{\partial\xi}\right)+\left(1-\eta^2\right)\left(f\frac{\partial\Psi}{\partial f}-\eta\frac{\partial\Psi}{\partial\eta}\right)\right|^2 \tag{5.5.22}$$

and finally two terms

$$\begin{aligned} A_{ang}(\Psi) = -\frac{\hbar^2}{16\mu f^2\left(\xi^2-\eta^2\right)}\Bigg|&\frac{i}{\sin\beta}\frac{\partial\Psi}{\partial\alpha}+\frac{\partial\Psi}{\partial\beta}-i\cot\beta\frac{\partial\Psi}{\partial\phi} \\ &-\exp(i\phi)\frac{\sqrt{\left(\xi^2-1\right)\left(1-\eta^2\right)}}{\xi^2-\eta^2}\left(\eta\frac{\partial\Psi}{\partial\xi}-\xi\frac{\partial\Psi}{\partial\eta}+\frac{i\xi\eta\left(\xi^2-\eta^2\right)}{\left(\xi^2-1\right)\left(1-\eta^2\right)}\frac{\partial\Psi}{\partial\phi}\right)\Bigg|^2 \end{aligned} \tag{5.5.23}$$

and

$$\begin{aligned} A'_{ang}(\Psi) = -\frac{\hbar^2}{16\mu f^2\left(\xi^2-\eta^2\right)}\Bigg|&\frac{i}{\sin\beta}\frac{\partial\Psi}{\partial\alpha}-\frac{\partial\Psi}{\partial\beta}-i\cot\beta\frac{\partial\Psi}{\partial\phi} \\ &-\exp(-i\phi)\frac{\sqrt{\left(\xi^2-1\right)\left(1-\eta^2\right)}}{\xi^2-\eta^2}\left(-\eta\frac{\partial\Psi}{\partial\xi}+\xi\frac{\partial\Psi}{\partial\eta}+\frac{i\xi\eta\left(\xi^2-\eta^2\right)}{\left(\xi^2-1\right)\left(1-\eta^2\right)}\frac{\partial\Psi}{\partial\phi}\right)\Bigg|^2 \end{aligned} \tag{5.5.24}$$

that we will refer to as *angular momentum coupling* terms. The physical significance, and hence the naming of these terms, will be discussed in more details in the next section. We end this section by stressing the fact that no approximations have been made in the derivations of the above expressions.

5.6 Separation of rotational coordinates

In this section we will derive the final expression for the rotational invariant A-term of the J-functional, to be used in the numerical implementation of the variational R-matrix formulation of the hydrogen proton scattering. As a prelude to this separation of rotational coordinates we first need an expression for the scattering wave function in terms of rotational invariant coordinates. The methodology for such a discussion was developed in chapter 4.

To repeat, the separation of translational coordinates was obtained through the transformation from the laboratory-fixed to space-fixed coordinates, followed by the elimination of the center-of-mass coordinate. To be more precise we write, using Eq. (4.2.10),

$$\Psi_{\vec{k}}\left(\vec{r}_a,\vec{r}_b,\vec{r}_e\right) = \exp\left(-i\vec{k}\cdot\vec{R}'_G/\hbar\right)\Psi_{\vec{0}}\left(\vec{r}',\vec{R}'\right) \tag{5.6.1}$$

We then put $\vec{R}'_G = \vec{0}$, and ignore the linear momentum label, leaving us with a translationally invariant scattering problem. Next we note that an arbitrary solution to the scattering problem can be expressed as a sum over wave functions with sharp angular momentum - that is

$$\Psi\left(\vec{r}',\vec{R}'\right)=\sum_{J=0}^{\infty}\sum_{m=-J}^{J}\Psi_{m}^{J}\left(\vec{r}',\vec{R}'\right) \tag{5.6.2}$$

To go from the space-fixed to the body-fixed coordinates we use Eq. (4.3.22)

$$\begin{aligned}\Psi\left(\vec{r}',\vec{R}'\right)&=\sum_{J=0}^{\infty}\sum_{m=-J}^{J}\sum_{m'=-J}^{J}\overline{\overline{D}}_{mm'}^{J*}\left(\alpha,\beta,0\right)\Psi_{m'}^{J}\left(\vec{r},R\right)\\&=\sum_{J=0}^{\infty}\sum_{m=-J}^{J}\sum_{m'=-J}^{J}\overline{\overline{D}}_{mm'}^{J*}\left(\alpha,\beta,0\right)\Phi_{m'}^{J}\left(\xi,\eta,\phi,f\right)\end{aligned} \tag{5.6.3}$$

where we have introduced the spheroidal coordinates and f in the last step. Since $\Phi_{m'}^{J}(\xi,\eta,\phi,f)$, by definition, is an eigenfunction of the z-component of the body-fixed angular momentum operator, Eq. (5.5.17), we can factor out the dependence on the ϕ coordinate.

$$\Phi_{m'}^{J}(\xi,\eta,\phi,f)=\exp(im'\phi)\Phi_{m'}^{J}(\xi,\eta,f) \tag{5.6.4}$$

Now using the complex conjugated of Eq. (4.3.11) - that is

$$\overline{\overline{D}}_{mm'}^{J*}\left(\alpha,\beta,\phi\right)=\exp\left(im\alpha\right)d_{mm'}^{J*}\left(\beta\right)\exp\left(im'\phi\right) \tag{5.6.5}$$

it should be evident that we can absorb the dependence on the ϕ coordinate into the rotation matrices, such that Eq. (5.6.3) becomes

$$\Psi\left(\vec{r}',\vec{R}'\right)=\sum_{J=0}^{\infty}\sum_{m=-J}^{J}\sum_{m'=-J}^{J}\overline{\overline{D}}_{mm'}^{J*}\left(\alpha,\beta,\phi\right)\Phi_{m'}^{J}\left(\xi,\eta,f\right) \tag{5.6.6}$$

This is exactly the desired expression in which the scattering wave function is expressed in terms of the rotational (and translational) invariant coordinates ξ,η and f. The next step is then to insert this expression for the wave function into the A-term of the J-functional, derived in the previous section, and integrate out the rotational coordinates α,β and ϕ. Before we can do this we need to know the action of the differential operators, depending on the rotational coordinates, on the complex conjugated of the rotation matrices. From the definition, Eq. (5.6.5), we can show, see Biedenharn and Louck [54] p. 64, the following eigenvalue equations

$$\begin{aligned}\mathbf{P}_{\pm}\overline{\overline{D}}_{mm'}^{J*}\left(\alpha,\beta,\phi\right)&=\exp\left(\pm i\phi\right)\sqrt{\left(J\mp m'\right)\left(J\pm m'+1\right)}\overline{\overline{D}}_{mm'\pm1}^{J*}\left(\alpha,\beta,\phi\right)\\\mathbf{P}_{z}\overline{\overline{D}}_{mm'}^{J*}\left(\alpha,\beta,\phi\right)&=m'\overline{\overline{D}}_{mm'}^{J*}\left(\alpha,\beta,\phi\right)\end{aligned} \tag{5.6.7}$$

where we have defined the differential operators[61]

---

61 As mentioned before in chapter 4 section 3, it is easy to show that the functions $\overline{\overline{D}}_{mm'}^{J*}(\alpha,\beta,\phi)$ are wave functions for a rotating symmetric top (a solid body with center-of-mass fixed in space) with a total angular momentum of J, a z-component of the angular momentum referred to space-fixed axis of m, and a z-component of the angular

$$\mathbf{P}_{\pm} \equiv \frac{\mathrm{i}\hbar}{\sin\beta}\frac{\partial}{\partial\alpha} \mp \hbar\frac{\partial}{\partial\beta} - \mathrm{i}\hbar\cot\beta\frac{\partial}{\partial\phi}$$
$$\mathbf{P}_{z} \equiv -\mathrm{i}\hbar\frac{\partial}{\partial\phi} \tag{5.6.8}$$

entering the A-terms of the J-functional. Now substituting Eq. (5.6.6) and Eq. (5.6.8) into Eq. (5.5.20-24), inserting Eq. (5.6.7), and finally integrating over the rotational coordinates, using the orthogonality relation Eq. (4.3.24) for the rotation matrices, we conclude[62]

$$\mathrm{A}(\Psi) = 8\pi^2\sum_{\mathrm{J}=0}^{\infty}\sum_{\mathrm{m}=-\mathrm{J}}^{\mathrm{J}}\int_0^{\infty}\mathrm{df}\,8\mathrm{f}^5\int_1^{\infty}\mathrm{d}\xi\int_{-1}^{1}\mathrm{d}\eta\left\{\mathrm{A}_{\mathrm{elec}}\left(\Phi_{\mathrm{m}}^{\mathrm{J}}\right) + \mathrm{A}_{\mathrm{radi}}\left(\Phi_{\mathrm{m}}^{\mathrm{J}}\right) + \mathrm{A}_{\mathrm{ang}}\left(\Phi_{\mathrm{m}}^{\mathrm{J}}\right) + \mathrm{A}'_{\mathrm{ang}}\left(\Phi_{\mathrm{m}}^{\mathrm{J}}\right)\right\} \tag{5.6.9}$$

where we have defined four terms; the *electronic term*

$$\begin{aligned}\mathrm{A}_{\mathrm{elec}}\left(\Phi_{\mathrm{m}}^{\mathrm{J}}\right) = &\left[\mathrm{E} - \frac{\mathrm{e}^2}{8\pi\varepsilon_0\mathrm{f}}\left(1 - \frac{4\xi}{\xi^2-\eta^2}\right)\right]\left(\xi^2-\eta^2\right)\left|\Phi_{\mathrm{m}}^{\mathrm{J}}\right|^2 \\ &- \frac{\hbar^2}{2\mu_{\mathrm{e}}\mathrm{f}^2}\left[\left(\xi^2-1\right)\left|\frac{\partial\Phi_{\mathrm{m}}^{\mathrm{J}}}{\partial\xi}\right|^2 + \left(1-\eta^2\right)\left|\frac{\partial\Phi_{\mathrm{m}}^{\mathrm{J}}}{\partial\eta}\right|^2 + \left(\frac{\mathrm{m}^2}{\xi^2-1} + \frac{\mathrm{m}^2}{1-\eta^2}\right)\left|\Phi_{\mathrm{m}}^{\mathrm{J}}\right|^2\right]\end{aligned} \tag{5.6.10}$$

the nuclear kinetic or *radial term*

$$\mathrm{A}_{\mathrm{radi}}\left(\Phi_{\mathrm{m}}^{\mathrm{J}}\right) = -\frac{\hbar^2}{8\mu\mathrm{f}^2\left(\xi^2-\eta^2\right)}\left|\left(\xi^2-1\right)\left(\mathrm{f}\frac{\partial\Phi_{\mathrm{m}}^{\mathrm{J}}}{\partial\mathrm{f}} - \xi\frac{\partial\Phi_{\mathrm{m}}^{\mathrm{J}}}{\partial\xi}\right) + \left(1-\eta^2\right)\left(\mathrm{f}\frac{\partial\Phi_{\mathrm{m}}^{\mathrm{J}}}{\partial\mathrm{f}} - \eta\frac{\partial\Phi_{\mathrm{m}}^{\mathrm{J}}}{\partial\eta}\right)\right|^2 \tag{5.6.11}$$

and finally two terms

$$\begin{aligned}\mathrm{A}_{\mathrm{ang}}\left(\Phi_{\mathrm{m}}^{\mathrm{J}}\right) = &-\frac{\hbar^2}{16\mu\mathrm{f}^2\left(\xi^2-\eta^2\right)}\left|\sqrt{(\mathrm{J}-\mathrm{m})(\mathrm{J}+\mathrm{m}+1)}\Phi_{\mathrm{m}+1}^{\mathrm{J}}\right. \\ &\left. - \frac{\sqrt{\left(\xi^2-1\right)\left(1-\eta^2\right)}}{\xi^2-\eta^2}\left(\eta\frac{\partial\Phi_{\mathrm{m}}^{\mathrm{J}}}{\partial\xi} - \xi\frac{\partial\Phi_{\mathrm{m}}^{\mathrm{J}}}{\partial\eta} - \frac{\mathrm{m}\xi\eta\left(\xi^2-\eta^2\right)}{\left(\xi^2-1\right)\left(1-\eta^2\right)}\Phi_{\mathrm{m}}^{\mathrm{J}}\right)\right|^2\end{aligned} \tag{5.6.12}$$

---

momentum referred to body-fixed axis of m'. The operators defined in Eq. (5.6.8) are exactly respectively the z-component, the step-up and step-down angular momentum operators referred to the body-fixed axis for a symmetric top.

62 Note that the integration over the rotational coordinates (α,β,ϕ) introduces (see Eq. (4.3.24)) a trivial sum over the index m going from -J to J, but as the functions $\Phi_{\mathrm{m}'}^{\mathrm{J}}(\xi,\eta,\mathrm{f})$ (see Eq. 5.6.6)) are independent of this index the summation simply reduces to the factor $2\mathrm{J}+1$ which is turn is canceled out by the inverse factor in Eq. 4.3.24. Finally for convenience we have substituted the lables $\mathrm{m}' \to \mathrm{m}$.

and

$$A'_{ang}\left(\Phi^J_m\right) = -\frac{\hbar^2}{16\mu f^2\left(\xi^2-\eta^2\right)}\left|\sqrt{(J+m)(J-m+1)}\Phi^J_{m-1}\right.$$
$$\left.-\frac{\sqrt{\left(\xi^2-1\right)\left(1-\eta^2\right)}}{\xi^2-\eta^2}\left(-\eta\frac{\partial\Phi^J_m}{\partial\xi}+\xi\frac{\partial\Phi^J_m}{\partial\eta}-\frac{m\xi\eta\left(\xi^2-\eta^2\right)}{\left(\xi^2-1\right)\left(1-\eta^2\right)}\Phi^J_m\right)\right|^2 \tag{5.6.13}$$

that we will refer to as *angular momentum coupling terms*. The electronic A-term came from $|\vec{\nabla}_r\Psi|^2$, Eq. (5.5.16), and is therefore clearly a pure electronic term. The nuclear kinetic or radial term includes derivatives with respect to both the two electronic coordinates ξ and η and the nuclear coordinate f, and therefore describes the radial non-adiabatic coupling of the nuclear and electronic motion. The last two terms couples wave functions with difference of unity in the m quantum number, and hence we refer to them as the angular non-adiabatic coupling terms or just the angular momentum coupling terms.

5.7 The clamped nucleus problem of the hydrogen molecular ion

The Born-Oppenheimer solutions and electronic structures of H_2^+ have been studied by a large number of theorists; thus, Burrau [12] in 1927, Hylleraas [13] in 1931, Jaffé [14] in 1934, Sandman [15] in 1935 and many others have performed Born-Oppenheimer approximate calculations on both the ground state and some of the excited states. In other words, the solutions to the Born-Oppenheimer treatment of the hydrogen molecular ion have roughly speaking been known to theorists since the introduction of quantum mechanics, and nowadays the results are included in nearly every textbook on introductory quantum chemistry. Nevertheless we are also going to study this approximate approach, for two reasons. First, since the Born-Oppenheimer approximation is well-known to be a "good approximation", we would definitely expect the electronic term of the J-functional, Eq. (5.5.21), to be the leading term, when we later on include the other terms to study the full three-body problem. Consequently the electronic term makes up the zero order term of the J-functional, and therefore it is of great importance that we design our numerical scheme, to be used on the full H_2^+ problem, in such a way that we obtain a good estimate of the electronic term. Secondly, since the Born-Oppenheimer solutions for H_2^+, are well-documented, in terms of tables of potential-energies, this also gives us the possibility to test and optimize the numerical scheme; a thing that would not have been possible to the same extent if we had moved on to the full three-body problem right away.

In the Born-Oppenheimer approximation, to repeat, we fix the nuclear separation R and solve the electronic problem using the variational method discussed previously - just now we

exclude the surface term (the R-matrix) since this is of course not a scattering situation[63]. For the hydrogen atom, by virtue of spherical symmetry of the system, the operators $\mathbf{L}^2$ and $\mathbf{L}_z$ both commute with the Hamiltonian, and hence, see chapter 4 section 1, we can characterize the wave function according to the values of (J, m). For H_2^+ on the other hand we do not have spherical symmetry, and we would find that $[\mathbf{L}^2, \mathbf{H}_{\text{elec}}] \neq 0$. In other words the total electronic orbital angular momentum is not a constant for H_2^+, and the wave functions can not be characterized by a sharp J. However, we do have axial symmetry, recalling that the two-body system of the protons belong to the point group $D_{\infty h}$. In the discussion on rotations in chapter 4 section 3, we "showed" that the generator of rotations about the z-axis is the z-component of the total orbital angular momentum, and hence we conclude that for H_2^+ we have $[\mathbf{L}_z, \mathbf{H}_{\text{elec}}] = 0$. Therefore the electronic wave function can be chosen to be an eigenfunction to $\mathbf{L}_z$. In the spheroidal coordinates we derived an expression for $\mathbf{L}_z$ in Eq. (5.5.17), and the normalized eigenfunctions of $\mathbf{L}_z$ then read as $(2\pi)^{-\frac{1}{2}} \exp(\text{im}\phi)$ where $\text{m} = 0, \pm 1, \pm 2, \pm 3, \ldots,$. As stated earlier, and to be verified soon, the electronic problem is separable in the spheroidal coordinates, and therefore we assume that we can write any electronic wave function $\Psi_{\text{m}}(\xi, \eta, \phi)$, with sharp[64] m quantum number, as the following product function

$$\Psi_{\text{m}}(\xi, \eta, \phi) = (2\pi)^{-\frac{1}{2}} \exp(\text{im}\phi) \Phi_{\text{m}}(\xi, \eta) \tag{5.7.1}$$

where

$$\Phi_{\text{m}}(\xi, \eta) = \sum_{\Omega=1}^{\text{M}_\eta} \varphi_\Omega^{\text{m}}(\eta) \psi_\Omega^{\text{m}}(\xi) \tag{5.7.2}$$

The number of (still undefined) product functions, $\varphi_\Omega^{\text{m}}(\eta)\psi_\Omega^{\text{m}}(\xi)$, included in the above expansion of $\Phi_{\text{m}}(\xi, \eta)$, is denoted by M_η. In principle the expansion is not strictly exact if this number is finite, but knowing that the numerical scheme presented here, is to be implemented on a computer, with a limited core memory, we write the upper limit of the summation as a finite number, and just bear in mind that this number should be "large" to ensure convergence. At other places in this chapter we shall use the same notation for an, in principle, infinite sum of terms. Inserting Eq. (5.7.1) into the electronic A-term, Eq. (5.5.21), and integrating over ϕ (ignoring the Euler angles α and β since the nuclear are fixed) we obtain the following variational functional for the electronic problem

---

63 We are seeking electronic *bound* states for the H_2^+ system (i.e. $\Psi_{\text{elec}} \in L^2(V_{\text{elec}})$), and hence if we choose the volume of the configuration space in Eq. (2.2.1) to be very large (in principle infinitely large), the wave function will have no amplitude on the surface enclosing V_{elec}. Consequently $\Phi_{\text{elec}} = 0$ in Eq. (2.2.1), and the surface term vanish. The working equation then reads as Eq. (2.2.27) except that the N'th row and column have vanished.

64 An arbitrary $\Psi(\xi, \eta, \phi)$ would then be expressed as a linear combination of these functions.

$$
\begin{aligned}
J'_{\text{elec}}(\Phi_m) &= \int_1^\infty d\xi \int_{-1}^1 d\eta \left\{ \left[\left(E - \frac{e^2}{8\pi\varepsilon_0 f} \right) (\xi^2 - \eta^2) + \frac{e^2 \xi}{2\pi\varepsilon_0 f} \right] |\Phi_m|^2 \right. \\
&\quad \left. - \frac{\hbar^2}{2\mu_e f^2} \left[(\xi^2 - 1) \left| \frac{\partial \Phi_m}{\partial \xi} \right|^2 + (1 - \eta^2) \left| \frac{\partial \Phi_m}{\partial \eta} \right|^2 + \left(\frac{m^2}{\xi^2 - 1} + \frac{m^2}{1 - \eta^2} \right) |\Phi_m|^2 \right] \right\} \\
&= \frac{\hbar^2}{2\mu_e f^2} \int_1^\infty d\xi \int_{-1}^1 d\eta \left\{ \frac{2\mu_e f^2}{\hbar^2} \left[\left(E - \frac{e^2}{8\pi\varepsilon_0 f} \right) (\xi^2 - \eta^2) + \frac{e^2 \xi}{2\pi\varepsilon_0 f} \right] |\Phi_m|^2 \right. \\
&\quad \left. - (\xi^2 - 1) \left| \frac{\partial \Phi_m}{\partial \xi} \right|^2 - (1 - \eta^2) \left| \frac{\partial \Phi_m}{\partial \eta} \right|^2 - \left(\frac{m^2}{\xi^2 - 1} + \frac{m^2}{1 - \eta^2} \right) |\Phi_m|^2 \right\}
\end{aligned}
\tag{5.7.3}
$$

As the nuclear are fixed in this treatment the first factor in Eq. (5.7.3) is just a constant, and we are free[65] to define a new variational functional without this factor giving the exact same physical solutions.

$$
\begin{aligned}
J_{\text{elec}}(\Phi_m) &= \int_1^\infty d\xi \int_{-1}^1 d\eta \left\{ \left[\lambda\xi - \kappa(\xi^2 - \eta^2) - \frac{m^2}{\xi^2 - 1} \right] |\Phi_m|^2 \right. \\
&\quad \left. - (\xi^2 - 1) \left| \frac{\partial \Phi_m}{\partial \xi} \right|^2 - (1 - \eta^2) \left| \frac{\partial \Phi_m}{\partial \eta} \right|^2 - \frac{m^2}{1 - \eta^2} |\Phi_m|^2 \right\}
\end{aligned}
\tag{5.7.4}
$$

where we have defined the parameters

$$
\begin{aligned}
\kappa &\equiv -\frac{2\mu_e f^2}{\hbar^2} \left(E - \frac{e^2}{8\pi\varepsilon_0 f} \right) \\
\lambda &\equiv \frac{\mu_e e^2 f}{\hbar^2 \pi\varepsilon_0}
\end{aligned}
\tag{5.7.5}
$$

so that, in favor of these parameters, the J-functional does not depend explicitly on the energy and the nuclear separation any more. Presently we are interested only in the bound states (i.e. $E < 0$) of the investigated system, and hence we choose $\kappa > 0$. Note also that the m quantum number only enters the variational functional in the form m^2. This implies that the energies of the states are independent of the sign of m, so that states with a given m quantum number are at least doubly degenerate. Without loss of generality we can therefore choose *m to be a positive integer or zero*.

We now proceed with a finite basis expansion of $\varphi_\Omega^m(\eta)$ in normalized associated Legendre polynomials[66], $\bar{P}_\ell^m(\eta)$. The use of associated Legendre polynomials in the

---

65 A constant factor does of course not effect the solutions obtained upon variation of a functional.

66 The explicit expression for the normalized associated Legendre polynomials of order m and degree ℓ reads as

$$
\bar{P}_\ell^m(\eta) \equiv \sqrt{\frac{(2\ell+1)(\ell-m)!}{2(\ell+m)!}} P_\ell^m(\eta), \quad 0 \le m \le \ell
$$

where the associated Legendre polynomials themselves are defined as

expansion of $\varphi_\Omega^{\mathrm{m}}(\eta)$ is an approach followed in most studies of the electronic H_2^+ system, for obvious reasons as we shall soon see. Furthermore since these functions are orthogonal polynomials they also define an underlying DVR grid as discussed in chapter 3 section 3. Hence this choice of primitive basis functions ensures that we can define a DVR scheme in the η coordinate to be used in the evaluation of the higher order terms of the J-functional. In order to adapt the DVR scheme discussed in chapter 3 section 3 directly, we will use *normalized* associated Legendre polynomials. We write

$$\varphi_\Omega^{\mathrm{m}}(\eta) = \sum_{\ell=1}^{N_\eta} C_{\ell\Omega} \overline{P}^{\mathrm{m}}_{\mathrm{m}+\ell-1}(\eta) \tag{5.7.6}$$

where

$$\int_{-1}^{1} d\eta \left\{ \overline{P}_\ell^{\mathrm{m}}(\eta) \overline{P}_{\ell'}^{\mathrm{m}}(\eta) \right\} = \delta_{\ell\ell'}, \quad 0 \le \mathrm{m} \le \ell, \ell' \tag{5.7.7}$$

When inserting the expansion, Eq. (5.7.6), into Eq. (5.7.2) and substituting the result into the functional, Eq. (5.7.4), it is clear that the two last terms in Eq. (5.7.4) introduce integrals over η of the type

$$\begin{aligned} I_{\ell\ell'} &\equiv \int_{-1}^{1} d\eta \left\{ \left(1-\eta^2\right) \frac{\partial \overline{P}_\ell^{\mathrm{m}}(\eta)}{\partial \eta} \frac{\partial \overline{P}_{\ell'}^{\mathrm{m}}(\eta)}{\partial \eta} \right\} + \int_{-1}^{1} d\eta \left\{ \frac{\mathrm{m}^2}{1-\eta^2} \overline{P}_\ell^{\mathrm{m}}(\eta) \overline{P}_{\ell'}^{\mathrm{m}}(\eta) \right\} \\ &= \left[\overline{P}_\ell^{\mathrm{m}}(\eta) \left(1-\eta^2\right) \frac{\partial \overline{P}_{\ell'}^{\mathrm{m}}(\eta)}{\partial \eta} \right]_{-1}^{1} - \int_{-1}^{1} d\eta \left\{ \overline{P}_\ell^{\mathrm{m}}(\eta) \left[\left(1-\eta^2\right) \frac{\partial^2 \overline{P}_{\ell'}^{\mathrm{m}}(\eta)}{\partial \eta^2} - 2\eta \frac{\partial \overline{P}_{\ell'}^{\mathrm{m}}(\eta)}{\partial \eta} \right] \right\} \\ &\quad + \int_{-1}^{1} d\eta \left\{ \frac{\mathrm{m}^2}{1-\eta^2} \overline{P}_\ell^{\mathrm{m}}(\eta) \overline{P}_{\ell'}^{\mathrm{m}}(\eta) \right\} \\ &= \int_{-1}^{1} d\eta \left\{ \overline{P}_\ell^{\mathrm{m}}(\eta) \left[\frac{\mathrm{m}^2}{1-\eta^2} \overline{P}_{\ell'}^{\mathrm{m}}(\eta) - \left(1-\eta^2\right) \frac{\partial^2 \overline{P}_{\ell'}^{\mathrm{m}}(\eta)}{\partial \eta^2} + 2\eta \frac{\partial \overline{P}_{\ell'}^{\mathrm{m}}(\eta)}{\partial \eta} \right] \right\} \end{aligned} \tag{5.7.8}$$

where we have made a simple integration by parts. It is at this very point that we can "justify" for the particular choice of basis functions, Eq. (5.7.6), in the η-coordinate; associated Legendre polynomials satisfy the characteristic second order differential equation [52]

$$P_\ell^{\mathrm{m}}(\eta) \equiv \frac{1}{2^\ell \ell!} \left(1-\eta^2\right)^{\mathrm{m}/2} \left(\frac{\mathrm{d}}{\mathrm{d}\eta} \right)^{\mathrm{m}+\ell} \left[\left(\eta^2-1\right)^\ell \right], \quad 0 \le \mathrm{m} \le \ell$$

and satisfy the orthogonality relation

$$\int_{-1}^{1} d\eta \left\{ P_\ell^{\mathrm{m}}(\eta) P_{\ell'}^{\mathrm{m}}(\eta) \right\} = \frac{2(\ell+\mathrm{m})!}{(2\ell+1)(\ell-\mathrm{m})!} \delta_{\ell\ell'}$$

$$\left(1-\eta^2\right)\frac{\partial^2 \mathrm{P}_\ell^{\mathrm{m}}(\eta)}{\partial\eta^2}-2\eta\frac{\partial \mathrm{P}_\ell^{\mathrm{m}}(\eta)}{\partial\eta}+\left[\ell(\ell+1)-\frac{\mathrm{m}^2}{1-\eta^2}\right]\mathrm{P}_\ell^{\mathrm{m}}(\eta)=0 \tag{5.7.9}$$

which does of course also hold for the normalized associated Legendre polynomials, such that

$$\frac{\mathrm{m}^2}{1-\eta^2}\overline{\mathrm{P}}_\ell^{\mathrm{m}}(\eta)-\left(1-\eta^2\right)\frac{\partial^2 \overline{\mathrm{P}}_\ell^{\mathrm{m}}(\eta)}{\partial\eta^2}+2\eta\frac{\partial \overline{\mathrm{P}}_\ell^{\mathrm{m}}(\eta)}{\partial\eta}=\ell(\ell+1)\overline{\mathrm{P}}_\ell^{\mathrm{m}}(\eta) \tag{5.7.10}$$

Inserting this into Eq. (5.7.8) then gives the simple result

$$\mathrm{I}_{\ell\ell'}=\ell(\ell+1)\int_{-1}^{1}\mathrm{d}\eta\left\{\overline{\mathrm{P}}_\ell^{\mathrm{m}}(\eta)\overline{\mathrm{P}}_{\ell'}^{\mathrm{m}}(\eta)\right\}=\ell(\ell+1)\delta_{\ell\ell'} \tag{5.7.11}$$

The ξ-derivative term in Eq. (5.7.4) is clearly diagonal in the expansion in normalized associated Legendre polynomials. However this is not the case for the first term of the variational functional since it involves integrals over η^2. As we will see this gives coupling in the different degrees, ℓ, of the normalized associated Legendre polynomials, but again we can derive an analytical expression for the integral, this time taking point of reference in the following recurrence relation[67] .

$$\eta\overline{\mathrm{P}}_\ell^{\mathrm{m}}(\eta)\equiv \mathrm{Y}_\ell^{\mathrm{m}}\overline{\mathrm{P}}_{\ell-1}^{\mathrm{m}}(\eta)+\mathrm{Y}_{\ell+1}^{\mathrm{m}}\overline{\mathrm{P}}_{\ell+1}^{\mathrm{m}}(\eta) \tag{5.7.12}$$

where we have defined the factor

$$\mathrm{Y}_\ell^{\mathrm{m}}\equiv\sqrt{\frac{(\ell+\mathrm{m})(\ell-\mathrm{m})}{(2\ell+1)(2\ell-1)}} \tag{5.7.13}$$

---

67 The associated Legendre polynomials satisfy the following recurrence relation [52]

$$\eta\mathrm{P}_\ell^{\mathrm{m}}(\eta)=\frac{\ell+\mathrm{m}}{2\ell+1}\mathrm{P}_{\ell-1}^{\mathrm{m}}(\eta)+\frac{\ell-\mathrm{m}+1}{2\ell+1}\mathrm{P}_{\ell+1}^{\mathrm{m}}(\eta)$$

and multiplying this relation by the normalization factor we obtain a recurrence relation for the normalized associated Legendre polynomials

$$\begin{aligned}\eta\overline{\mathrm{P}}_\ell^{\mathrm{m}}(\eta)&=\frac{\ell+\mathrm{m}}{2\ell+1}\sqrt{\frac{(2\ell+1)(\ell-\mathrm{m})!}{2(\ell+\mathrm{m})!}}\mathrm{P}_{\ell-1}^{\mathrm{m}}(\eta)+\frac{\ell-\mathrm{m}+1}{2\ell+1}\sqrt{\frac{(2\ell+1)(\ell-\mathrm{m})!}{2(\ell+\mathrm{m})!}}\mathrm{P}_{\ell+1}^{\mathrm{m}}(\eta)\\&=\sqrt{\frac{(\ell+\mathrm{m})(\ell-\mathrm{m})}{(2\ell+1)(2\ell-1)}}\sqrt{\frac{(2\ell-1)(\ell-1-\mathrm{m})!}{2(\ell-1+\mathrm{m})!}}\mathrm{P}_{\ell-1}^{\mathrm{m}}(\eta)+\sqrt{\frac{(\ell+\mathrm{m}+1)(\ell+1-\mathrm{m})}{(2\ell+3)(2\ell+1)}}\sqrt{\frac{(2\ell+3)(\ell+1-\mathrm{m})!}{2(\ell+1+\mathrm{m})!}}\mathrm{P}_{\ell+1}^{\mathrm{m}}(\eta)\\&=\sqrt{\frac{(\ell+\mathrm{m})(\ell-\mathrm{m})}{(2\ell+1)(2\ell-1)}}\overline{\mathrm{P}}_{\ell-1}^{\mathrm{m}}(\eta)+\sqrt{\frac{(\ell+\mathrm{m}+1)(\ell+1-\mathrm{m})}{(2\ell+3)(2\ell+1)}}\overline{\mathrm{P}}_{\ell+1}^{\mathrm{m}}(\eta)\equiv\mathrm{Y}_\ell^{\mathrm{m}}\overline{\mathrm{P}}_{\ell-1}^{\mathrm{m}}(\eta)+\mathrm{Y}_{\ell+1}^{\mathrm{m}}\overline{\mathrm{P}}_{\ell+1}^{\mathrm{m}}(\eta)\end{aligned}$$

The η^2-integral then reads as

$$\begin{aligned}\int_{-1}^{1} d\eta\left\{\overline{P}_{\ell}^{m}(\eta)\eta\eta\overline{P}_{\ell'}^{m}(\eta)\right\} &= Y_{\ell}^{m}Y_{\ell'}^{m}\int_{-1}^{1} d\eta\left\{\overline{P}_{\ell-1}^{m}(\eta)\overline{P}_{\ell'-1}^{m}(\eta)\right\} + Y_{\ell}^{m}Y_{\ell'+1}^{m}\int_{-1}^{1} d\eta\left\{\overline{P}_{\ell-1}^{m}(\eta)\overline{P}_{\ell'+1}^{m}(\eta)\right\} \\ &+ Y_{\ell+1}^{m}Y_{\ell'}^{m}\int_{-1}^{1} d\eta\left\{\overline{P}_{\ell+1}^{m}(\eta)\overline{P}_{\ell'-1}^{m}(\eta)\right\} + Y_{\ell+1}^{m}Y_{\ell'+1}^{m}\int_{-1}^{1} d\eta\left\{\overline{P}_{\ell+1}^{m}(\eta)\overline{P}_{\ell'+1}^{m}(\eta)\right\} \quad (5.7.14) \\ &= \left(Y_{\ell}^{m}\right)^2\delta_{\ell\ell'} + Y_{\ell}^{m}Y_{\ell-1}^{m}\delta_{\ell\ell'+2} + Y_{\ell+1}^{m}Y_{\ell+2}^{m}\delta_{\ell\ell'-2} + \left(Y_{\ell+1}^{m}\right)^2\delta_{\ell\ell'}\end{aligned}$$

and we conclude that terms of this type couples the normalized associated Legendre polynomial of degree ℓ to polynomials of degree $\ell \pm 2$. In other words we obtain a very simple band structure for the matrix representation of the J-functional in the normalized associated Legendre polynomials, see figure 13.

	$\overline{P}_{m}^{m}$	$\overline{P}_{m+1}^{m}$	$\overline{P}_{m+2}^{m}$	$\overline{P}_{m+3}^{m}$	$\overline{P}_{m+4}^{m}$	$\overline{P}_{m+5}^{m}$	$\overline{P}_{m+6}^{m}$
$\overline{P}_{m}^{m}$		$\overline{\overline{0}}$		$\overline{\overline{0}}$	$\overline{\overline{0}}$	$\overline{\overline{0}}$	$\overline{\overline{0}}$
$\overline{P}_{m+1}^{m}$	$\overline{\overline{0}}$		$\overline{\overline{0}}$		$\overline{\overline{0}}$	$\overline{\overline{0}}$	$\overline{\overline{0}}$
$\overline{P}_{m+2}^{m}$		$\overline{\overline{0}}$		$\overline{\overline{0}}$		$\overline{\overline{0}}$	$\overline{\overline{0}}$
$\overline{P}_{m+3}^{m}$	$\overline{\overline{0}}$		$\overline{\overline{0}}$		$\overline{\overline{0}}$		$\overline{\overline{0}}$
$\overline{P}_{m+4}^{m}$	$\overline{\overline{0}}$	$\overline{\overline{0}}$		$\overline{\overline{0}}$		$\overline{\overline{0}}$	
$\overline{P}_{m+5}^{m}$	$\overline{\overline{0}}$	$\overline{\overline{0}}$	$\overline{\overline{0}}$		$\overline{\overline{0}}$		$\overline{\overline{0}}$
$\overline{P}_{m+6}^{m}$	$\overline{\overline{0}}$	$\overline{\overline{0}}$	$\overline{\overline{0}}$	$\overline{\overline{0}}$		$\overline{\overline{0}}$	

Figure 13 Band structure of the S-matrix

We now define the expansion coefficients, $C_{\ell\Omega}$, in Eq. (5.7.2), as the elements of the real unitary $N_\eta \times M_\eta$ matrix $\overline{\overline{C}}$ which diagonalizes the $N_\eta \times N_\eta$ matrix $\overline{\overline{S}}$ (see figure 13 where $N_\eta = 7$) defined as[68]

$$\begin{aligned}S_{\ell\ell'} \equiv{}& \kappa Y_{m+\ell}^{m}Y_{m+\ell+1}^{m}\delta_{\ell\ell'-2} + \kappa Y_{m+\ell-1}^{m}Y_{m+\ell-2}^{m}\delta_{\ell\ell'+2} \\ &+\left[\kappa\left(Y_{m+\ell-1}^{m}\right)^2 + \kappa\left(Y_{m+\ell}^{m}\right)^2 - (m+\ell-1)(m+\ell)\right]\delta_{\ell\ell'}\end{aligned} \quad (5.7.15)$$

That is

$$\overline{\overline{C}}^{T}\overline{\overline{S}}\overline{\overline{C}} = \overline{\overline{\Lambda}} \quad (5.7.16)$$

---

68 To obtain row and column index for the matrix, going from 1 to N_η, we have made the substitutions $\ell \to m + \ell - 1$ and $\ell' \to m + \ell' - 1$. Consequently for $1 \le \ell \le 2$ or $N_\eta - 1 \le \ell \le N_\eta$ the corresponding off diagonal terms should not enter the definition of $\overline{\overline{S}}$.

In this way we have constructed a set of basis functions, $\{\varphi_\Omega^m(\eta), \Omega = 1,\ldots,M_\eta\}$, in which the matrix representation of the J-functional is now block diagonal - as opposed to the block structure illustrated in figure 13. Finally we insert the expansion, Eq. (5.7.2), into the functional, Eq. (5.7.4), use the definition of the matrix $\overline{\overline{C}}$ in Eq. (5.7.15,16) and the fact that the basis functions, $\varphi_\Omega^m(\eta)$, are orthonormal[69], and obtain the following J-functional

$$J_{elec}(\Phi_m) = \sum_{\Omega=1}^{M_\eta} \int_1^\infty d\xi \left\{ \left[\lambda\xi - \kappa\xi^2 + \Lambda_\Omega^m - \frac{m^2}{\xi^2-1} \right] \left|\psi_\Omega^m\right|^2 - \left(\xi^2-1\right) \left| \frac{\partial \psi_\Omega^m}{\partial \xi} \right|^2 \right\} \qquad (5.7.17)$$

where we have denoted the elements of the $M_\eta \times M_\eta$ diagonal matrix $\overline{\overline{\Lambda}}$, in Eq (5.7.16), by Λ_Ω^m.

The next step is the expansion of $\psi_\Omega^m(\xi)$, Eq. (5.7.2), in a suitable set of basis functions, followed by the integration of the variational functional in the ξ coordinate. If we were "just" to solve the electronic problem, a natural choice would be to use the Hylleraas [13] or the Jaffé [14] expansion[70] resulting in simple three-term recursion relations, much like the one we obtained in the normalized associated Legendre expansion of $\varphi_\Omega^m(\eta)$. Nevertheless this is not the type of expansion that we will use. Besides convergence of the electronic term, the important point that must be taken into consideration in choosing the form of expansion is the simplicity of the numerical scheme that is to be implemented on the non-adiabatic terms of the J-functional. In other words a direct application using one of the "standard" expansions for the electronic term, would result in integrals for the non-adiabatic terms that could not "easily" be dealt with numerically. When I started out with this project, at the University of Aarhus, I spent some time implementing a FEM-expansion of $\psi_\Omega^m(\xi)$ in Hermite type functions (see Appendix C) known from Spline type interpolation. This was a relatively easy task, but as I later on was to include the non-adiabatic terms, it soon became clear to me that this was far from trivial in the FEM formulation. Though I had no reason to believe that it was practically impossible to carry out such an implementation, I started to look for a different numerical approach, and for this reason I have moved the description of the Hermite-type FEM to an appendix (C). Eventually I spent two weeks with Professor Claude

---

69 The normalized associated Legendre polynomials are orthonormal, Eq. (5.7.7), and since the matrix $\overline{\overline{C}}$, through the definition Eq. (5.7.16), is real unitary the basis functions $\varphi_\Omega^m(\eta)$ are also orthonormal - that is

$$\int_{-1}^{1} d\eta \left\{ \varphi_\Omega^m(\eta) \varphi_{\Omega'}^m(\eta) \right\} = \delta_{\Omega\Omega'}, \quad 0 \le m \le \Omega, \Omega'$$

70 The Jaffé [14] expansion reads as

$$\psi_\Omega^m(\xi) = \left(\xi^2-1\right)^{m/2} (\xi+1)^\sigma e^{-p\xi} \sum_{n=1}^{\infty} C_n^\Omega \left(\frac{\xi-1}{\xi+1} \right)^{n-1}$$

where $\sigma = R/(2p) - m - 1$ and $p = -\frac{1}{4}R^2E$. Hylleraas [13] on the other hand uses associated Laguerre polynomials in the expansion of $\psi_\Omega^m(\xi)$

$$\psi_\Omega^m(\xi) = \left(\xi^2-1\right)^{m/2} e^{-u/2} \sum_{n=1}^{\infty} \frac{C_n^\Omega}{(m+n-1)!} L_{m+n-1}^m(u)$$

where $u = 2p(\xi-1)$.

Leforestier [7] studying the discrete variable representation method discussed in chapter 3 section 3. The only problem was now to construct an expansion of $\psi_\Omega^m(\xi)$ upon which a DVR quadrature scheme could most conveniently be based. Somewhat inspired by the original Hylleraas expansion [13] I came up with a formulation, which, in my opinion, provides a very straightforward and easy numerical scheme.

As the formulation to be described now, is based on an expansion of $\psi_\Omega^m(\xi)$ in associated Laguerre polynomials[71], $L_n^m(x)$, we shall first have to introduce a new coordinate, say ζ[72], that has a domain of definition from zero to infinity rather than from 1 to infinity as is the range for the spheroidal coordinate ξ. We define the following change of coordinate, $\xi \to \zeta$,

$$\zeta \equiv c(\xi - 1) \quad \Rightarrow \quad \begin{cases} \xi = \dfrac{\zeta}{c} + 1 \quad \Rightarrow \quad \dfrac{d\xi}{d\zeta} = \dfrac{1}{c} \\ c^2(\xi^2 - 1) = \zeta(\zeta + 2c) \end{cases} \tag{5.7.18}$$

where c is a scaling constant. This change of coordinate leads to the functional[73]

$$J_{elec}(\Phi_m) = \sum_{\Omega=1}^{M_\eta} \int_0^\infty d\zeta \left\{ \left[\lambda\left(\frac{\zeta}{c} + 1\right) - \kappa\left(\frac{\zeta}{c} + 1\right)^2 + \Lambda_\Omega^m - \frac{m^2 c^2}{\zeta(\zeta + 2c)} \right] \left|\psi_\Omega^m\right|^2 - \zeta(\zeta + 2c) \left| \frac{\partial \psi_\Omega^m}{\partial \zeta} \right|^2 \right\} \tag{5.7.19}$$

We now write $\psi_\Omega^m(\zeta)$ as an expansion

$$\psi_\Omega^m(\zeta) = \sum_{\Lambda=1}^{M_\zeta} \sum_{n=1}^{N_\zeta} D_{n\Lambda}^\Omega \phi_{n-1}^m(\zeta) \tag{5.7.20}$$

in the so-called normalized associated Laguerre *functions*

$$\phi_n^m(\zeta) \equiv \sqrt{\frac{n!}{(n+m)!}} e^{-\zeta/2} \zeta^{m/2} L_n^m(\zeta), \quad m, n \geq 0 \tag{5.7.21}$$

that satisfy

---

71 In this thesis we use the following definition for the associated Laguerre polynomials [52]

$$L_n^m(x) \equiv \frac{e^x x^{-m}}{n!} \frac{d^n}{dx^n}\left[e^{-x} x^{n+m}\right], \quad n, m \geq 0$$

Some authors, for m a positive integer or zero, define the associated Laguerre polynomials by the equation

$$\mathcal{L}_n^m(x) \equiv \frac{d^m}{dx^m}\left[\mathcal{L}_n(x)\right], \quad \text{where} \quad \mathcal{L}_n(x) \equiv e^x \frac{d^n}{dx^n}\left[e^{-x} x^n\right]$$

such that

$$\mathcal{L}_{n+m}^m(x) = (-1)^m (n+m)! L_n^m(x)$$

72 Though the reader might confuse the new Greek letter ζ (zeta) with the old ξ (xi), the former has been chosen for this exact same similarity, simply to stress the fact that this change of coordinate is a mere mathematical redefinition of a variable, and as such has no underlying physical meaning as did characterize the change of coordinates described up till now.

73 We have ignored the constant scaling parameter c entering the functional from the change of the volume element.

$$\int_0^\infty d\xi \left\{ \phi_n^m(\xi) \phi_{n'}^m(\xi) \right\} = \delta_{nn'}, \quad m, n, n' \geq 0 \tag{5.7.22}$$

When inserting the expansion, Eq. (5.7.20), into Eq. (5.7.19) the last term of the functional introduces integrals that can be rewritten in terms of a simple integration by parts

$$\begin{aligned} I_{nn'} &= \int_0^\infty d\xi \left\{ \xi(\xi + 2c) \frac{\partial \phi_n^m(\xi)}{\partial \xi} \frac{\partial \phi_{n'}^m(\xi)}{\partial \xi} \right\} \\ &= \left[\phi_n^m(\xi) \xi(\xi + 2c) \frac{\partial \phi_{n'}^m(\xi)}{\partial \xi} \right]_0^\infty - \int_0^\infty d\xi \left\{ \left(2(\xi + c) \frac{\partial \phi_{n'}^m(\xi)}{\partial \xi} + (\xi + 2c) \xi \frac{\partial^2 \phi_{n'}^m(\xi)}{\partial^2 \xi} \right) \phi_n^m(\xi) \right\} \end{aligned} \tag{5.7.23}$$

where the first term vanishes due to the asymptotic behavior of the associated Laguerre functions[74]. The associated Laguerre functions satisfy the following second order differential equation [52]

$$\xi \frac{\partial^2 \phi_n^m(\xi)}{\partial^2 \xi} = -\frac{\partial \phi_n^m(\xi)}{\partial \xi} + \left(\frac{m^2}{4\xi} + \frac{\xi}{4} - n - \frac{m}{2} - \frac{1}{2} \right) \phi_n^m(\xi) \tag{5.7.24}$$

Inserting this relation into Eq. (5.7.23), and collecting terms in $\partial \phi_n^m / \partial \xi$ gives

$$I_{nn'} = -\int_0^\infty d\xi \left\{ \xi \frac{\partial \phi_{n'}^m(\xi)}{\partial \xi} + (\xi + 2c) \left(\frac{m^2}{4\xi} + \frac{\xi}{4} - n' - \frac{m}{2} - \frac{1}{2} \right) \phi_{n'}^m(\xi) \right\} \phi_n^m(\xi) \tag{5.7.25}$$

Further for the associated Laguerre functions we have the recursion relation [52]

$$\xi \frac{\partial \phi_n^m(\xi)}{\partial \xi} = \left(\frac{m}{2} + n - \frac{\xi}{2} \right) \phi_n^m(\xi) - \sqrt{n(n+m)} \phi_{n-1}^m(\xi) \tag{5.7.26}$$

and inserting this into the expression for $I_{nn'}$, Eq. (5.7.25), gives

$$I_{nn'} = -\int_0^\infty d\xi \left\{ \left[\frac{m}{2} + n' - \frac{\xi}{2} + (\xi + 2c) \left(\frac{m^2}{4\xi} + \frac{\xi}{4} - n' - \frac{m}{2} - \frac{1}{2} \right) \right] \phi_{n'}^m(\xi) - \sqrt{n'(n'+m)} \phi_{n'-1}^m(\xi) \right\} \phi_n^m(\xi) \tag{5.7.27}$$

Finally we can rewrite the whole electronic J-functional[75]

---

74 The associated Laguerre functions, as opposed to the polynomials themselves, are elements in the Hilbert space. From the definition Eq. (5.7.21) we deduce the correct asymptotic behavior of the functions

$$\lim_{\xi \to \infty} \left[\phi_n^m(\xi) \right] = 0$$

75 In the rewriting of the J-functional we have used the identity

$$-\frac{m^2 c^2}{\xi(\xi + 2c)} + (\xi + 2c) \frac{m^2}{4\xi} = \frac{m^2(\xi + 4c)}{4(\xi + 2c)}$$

and ignored the constant factor, c^{-1}, entering the volume element of the functional. Note also that in Eq. (5.7.28) the last term should only be included for $2 \leq n' \leq N_\xi$.

$$J_{elec}(\Phi_m) = \sum_{\Omega=1}^{M_\eta}\sum_{\Lambda=1}^{M_\xi}\sum_{\Lambda'=1}^{M_\xi}\sum_{n=1}^{N_\xi}\sum_{n'=1}^{N_\xi} D_{n\Delta}^{\Omega} D_{n'\Lambda'}^{\Omega} \int_0^\infty d\xi \Bigg\{ \Bigg[\lambda\left(\frac{\xi}{c}+1\right) - \kappa\left(\frac{\xi}{c}+1\right)^2 + \Lambda_\Omega^m + \frac{m^2(\xi+4c)}{4(\xi+2c)} + \frac{m}{2} + (n'-1) - \frac{\xi}{2} + (\xi+2c)\left(\frac{\xi}{4} - (n'-1) - \frac{m}{2} - \frac{1}{2}\right) \Bigg] \phi_{n'-1}^m(\xi) - \sqrt{(n'-1)(m+n'-1)}\,\phi_{n'-2}^m(\xi) \Bigg\} \phi_{n-1}^m(\xi) \tag{5.7.28}$$

Next we discuss how to obtain numerical values for the integrals entering in the above variational functional. The associated Laguerre functions satisfy the recurrence relation [52]

$$\xi\phi_n^m(\xi) = -B_{n+1}^m \phi_{n+1}^m(\xi) + A_n^m \phi_n^m(\xi) - B_n^m \phi_{n-1}^m(\xi) \tag{5.7.29}$$

where we have defined the two factors

$$A_n^m \equiv 2n + m + 1, \quad B_n^m \equiv \sqrt{n(n+m)} \tag{5.7.30}$$

so that

$$\int_0^\infty d\xi \left\{ \phi_n^m(\xi)\xi\phi_{n'}^m(\xi) \right\} = -B_{n+1}^m \delta_{n+1n'} + A_n^m \delta_{nn'} - B_n^m \delta_{n-1n'} \tag{5.7.31}$$

and

$$\int_0^\infty d\xi \left\{ \phi_n^m(\xi)\xi^2\phi_{n'}^m(\xi) \right\} = B_n^m B_{n-1}^m \delta_{n-2n'} - \left[A_n^m B_n^m + A_{n-1}^m B_n^m \right] \delta_{n-1n'} + \left[\left(B_n^m\right)^2 + \left(A_n^m\right)^2 + \left(B_{n+1}^m\right)^2 \right] \delta_{nn'} - \left[A_{n+1}^m B_{n+1}^m + A_n^m B_{n+1}^m \right] \delta_{n+1n'} + B_{n+2}^m B_{n+1}^m \delta_{n+2n'} \tag{5.7.32}$$

Using the orthonormality of the associated Laguerre functions and the above two relations, Eq. (5.7.31,32), the integrals in the variational functional, Eq. (5.7.28), can be determined analytically, except for the one term where ξ enters the denominator. To evaluate this terms we will have to use a numerical method, and as suggested before we are going to use the DVR method. Following the exact procedure outlined in chapter 3 section 3, we write

$$\int_0^\infty dx \left\{ \phi_n^m(\xi) \frac{m^2(\xi+4c)}{4(\xi+2c)} \phi_{n'}^m(\xi) \right\} \approx \sum_{p=1}^{N_\xi}\sum_{q=1}^{N_\xi} U_{pn}^m U_{qn'}^m \left\langle X_p \left| \frac{m^2(\xi+4c)}{4(\xi+2c)} \right| X_q \right\rangle = \sum_{p=1}^{N_\xi} U_{pn}^m U_{pn'}^m \frac{m^2(\xi_p+4c)}{4(\xi_p+2c)} \tag{5.7.33}$$

where we have used Eq. (3.3.20,21). We now proceed by defining the following two $N_\xi \times N_\xi$ matrices

$$H^{\Omega}_{nn'} = \int_0^{\infty} d\xi \left\{ \left[\xi^2 \left(\frac{1}{4} - \frac{\kappa}{c^2} \right) + \xi \left(\frac{c}{2} + \frac{1-2\kappa}{c} - \frac{m}{2} - n' \right) + \left(\Lambda^m_{\Omega} - \kappa + \frac{m}{2} + n' + c(1-m-2n') \right) \right.\right.$$
$$\left.\left. + \frac{m^2(\xi+4c)}{4(\xi+2c)} \right] \phi^m_{n'-1}(\xi) - \sqrt{(n'-1)(m+n'-1)}\,\phi^m_{n'-2}(\xi) \right\} \phi^m_{n-1}(\xi) \tag{5.7.34}$$

and

$$S_{nn'} = \int_0^{\infty} d\xi \left\{ \phi^m_{n-1}(\xi) \left(\frac{\xi}{c} + 1 \right) \phi^m_{n'-1}(\xi) \right\} \tag{5.7.35}$$

where Eq. (5.7.31-33) are used to obtain the numerical values. Note that the matrix $\overline{\overline{S}}$ has a very simple tridiagonal structure (see Eq. (5.7.31)), as opposed to the matrix $\overline{\overline{H}}$, where integrals of the type discussed in connection with Eq. (5.7.33) enter. The variational functional now reads as

$$J_{elec} = \sum_{\Omega=1}^{M_\eta} \sum_{\Lambda=1}^{M_\xi} \sum_{\Lambda'=1}^{M_\xi} \sum_{n=1}^{N_\xi} \sum_{n'=1}^{N_\xi} D^{\Omega}_{n\Lambda} D^{\Omega}_{n'\Lambda'} \left\{ \lambda S_{nn'} - H^{\Omega}_{nn'} \right\} \tag{5.7.36}$$

To obtain the desired electronic bound states of the hydrogen molecular ion, we have to look for the stationary points of the above variational functional. Variation of Eq. (5.7.36) with respect to the expansion coefficients, $\partial J_{elec} / \partial D^{\Omega}_{n'\Lambda'} = 0$, leads, for each value of Ω, to the following secular equation

$$\overline{\overline{H}}\,\overline{\overline{D}} = \overline{\overline{S}}\,\overline{\overline{D}}\,\overline{\overline{\Gamma}} \tag{5.7.37}$$

where $\overline{\overline{D}}$ is an $N_\xi \times M_\xi$ matrix and where the Δ'th diagonal element of the $M_\xi \times M_\xi$ matrix $\overline{\overline{\Gamma}}$ denotes the λ value (see Eq. (5.7.5)) for the eigenstate

$$\psi^m_{\Omega\Lambda}(\xi) = \sum_{n=1}^{N_\xi} D^{\Omega}_{n\Lambda} \phi^m_{n-1}(\xi) \tag{5.7.38}$$

that is $\Gamma^{\Omega}_{\Lambda} = \lambda$. Eq. (5.7.37) is a so-called *generalized eigenvalue equation*, where the eigenvectors (given as the columns of $\overline{\overline{D}}$) are normalized over the matrix $\overline{\overline{S}}$

$$\overline{\overline{D}}^T \overline{\overline{H}}\,\overline{\overline{D}} = \overline{\overline{D}}^T \overline{\overline{S}}\,\overline{\overline{D}}\,\overline{\overline{\Gamma}} = \overline{\overline{\Gamma}} \tag{5.7.39}$$

It should be noted that Eq. (5.7.37) is not an eigenvalue equation of the energy of the system, such that the resulting states, $\psi^{m}_{\Omega\Delta}(\zeta)$, are not states in the "normal" sense. The following remark is intended to clarify this situation.

In the scheme outlined above we fixed the parameter κ and then solved the eigenvalue equations Eq. (5.7.17) and Eq. (5.7.38) to obtain a set of the two solution matrices $\overline{\overline{C}}$ and $\overline{\overline{D}}$ and a spectrum of the parameter λ (given as the diagonal elements of $\overline{\overline{\Gamma}}$). Using the definitions in Eq. (5.7.5) we then obtain a spectrum in f

$$f = \frac{\pi\hbar^2\varepsilon_0}{e^2\mu_e}\lambda \tag{5.7.40}$$

and in the energy

$$E = \frac{1}{2f}\left(\frac{e^2}{4\pi\varepsilon_0} - \frac{\hbar^2}{\mu_e f}\kappa\right) = 2\mu_e\left(\frac{e^2}{4\pi\varepsilon_0\hbar}\right)^2\frac{\lambda - 4\kappa}{\lambda^2} \tag{5.7.41}$$

To repeat, the basis functions, $\psi^{m}_{\Omega\Delta}(\zeta)$, are not eigenfunctions of the energy E of the system with a fixed nuclear separation f, but solutions where all the members of the set $\{\psi^{m}_{\Omega\Delta}(\zeta),\ \Omega = 1,..,M_\eta;\ \Delta = 1,..M_\xi\}$ correspond to the same value of the parameter κ. These circumstances resembles a situation where the potential in a Schrödinger equation is scaled in such a way that all the solutions correspond to the same value of the energy. Such a set of solutions are referred to as a *Sturmian basis-set* [6, 62]. To emphasize the connection with these functions, we shall call the bound states obtained from the scheme discussed above "Sturmian-like functions". The explicit expression for the eigenstates of the electronic H_2^+ system now read as

$$\begin{aligned}\Phi_m(\zeta,\eta) &= \sum_{\Omega=1}^{M_\eta}\sum_{\ell=1}^{N_\eta}\sum_{\Delta=1}^{M_\xi}\sum_{n=1}^{N_\xi} C_{\ell\Omega} D^{\Omega}_{n\Delta}\,\overline{P}^{m}_{m+\ell-1}(\eta)\phi^{m}_{n-1}(\zeta) \\ &= \sum_{(\Omega\Delta)}\sum_{(\ell n)} B_{(\ell n)(\Omega\Delta)}\overline{P}^{m}_{m+\ell-1}(\eta)\phi^{m}_{n-1}(\zeta)\end{aligned} \tag{5.7.42}$$

where we have defined the $(N_\eta + N_\xi)\times(M_\eta + M_\xi)$ matrix $\overline{\overline{B}}$. Each columns of this matrix correspond to an eigenfunction expressed in the primitive basis of the normalized associated Legendre and Laguerre functions. According to Eq. (5.7.1) the total (real) electronic wave function is then given as one of these eigenfunctions multiplied by the factor $(2\pi)^{-1/2}\cos(m\phi)$. In figure 14 below the explicit structure and construction of the matrix $\overline{\overline{B}}$ is illustrated. The hatched rectangles in this figure correspond to columns of $\overline{\overline{D}}$ (column vector) weighted by an element of the matrix $\overline{\overline{C}}$.

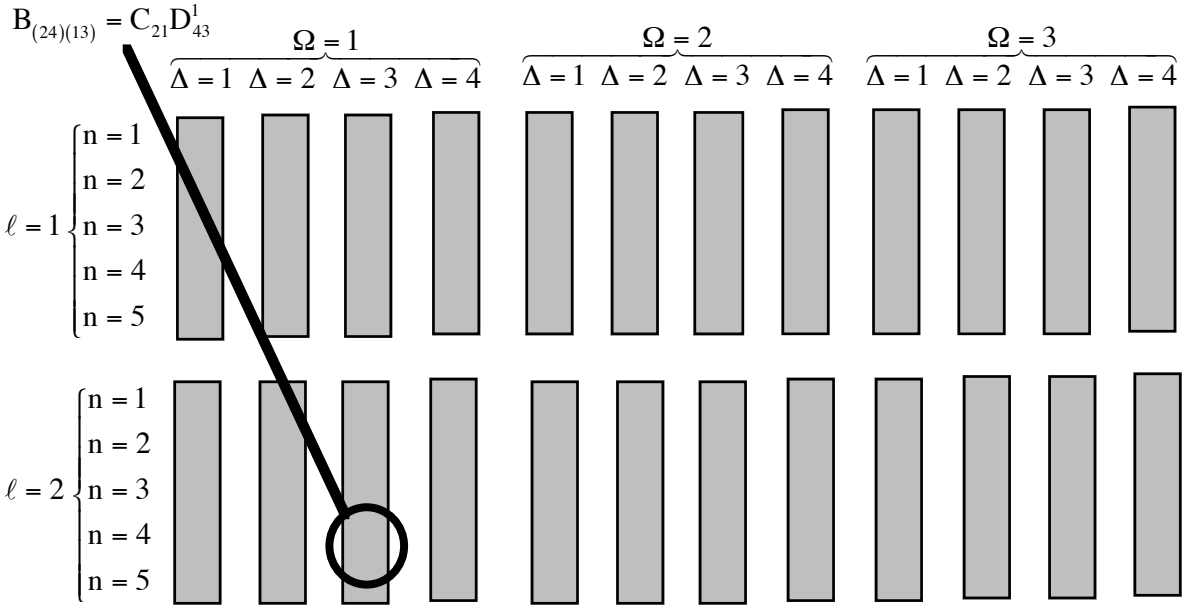

Figure 14 Construction of the basis-matrix

Before we move on to discussing the full three-body problem, we will shortly comment on the symmetry properties and labeling of the electronic states of the hydrogen molecular ion (corresponding to the columns of $\overline{\overline{B}}$). The two center system of H_2^+ that we are considering processes the following types of geometrical symmetry elements: an infinite-fold rotational axis C_∞ along the z-axis, an infinite number of C_2 axis and mirror planes σ_v perpendicular to the z-axis, a point of inversion at the nuclear center and finally a symmetry plane σ_h in the xy-plane. Thus it belongs to the point group $D_{\infty h}$. The reflection symmetry through the xy-plane leads to the fact that the eigenfunctions have definite η (or z) parity[76], and hence the eigenfunctions can be classified according to their parity. For even electronic wave functions, we use the subscript "g" (from the German word "gerade", meaning even); for odd wave functions we use "u" (from "ungerade"). As mentioned in the beginning of this section the z-component of the orbital angular momentum is conserved due to the rotationally symmetry around the z-axis, and consequently we could define the quantum number m. Following molecular physics, we then classify the eigenstates according to |±m| by Greek letters:

|±m|	0	1	2	3	4	.....
Symbol	σ	π	δ	ϕ	γ	.....

76 The inversion of the electronic coordinates (ζ, η, ϕ) through the nuclear center corresponds to the transformations

$$\zeta \to \zeta, \quad \eta \to -\eta, \quad \phi \to \phi + \pi$$

From the form, Eq. (5.7.1), of the ϕ eigenfunctions we see that the transformation $\phi \to \phi + \pi$ introduces a factor $(-1)^m$ in addition to any sign change from the transformation $\eta \to -\eta$.

Besides classifying the states of H_2^+ according to their η parity and the magnetic quantum number $|\pm m|$, we also give the eigenstates additional labels according to the usual atomic quantum numbers "n, l" in united atom limit (i.e. "$H_2^+ \xrightarrow[R\to 0]{} He^+$"), where

l	0	1	2	3	4	.....
Symbol	s	p	d	f	g	.....

as is customary in molecular physics, even though n and l are not good quantum numbers for $R \neq 0$. Following exactly the same procedure of Power [63], it can be shown that the number of nodes (for $\Psi_m(\xi,\eta,\phi)$) in each of the coordinates (ξ, η, ϕ) does not change with R, i.e. nodes are conserved. This conservation law enables us to find the correspondence relation between the united atom quantum numbers (n, l, m) and the number of nodes in (ξ, η, ϕ), i.e.[77] the function labels Ω, Δ and m in Eq. (5.7.42). The number of nodes in ϕ is simply m, and in coordinates ζ and η they are respectively $n - l - 1$ and $l - m$. We can then write

$$\Delta = n - l, \quad \Omega = l - m + 1 \tag{5.7.43}$$

or

$$n = \Omega + \Delta + m - 1, \quad l = \Omega + m - 1 \tag{5.7.44}$$

Using these relations and that fact that the parity is also conserved with R, we can construct the following table

Table 1 Labeling of the electronic states

State	$1s\sigma_g$	$2s\sigma_g$	$3s\sigma_g$	$2p\sigma_u$	$3p\sigma_u$	$4p\sigma_u$	$3d\sigma_g$	$4f\sigma_u$	$2p\pi_u$	$3d\pi_g$	$4f\pi_g$
Δ	1	2	3	1	2	3	1	1	1	1	1
Ω	1	1	1	2	2	2	3	4	1	2	3
n	1	2	3	2	3	4	3	4	2	3	4
l	0	0	0	1	1	1	2	3	1	2	3
m	0	0	0	0	0	0	0	0	1	1	1

77 In the united atom limit (He^+) the wave function is simply given by

$$\Psi_{n/m}(r,\theta,\phi) = e^{-\rho/2}\rho^l L_{n+l}^{2l+1}(\rho) Y_l^m(\theta,\phi)$$

where $r = \xi R/2$ $(R \to 0)$, $\rho = 2r/n$ and $\eta = \cos(\theta)$. Using this expression it is easy to see that we have $n - l - 1$ nodes in ξ, $l - m$ nodes in η and m nodes in ϕ. Now recalling that the lowest eigenfunction in any of the three coordinates has zero nodes, the first excited eigenfunction has one node, and so on, we can readily obtain Eq. (5.7.43). Further $Y_l^m(\theta,\phi)$ is even in $\eta = \cos(\theta)$ for $l - m$ even.

If for instance $m = 0$ the columns of the matrix $\overline{\overline{B}}$, in figure 14, correspond to states carrying the following labels $1s\sigma_g, 2s\sigma_g, 3s\sigma_g, 4s\sigma_g, 2p\sigma_u, 3p\sigma_u, ...$, and we note that the columns of $\overline{\overline{B}}$ represent states with changing parity for every M_ξ state.

5.8 The full hydrogen molecular ion problem

We are now going to derive a numerical scheme for the evaluation of the full three particle variational R-matrix functional determined in section 6 of this chapter. The scheme will largely be based on the numerical methods and results obtained in chapter 3, section 2 and 3, and especially on the scheme derived in the previous section of this chapter. The working equation and starting point for this discussion is, to repeat, the translational and rotational invariant functional Eq. (5.6.10-13). In this functional each term (J, m) is uncoupled to the others, and in the following we deal with only one term and drop the labels (J, m). The variational form gives a set of coupled, partial differential equations in the m'th quantum number, but we proceed with a basis-set approach. Our first "ansatz" is a FEM expansion of $\Phi_m(\xi, \eta, f)$ in linear elements (see figure 6) in the f coordinate. This approach was discussed in chapter 3 section 2, and consequently we obtain a numerical formulation that enables us to directly apply the R-matrix algorithm derived in the end of that section. We write

$$\Phi_m(\xi, \eta, f) = \sum_{j=1}^{M_f} \Phi_m^j(\xi, \eta) F_j(f) \tag{5.8.1}$$

where the linear FEM elements, $F_j(f)$, are defined in Eq. (3.2.8). The integration over f in the functional then becomes a sum of discrete integrals over the grid points, $\{ f_j,\ j = 1,..,M_f \}$. As noted before, by virtue of the success of the Born-Oppenheimer approximation, the electronic A-term of the J-functional makes up the zero order term of the complete non-adiabatic functional. Therefore the numerical scheme to be derived now should at least give good convergence for this term. Consequently we first restrict our attention to the three particle electronic term, and then proceed with the addition of non-adiabatic terms hereafter. This correspond to considering the limit $1/\mu \to 0$ (see Eq. (5.3.5)) in Eq. (5.6.10-13), and we find that the functional has no derivatives with respect to f. For the integrals to be considered, over f, we introduce the following notation for the M_f f-diagonal[78] terms

$$\begin{aligned} \left\langle f^k \right\rangle_1 &\equiv \int_{f_1}^{f_2} df \left\{ f^k F_1(f) F_1(f) \right\}, \quad \left\langle f^k \right\rangle_{M_f} \equiv \int_{f_{M_f}-1}^{f_{M_f}} df \left\{ f^k F_{M_f}(f) F_{M_f}(f) \right\} \\ \left\langle f^k \right\rangle_j &\equiv \int_{f_{j-1}}^{f_{j+1}} df \left\{ f^k F_j(f) F_j(f) \right\}, \quad j = 2,..., M_f - 1 \end{aligned} \tag{5.8.2}$$

78 The terms f-diagonal and f-off-diagonal refer to the tridiagonal block structure (see Eq. (3.2.10)), of matrices written in a basis of simple linear FEM functions as expressed in Eq. (5.8.1).

and

$$\left\langle f^k \right\rangle_j' \equiv \int_{f_j}^{f_{j+1}} df \left\{ f^k F_j(f) F_{j+1}(f) \right\}, \quad j = 1,\ldots,M_f - 1 \tag{5.8.3}$$

for the $M_f - 1$ f-off-diagonal terms. The explicit expressions for these integrals are easily obtained using Eq. (3.2.4). It should be clear from figure 6 that the overlap $\left\langle f^k \right\rangle_j$ is larger than $\left\langle f^k \right\rangle_j^{\copyright}$. Actually, if we choose a very dense grid in f, $\{f_j,\ j = 1,..,M_f\}$, the f-diagonal elements will be close to four time as large as the corresponding f-off-diagonal terms. We then conclude that the electronic, f-diagonal terms will contribute most to the total variational functional, and consequently we will construct the numerical scheme in such a way that it is accurate[79] for these terms of the functional. In other words we wish to evaluate the whole functional in a basis-set of eigenfunctions for the f-diagonal electronic term. This is precisely a type of preconditioning, that we discussed in end of section 3, chapter 3 (see Eq. (3.3.27-32), and, to repeat, this yields a compact basis-set for the full problem. As it is only the so-called angular momentum coupling terms, Eq. (5.6.12-13), that introduces coupling in the m quantum number, we consider only one term in m (in addition to fixed J label). From Eq. (5.6.10) it follows that the contribution to the functional which is sesquilinear in $\Phi_m^i(\xi,\eta)$ (i.e. f-diagonal) read as

$$\begin{aligned} A_{elec}\left(\Phi_m^j\right) &= 8\int_1^\infty d\xi \int_{-1}^1 d\eta \left\{ \left[\left(E\left\langle f^5 \right\rangle_j - \frac{e^2}{8\pi\varepsilon_0}\left\langle f^4 \right\rangle_j \right)\left(\xi^2 - \eta^2\right) + \frac{e^2\xi}{2\pi\varepsilon_0}\left\langle f^4 \right\rangle_j \right] \left|\Phi_m^j\right|^2 \right. \\ &\left. - \frac{\hbar^2}{2\mu_e}\left\langle f^3 \right\rangle_j \left[\left(\xi^2 - 1\right)\left|\frac{\partial\Phi_m^j}{\partial\xi}\right|^2 + \left(1 - \eta^2\right)\left|\frac{\partial\Phi_m^j}{\partial\eta}\right|^2 + \left(\frac{m^2}{\xi^2 - 1} + \frac{m^2}{1 - \eta^2}\right)\left|\Phi_m^j\right|^2 \right] \right\} \\ &= \frac{4\hbar^2}{\mu_e}\left\langle f^3 \right\rangle_i \int_1^\infty d\xi \int_{-1}^1 d\eta \left\{ \left[\lambda_j \xi - \kappa_j\left(\xi^2 - \eta^2\right) \right] \left|\Phi_m^j\right|^2 \right. \\ &\left. - \left(\xi^2 - 1\right)\left|\frac{\partial\Phi_m^j}{\partial\xi}\right|^2 - \left(1 - \eta^2\right)\left|\frac{\partial\Phi_m^j}{\partial\eta}\right|^2 - \left(\frac{m^2}{\xi^2 - 1} + \frac{m^2}{1 - \eta^2}\right)\left|\Phi_m^j\right|^2 \right\} \end{aligned} \tag{5.8.4}$$

where we have defined the parameters

$$\kappa_j \equiv -\frac{2\mu_e}{\hbar^2\left\langle f^3 \right\rangle_j}\left(E\left\langle f^5 \right\rangle_j - \frac{e^2}{8\pi\varepsilon_0}\left\langle f^4 \right\rangle_j \right), \quad \lambda_j \equiv \frac{\mu_e e^2}{\hbar^2\pi\varepsilon_0}\frac{\left\langle f^4 \right\rangle_j}{\left\langle f^3 \right\rangle_j} \tag{5.8.5}$$

by analogy with Eq. (5.7.3-5). Eq. (5.8.4) clearly resemble Eq. (5.7.4), and we proceed with the change of variable $\xi \to \zeta$ and an expansion of $\Phi_m^j(\xi,\eta)$ in a primitive product basis of normalized associated Legendre polynomials and Laguerre functions. We then follow the

---

79 Strictly speaking the scheme will of course only be accurate if the primitive basis is chosen large enough.

exact same procedure as outlined in the previous section, to yield a Sturmian-like basis-set, $\{\Psi^{j}_{\Omega\Lambda}(\zeta,\eta)\}$, given as the columns of the $\overline{\overline{B}}_j$ matrix. Expressing $\Phi^{j}_{m}(\xi,\eta)$ in terms of this basis

$$\Phi^{j}_{m}(\zeta,\eta)=\sum_{(\Omega\Lambda)}C^{j}_{(\Omega\Lambda)}\Psi^{j}_{\Omega\Lambda}(\zeta,\eta),\quad \Psi^{j}_{\Omega\Lambda}(\zeta,\eta)=\sum_{(\ell n)}B^{j}_{(\ell n)(\Omega\Lambda)}\overline{P}^{m}_{m+\ell-1}(\eta)\phi^{m}_{n-1}(\zeta) \tag{5.8.6}$$

gives a diagonal form of the functional

$$A_{adi}\left(\Phi^{j}_{m}\right)=\frac{4\hbar^2}{\mu_e}\left\langle f^3\right\rangle_j\sum_{(\Omega\Lambda)}\left\{\left(\lambda_j-\Gamma^{\Omega}_{\Lambda}\right)\left|C^{j}_{\Omega\Lambda}\right|^2\right\} \tag{5.8.7}$$

where $\Gamma^{\Omega}_{\Lambda}$ denotes the diagonal elements of the $M_\zeta\times M_\zeta$ matrix $\overline{\overline{\Gamma}}$ resulting from the solution of the generalized eigenvalue equation given in Eq. (5.7.37).

To include the f-off-diagonal (see Eq. (3.2.10)) electronic terms we make the substitution $\left\langle f^k\right\rangle_j\rightarrow\left\langle f^k\right\rangle^{\mathbb{C}}_j$ in Eq. (5.8.4,5). As the parameters λ_j and κ_j have now changed values, clearly the corresponding f-off-diagonal A-term of the J-functional will not take a simple linear form (Eq. (5.8.7)) in the Sturmian-like basis-set obtained from the diagonalization of the f-diagonal A-terms. Consequently we shall have to determine explicitly the $(N_\zeta+N_\eta)\times(N_\zeta+N_\eta)$ matrices $\overline{\overline{A}}_j$ of the f-off-diagonal electronic terms in the primitive basis-set $\{\overline{P}^{m}_{\ell}(\eta),\phi^{m}_{n}(\zeta)\}$, and then transform it to the Sturmian-like basis-set to obtain a $(M_\zeta+M_\eta)\times(M_\zeta+M_\eta)$ matrix $\overline{\overline{A}}_j{}'$ - that is

$$\overline{\overline{A}}_j{}'=\overline{\overline{B}}^{T}_j\overline{\overline{A}}_j\overline{\overline{B}}_{j+1} \tag{5.8.8}$$

The block structure of $\overline{\overline{A}}_j$ is shown in figure 13, where the η-off-diagonal[80] terms read as

$$A^{j}_{(\ell n)(\ell+2n')}=\frac{4\hbar^2}{\mu_e c}\kappa_j\left\langle f^3\right\rangle_j{}'Y^{m}_{m+\ell}Y^{m}_{m+\ell+1}\delta_{nn'} \tag{5.8.9}$$

and the η-diagonal terms[81]

$$\begin{aligned}A^{j}_{(\ell n)(\ell n')}=\frac{4\hbar^2}{\mu_e}\left\langle f^3\right\rangle_j{}'\int_0^\infty d\xi\Bigg\{\Bigg[&\xi^2\left(\frac{1}{4}-\frac{\kappa_j}{c^2}\right)+\xi\left(\frac{\lambda_j}{c}+\frac{c}{2}-\frac{2\kappa_j}{c}-\frac{m}{2}-n'\right)+\left(\frac{m}{2}-\kappa_j+n'\right.\\&\left.-1+c(1-m-2n')+\lambda_j+\kappa_j\left(Y^{m}_{m+\ell-1}\right)^2+\kappa_j\left(Y^{m}_{m+\ell}\right)^2-(m+\ell-1)(m+\ell)\right)\\&+\frac{m^2(\xi+4c)}{4(\xi+2c)}\Bigg]\phi^{m}_{n'-1}(\xi)-\sqrt{(n'-1)(m+n'-1)}\phi^{m}_{n'-2}(\xi)\Bigg\}\phi^{m}_{n-1}(\xi)\end{aligned} \tag{5.8.10}$$

In the evaluation of Eq.(5.8.10) we used Eq. (5.7.30-33) derived in the previous section.

---

80 The terms η-diagonal and η-off-diagonal refer to the band tridiagonal block structure (see figure 13), of matrices written in a basis of normalized associated Legendre functions as expressed in Eq. (5.8.1).

81 In the derivation of Eq. (5.8.10) we have used Eq. (5.7.34) and substituted Λ^{m}_{Ω} with Eq. (5.7.15).

The next step is now to include non-adiabatic corrections to the variational functional. As a first "ansats" we will only include the radial non-adiabatic A-term, Eq. (5.6.11), for several reasons. First this term can be expected to be dominant over the angular non-adiabatic terms due the f-derivative term entering the former. Secondly there seems no point in adding further non-adiabatic corrections to the functional, if it should turn out that the algorithm, already at this point is numerically unstable. Finally the addition of the angular momentum coupling terms will complicate the numerical scheme unnecessarily for a first evaluation of the algorithm, due to the coupling in m entering these terms. This complicating aspects in connection with the addition of the angular momentum coupling terms will be discussed in the next chapter. We start with the radial non-adiabatic term, Eq. (5.6.11), and rewrite it to obtain

$$A_{radi}(\Phi_m) = \int_{f_{min}}^{f_{max}} df \int_{-1}^{1} d\eta \int_{1}^{\infty} d\xi \left\{ \frac{\hbar^2 f^3}{\mu(\xi^2-\eta^2)} \left| \left\{ (\xi^2-\eta^2) f \frac{\partial}{\partial f} + (\xi-\xi^3)\frac{\partial}{\partial \xi} + (\eta^3-\eta)\frac{\partial}{\partial \eta} \right\} \Phi_m \right|^2 \right\} \quad (5.8.11)$$

where we have specified the domain of definition of f in order to obtain a simple notation for integrals over this variable[82]. Next we change variable $\xi \to \zeta$ and introduce the operator $\not{\alpha}$

$$A_{radi}(\Phi_m) = \frac{\hbar^2}{\mu} \int_{f_{min}}^{f_{max}} df \int_{-1}^{1} d\eta \int_{0}^{\infty} d\zeta \left\{ \left| \left\{ \sqrt{(\xi^2(\zeta)-\eta^2) f^5}\, \frac{\partial}{\partial f} + \sqrt{\frac{f^3}{\xi^2(\zeta)-\eta^2}}\, \not{\alpha} \right\} \Phi_m \right|^2 \right\} \quad (5.8.12)$$

where

$$\not{\alpha} \equiv \xi(\zeta) - \xi^3(\zeta)\frac{\partial}{c\partial\zeta} + (\eta^3-\eta)\frac{\partial}{\partial\eta} \quad (5.8.13)$$

As with the off-diagonal electronic terms in f, discussed above, the procedure is now to evaluate Eq. (5.8.12) in the primitive basis set $\{\bar{P}_\ell^m(\eta), \phi_n^m(\zeta)\}$, and then transform it to the Sturmian-like basis-set using Eq. (5.8.8). As a prelude to this evaluation we deduce the action of the operator $\not{\alpha}$ on the primitive basis

$$\begin{aligned} \not{\alpha}\left[\bar{P}_\ell^m(\eta)\phi_n^m(\zeta)\right] &= \frac{\xi(\zeta)-\xi^3(\zeta)}{c}\bar{P}_\ell^m(\eta)\frac{\partial}{\partial\zeta}\phi_n^m(\zeta) + \phi_n^m(\zeta)(\eta^3-\eta)\frac{\partial}{\partial\eta}\bar{P}_\ell^m(\eta) \\ &= \frac{\xi(\zeta)-\xi^3(\zeta)}{c\zeta}\bar{P}_\ell^m(\eta)\left\{\left(\frac{m}{2}+n-\frac{\zeta}{2}\right)\phi_n^m(\zeta) - \sqrt{n(n+m)}\phi_{n-1}^m(\zeta)\right\} \\ &+ \eta\left\{\ell\eta\bar{P}_\ell^m(\eta) - \frac{\sqrt{(\ell^2-m^2)(2\ell+1)}}{2\ell-1}\bar{P}_{\ell-1}^m(\eta)\right\}\phi_n^m(x) \end{aligned} \quad (5.8.14)$$

82 It is assumed that the reader by now is familiar with the nature and definition of the linear FEM basis functions.

where we have used the recursion relations Eq. (5.7.26) and [52]

$$\left(\eta^2-1\right)\frac{\partial}{\partial\eta}\overline{P}_\ell^m(\eta)=\ell\eta\overline{P}_\ell^m(\eta)-\frac{\sqrt{\left(\ell^2-m^2\right)(2\ell+1)}}{2\ell-1}\overline{P}_{\ell-1}^m(\eta) \tag{5.8.15}$$

After inserting Eq. (5.8.14) into Eq. (5.8.12) a fairly complicated integral over the two[83] variables ξ and η appears. It is at this very point that the DVR scheme will prove very useful as we can use a two dimensional DVR scheme as described in chapter 3 section 3. Each primitive basis function, $\left|\phi_n^m\right\rangle$ and $\left|\overline{P}_\ell^m\right\rangle$, is expressed in terms of an orthogonal basis-set $\left\{\left|\xi_q\right\rangle\right\}$ and $\left\{\left|\eta_p\right\rangle\right\}$[84] through the unitary transformations, (see Eq. (3.3.20))

$$\begin{aligned}\left|\phi_{n-1}^m\right\rangle &\approx \sum_{q=1}^{N_\xi}\sqrt{\Theta_q}\phi_{n-1}^m(\xi_q)\left|\xi_q\right\rangle \equiv \sum_{q=1}^{N_\xi}V_{qn}^m\left|\xi_q\right\rangle, \quad n=1,2,\ldots N_\xi\\ \left|\overline{P}_{m+\ell-1}^m\right\rangle &\approx \sum_{p=1}^{N_\eta}\sqrt{\Omega_p}\overline{P}_{m+\ell-1}^m(\eta_p)\left|\eta_p\right\rangle \equiv \sum_{p=1}^{N_\eta}U_{p\ell}^m\left|\eta_p\right\rangle, \quad \ell=1,2,\ldots N_\eta\end{aligned} \tag{5.8.16}$$

where ξ_q / η_p and Θ_q / Ω_p are respectively the abscissa and weights for the normalized associated Legendre polynomials and the normalized associated Laguerre functions. Using Eq. (3.3.21) we deduce the following very simple relation for a general two dimensional integral

$$\int_{-1}^{1}d\eta\int_0^\infty d\xi\left\{\overline{P}_{m+\ell-1}^m(\eta)\phi_{n-1}^m(\xi)g(\xi,\eta)\overline{P}_{m+\ell'-1}^m(\eta)\phi_{n'-1}^m(\xi)\right\}\approx\sum_{q=1}^{N_\xi}\sum_{p=1}^{N_\eta}\left\{V_{qn}^mV_{qn'}^mU_{p\ell}^mU_{p\ell'}^mg(\xi_q,\eta_p)\right\} \tag{5.8.17}$$

Expressed in the primitive product basis $\{F_j(f),\overline{P}_\ell^m(\eta),\phi_n^m(\xi)\}$ the nuclear-kinetic term of the J-functional then reads as

$$\begin{aligned}A_{(\ell n)(\ell' n')}^{ij}=-\frac{\hbar^2}{\mu}\sum_{p=1}^{N_\eta}\sum_{q=1}^{N_\xi}\Big\{&U_{p\ell}U_{p\ell'}V_{qn}V_{qn'}\left[\xi^2(\xi_q)-\eta_p^2\right]\left\langle f^5\right\rangle_{ij}+U_{p\ell}V_{qn}\alpha_{pq}^{n'\ell'}\left\langle f^4\right\rangle_{ji}\\&+U_{p\ell'}V_{qn'}\alpha_{pq}^{n\ell}\left\langle f^4\right\rangle_{ij}+\alpha_{pq}^{n\ell}\alpha_{pq}^{n'\ell'}\left[\xi^2(\xi_q)-\eta_p^2\right]^{-1}\left\langle f^3\right\rangle_{ij}\Big\}\end{aligned} \tag{5.8.18}$$

where we have defined

---

83 The integration over the linear FEM basis functions in f is considered trivial.

84 In order not to confuse the abscissa ξ_q and η_p with the DVR functions $\left|\xi_q\right\rangle$ and $\left|\eta_p\right\rangle$ we have used a Bra-ket notation.

$$\alpha_{pq}^{n\ell} = \left[\frac{\xi(\zeta_q) - \xi^3(\zeta_q)}{c\zeta_q} \left\{ \left(\frac{m}{2} + n - 1 - \frac{\zeta_q}{2} \right) V_{qn} - \sqrt{(n-1)(n-1+m)}\, V_{qn-1} \right\} U_{p\ell} \right.$$
$$\left. + \eta_p \left\{ (\ell + m - 1)\eta_p U_{p\ell} - \frac{\sqrt{\left((\ell + m - 1)^2 - m^2\right)(2\ell + 2m - 1)}}{2\ell + 2m - 3} U_{p\ell-1} \right\} V_{qn} \right] \tag{5.8.19}$$

and

$$\left\langle f^3 \right\rangle_{ij} = \int_{f_{min}}^{f_{max}} df \left\{ F_i(f) f^3 F_j(f) \right\}$$
$$\left\langle f^4 \right\rangle_{ij} = \int_{f_{min}}^{f_{max}} df \left\{ F_i(f) f^4 \frac{\partial F_j(f)}{\partial f} \right\} \tag{5.8.20}$$
$$\left\langle f^5 \right\rangle_{ij} = \int_{f_{min}}^{f_{max}} df \left\{ \frac{\partial F_i(f)}{\partial f} f^5 \frac{\partial F_j(f)}{\partial f} \right\}$$

5.9 Representation of the transition dipole moment

As mentioned in the "general motivation" of this project, we wish to give a more detailed description of the transitions among states of H_2^+ in white dwarfs (WD), than have been presented in the literature up till now [9, 17, 18]. The main improvement from these previous works on H_2^+, to repeat, will be to work in a complete non-adiabatic picture, where the H_2^+-system is treated as a full three body problem as described in the preceding sections. A fully consistent treatment of this problem, however, would require that the field *as well as* the three particles should be subject to quantum conditions. In other words the Hamiltonian for the radiation field should be included with those for the particles, leading to a far more complicated variational problem (J-functional), than the one described in the previous section. The use of such a J-functional permits interchange of energy between the molecular states of H_2^+ and the field states, implying that the radiation field participates in the dynamical processes. However, such a non-adiabatic treatment of H_2^+ in the framework of quantum electrodynamics [48] would be very troublesome, and thus approximations must be made. Instead we will use semiclassical electrodynamics[85], where the Hamiltonian has only the atomic or molecular terms, plus a term for interaction with the radiation. The particles are subject to quantum conditions, but the radiation field is taken to be classical and prescribed as a fixed external agent - the so-called "driving field" viewpoint. Solving non-adiabatic quantum mechanical calculations for many particle systems in this semiclassical picture is

---

85 If the Hamiltonian for the radiation field is not part of the complete Hamiltonian (as in the semiclassical theory) spontaneous decay cannot be accounted for. In the Semiclassical Electrodynamics this lead to the introduction of the Einstein A-coefficient. However in this thesis we choose to ignore such phenomena in which energy is transferred between molecular system and radiation field.

difficult enough, and moreover acceptable when the radiation field is so strong that any influence on it by the matter present is negligibly small. As discussed in the excellent text book by Craig and Thirunamachandran [48] the inclusion of the interaction term gives the well-known electric dipole interaction moment plus higher order terms[86]. Again approximations will be made. When the radiation wavelength is long compared with the molecular dimension the variation of the vector potential (using the Coulomb gauge formulation [48]) can be neglected. Consequently the magnetic field vanishes and the electric field is uniform over the extent of the molecule, so that there is no magnetic interaction and the electric dipole moment is the only term entering the interaction operator at this level. This is the so-called *electric dipole approximation* which we are going to apply to the study of transitions among states of H_2^+ in WD's. Thus the starting point for the this study is to derive a numerical scheme for the electric transition dipole moment for H_2^+, which will be the topic for this section.

In the previous section we described how to evaluate the $\overline{\overline{A}}_{ij}$ matrices entering the algorithm presented in the end of section 2 chapter 3. The outcome of this algorithm are the amplitudes $\overline{C}_j$, expressing the total three particle wave function in a Sturmian-like basis-set. The next step is then to generate the full three particle transition dipole moment from these amplitudes. To do this we need to derive an explicit expression for the matrix representation of the translationally and rotationally invariant transition dipole moment operator, $\vec{\mu}$, in the basis of Sturmian-like functions. In the laboratory fixed frame of reference, presented in section 2 of this chapter, the electric dipole moment operator simply reads as

$$\vec{\mu} = e\left(\vec{r}_a + \vec{r}_b - \vec{r}_e\right) \tag{5.9.1}$$

To express $\vec{\mu}$ in terms of space fixed coordinates we invert the matrix equation Eq. (5.3.2)

$$\left[\vec{r}_a, \vec{r}_b, \vec{r}_e\right] = \left[\vec{r}', \vec{R}', \vec{R}'_G\right] \begin{bmatrix} -\frac{m_e}{M} & -\frac{m_e}{M} & \frac{m_a + m_b}{M} \\ \frac{m_b}{m_a + m_b} & -\frac{m_a}{m_a + m_b} & 0 \\ 1 & 1 & 1 \end{bmatrix} = \left[\vec{r}', \vec{R}', \vec{R}'_G\right] \begin{bmatrix} -\frac{m_e}{M} & -\frac{m_e}{M} & 2\frac{m}{M} \\ \frac{1}{2} & -\frac{1}{2} & 0 \\ 1 & 1 & 1 \end{bmatrix} \tag{5.9.2}$$

where we have used $m_a = m_b = m$ for the H_2^+-system. Hence we find

$$\begin{aligned} \vec{\mu} &= e\left\{\left(-\frac{m_e}{M}\vec{r}' + \frac{1}{2}\vec{R}' + \vec{R}'_G\right) + \left(-\frac{m_e}{M}\vec{r}' - \frac{1}{2}\vec{R}' + \vec{R}'_G\right) - \left(2\frac{m}{M}\vec{r}' + \vec{R}'_G\right)\right\} \\ &= -2\frac{e\left(m + m_e\right)}{M}\vec{r}' + e\vec{R}'_G \end{aligned} \tag{5.9.3}$$

---

86 When spatial variation of the vector potential is taken account for higher order terms enter the interaction operator between the matter and the radiation field. If a linear variation of the vector potential is assuming, an electric quadrupole moment and a magnetic dipole moment enter the interaction operator in addition to the electric dipole moment.

Before we go any further let us consider the contribution to the *transition* dipole moment from the last term in Eq. (5.9.3). Let $\Psi_i\left(\vec{r}',\vec{R}',\vec{R}'_G\right)$ denote the initial state and $\Psi_f\left(\vec{r}',\vec{R}',\vec{R}'_G\right)$ the final state. From the general discussion in chapter 4 section 2 and Eq. (4.2.10) we deduce

$$\left\langle \Psi_i\left(\vec{r}',\vec{R}',\vec{R}'_G\right)\middle| e\vec{R}'_G \middle| \Psi_f\left(\vec{r}',\vec{R}',\vec{R}'_G\right)\right\rangle = e\left\langle e^{i\vec{K}_i\vec{R}'_G}\middle|\vec{R}'_G\middle|e^{i\vec{K}_f\vec{R}'_G}\right\rangle\left\langle \Psi_i\left(\vec{r}',\vec{R}'\right)\middle|\Psi_f\left(\vec{r}',\vec{R}'\right)\right\rangle \tag{5.9.4}$$

Noting that $\Psi_i\left(\vec{r}',\vec{R}'\right)$ and $\Psi_f\left(\vec{r}',\vec{R}'\right)$ refer to two different quantum states (hence the name *transition* dipole moment) they are, by definition, characterized by a different set of quantum numbers and have zero overlap. In other words the last term of Eq. (5.9.4) is always zero, and we conclude (as was expected) that the center-of-mass does not contribute to the transition dipole moment and can therefore be eliminated.

$$\vec{\mu} = -2\frac{e\left(m+m_e\right)}{M}\vec{r}' \tag{5.9.5}$$

Next we shift to a body fixed frame of reference (see Eq. (5.4.4)) in which the electronic *Cartesian components* are x, y and z, then the spheroidal coordinates (see Eq. (5.5.4)) are introduced, and finally the result is express in *spherical components* (see Eq. (4.3.9,16)) - that is

$$\begin{aligned}\vec{r}' &= \overline{\overline{R}}(\alpha,\beta,0)\begin{bmatrix}x\\y\\z\end{bmatrix} = \overline{\overline{R}}(\alpha,\beta,0)\begin{bmatrix}f\sqrt{\left(\xi^2-1\right)\left(1-\eta^2\right)}\cos\phi\\ f\sqrt{\left(\xi^2-1\right)\left(1-\eta^2\right)}\sin\phi\\ f\xi\eta\end{bmatrix}\\ &= \overline{\overline{D}}^{1*}(\alpha,\beta,\phi)\begin{bmatrix}2^{-1/2}f\sqrt{\left(\xi^2-1\right)\left(1-\eta^2\right)}\\ 2^{-1/2}f\sqrt{\left(\xi^2-1\right)\left(1-\eta^2\right)}\\ f\xi\eta\end{bmatrix}\end{aligned} \tag{5.9.6}$$

where the Euler angle ϕ has been absorbed[87] into the rotation matrix in the last step. The spherical components of the body fixed dipole moment then read as

---

87 For the change from the Cartesian basis to Spherical basis Eq. (5.4.18) and Eq. (5.5.4) give us

$$\begin{aligned}\vec{r} &\equiv x\vec{e}_x + y\vec{e}_y + z\vec{e}_z = x\frac{1}{\sqrt{2}}\left(\vec{e}_{+1}+\vec{e}_{-1}\right) - y\frac{i}{\sqrt{2}}\left(\vec{e}_{+1}-\vec{e}_{-1}\right) + z\vec{e}_0\\ &= \frac{d_{\pm1}}{\sqrt{2}}\left(\cos\phi - i\sin\phi\right)\vec{e}_{+1} + \frac{d_{\pm1}}{\sqrt{2}}\left(\cos\phi + i\sin\phi\right)\vec{e}_{-1} + d_0\vec{e}_0 = \frac{d_{\pm1}}{\sqrt{2}}\exp\left(-i\phi\right)\vec{e}_{+1} + \frac{d_{\pm1}}{\sqrt{2}}\exp\left(i\phi\right)\vec{e}_{-1} + d_0\vec{e}_0\end{aligned}$$

where we have defined

$$d_{\pm1} \equiv f\sqrt{\left(\xi^2-1\right)\left(1-\eta^2\right)}, \quad d_0 \equiv f\xi\eta$$

The factors $\exp\left(\pm i\phi\right)$ can then be absorbed into the rotation matrix in Eq. (5.9.6) using Eq. (5.6.5).

$$\mu_i = \sum_{j=-1}^{1} \overline{\overline{D}}_{ij}^{1*}(\alpha,\beta,\phi)\mathbf{d}_j\,, \quad \vec{\mathbf{d}} \equiv -\frac{e(m+m_e)f}{M}\begin{bmatrix}\sqrt{(\xi^2-1)(1-\eta^2)}\\ \sqrt{(\xi^2-1)(1-\eta^2)}\\ \sqrt{2}\xi\eta\end{bmatrix} \tag{5.9.7}$$

To evaluate the transition dipole moment between an initial state $\Psi_{J_i m_i}(\vec{r}',\vec{R}')$ and a finale state $\Psi_{J_f m_f}(\vec{r}',\vec{R}')$ we make use of Eq. (5.6.6)

$$\begin{aligned}\langle J_i m_i|\mu_i|J_f m_f\rangle = \sum_{\Lambda_i=-J_i}^{J_i}\sum_{\Lambda_f=-J_f}^{J_f}\Bigg[\int d\Omega\Bigg\{\sum_{j=-1}^{1}\overline{\overline{D}}_{m_f\Lambda_f}^{J_f*}(\Omega)\overline{\overline{D}}_{m_i\Lambda_i}^{J_i}(\Omega)(-1)^{i-j}\overline{\overline{D}}_{-i-j}^{1}(\Omega)\Bigg\}\\ \times\int 8f^5(\xi^2-\eta^2)d\xi d\eta df\left\{\Phi_{J_f\Lambda_f}^{*}(\xi,\eta,f)\mathbf{d}_i\Phi_{J_i\Lambda_i}(\xi,\eta,f)\right\}\Bigg]\end{aligned} \tag{5.9.8}$$

where we have denoted the Euler angles collectively by Ω and used the symmetry relation $\overline{\overline{D}}_{m'm}^{J*}(\Omega) = (-1)^{m'-m}\overline{\overline{D}}_{-m'-m}^{J}(\Omega)$. To integrate over the rotation matrices we use Eq. (4.3.25) and arrive at the following central result

$$\langle J_i m_i|\mu_i|J_f m_f\rangle = \langle J_i\|\mu_i\|J_f\rangle C_{m_i\,-i\,m_f}^{J_i\,1\,J_f} \tag{5.9.9}$$

where we have defined the matrix element

$$\langle J_i\|\mu_i\|J_f\rangle \equiv \frac{2\pi}{2J_f+1}\sum_{\Lambda_i=-J_i}^{J_i}\sum_{\Lambda_f=-J_f}^{J_f}\sum_{j=-1}^{1}(-1)^{i-j}C_{\Lambda_i\,-j\,\Lambda_f}^{J_i\,1\,J_f}\langle J_i\Lambda_i|\mathbf{d}_j|J_f\Lambda_f\rangle \tag{5.9.10}$$

and

$$\langle J_i\Lambda_i|\mathbf{d}_j|J_f\Lambda_f\rangle = \int 8f^5(\xi^2-\eta^2)d\xi d\eta df\left\{\Phi_{J_f\Lambda_f}^{*}(\xi,\eta,f)\mathbf{d}_j\Phi_{J_i\Lambda_i}(\xi,\eta,f)\right\} \tag{5.9.11}$$

The quantity, $\langle J_i\|\mu_i\|J_f\rangle$, in Eq. (5.9.10) is Condon and Shortley's [64] notation for a *reduced matrix element* and is, as its definition shows, independent of all projection quantum numbers (m_i and m_f) and hence a rotational invariant. Eq. (5.9.9,10) are actually the manifestation of a very fundamental "physical circumstance" - known as the *Wigner-Eckart Theorem*; "Each matrix element in an angular momentum basis of an irreducible tensor operator is a product of two factors; a purely angular momentum dependent factor (the Wigner coefficient in Eq. (5.9.9)) and a factor that is independent of projection quantum numbers (the reduced matrix element in Eq. (5.9.10))." The electric dipole moment operator is a vector operator (also called an irreducible tensor of rank J=1) and hence the Wigner-Eckart theorem applies to matrix elements of μ_i in a basis of functions with a sharp angular momentum. Biedenharn and Louck [54] expresses the essence of the Wigner-Eckart theorem in the following way; "The most striking feature of the Wigner-Eckart theorem is the clear-cut separation of the generic (group-theoretic) aspects of an operator from its particularities - the reduced matrix element - that relate to the physical measurement in question.

Conventionally one expresses this by saying that one has separated the geometric aspect from the physics of the problem." Applying the relations for non-vanishing Wigner coefficients[88] to Eq. (5.9.9) give us the following *selection rules* for dipole allowed transitions[89].

$$\Delta J = 0, \pm 1 \quad \text{and} \quad \Delta m = 0, \pm 1 \tag{5.9.12}$$

We also note in general that, if $J_f = J_i = 0$, all Wigner coefficients are zero, such that $J = 0 \nrightarrow 0$ transitions are forbidden in the dipole approximation. The Wigner coefficients in Eq. (5.9.10), on the other hand, select the body fixed components of $\vec{\mathbf{d}}$ that give a non-zero contribution to the transition dipole moment. If we restrict ourselves to considering transitions among the three lowest electronic states of H_2^+, the contribution to the transition dipole moments are listed in table 2 where we have denoted the components of $\vec{\mathbf{d}}$ according to the orientation along the nuclear axis (i.e. $\mathbf{d}_{\parallel} \equiv \mathbf{d}_0$ and $\mathbf{d}_{\perp} \equiv \mathbf{d}_{\pm 1}$), and substituted $J \rightarrow l$ since we neglect any spin angular momentum from the particles.

Table 2 Transition dipole moments

$\langle i\|\vec{\mu}\|f\rangle$	$1s\sigma_g$	$2p\sigma_u$	$2p\pi_u$
$1s\sigma_g$	0	$\langle 0,0\|\mathbf{d}_{\parallel}\|1,0\rangle$	$\langle 0,0\|\mathbf{d}_{\perp}\|1,\pm 1\rangle$
$2p\sigma_u$	$\langle 1,0\|\mathbf{d}_{\parallel}\|0,0\rangle$	0	0
$2p\pi_u$	$\langle 1,\pm 1\|\mathbf{d}_{\perp}\|0,0\rangle$	0	0

Thus we need to evaluate the two different types of matrix elements listed in table 2 and defined in Eq. (5.9.11). The wave functions are expanded in simple linear FEM elements (see Eq. (5.8.1)) and in both cases we get the following contribution from the integration of f in Eq. (5.9.11).

$$8\left\langle f^6 \right\rangle_{ij} \equiv 8\int_{f_i}^{f_j} df\left\{f^5 f\right\} \tag{5.9.13}$$

where i and j denote the grid points in f. The strategy is now as follows; first we evaluate Eq. (5.9.11) in a basis of associated Legendre polynomials and Laguerre functions (see Eq. (5.8.6)), and next we transform the resulting matrix representation of $\mathbf{d}_j$ into the Sturmian-like basis using Eq. (5.8.8). Then we determine the transition moment using the amplitudes $\overline{C}_i$ obtained from the scattering calculation discussed in section 2 chapter 3, and finally we

---

88 See the end of section 3 chapter 4.

89 These selection rules could have been obtained more directly from the fact that $\vec{\mu}$ is a vector operator with respect to rotations of physical space generated by the total angular momentum $\vec{\mathbf{J}}$ and changes sign under spatial inversion (i.e. odd parity). Group theory tells us that any matrix element is zero unless it is totally symmetrical under the symmetry operations of the system, such that the only allowed electric dipole transitions are those involving a change of parity. This is exactly what table 2 shows; $g \nleftrightarrow g$ $u \nleftrightarrow u$ $g \leftrightarrow u$.

sum the different contributions over the f-grid points. Let us first consider the matrix elements over $\mathbf{d}_{\parallel}$ where $\Delta m = 0$.

$$D^{\parallel}_{(\ell n)(\ell' n')} \equiv \int_{-1}^{1} d\eta \int_{0}^{\infty} d\xi \left\{ \bar{P}^{m}_{m+\ell-1}(\eta)\phi^{m}_{n-1}(\xi) c^{-1}\left(\xi^2(\xi)-\eta^2\right)\xi(\xi)\eta \bar{P}^{m}_{m+\ell'-1}(\eta)\phi^{m}_{n'-1}(\xi)\right\} \qquad (5.9.14)$$

where we have introduced the new variable ξ defined in Eq. (5.7.18). We could now derive an analytical expression for these matrix elements, using Eq. (5.7.12) and Eq. (5.7.29), to discover that $\overline{\overline{D}}^{\parallel}$ has a very simple band structure, but instead we simply use the straightforward multi dimensional DVR scheme (see Eq. (5.8.17)). Next we consider the matrix elements over $\mathbf{d}_{\perp}$ where $\Delta m = \pm 1$, and for simplicity we assume that $m' = m + 1$.

$$D^{\perp}_{(\ell n)(\ell' n')} \equiv \int_{-1}^{1} d\eta \int_{0}^{\infty} d\xi \left\{ \bar{P}^{m}_{m+\ell-1}(\eta)\phi^{m}_{n-1}(\xi) c^{-1}\left(\xi^2(\xi)-\eta^2\right)\sqrt{\left(\xi^2(\xi)-1\right)\left(1-\eta^2\right)}\bar{P}^{m+1}_{m+\ell'}(\eta)\phi^{m+1}_{n'-1}(\xi)\right\} \qquad (5.9.15)$$

Clearly we will have to use a numerical method to evaluate these matrix elements, and the "natural choice" is again a multi dimensional DVR. However there is a catch somewhere; from the discussion on the DVR method in chapter 3 section 3, we recall that when we defined the DVR scheme we first had to determine some quadrature points defined as the roots of the orthogonal polynomials - but for different values of m we will find different sets of quadrature points. In other words we have two different FBR's and hence also to different DVR's. A general discussion on this problem is given in the paper [65] by Leforestier. Nevertheless in our case with two different FBR's of associated Legendre polynomials and Laguerre functions the problem is easily dealt with. The idea is simply to express the functions of order m+1 in functions of order m and then evaluate the matrix elements in a DVR defined from the FBR of order m. This is possible because there exist a set of recursion relations[90] for associated Legendre and Laguerre polynomials. For the normalized associated Legendre polynomials and associated Laguerre functions we have

$$\sqrt{1-\eta^2}\,\bar{P}^{m+1}_{\ell}(\eta) = A^{m}_{\ell}(\eta)\bar{P}^{m}_{\ell}(\eta) + B^{m}_{\ell-1}\bar{P}^{m}_{\ell-1}(\eta), \quad \begin{cases} A^{m}_{\ell}(\eta) \equiv -\eta\sqrt{\dfrac{\ell-m}{\ell+m+1}} \\ B^{m}_{\ell} \equiv \sqrt{\dfrac{(2\ell+3)(\ell+m+1)}{(2\ell+1)(\ell+m+2)}} \end{cases} \qquad (5.9.16)$$

and

---

90 From reference [52] we have the following recursion relations for respectively the associated Legendre and Laguerre polynomials

$$\sqrt{1-\eta^2}\,P^{m+1}_{\ell}(\eta) = (m-\ell)\eta P^{m}_{\ell}(\eta) + (\ell+m)P^{m}_{\ell-1}(\eta), \quad L^{m+1}_{n}(\xi) = \frac{1}{\xi}\left[(\xi-n)L^{m}_{n}(\xi) + (m+n)L^{m}_{n-1}(\xi)\right]$$

$$\phi_n^{m+1}(\xi) = X_n^m(\xi)\phi_n^m(\xi) + Y_{n-1}^m(\xi)\phi_{n-1}^m(\xi), \quad \begin{cases} X_n^m(\eta) \equiv \dfrac{\xi - n}{\sqrt{\xi(n+m+1)}} \\ Y_n^m(\xi) \equiv \sqrt{\dfrac{(n+1)(n+m+1)}{\xi(n+m+2)}} \end{cases} \tag{5.9.17}$$

Substituting Eq. (5.9.16,17) into Eq. (5.9.15) leads to the following expression

$$\begin{aligned} D^{\perp}_{(\ell n)(\ell' n')} = c^{-1}\Big[&\langle \ell, n|A_\ell^m(\eta)X_n^m(\xi) + \langle \ell, n-1|A_\ell^m(\eta)Y_{n-1}^m(\xi) + \\ &\langle \ell-1, n|B_{\ell-1}^m X_n^m(\xi) + \langle \ell-1, n-1|B_{\ell-1}^m Y_{n-1}^m(\xi)\Big] g(\xi,\eta)|\ell', n'\rangle \end{aligned} \tag{5.9.18}$$

where we have defined the function

$$g(\xi,\eta) \equiv \left(\xi^2(\xi) - \eta^2\right)\sqrt{\left(\xi^2(\xi) - 1\right)} \tag{5.9.19}$$

Eq. (5.9.18) is then easily evaluated using Eq. (5.8.17). Next we transform $\overline{\overline{D}}^{\nu}$ into the Sturmian-like basis, evaluate the transition moment in the discrete f-points using the amplitudes $\overline{C}_i$ obtained from the scattering calculation discussed in section 2 chapter 3, and finally sum the different contributions over the f-grid points - that is

$$\langle \text{init}|\mathbf{d}_\nu|\text{final}\rangle = \sum_{ij}\left\{8\langle f^6\rangle_{ij}\left[\overline{C}_i^T\overline{\overline{B}}_i^T\right]_{\text{init}}\overline{\overline{D}}^{\nu}\left[\overline{\overline{B}}_j\overline{C}_j\right]_{\text{final}}\right\}, \quad i-j = 0,\pm 1, \quad \nu = \perp \text{ or } \| \tag{5.9.20}$$

where care should of course be taken in the first and last f-grid point.

6 Numerical results for the hydrogen molecular ion

6.1 Introduction

With the completion of a numerical scheme to describe the hydrogen proton scattering it is now finally time to present and discuss some concrete numerical results. However before we do so, I would like to comment on the derived algorithms in terms of flow charts and stress the fact that a *lot* of effort and time has been put into the actual implementation of this scheme on a computer. Actually, it is no secret that far the most of the time spent on this project was dedicated to this step of passing from chapter 5 to chapter 6. The reason why this step turned out to be so effortful was partly that many of the numerical subroutines needed to carry out the calculations were not available in any standard library on the computers. Consequently I had to develop and program my own numerical routines. Also the algorithms that successively compute the R-matrix and next propagate the scattering wave function via a recursive procedure (Eq. (3.2.21-22)) turned out to be more complicated to implement, and especially optimize, than expected. Further it should of course also be noted that this type of numerical problem - a full quantum mechanical description of a three particle system - simply is a very computationally intensive task, which is obviously also reflected in the complexity of the source code itself. During this project I have programmed many thousand lines of FORTRAN-77 code (and c-shell scripts), and although these computer routines naturally form a very significant part of my contribution to this research project, I have decided not to take up space in this (admitted already quite extensive) thesis with a presentation of the source codes. However, should the reader have any desire for such an insight to the actual source codes used in this project, I will gladly provide him/her with a copy.

Programming and optimizing several thousand lines of code evidently implies a *lot* of tedious debugging, and although you tend to develop quite good skills in programming with time, this does not seem to have any serious positive influence on the actual time spent on debugging. The fact that you have become a “better programmer” (i.e. developed more sophisticated programming techniques) often just results in more “complex bugs” to be resolved; the decline in the frequency of bugs tends to be canceled out by the “growing size” of the bugs. Actually at some stages of programming I had the feeling that in addition to the celebrated laws and postulates of quantum mechanics, another much more elusive and deceptive “law” appeared to control my project; Murphy’s law (“anything that can go wrong will go wrong” - and, if I might add, probably at the least expected time). As a matter of fact I some times felt that Murphy was an optimist. However I would also like to draw the reader's attention to the fact that the sort of approach to the three body problem of H_2^+ , presented in this thesis, has never been attempted before. Therefore neither does it come to me as a shock to realize that the project, as it was originally formulated by me two and a half year ago, is not

yet fully completed. To be more specific I am still in the phase of *debugging* the code evaluating the transition dipole moments for the non-adiabatic states of H_2^+. In other words the last (astrophysical) part of this project, concerning the application of my results to a detailed model for the role of H_2^+ absorption in DA white dwarfs, and the subsequent comparison with absorption spectra recorded by the International Ultraviolet Explorer Satellite, still has to be looked at. However nothing so far have suggested that this last part of the project cannot be carried out, and I feel absolutely confident that it will be in the foreseeable future.

6.2 Schematic outline of programs and routines

As mentioned above the actual source code will not be presented in this thesis, but instead I will shortly go through the overall structure of the four most central programs and routines used in the study of H_2^+. So before I move on to a presentation and discussion of the results in the next section, flow charts for the computer routines will be presented and a short comment on the programs follows. As outlined in section 5.7-9 the numerical schemes derived for the Born-Oppenheimer and the full three body treatment of H_2^+, are based on respectively a one- and two-dimensional DVR. Since no routines were available to generate the abscissas and weights for a general N-point normalized associated Legendre or Laguerre DVR of order m, I had to develop my own routine. The mathematical basis for this routine was discussed in section 3.3, and a schematic outline is given in figure 15 below where $\overline{P}_n^m(x)$ denotes both the Legendre and Laguerre polynomials.

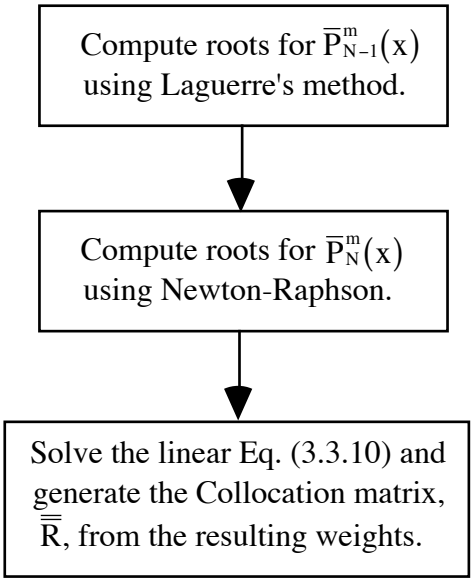

Figure 15 DVR subroutine

From the explicit expressions for the polynomial coefficients, given in reference [52], the first block in figure 15 computes the roots of the polynomial of degree N-1 (the order, m, is fixed throughout the routine) using the direct Laguerre's method [53]. This is a very fast

straightforward method using complex arithmetic. However, the catch is that exactly because it uses a direct method to evaluate $\overline{P}_n^m(x)$, in a general point x, the accuracy on the resulting roots drops dramatically as the degree, n, increases. To understand this, one should note that the numerical values of the polynomial coefficients increase very rapidly with growing degree, such that with the alternating signs of the coefficients, a direct method successively adds and subtracts very large numerical components of $\overline{P}_n^m(x)$, and thus effects a poor accuracy on the numerically small result. Conventionally one expresses this by saying that the direct approach is "numerically unstable" for large degree, n, in the sense that the calculations "explode numerically". An easy way to overcome this problem is to implement a method, for finding the roots of $\overline{P}_n^m(x)$, which does not explicitly make use of the algebraic expression for $\overline{P}_n^m(x)$, such that the very convenient recurrence relations, existing for the orthogonal polynomials[91], can be used instead. My choice fell on the well-known Newton-Raphson method discussed in reference [53]. However this root-finding scheme is slower than the direct Laguerre's method, so I decided to combine the speed of the later and the accuracy of the former in the following way: The polynomial $\overline{P}_n^m(x)$ can easily be shown to have exactly n distinct roots in the domain of definition. Moreover, it can be shown that the N roots of $\overline{P}_N^m(x)$ "interleave" the N-1 roots of $\overline{P}_{N-1}^m(x)$, i.e. there is exactly one root of the former in between each two adjacent roots of the latter. This fact came in handy when the two different root-finding schemes was to be combined into one fast and accurate routine, figure 15. The first block in figure 15 generates the approximate location of the N-1 roots of $\overline{P}_{N-1}^m(x)$ and then, in turn, the second block bracket the N roots of $\overline{P}_N^m(x)$, pinning them down more precisely by the Newton-Raphson method. Next the resulting abscissas (or roots) are substituted into Eq. (3.3.10) and the linear equation is solved in the third block in figure 15 using a "Singular Value Decomposition" technique (SVD) [53] that allows for an ill-conditioned[92] coefficient matrix. This procedure of solving Eq. (3.3.10) directly, to obtain the weights, is probably the only questionable step in the overall DVR routine, as we have no control over the conditioning of the coefficient matrix (i.e. it can be close to singular). However it was my experience that the routine was numerically stable for up to N=60 - thus the upper limit was a 60-point DVR scheme, but indeed, as we will see in the next section, this was sufficient. Finally the weights and abscissas are used to construct the Collocation matrix, $\overline{\overline{R}}$, and the unitary matrix, $\overline{\overline{U}}$, defined in Eq. (3.3.17).

Next we go through the routine computing the pure electronic potential energies, E, as

---

91 From reference [52] we deduce

$$(\ell - m)P_\ell^m(\eta) = \eta(2\ell-1)P_{\ell-1}^m(\eta) - (\ell+m-1)P_{\ell-2}^m(\eta), \quad \text{where} \quad \begin{cases} P_m^m(\eta) = (-1)^m(2m-1)!!\left(1-\eta^2\right)^{m/2} \\ P_{m+1}^m(\eta) = \eta(2m+1)P_m^m(\eta) \end{cases}$$

and

$$nL_n^m(\xi) = (2n+m-1-\xi)L_{n-1}^m(\xi) - (n+m-1)L_{n-2}^m(\xi), \quad \text{where} \quad \begin{cases} L_0^m(\xi) = 1 \\ L_1^m(\xi) = m+1-\xi \end{cases}$$

92 i.e. the matrix is close to singular in terms of the machine's floating point precision.

function of the inter-nuclear separation, R. The numerical scheme for the Born-Oppenheimer approximate treatment of the H_2^+ was discussed in section 5.7, and a schematic outline of the program is given in figure 16 below.

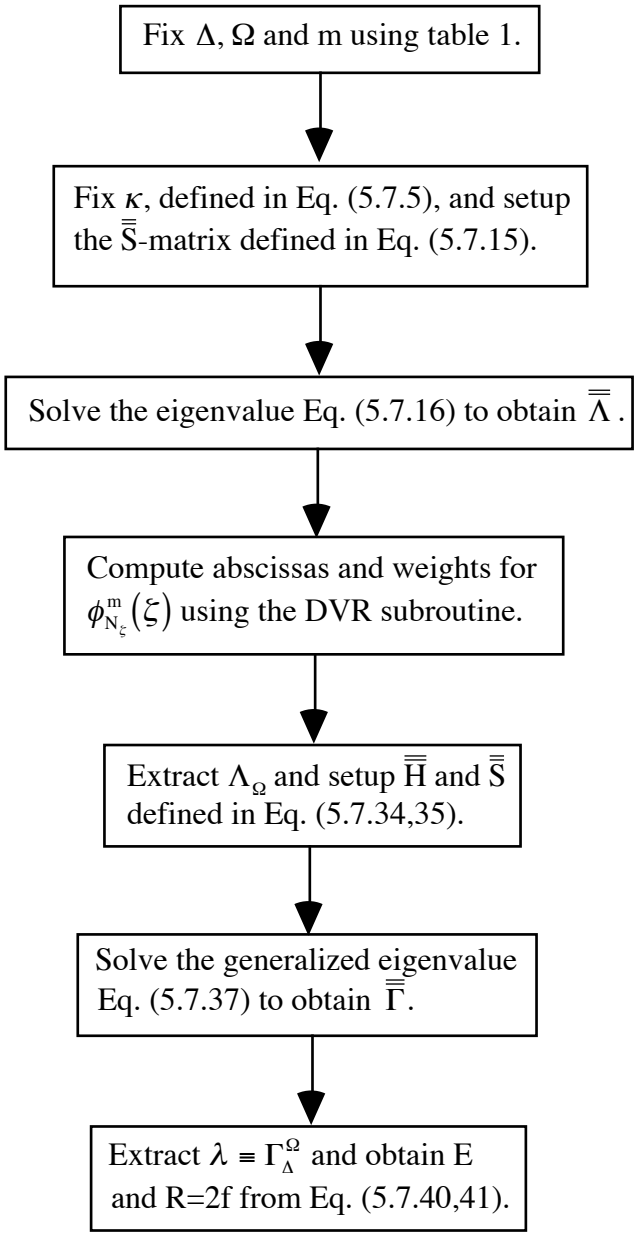

Figure 16 BO program

To solve the eigenvalue equation in block three in figure 16 a "Householder reduction method" followed by a "Tridiagonal QL Implicit" algorithm was implemented. The Householder algorithm (TRED2 in [53]) reduces the $N_\eta \times N_\eta$ symmetric matrix $\bar{\bar{S}}$ (see figure 13) to a tridiagonal form, which in turn can be diagonalized by the "Tridiagonal QL Implicit" algorithm (TQLI in [53]). The combination of TRED2 and TQLI (269 lines of

FORTRAN-77 code) is believed to be the most effective known technique for finding all the eigenvalues (and/or eigenvectors) of a real, symmetric matrix. The generalized eigenvalue problem in block 6, on the other hand, forms a much bigger computational task. No algorithms are discussed in Numerical Recipes [53] for this type of eigenvalue problem, and no standard subroutine libraries (e.g. "The Numerical Algorithms Group (NAG) library") offer routines that most effectively can solve such generalized eigenvalue equations. First I was provided with a software package that solves a generalized eigenvalue problem using an implementation of the "Spectral Transform Lanczos Method" (STLM) developed by Ruhe and Ericsson [66]. A short outline of the algorithm is given in reference [23]. The STLM package is quite large (6268 lines of FORTRAN-77 code) and involving to implement in the sense that a "black-box-user" has to provide many "strange" input parameters and additional CPU-time- and random-number-generating subroutines, but nevertheless it is a very effective and powerful routine to find a *subset* of eigenvalues and eigenvectors of a generalized eigenvalue matrix problem when the dimension is *large*. However the matrix dimension in the eigenvalue problems I considered was typically of the order 30-40, and therefore the STLM routine turned out to be quite inefficient and most of all slow. The use of the STLM package was simply an "overkill" for the sort of problems I had at hand. Unfortunately it took me a while before I realized this, and besides nor was I motivated to think in terms of a replacement since it seemed I had no alternative to the STLM routine. Eventually I got hold on a software package (RGG) developed by Garbow [67] that very efficiently solves a generalized eigenvalue equation for *all* the eigenvalues (and/or eigenvectors) using an implementation of a "QZ algorithm" [68]. This routine is much smaller (only 1245 lines of FORTRAN-77 code), easy to implement and, perhaps most importantly, for the dimensions I was considering, it proved to be substantially faster than the STLM routine. Actually it took 15 seconds[93] to solve a 30×30 generalized eigenvalue problem using STLM whereas it only took 0,15 seconds to solve the same problem using RGG. Again these numbers should be compared with the CPU-times spent in the other blocks in figure 16, which is illustrated in figure 17 below for $N_\xi = N_\eta = 30$. Thus a tremendous speed-up followed when I changed from STLM to RGG - a factor of 100 for the generalized eigenvalue routine itself when $N_\xi = 30$, as in figure 17. It should be noted that in figure 17 the CPU-time is shown for the different subroutines for the instance where only *one* eigenpair, (E, R), was desired - in which case the DVR subroutine was clearly the far most time consuming single subroutine. However this subroutine is only called one time per execution of the BO program, such that when hundreds of eigenpairs were desired, the real "bottle-neck" in the BO program was the RGG routine.

---

93 All the elapsed execution times presented in this thesis are measured as the CPU-time it took to execute a scalar optimized and vectorized (O2) FORTRAN-77 routine on a CONVEX C3240 with four CPU's of each 43Mflop.

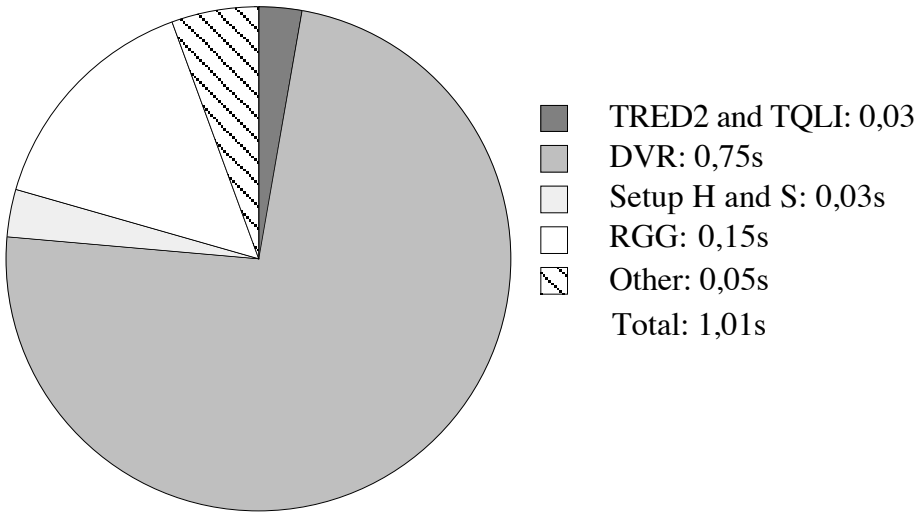

Figure 17 CPU-time in BO program

Finally I will go through the programs that computes the full three particle wave function for the H_2^+ system. The program was split up into two different parts; the first program (BASIS) computes the Born-Oppenheimer approximated energy dependent Sturmian-like basis functions (see the $\overline{\overline{B}}_j$ matrices in Eq. (5.7.42) and Eq. (5.8.8)), and the second program (SCATT) generates the R-matrix and propagates the wave function, in this electronic Sturmian basis-set, for a selected initial electronic state. Schematic outlines of the BASIS and the SCATT programs are given in figure 18 and 19, respectively. Clearly the BASIS program resembles the BO program discussed above, and evidently the same eigenvalue routines were used in both programs. Thus figure 17 also gives a description of the elapsed execution times in the BASIS program, just in this algorithm we sum over all the grid points in f and each of the eigenstates in the *truncated* ($M_\eta < N_\eta$) basis-set obtained from the diagonalization of Eq. (5.7.16). For $N_f = 500$, $N_\xi = N_\eta = 30$ and $M_\xi = M_\eta = 10$, the total CPU-time was estimated to 18 minutes and 7 seconds. Due to the limited core memory the energy dependent basis-set matrices, $\left\{\overline{\overline{C}}_j \; j = 1,...N_f\right\}$ and $\left\{\overline{\overline{D}}_\Omega^j, \; j = 1,....N_f \wedge \Omega = 1,...M_\eta\right\}$, computed by the BASIS program, had to be stored off-core. The high I/O performance of the super-computers (typically $20Mb/s$) made this disk buffering practical, such that $\overline{\overline{C}}_j$ and $\overline{\overline{D}}_\Omega^j$ were easily accessible to the SCATT program. In SCATT the successive computation of the R-matrix and the following propagation of the scattering wave function, using the recursive procedure derived in section 3.2, are all performed in the basis of electronic Sturmian-like functions. These electronic basis functions are represented by the $\overline{\overline{B}}_j$ matrices, introduced in section 5.7 (should not be confused with the $\overline{\overline{B}}_j$'s defined in section 3.2), and they are in turn constructed from the $\overline{\overline{C}}_j$ and $\overline{\overline{D}}_\Omega^j$ matrices, computed in BASIS. To repeat, these $\overline{\overline{B}}_j$ matrices are the transformation matrices from the primitive basis of Legendre and Laguerre functions to the Sturmian-like basis in which the zero order A-term of the J-functional is diagonal. The algorithm is started by initiating the scattering wave function, $\overline{u}_N$ (see end of section 3.2) at the boundary, $f = f_N$, by a specific electronic state characterized by

the quantum numbers Λ, Ω and m. Thus in accordance with the structure of $\overline{\overline{B}}_N$ (see figure 14), $\bar{u}_N$ is initiated as the $\left[(\Omega-1)M_\zeta + \Lambda\right]$´s unit-vector in the second block in figure 18.

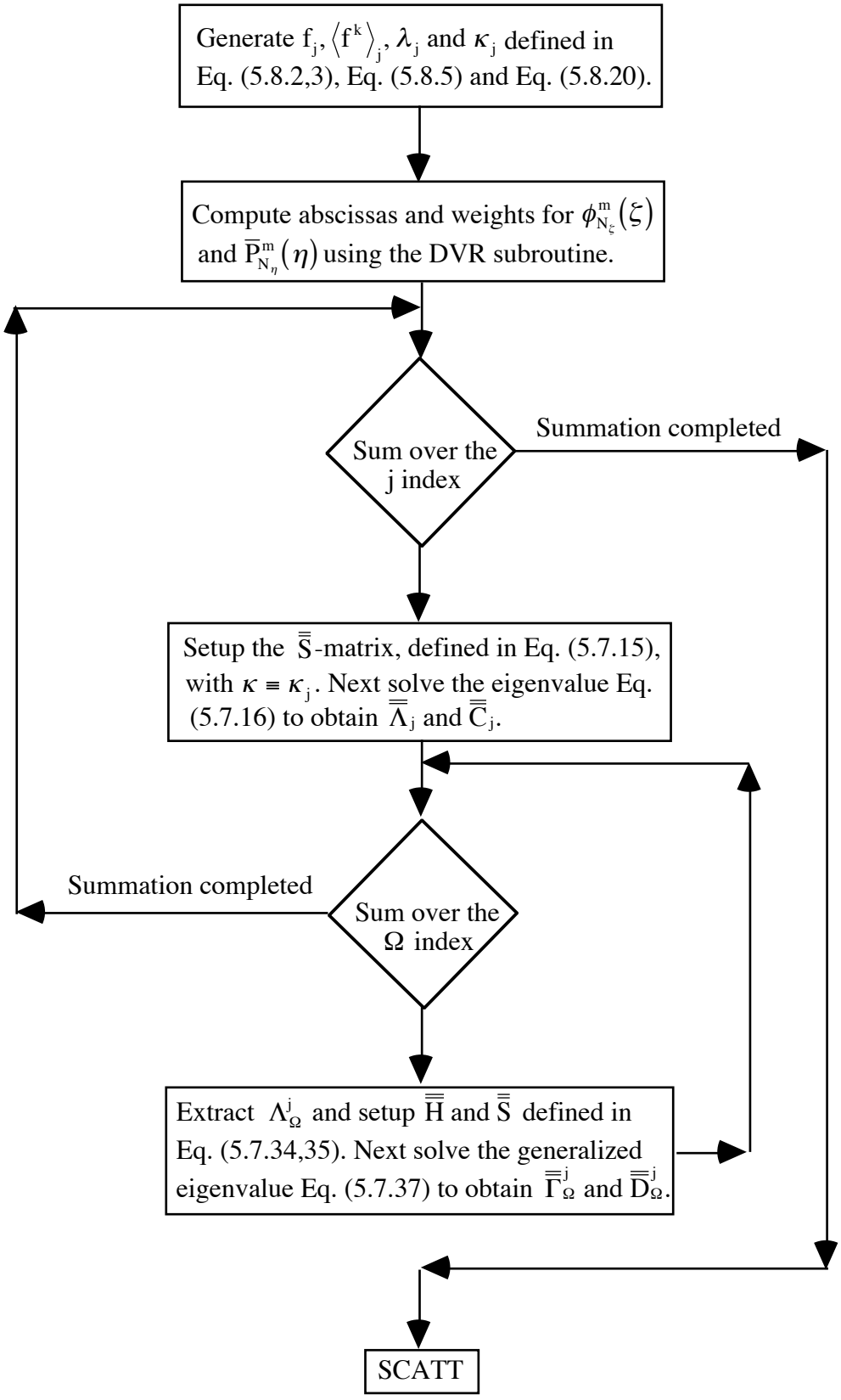

Figure 18 BASIS program

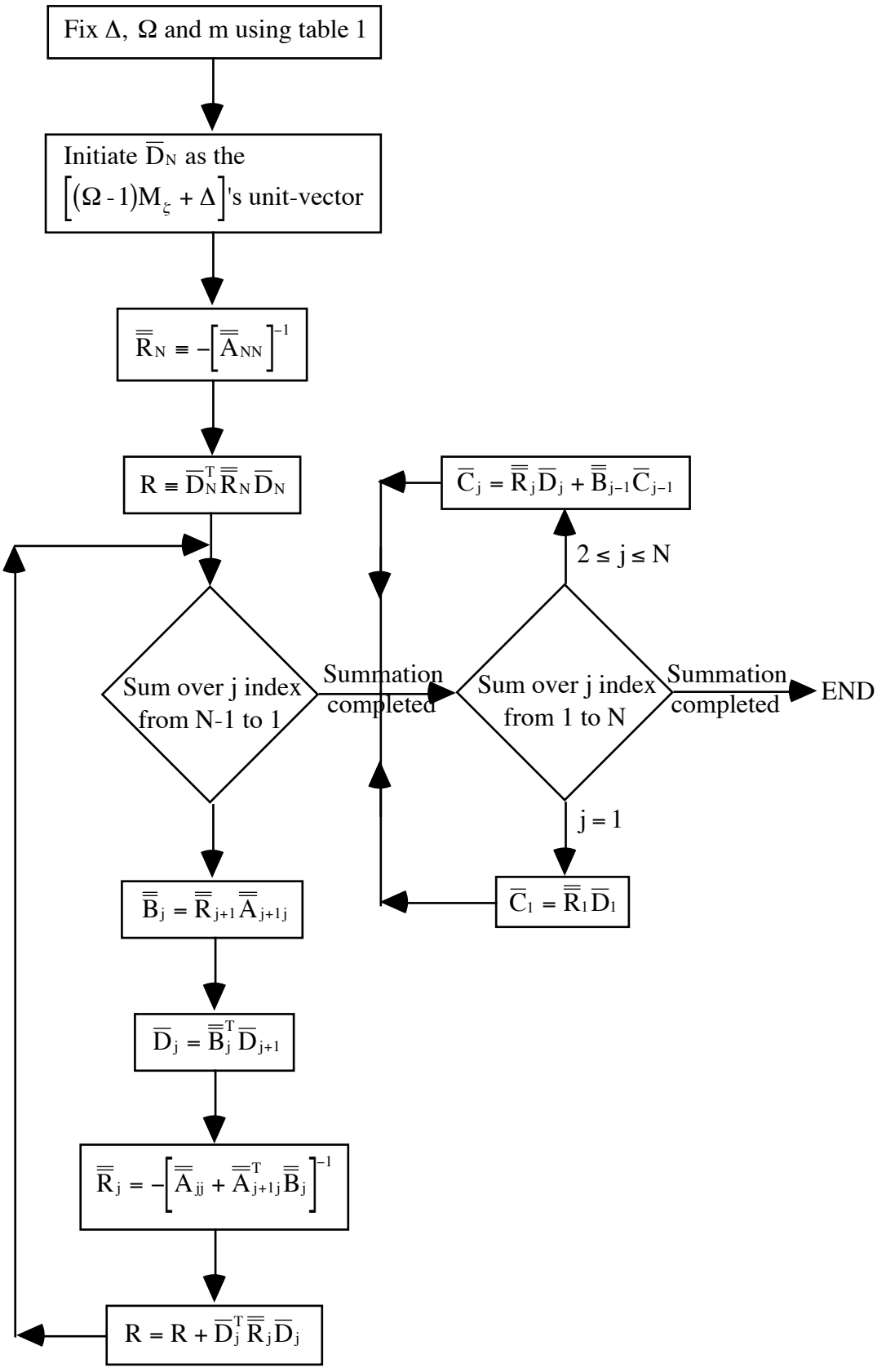

Figure 19 SCATT program

To allow for possibly ill-conditioned $\overline{\overline{A}}_{ij}$-matrices, the matrix inversions in SCATT (see figure 19) were carried out using an implementation of the "Singular Value Decomposition"

technique (SVD) [53] previously used to solve the linear equations in the DVR subroutine just discussed. This was, as we shall soon see in the next section, a necessary precaution because the variational R-matrix scheme could occasionally display "mild singularities" in agreement with the predictions made in the end of section 2.2. The f-diagonal $\overline{\overline{A}}_{jj}$-matrices, entering the block where $\overline{\overline{R}}_j$ is computed in figure 19, were constructed using Eq. (5.8.7) for the electronic part and Eq. (5.8.18,19) for the radial non-adiabatic part, followed by a transformation into the Sturmian-like basis-set using Eq. (5.8.8). The f-off-diagonal $\overline{\overline{A}}_{j+1j}$-matrices were constructed using the same scheme, just in this case Eq. (5.8.9,10) replaced Eq. (5.8.7). In order to optimize the code I extracted the four terms of the two dimensional DVR, Eq. (5.8.18,19), that were independent of f. In this way the very time-consuming 2-D DVR (25 minutes and 18 seconds for $N_\xi = N_\eta = 30$) would only have to be computed one time per scattering calculation. Actually, for fixed N_ξ and N_η, it turned out that with the high I/O performance of the super-computers, disk buffering was substantially faster than re-calculating the radial non-adiabatic elements. Once the shared data had been computed and stored on disk, additional scattering calculations could be computed with a significant speed-up. When this was done the real "bottle-neck" in the SCATT program was actually the transformation from the primitive basis of Legendre and Laguerre functions to the Sturmian-like basis given in Eq. (5.8.8). In figure 20 below the CPU-times are shown for the different steps in the SCATT program for *one iteration* with $N_\xi = N_\eta = 30$ and $M_\xi = M_\eta = 10$. Note that the two largest wedges in figure 20 represent the following steps: first the matrices $\left\{\overline{\overline{A}}_{ij}, \overline{\overline{C}}_i, \overline{\overline{C}}_j, \overline{\overline{D}}^i_\Omega \text{ and } \overline{\overline{D}}^j_\Omega \; \Omega = 1,...M_\eta\right\}$ are read from the disk ($\approx 2s$), then $\overline{\overline{B}}_i$ and $\overline{\overline{B}}_j$ are construct as described in section 5.7 (<< 1s), and finally the transformation given in Eq. (5.8.8) is performed ($\approx 15-16s$). In the case of $N_f = 500$ the total CPU-time was estimated to 4 hours 56 minutes and 23 seconds.

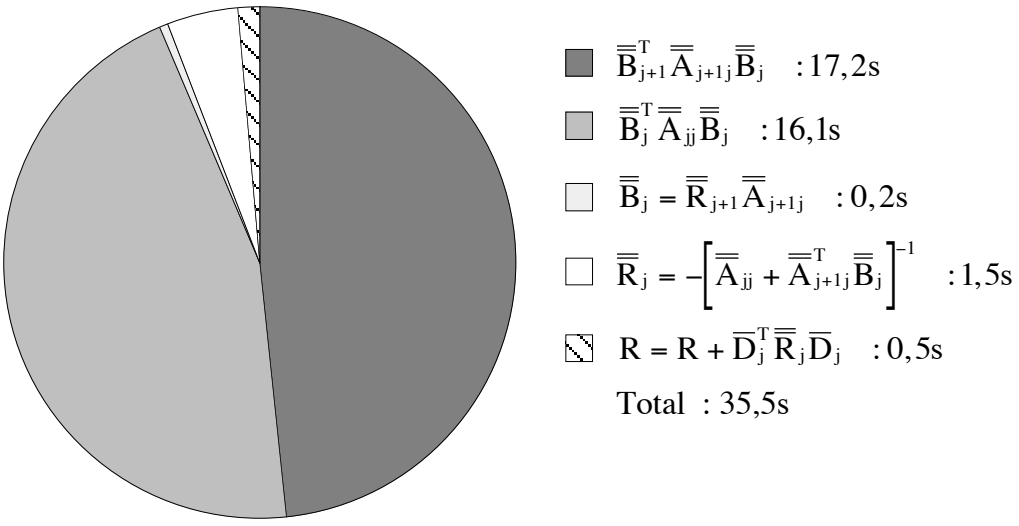

Figure 20 CPU-time in SCATT program

6.3 Results

As a prelude to the presentation of the results from the full scattering calculations, I will first discuss the results obtained for the Born-Oppenheimer approximate treatment of H_2^+. To repeat, this part of the project was only included to test the accuracy and stability of the DVR, BO and BASIS routines against some exact tabulated results. Thus the results to be presented now, for the electronic states, are not exciting in the sense that they have been reproduced many times before. However this comparison is very interesting in the present context of a full three body calculation in a basis of electronic states, as it will give us a first impression of the accuracy for the zero order term in this scattering calculation.

As mentioned in the introduction to section 5.7, a large number of theorists have already studied the clamped nucleus problem of the hydrogen molecular ion, and it is well-known that the resulting ordinary differential equations can, ideally speaking, be solved to any desired accuracy. The first extensive calculations have been carried out for several states of the molecule by Bates *et al.* in 1953 [69]. However these eigenvalues are only tabulated with 4-5 significant figures. For the lowest $1s\sigma_g$ and $2p\sigma_u$ states more extensive calculations in the Born-Oppenheimer approximation have been performed by Peek in 1965 [70]. Actually these results are accurate to 10-12 significant figures, and thus for these states the tables of eigenvalues should replace the better known ones of Bates *et al.* Also Peek's results for $1s\sigma_g$ and $2p\sigma_u$ were confirmed to the last figure by Montgomery Jr. in 1977 [71].

When I started out with this project, at the University of Aarhus, I spent some time implementing a FEM-expansion of $\psi_\Omega^m(\xi)$ (see Eq. (5.7.17)) in Hermite type functions (see Appendix C) known from Spline type interpolation. This was a relatively easy task for the clamped nucleus problem, but as I later on was to include the non-adiabatic terms, I decided to use the DVR method instead. Thus I have also calculated the electronic eigenvalues using a FEM approach, but as this technique was not used for the full three body problem, I find it irrelevant to present these results here. I will just state that the routine was written, and that it gave very accurate results. Before we compare my results for the electronic energies, using the DVR method, with the ones mentioned above, I would like to comment on the convergence of the numerical schemes. First we should note that the electronic states computed by the BO and BASIS routines, are Sturmian-like eigenfunctions with the same value of the parameter κ. In other words this parameter had to be fitted or adjusted to a specific value in order to obtain the electronic energy, E, for a given inter-nuclear separation, R. This, in turn, meant that the accuracy of the computed eigenpair, (E, R), was largely determined by the precision with which the specific κ parameter could be pinned down. The accuracy on κ itself was given by the floating point precision of the computer (typically $10^{-13} - 10^{-14}$), such that the precision on R (and E) varied from 10^{-13} at small distances and up to 10^{-9} at larger R. Thus it should be emphasized that when comparing the exact energies with the computed eigenvalues, at a given separation R, the precision with which the

eigenvalue R could the determined, should also be considered. Below I have tabulated the convergence of the energy of $1s\sigma_g$ at the fixed separation R=2.0 a_0 for different values of the parameters N_ξ and N_η entering the numerical scheme discussed in section 5.7. $1s\sigma_g$ was chosen since for this state we have exact values for E, and the separation R=2.0 a_0 was then picked because at small distances the κ parameter could be pinned down to give R with almost the floating point precision of the machine (i.e. $R = 2.0 \pm 10^{-13}$).

Exact value -0.6026342144949 [70, 71]				
E/au	N_ξ=5	10	30	50
N_η=5	-0.6	-0.6026342	-0.6026342	-0.6026342
10	-0.6	-0.6026342	-0.60263421449	-0.602634214495
30	-0.6	-0.6026342	-0.60263421449	-0.6026342144949
50	-0.6	-0.6026342	-0.60263421449	-0.6026342144949

It should be clear from these numbers that less than 10 functions in any of the two coordinates, ξ or η, was insufficient. Also we see that the accuracy of the scheme was largely determined by the number, N_ξ, of associated Laguerre polynomials included in the expansion of the wave function, and thus less dependent on N_η - just as long as this number was higher than 10. However the most exciting conclusion that can be drawn from the above numbers is of course that with a sufficiently large basis-set ($N_\xi \geq 50$ and $N_\eta \geq 30$) I obtained an eigenvalue that was in *complete* agreement with the exact results [70, 71] - correct to 13 decimal places. It is no secret that I was beside myself with joy when I first realized that my DVR approach to this problem gave literally exact results down to the floating point precision of the machine. Actually the joy was amplified by the fact that my scheme first appeared to give energies that were only correct to 3 decimal places. The problem was, as it turned out, that in all the calculations done by Bates, Peek and Montgomery Jr. the mass factor, μ_e (see Eq. (5.3.5)), had been put to unity. In other words they all ignored the finiteness of the mass of the protons, which is of course the central assumption in the Born-Oppenheimer approximation - but nevertheless, here I was, completely focused on how to go beyond the Born-Oppenheimer approximation, and thus not thinking in terms of infinite nuclear masses. Anyway, once the mistake was discovered, I was very pleased to see the exact agreement. In table 3 below the converted eigenvalues are shown for the $1s\sigma_g$ state at other values of R. In the first column the inter-nuclear separation is given with the precision of R listed in parentheses. The next column shows my results with $\mu_e \equiv 1$, and the third column with μ_e fixed to its real value listed in Eq. (5.3.5). The fourth column shows the exact results [70, 71], and the last column gives the eigenvalues obtained when adiabatic corrections have been

added to the Hamiltonian (see end of section 1.3) [72]. When the precision of the fitted nuclear separation, R, is taken into consideration, we see that my results are in *complete agreement* with the exact results [70, 71]. Further we note that the inclusion of adiabatic corrections increase the energies slightly at the fourth decimal place. Also it is interesting to see that just changing the mass-factor, μ_e, to its real value actually results in electronic energies that are closer to the adiabatic energies. In table 4 the computed electronic energies for the $2p\sigma_u$ state are compared against the exact results [70, 71], and again we see a complete agreement with the precision of R. In table 5 I have tabulated the computed energies for $2s\sigma_g$ against Bates' [69] results. Once more we see a complete agreement, to at least five decimal places. Instead of taking up more space with tabulating energies for the higher excited states of H_2^+, I have chosen to present the potential curves for the ten lowest electronic states graphically in figure 21, and then just state that they are all in agreement with Bates' [69] results. Besides, for the study of non-adiabatic transitions between $1s\sigma_g$ and $2p\sigma_u$, the curves for the two lowest states, are of particular interest, since they are typical of the behavior for bonding and anti-bonding orbitals in molecular orbital (MO) theory. From figure 21 we see that, for large inter-nuclear separations, R, the energy for both states is equal to the energy of a hydrogen atom in its ground state, 1s - that is with no inter-nuclear repulsion, $\frac{1}{R}$ (in au), we have $E_{1s\sigma_g/2p\sigma_u} \xrightarrow[R\to\infty]{} E_{1s} = -\frac{1}{2}\text{hartree}$[94]. Thus the wave functions must also go over into a linear combination of the ground states, $1s_a$ and $1s_b$ of an electron centered on nuclei a, b. As the wave function for $1s\sigma_g$ has positive parity with respect to inversion, and $2p\sigma_u$ negative parity, we obtain the well-known correlations

$$\begin{aligned} \Psi_{1s\sigma_g} &\xrightarrow[R\to\infty]{} \Psi_{1s_a} + \Psi_{1s_b} \equiv \sigma(1s) \\ \Psi_{2p\sigma_u} &\xrightarrow[R\to\infty]{} \Psi_{1s_a} - \Psi_{1s_b} \equiv \sigma^*(1s) \end{aligned} \tag{6.3.1}$$

The last two expressions for the molecular orbitals in Eq. (6.3.1) are the separate-atom designation. Here, to distinguish from the united-atom notation defined in section 5.7, the symmetry symbol is given first followed by the appropriate state of the separated atoms in parenthesis. An asterisk is used to distinguish anti-bonding orbitals, which are characterized by a nodal surface bisecting the inter-nuclear axis, that is by anti-symmetry under the transformation $\eta \to -\eta$ of Eq. (5.7.42)[95]. In figure 22 I have plotted the variation of purely electronic energy for the ten lowest states of H_2^+ (i.e. $E(R) - \frac{1}{R}(\text{au})$). At R=0, the two protons have come together to form the He^+ ion with the ground-state energy: $-\frac{1}{2}(2)^2\text{hartree}$=-2 hartree. Hence, we note that the lowest curve in figure 22 goes to the value -2 for $R \to 0$, even though this is not shown. Next, I would like to discuss the results from the scattering

---

94 For the hydrogen-like atoms we have the energy levels

$$E_n = -\frac{m_e}{2\hbar^2}\left(\frac{Ze^2}{4\pi\varepsilon_0}\right)^2 \frac{1}{n^2} = -\frac{1}{2}\left(\frac{Z}{n}\right)^2 \text{hartree(au)}$$

95 See also fodnote 76.

calculations.

It is difficult, if not impossible, at this point to give any conclusive verification of the results to be presented now - at least in terms of a decisive quantitative check. Besides the fact that this sort of calculation has never been attempted before, I am faced with the problem of having to comment on something as "abstract" as a three particle wave function. In other words the final evaluation of this sort of approach to the three particle problem, will have to wait until the next step in this project has been completed; namely the computation of the transition dipole moments between the calculated states, and the subsequent comparison with the absorption spectra recorded in DA white dwarfs. However when this has been said, I would like too add that with a "little intuition and common knowledge" about theoretical chemistry, I definitely believe that useful conclusions and information can be drawn from my results, even at this point. Especially when using semi-classical arguments, we can obtain valuable information about the asymptotic behavior of the channel wave functions: As argued in connection with Eq. (6.3.1), the electronic part of the total wave function can, for large values of the inter-nuclear separation, approximately be expressed as some linear combination of states for the hydrogen atom. Thus asymptotically we would expect the total wave functions to roughly converge to a product of some wave function for a hydrogen atom and a free-particle wave function for a proton - that is

$$\Psi_{H_2^+}\left(\vec{r},\vec{R}\right)\xrightarrow[R\to\infty]{} e^{i\vec{k}\vec{R}}\Psi_H\left(\vec{r}\right) \tag{6.3.2}$$

and

$$E_{tot} \approx E_{elec} + \frac{\hbar^2 k^2}{2\mu} \tag{6.3.3}$$

where $k = 2\pi/\lambda$ and the mass factor , μ, is given in Eq. (5.3.5). Hence a rough estimate of the asymptotic wave length in the radial motion is given by

$$\lambda \approx \frac{2\pi\hbar}{\sqrt{2\left(E_{tot} - E_{elec}\right)\mu}} \tag{6.3.4}$$

In other words, we expect the wave functions to asymptotically approach a periodic (cosine) function with a wave length approximately given by this expression. Moreover, using the "topology" of the potential energy curves, shown in figure 21, in a more general qualitative respect, we can deduce the expected classical behavior of the channel wave functions in the whole range of the inter-nuclear separation, R. Deviations from this expected classical behavior, should then be ascribed the quantum mechanical phenomena's as tunneling. Finally, the relative amplitudes of the "adiabatic forbidden or closed-channel" wave functions give a feeling of the validity of the Born-Oppenheimer approximation - which we of course expect to be quite good, even for a light system as H_2^+.

In the following I have shown the results from three different scattering calculations:

One where the incoming channel was fixed to the electronic ground-state, $1s\sigma_g$, with a total energy of -0.45 hartree, and two where the wave functions were initiated with the electronically excited states $2p\sigma_u$ and $2p\pi_u$ with a total energy of -0.1245 hartree. The total energies were fixed more or less arbitrarily; though as a rough guidance the energy in the $1s\sigma_g$ calculation was fixed such that asymptotically the kinetic energy in the radial motion corresponded to a typical temperature in the DA white dwarfs, i.e. 16000 K $\approx$[96] 0.05 hartree $= -0.45-(-0.50)$hartree. The total energies in the scattering calculations, initiated with the excited electronic states, were then fixed such that a transition would correspond to the line recorded in the absorption spectra, i.e. 1400Å $\approx$[97] 0.3255 hartree $= -0.1245-(-0.45)$ hartree. In all the calculations the parameters introduced in the numerical schemes discussed in chapter 5 were fixed to the following: $N_\xi = N_\eta = 30$, $M_\xi = M_\eta = 10$ and $N_f = 500$. Thus the BASIS routine computed 30×30 Sturmian-like electronic basis-functions in each grid point in f(=R/2), and in the SCATT routine this basis-set was then truncated to the 10×10 lowest eigenfunctions. A very important step in the construction of the Sturmian-like basis-set, was to define the *phases* of the eigenfunctions consistently from one grid point in f to the next. This was done in the BASIS routine, by a simple test of normalization of the matrices $\overline{\overline{C}}_j$ and $\overline{\overline{D}}_\Omega^j$ on $\overline{\overline{C}}_{j-1}$ and $\overline{\overline{D}}_\Omega^{j-1}$ using Eq. (5.7.16,39). The N_f parameter was then fixed such that the overlaps between the successive computed basis matrices were larger than 0.7. From table 3 I argued that inclusion of adiabatic terms introduced corrections to the electronic energies at the third decimal place, and thus there seemed no point in evaluating the electronic Sturmian-like basis functions to 13 decimal places, when the non-adiabatic calculations were performed. However as these calculations involved a 2 dimensional DVR, I fixed, on a rough estimate, N_ξ and N_η to 30.

In the following plots the amplitudes of the radial scattering wave functions have been normalized such that the wave function in the incoming channel ($1s\sigma_g$, $2p\sigma_u$ or $2p\pi_u$) has unit amplitude on the surface (R=8 au), after the scattering has taken place. In figure 23 I have depicted the radial variation of the $1s\sigma_g$-channel wave function for a scattering situation with a pure $1s\sigma_g$ electronic state in the incoming channel. Asymptotically we observe the expected periodic oscillation, discussed in connection with Eq. (6.3.2), and as we move in the R-axis the wave length decreases slightly to reach a minimum at R=2 au. Also the amplitude has a very large maximum at this point. Thus gradually more energy in transferred from the electronic degree of freedom into the kinetic radial motion when R is decreased. When moving further in the R-axis, λ increases dramatically, and at inter-nuclear separations smaller than 1 au, the wave function "dies out" very rapidly. All in all this behavior is in excellent agreement with the *attractive* potential energy curve for $1s\sigma_g$, shown in figure 21. This curve has a deep *minimum* at R=2 au, and for $E_{tot} = -0.45$hartree we find the *classical*

---

96 To convert from energy in atomic units (hartree) to an absolut temparature we have used $T = \left[\frac{E_h}{3.1668 \cdot 10^{-6}}\right]^o K$.

97 To convert from energy in atomic units (hartree) to wavelength in Angstrom we have used $\lambda = \frac{h \cdot c}{E} = \left[\frac{455.6}{E_h}\right]$Å.

turning-point to be at R=1 au. Using Eq. (6.3.4) with $E_{elec} \approx -0.50$ hartree we expect the wave length to be close to 0.66 au for large inter-nuclear separation. With an accuracy of two hundredth au this is exactly what we observe in figure 25 ($\lambda \approx (0.64 \pm 0.02)$ au). In this figure I have also plotted the actual position of the points, and we see that with 500 points in the f(=R/2) coordinate, in the range from 0.2 au to 8.0 au (i.e. $\Delta f = 0.0312$ au), the grid-density is large enough to ensure a good resolution of the wave function, and thus effect a converting propagation from one grid point to the next. As mentioned before, I had 100 open (electronic) channels ($M_\xi = M_\eta = 10$) in each of the three scattering calculations presented, and in figure 24 and 26 I have shown a plot of the radial variation for the three outgoing channel wave functions with largest amplitude. The first thing that we note is that these components of the total wave function are very small compared to the component from the incoming channel. This is a strong indication of the validity of the Born-Oppenheimer approximation, which classically assumes that these channels are closed, see figure 21. In agreement with the potential curves for respectively the $2s\sigma_g$ and $3d\sigma_g$ states we observe, in figure 24, that the later component is killed much earlier than the former. The dramatic change in the amplitudes at the surface, in figure 26 (and figure 36), should be ascribed to a boundary effect from the Finite Element Method, but we also note that it is relatively small since this behavior is not observed in any of the plots of channel wave functions with a larger amplitude. In figure 27 and 28 I have graphically illustrated the coupling between the incoming $1s\sigma_g$ channel wave function and the $2s\sigma_g$ and $3d\sigma_g$ outgoing channel wave functions, as a simple smoothened plot of the ratio of the amplitudes. In these figures it is even more evident, that the non-adiabatic corrections to the Born-Oppenheimer approximation are very small. Note also the maximum at respectively R=2.5 au and R=4.7 au which suggests a maximum coupling at these inter-nuclear separations.

In figure 29 to 37 I have shown similar plots for the results obtained from the $2p\sigma_u$ and $2p\pi_u$ initiated scattering calculations. Instead of going into a long tiresome discussion and interpretation of these results I will just emphasize the most distinct features of the plots, and then leave the detailed study of the graphs to the reader. An outline of the sort of information that can be extracted from the plots was given above, and moreover I think that most of the figures speak for themselves. In figure 29 we notice, a much faster oscillatory behavior of the incoming channel wave function, than we say in figure 23, which is clearly due to the higher channel energy ($E_{tot} = -0.1245$ hartree). The wave length increases all the way in the R-axis, and the maximum amplitude at R=2 is considerably smaller than the one observed in figure 23. After R=2 au the function is killed very rapidly. Again this classical turning-point and the overall behavior observed for the wave function is in excellent agreement with the very *repulsive* $2p\sigma_u$ potential curve shown in figure 21. Using Eq. (6.3.4) with $E_{elec} \approx -0.50$ hartree, we expect the wave length to be close to 0.23 au for large inter-nuclear separation, and from figure 31 we find $\lambda = (0.24 \pm 0.02)$ au. In figure 33 and 34 we see a much larger coupling between the channel wave functions, than in figure 27 and 28,

which is caused by the fact that the potential curves for the involved electronic states in this case lie notably closer, see figure 21. The small top in figure 33 is a point of singularity from the ration of the two wave function, and hence has no physical significance. In figure 35 I have shown the radial variation of the $2p\pi_u$ incoming channel wave function. As the potential curve lies substantially higher than the once for the $1s\sigma_g$ and $2p\sigma_u$ states, we see a very slow and weak oscillation in this case. Actually we only have "$1\frac{3}{4}$ oscillations" in this plot, and consequently it is very difficult to speak of a true asymptotic value of the wave length at a specific inter-nuclear separation. However, if we take an averaged value of λ, in the interval from $R = (6.60 \pm 0.01)$au to $R = (7.34 \pm 0.01)$au, we obtain an approximate wave length on (1.48 ± 0.04)au. In this interval of R the E_{elec} varies from -0.133 hartree to -0.134 hartree (see figure 21), and thus when using Eq. (6.3.4) we obtain an expected λ on (1.55 ± 0.05)au. As the kinetic energy in the radial motion is low (about 0.009hartree for large R), we observe very little coupling in between the wave function in the incoming channel and the other channel wave functions. The only notable coupling in shown in figure 37, where we also observe a minimum close to the classical turning-point in the $2p\pi_u$ channel, followed by a maximum at R=4 au. At present time I can not come up with any rational explanation for this feature in figure 37, but definitely this must be ascribed to some kind of tunneling phenomenon as the $3p\pi_u$ channel is classically closed. Finally in figure 38, 39 and 40 I have plotted the partial components of the R-matrix computed in the three different scattering calculations. These partial components correspond to the *individual* terms in the sum in Eq. (3.2.20). In the figures for the $1s\sigma_g$ and the $2p\sigma_u$ cases, we observe several discontinuities in the successive construction of the R-matrix. In figure 40, for the $2p\pi_u$ scattering, these discontinuities are even more striking (note the logarithmic scale), and in this case we could indeed speak of a singularity-like behavior of the R-matrix. This situation resembles, to a limited extend, the "Kohn anomalies" [31] inherited in the Kohn variational principle discussed in the end of section 1.4, and as argued in the end of section 2.2 the applied variational R-matrix method was also excepted to display these spurious unphysical singularities and thus *potentially* be plagued by Kohn anomalies. However, and this can not be overemphasized, the numerical scheme seemed to be very stable and reliable in the sense that the wave functions converted nicely, and no singularities or discontinuities were observed for the wave functions in any of the calculations - even in the cases where "close-to-singularities" appeared as shown in figure 40. Thus I did *not* note any behavior in the overall numerical scheme that could justify the term "Kohn anomalies" when used in its original meaning, as in reference [31, 39], but if the same sort of terminology was to be used we could phrase it provocatively as follows; "the applied variational R-matrix method displays numerically insignificant singularities that could be referred to as integrable Kohn anomalies".

As a "colorful" completion of this section I have included two pictures, figure 41 and 42 (see also front-page), each showing two iso-surfaces (of which one is transparent) and one

contour-surface of the total wave function resulting from a scattering calculation where the incoming channel was respectively a pure electronic $1s\sigma_g$ and $2p\sigma_u$ state. The pictures are 3D-scalar plots in the coordinates ξ, η and ϕ where the inter-nuclear separation, $R = 2f$, was fixed to 2 au. Note that the selected color-map is cyclic, such that a cycle of the color-scale does not necessarily correspond to a node-plane. This was preferred in order to obtain more colors in the pictures. The plots were created using the very powerful software package AVS (Application Visualization System).

Table 3 Data for $\mathbf{1s\sigma_g}$

R/au	BO-approx. Present/au $\mu_e \equiv 1$	BO-approx. Present/au $\mu_e = 0.99972776$	BO-approx. Exact [70, 71]/au $\mu_e \equiv 1$	Adiabatic Exact [72]/au $\mu_e = 0.99972776$
1.0(13)	-0.4517863133781	-0.4515214744047	-0.4517863133781	-0.45170606
1.5(13)	-0.5823232054550	-0.5821225574873	-0.5823232054550	-0.58211045
2.0(13)	-0.6026342144949	-0.6024702982357	-0.6026342144949	-0.60237486
2.5(13)	-0.5938235109905	-0.5936814005940	-0.5938235109905	-0.59354587
3.0(12)	-0.577562864049	-0.5774335761403	-0.5775628640490	-0.57727792
3.5(12)	-0.560855538798	-0.560733234764	-0.5608555387980	-0.56056794
4.0(11)	-546084883713	-0.54596561189	-0.5460848837129	-0.54579676
4.5(11)	-0.533940031109	-0.53382113487	-0.5339400311092	-0.5336552
5.0(11)	-0.524420295168	-0.524300105543	-0.5244202951676	-0.52413409
5.5(12)	-0.517231507858	-0.517109134078	-0.5172315078579	-0.51694708
6.0(10)	-0.51196904847	-0.51184418352	-0.5119690484667	-0.51168644
6.5(10)	-0.50821546996	-0.50808819645	-0.5082154699635	-0.50793509
7.0(10)	-0.50559400424	-0.50546461996	-0.5055940042393	-0.50531547
7.5(11)	-0.50379296471	-0.50366184915	-0.5037929647147	-0.50351601
8.0(10)	-0.5025703886	-0.50243791995	-0.5025703886000	-0.50229471
8.5(10)	-0.50174718746	-0.50161369632	-0.5017471874643	-0.50147248
9.0(10)	-0.5011954529	-0.50106120890	-0.5011954528984	-0.50092147
9.5(9)	-0.500826207	-0.5006914181	-0.5008262065266	-0.50055276
10.0(9)	-0.50057873	-0.5004435550	-0.5005787289439	-0.50030566

Table 4 Data for $2p\sigma_u$

R/au	BO-approx. Present/au $\mu_e \equiv 1$	BO-approx. Present/au $\mu_e = 0.99972776$	BO-approx. Exact [70, 71]/au $\mu_e \equiv 1$
1.0(14)	0.4351863748985	0.4353718111477	0.4351863748985
1.5(13)	0.04349846453898	0.0437121627581	0.04349846453898
2.0(12)	-0.1675343922024	-0.1673155490316	-0.1675343922024
2.5(11)	-0.292072048783	-0.291861964854	-0.2920720487832
3.0(11)	-0.3680850000399	-0.3678879284367	-0.3680850000399
3.5(11)	-0.415495726456	-0.415311449993	-0.4154957264561
4.0(12)	-0.4455506393605	-0.4453774215001	-0.4455506393605
4.5(11)	-0.46483897466	-0.464664781054	-0.4648389746611
5.0(10)	-0.47729161323	-0.477134555039	-0.4772916132283
5.5(10)	-0.485383144066	-0.485231611058	-0.4853831440662
6.0(10)	-0.49064389237	-0.49049656837	-0.4906438923684
6.5(10)	-0.49406031671	-0.49391615337	-0.4940603167091
7.0(10)	-0.49627171254	-0.49612989067	-0.4962717125439
7.5(10)	-0.49769564367	-0.49755553374	-0.4976956436628
8.0(10)	-0.4986960156	-0.49846714126	-0.4986960156017
8.5(10)	-0.49918273308	-0.49900447392	-0.4991827330795
9.0(10)	-0.49954382946	-0.49940645523	-0.4995438294691
9.5(9)	-0.499766514	-0.49962957102	-0.4997665142042
10.0(9)	-0.49990107	-0.49976442234	-0.4999010686027

Table 5 Data for $2s\sigma_g$

R/au	BO-approx. Present/au $\mu_e \equiv 1$	BO-approx. Present/au $\mu_e = 0.99972776$	BO-approx. Bates [69]/au $\mu_e \equiv 1$
1.0(14)	0.5770754112160	0.5771697336712	0.57708
1.4(13)	0.3194077319428	0.3194907915564	0.31941
2.0(12)	0.1391351246605	0.139206100001	0.13914
2.4(12)	0.0743942884928	0.074459281677	0.074397
3.0(11)	0.014446279533	0.01450433047	0.014448
3.4(12)	-0.011527483115	-0.01147307477	-0.011527
4.0(11)	-0.038514867457	-0.03846484360	-0.038515
4.4(11)	-0.051312574673	-0.05126490795	-0.051312
5.0(11)	-0.065505814677	-0.06546101890	-0.065505
5.5(11)	-0.07418097328	-0.07413807373	-0.074182
6.0(11)	-0.08088792282	-0.08084655183	-0.080888
6.5(11)	-0.08617579900	-0.08613564906	-0.086174
7.0(10)	-0.09042225667	-0.09038307413	-0.090423
7.5(11)	-0.093892813458	-0.09385438459	-0.093892
8.0(11)	-0.096777332868	-0.09673948282	-0.096775
8.5(10)	-0.09921332940	-0.0991759167	-0.099213
9.0(11)	-0.10130135623	-0.1012642688	-0.10130
9.5(11)	-0.103115483793	-0.1030786351	-0.10312
10(10)	-0.104710625912	-0.1046739512	-0.10471

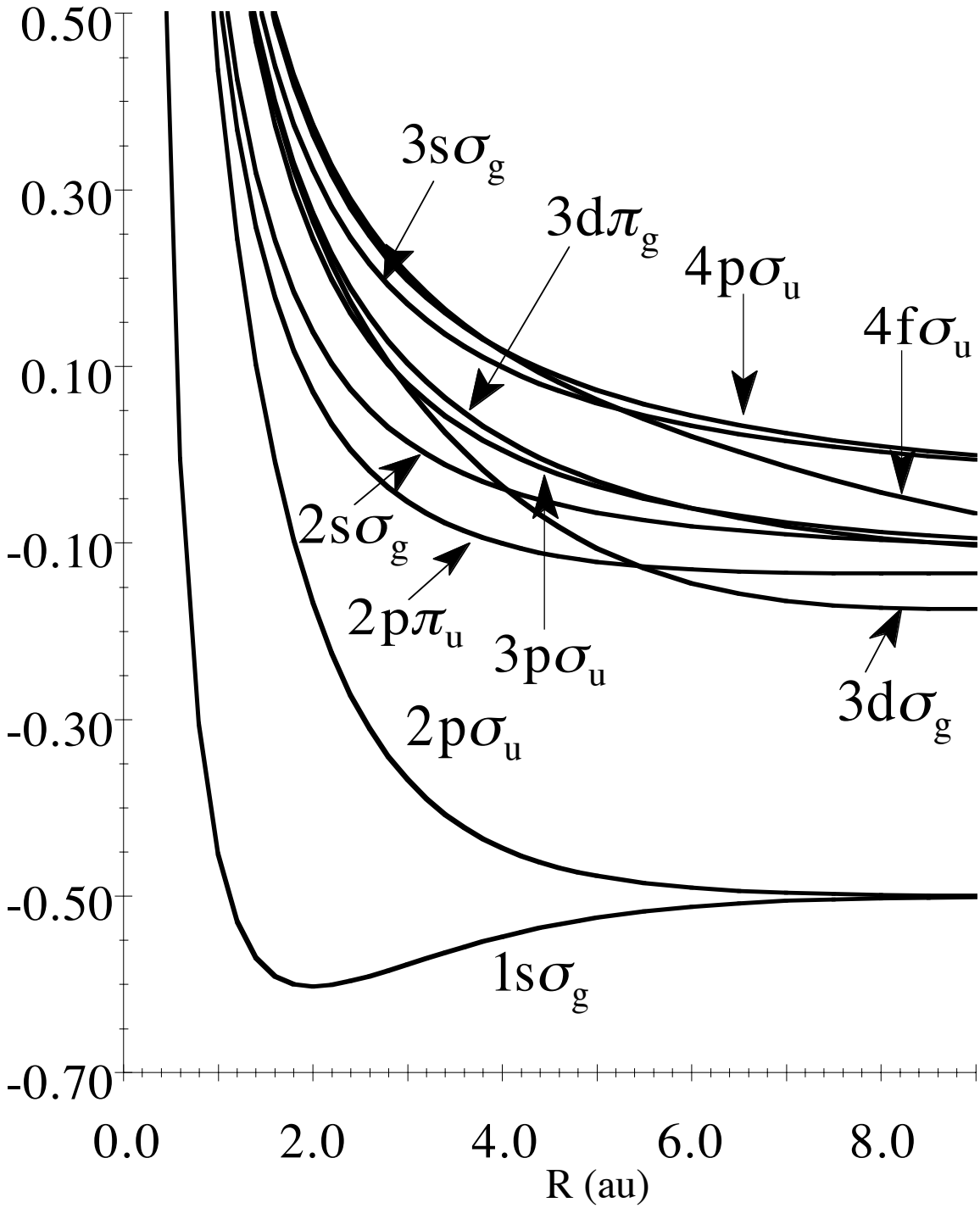

Figure 21 Potential energy curves

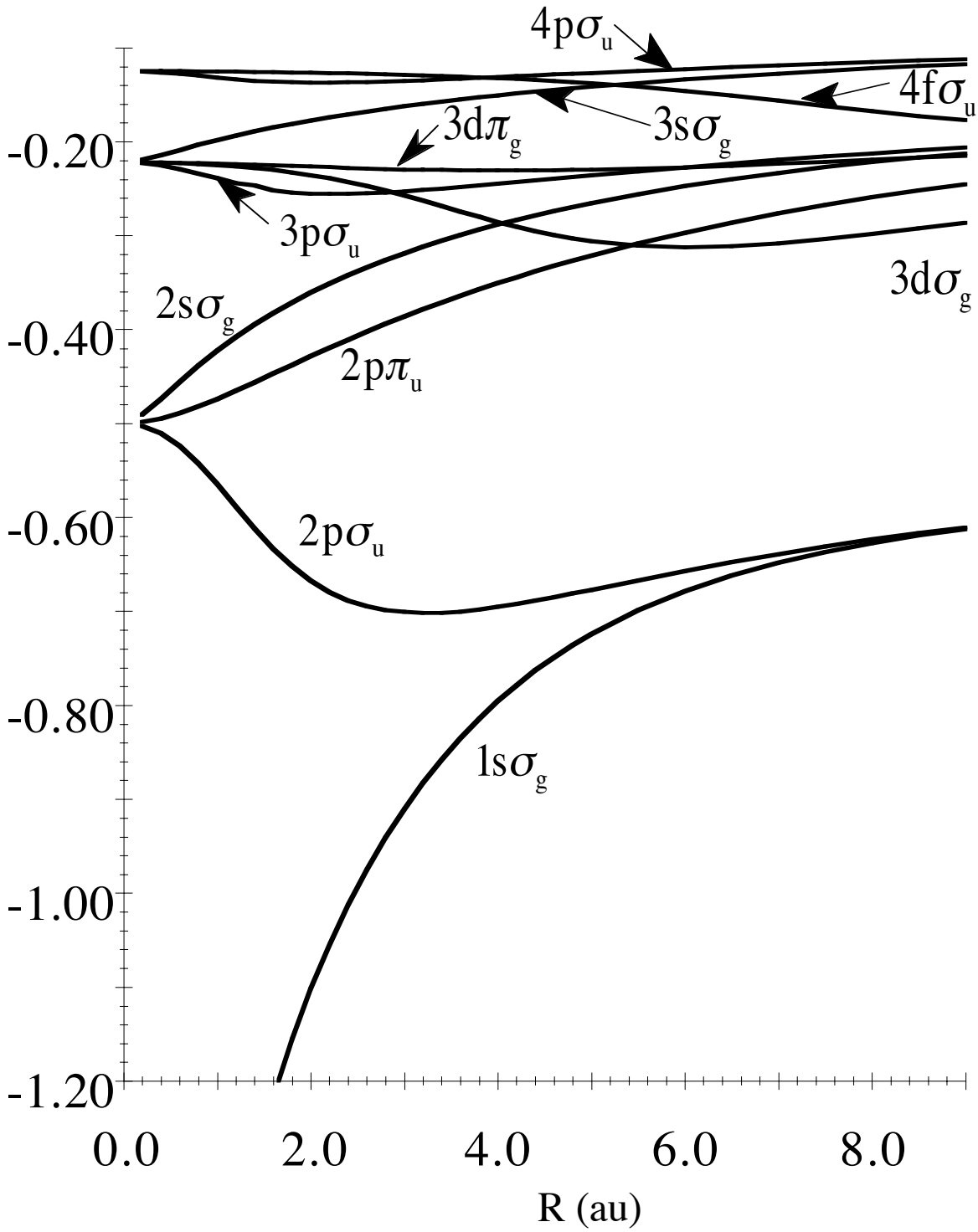

Figure 22 Pure electronic energy curves (E(R)-1/R)

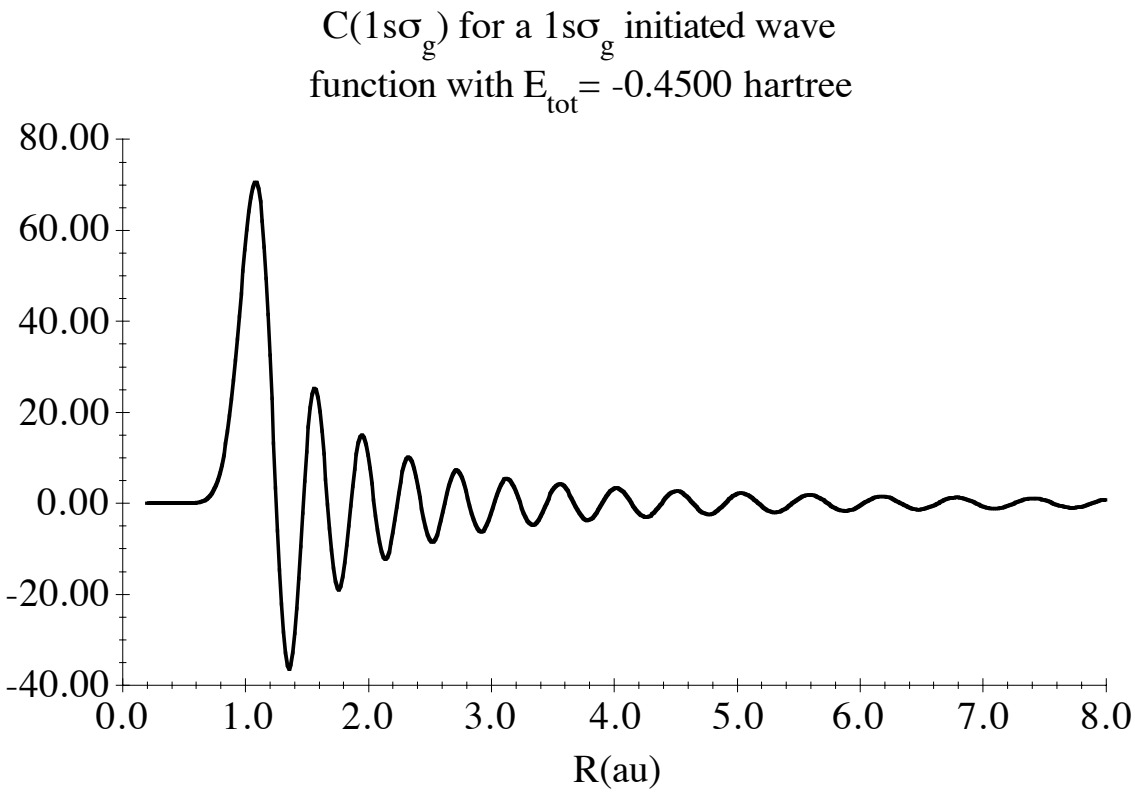

Figure 23 Plot of $\mathbf{C}\left(\mathbf{1s}\sigma_{\mathbf{g}}\right)$

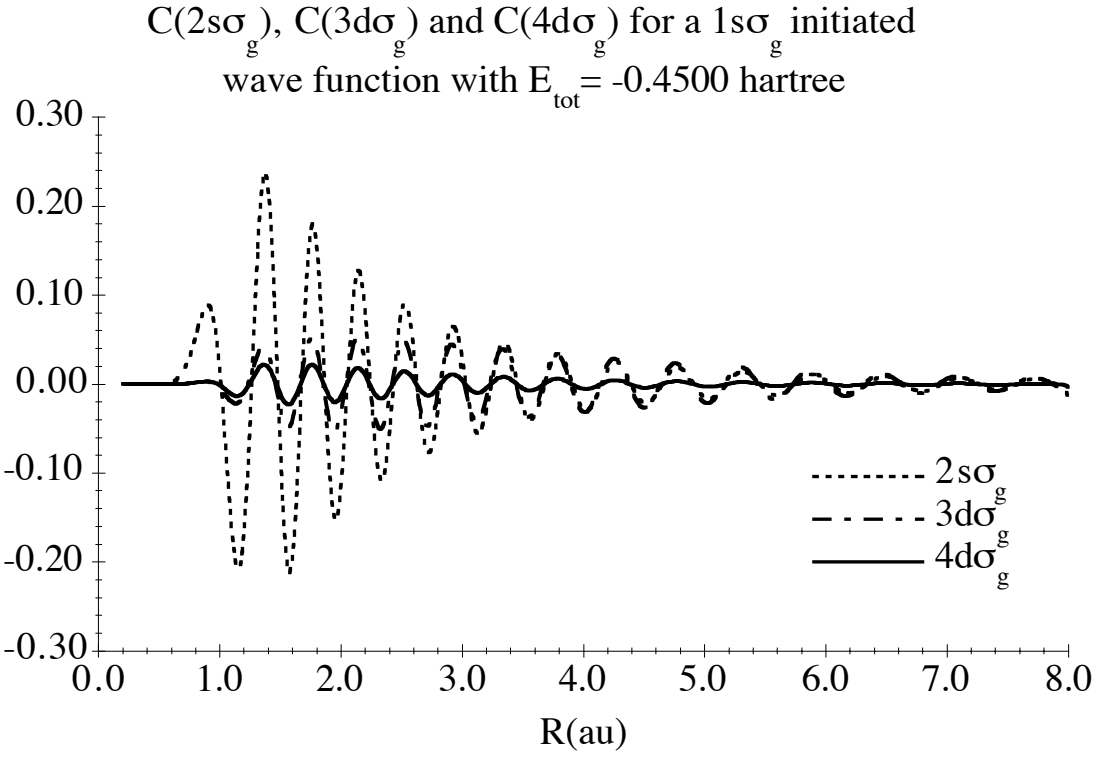

Figure 24 Plot of $\mathbf{C}\left(\mathbf{2s}\sigma_{\mathbf{g}}\right)$, $\mathbf{C}\left(\mathbf{3d}\sigma_{\mathbf{g}}\right)$ **and** $\mathbf{C}\left(\mathbf{4d}\sigma_{\mathbf{g}}\right)$

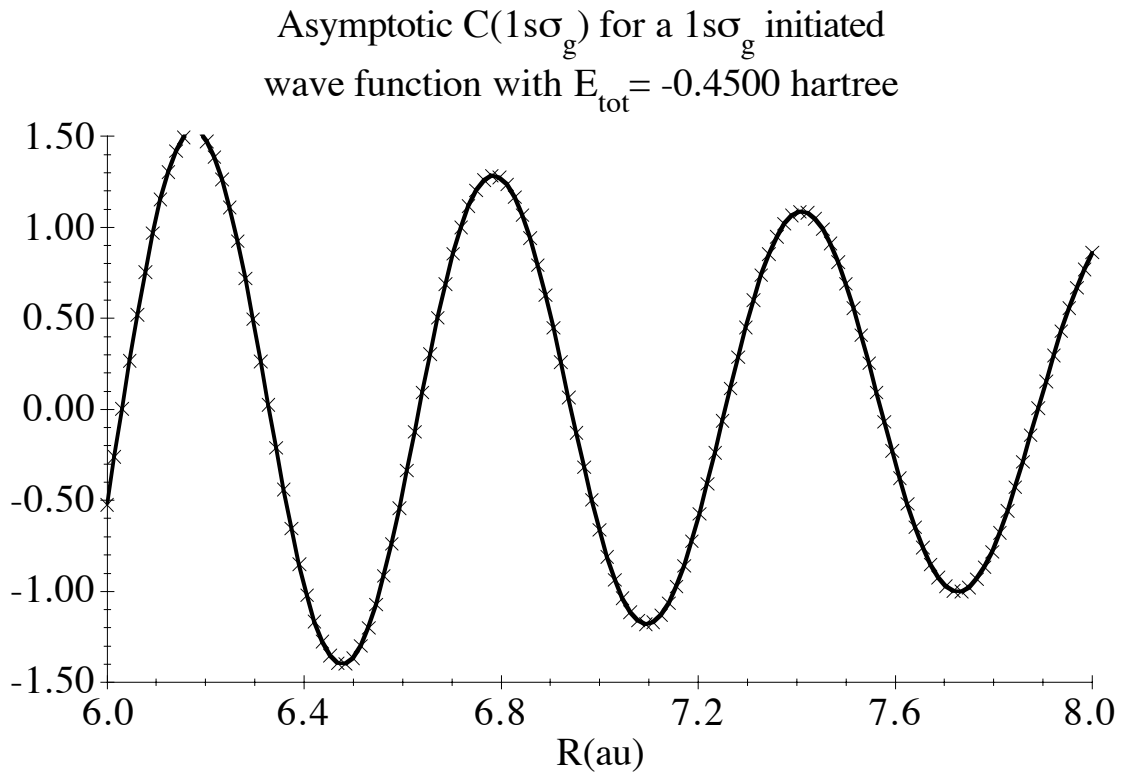

Figure 25 Plot of asymptotic $\mathbf{C}\left(\mathbf{1s}\sigma_{\mathbf{g}}\right)$

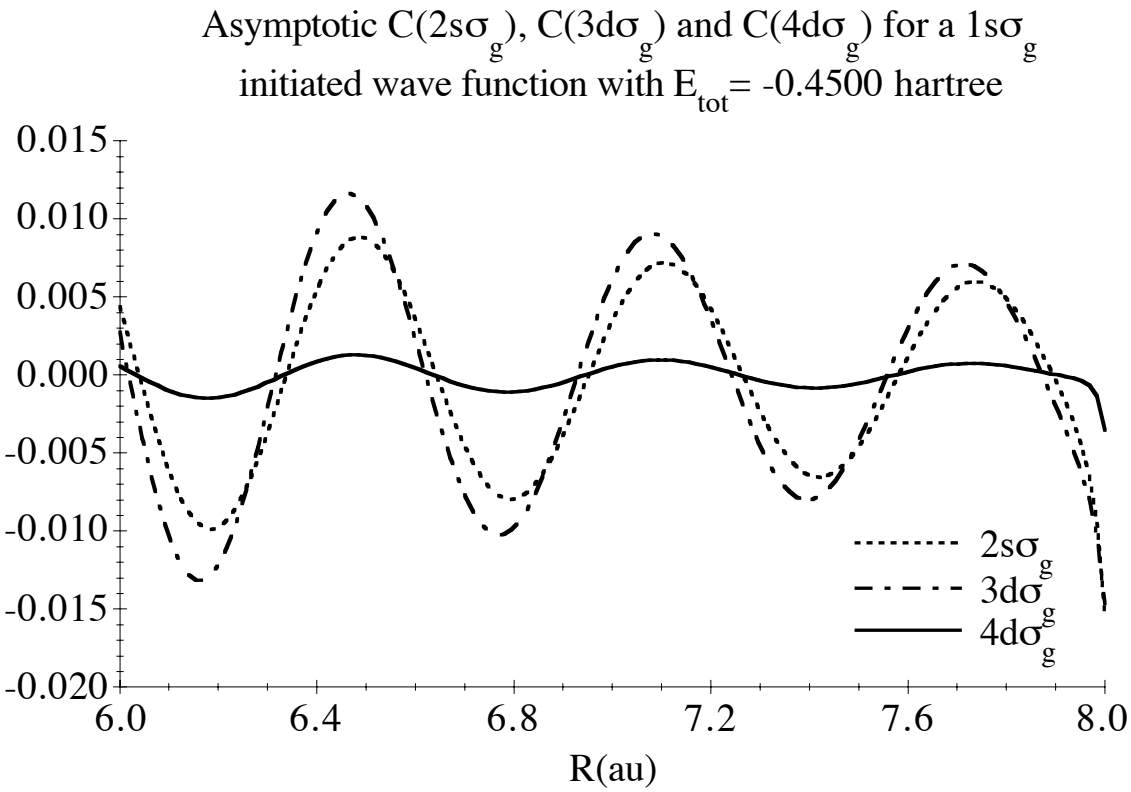

Figure 26 Plot of asymptotic $\mathbf{C}\left(\mathbf{2s}\sigma_{\mathbf{g}}\right)$, $\mathbf{C}\left(\mathbf{3d}\sigma_{\mathbf{g}}\right)$ **and** $\mathbf{C}\left(\mathbf{4d}\sigma_{\mathbf{g}}\right)$

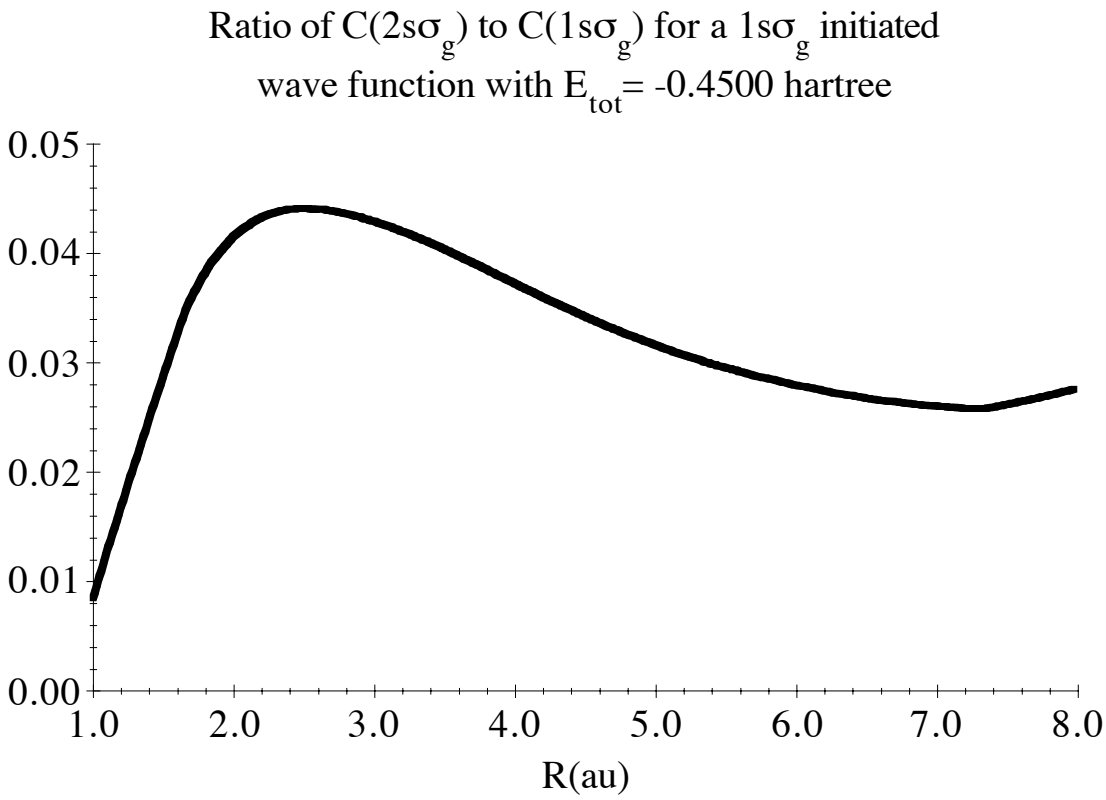

Figure 27 Plot of $\mathbf{C}\left(\mathbf{2s}\sigma_{\mathbf{g}}\right)/\mathbf{C}\left(\mathbf{1s}\sigma_{\mathbf{g}}\right)$

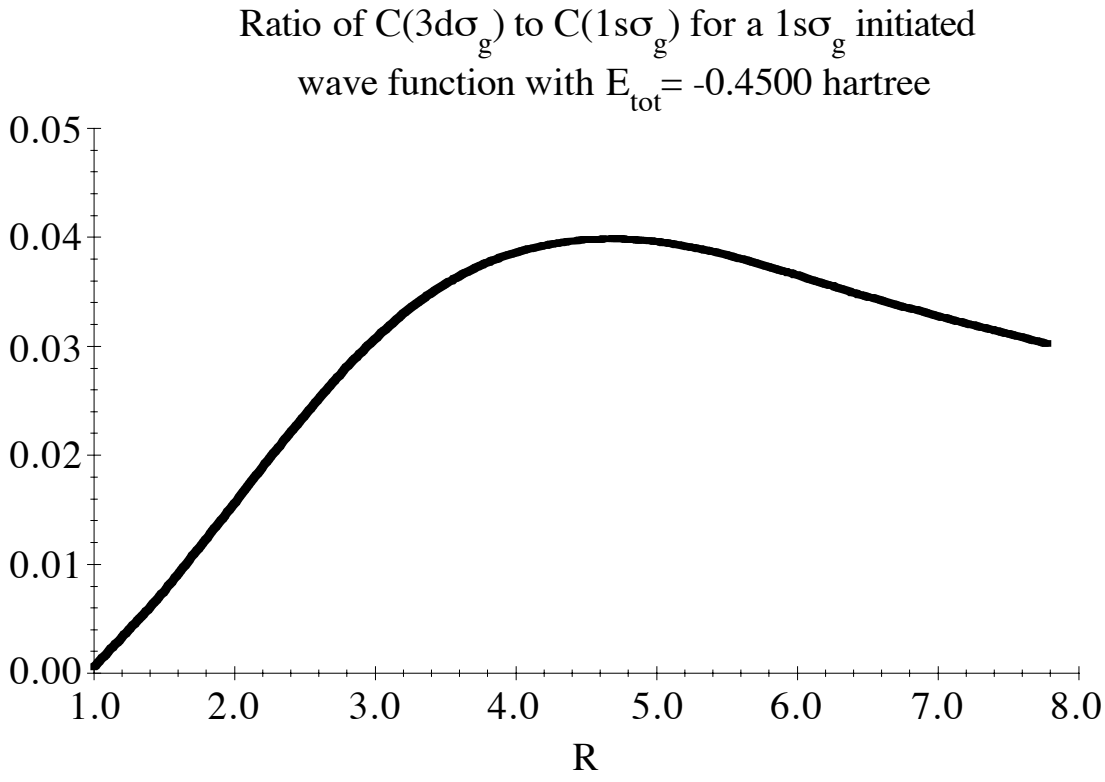

Figure 28 Plot of $\mathbf{C}\left(\mathbf{3d}\sigma_{\mathbf{g}}\right)/\mathbf{C}\left(\mathbf{1s}\sigma_{\mathbf{g}}\right)$

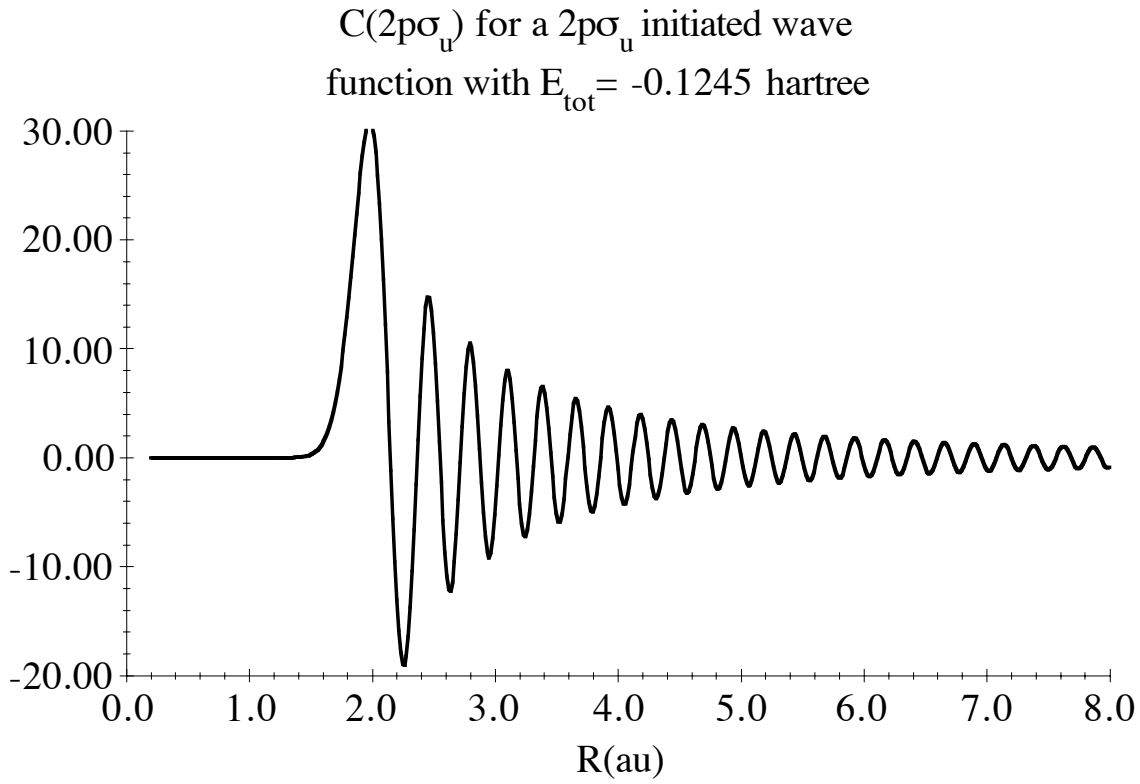

Figure 29 Plot of $\mathbf{C(2p\sigma_u)}$

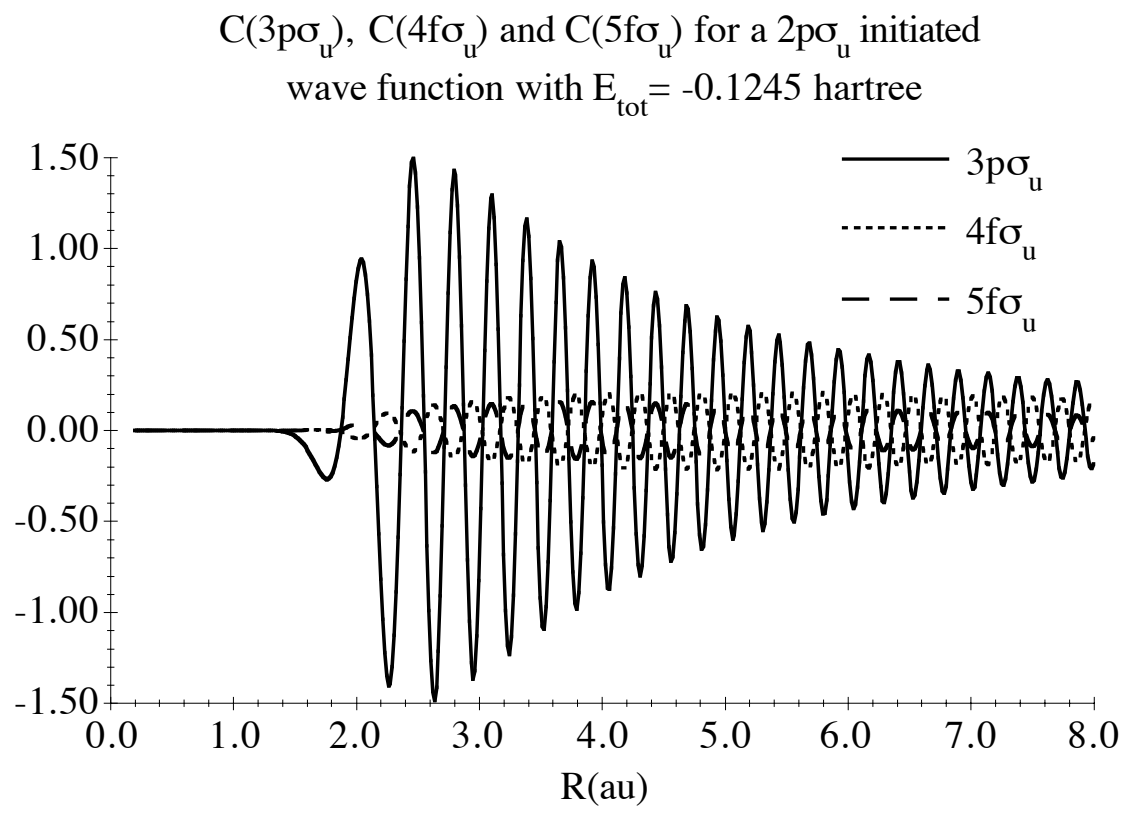

Figure 30 Plot of $\mathbf{C(3p\sigma_u)}$, $\mathbf{C(4f\sigma_u)}$ **and** $\mathbf{C(5f\sigma_u)}$

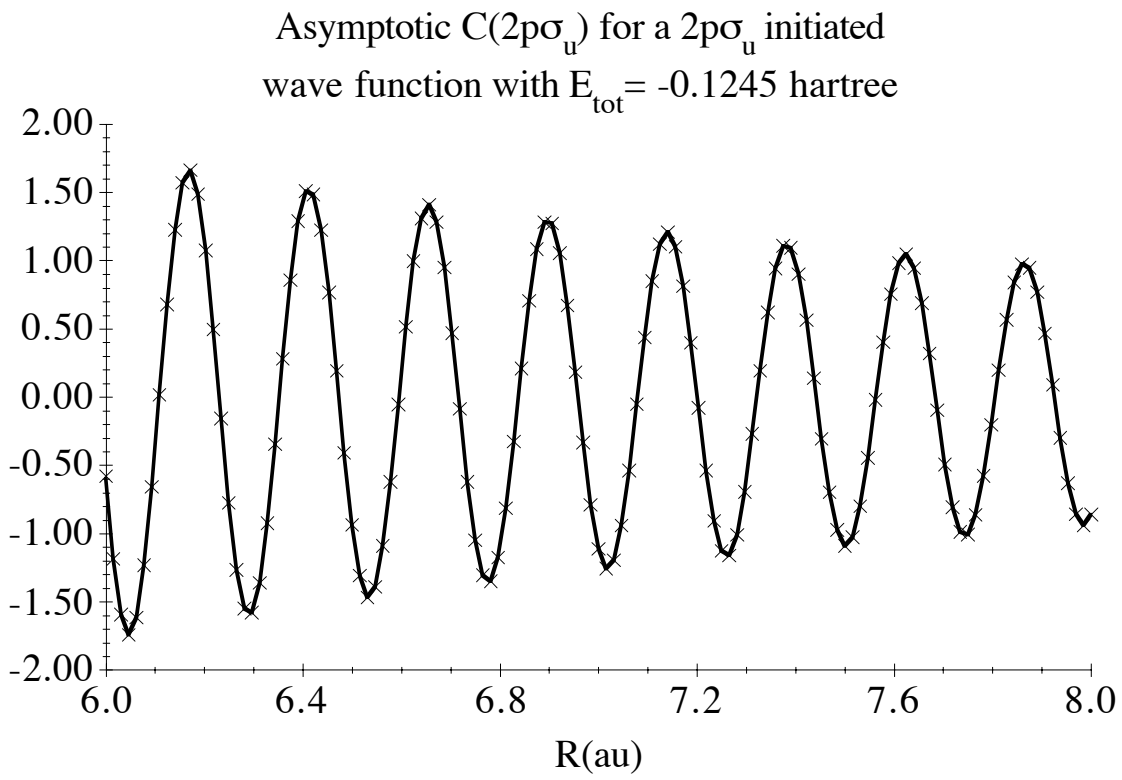

Figure 31 Plot of asymptotic $\mathbf{C(2p\sigma_u)}$

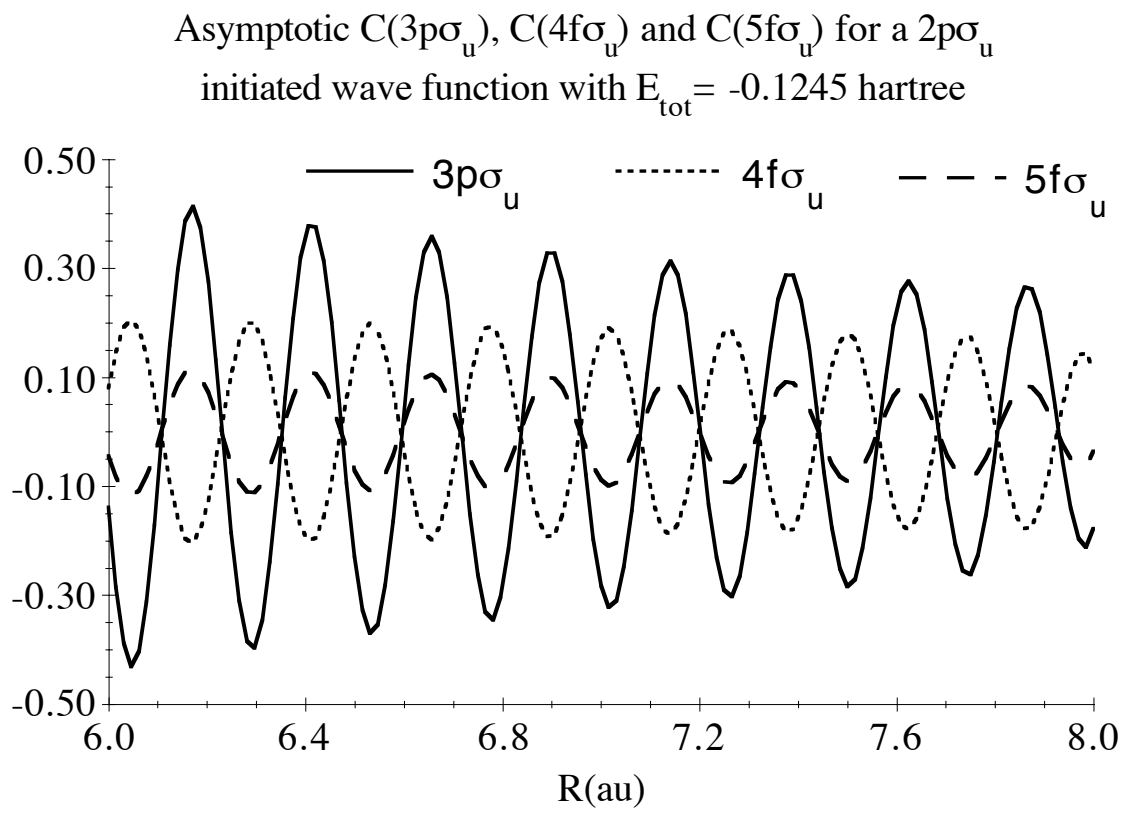

Figure 32 Plot of asymptotic $\mathbf{C(3p\sigma_u)}$, $\mathbf{C(4f\sigma_u)}$ **and** $\mathbf{C(5f\sigma_u)}$

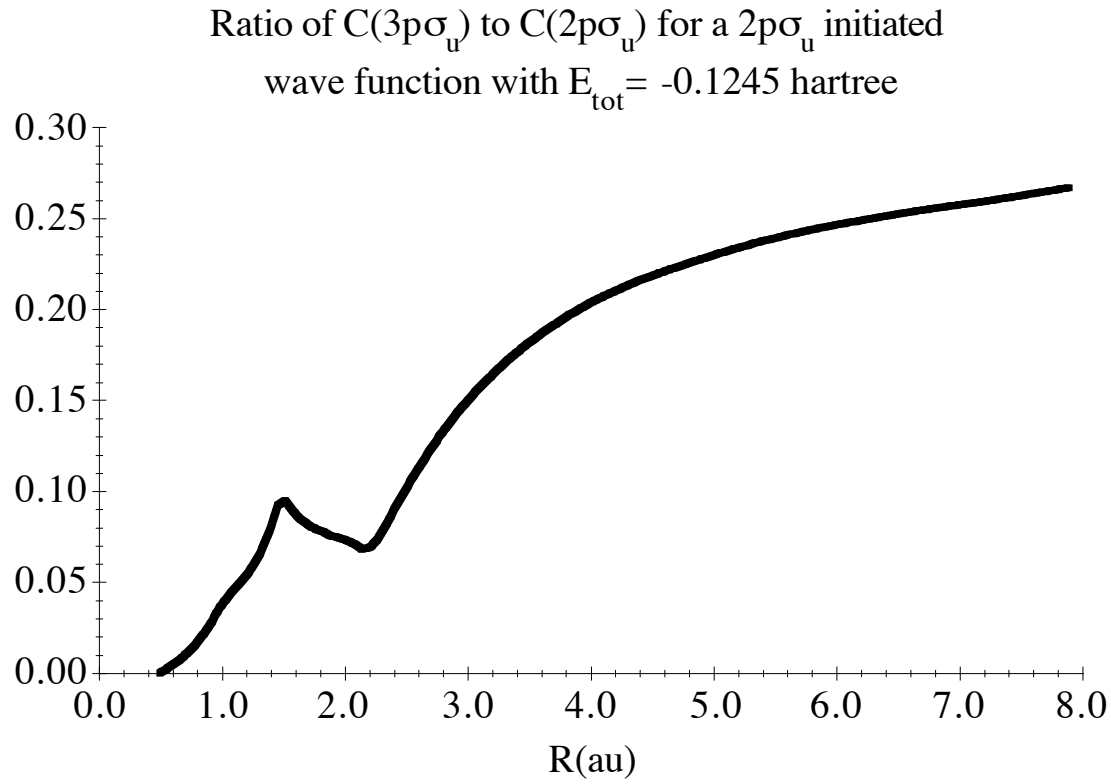

Figure 33 Plot of $\mathbf{C(3p\sigma_u)/C(2p\sigma_u)}$

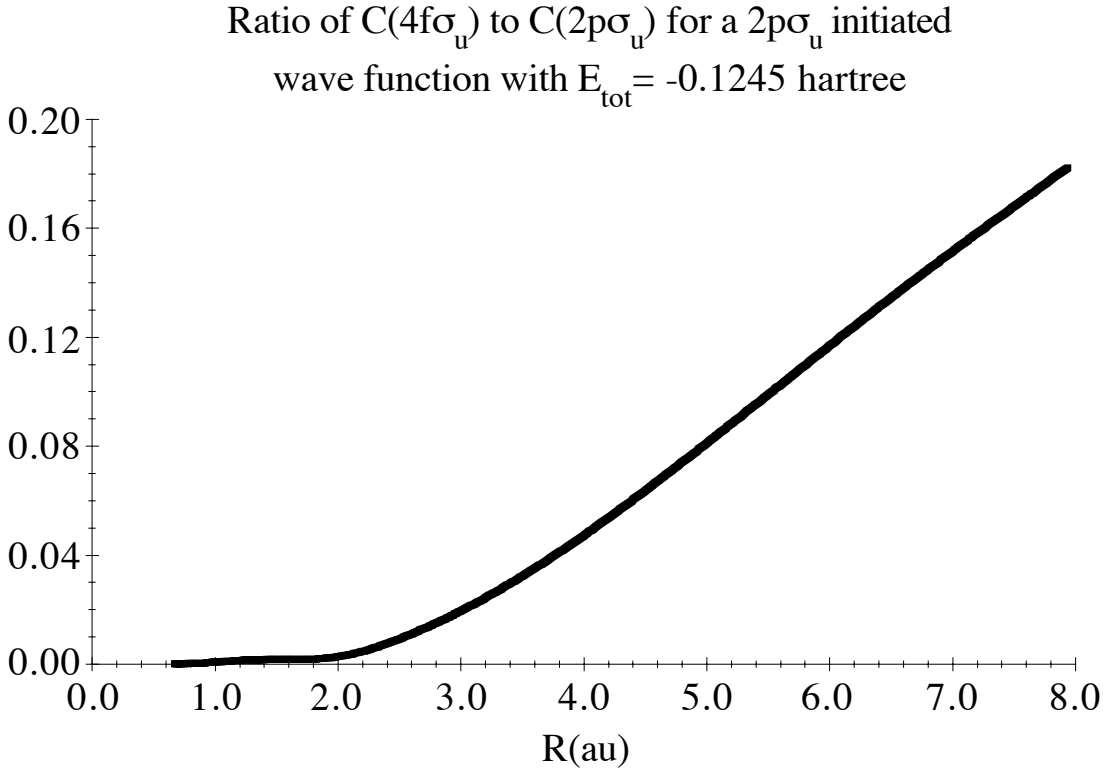

Figure 34 Plot of $\mathbf{C(4f\sigma_u)/C(2p\sigma_u)}$

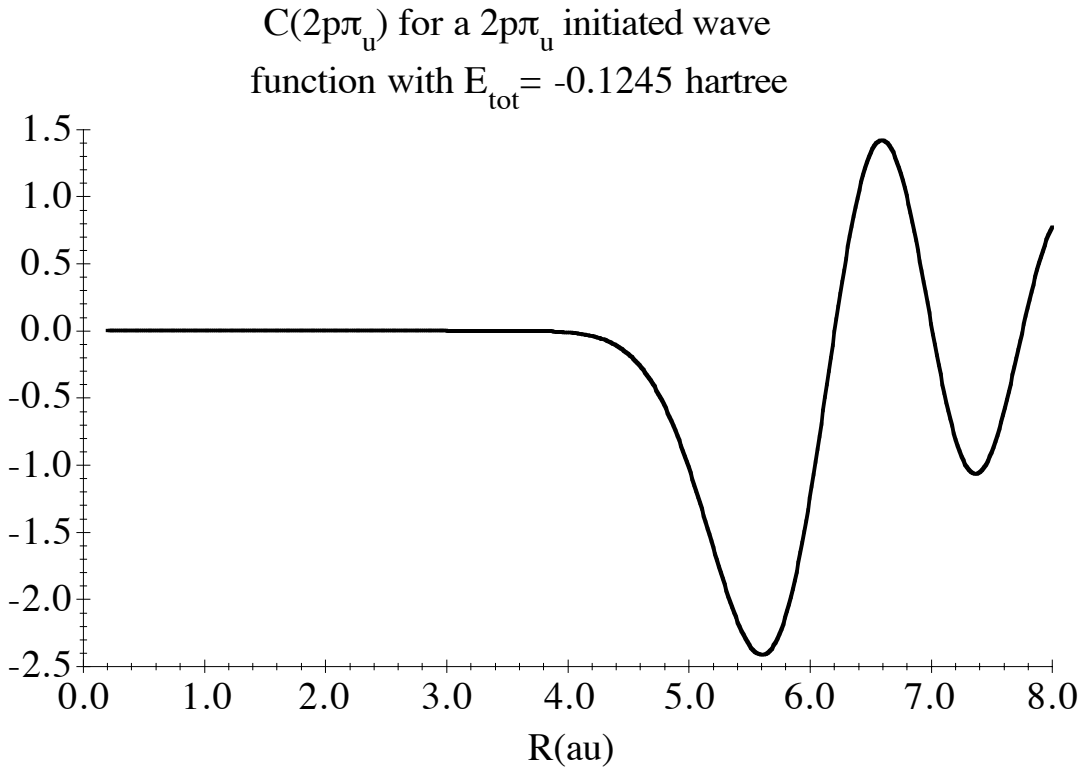

Figure 35 Plot of $\mathbf{C(2p\pi_u)}$

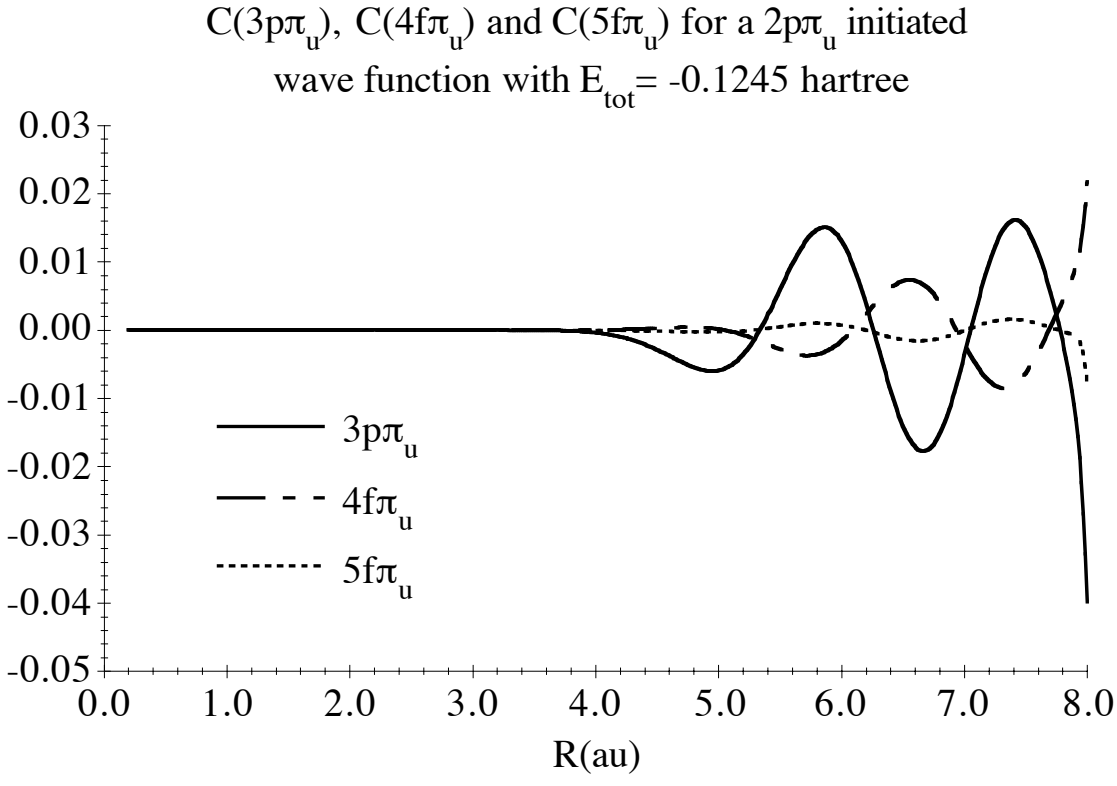

Figure 36 Plot of $\mathbf{C(3p\pi_u)}$, $\mathbf{C(4f\pi_u)}$ **and** $\mathbf{C(5f\pi_u)}$

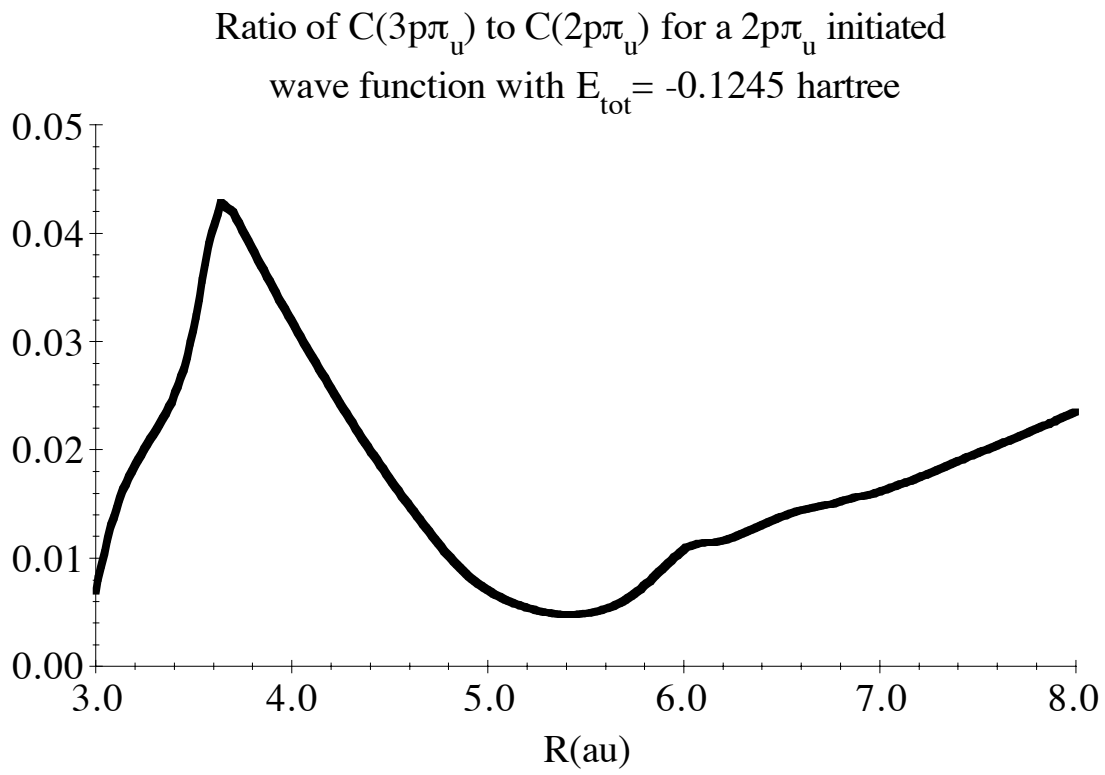

Figure 37 Plot of $\mathbf{C}(\mathbf{3p}\pi_{\mathbf{u}})/\mathbf{C}(\mathbf{2p}\pi_{\mathbf{u}})$

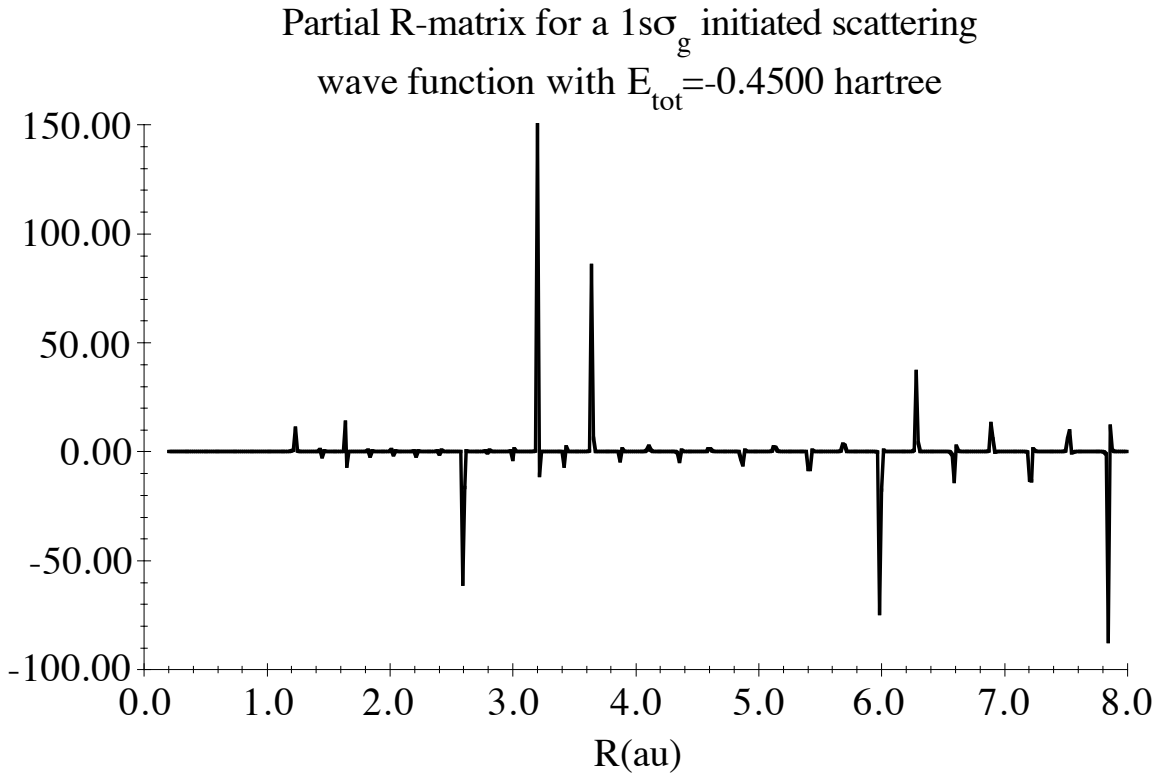

Figure 38 Plot of partial R-matrix for $\mathbf{C}(\mathbf{1s}\sigma_{\mathbf{g}})$

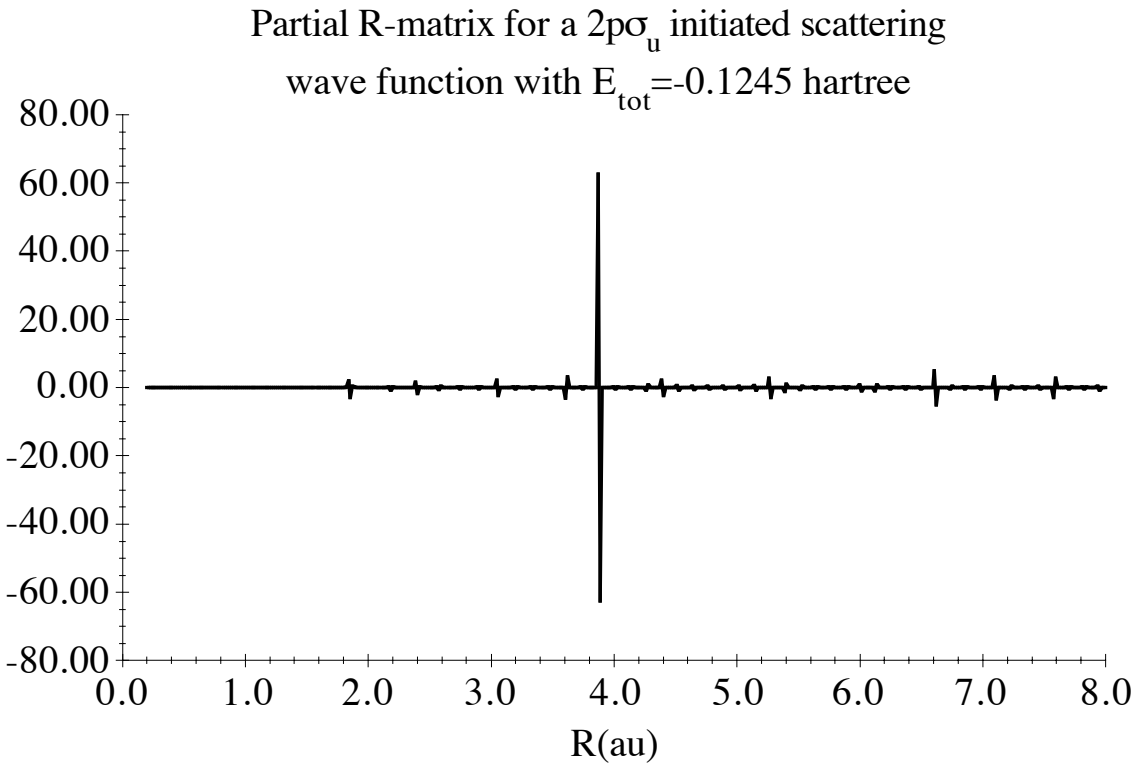

Figure 39 Plot of partial R-matrix for $\mathbf{C(2p\sigma_u)}$

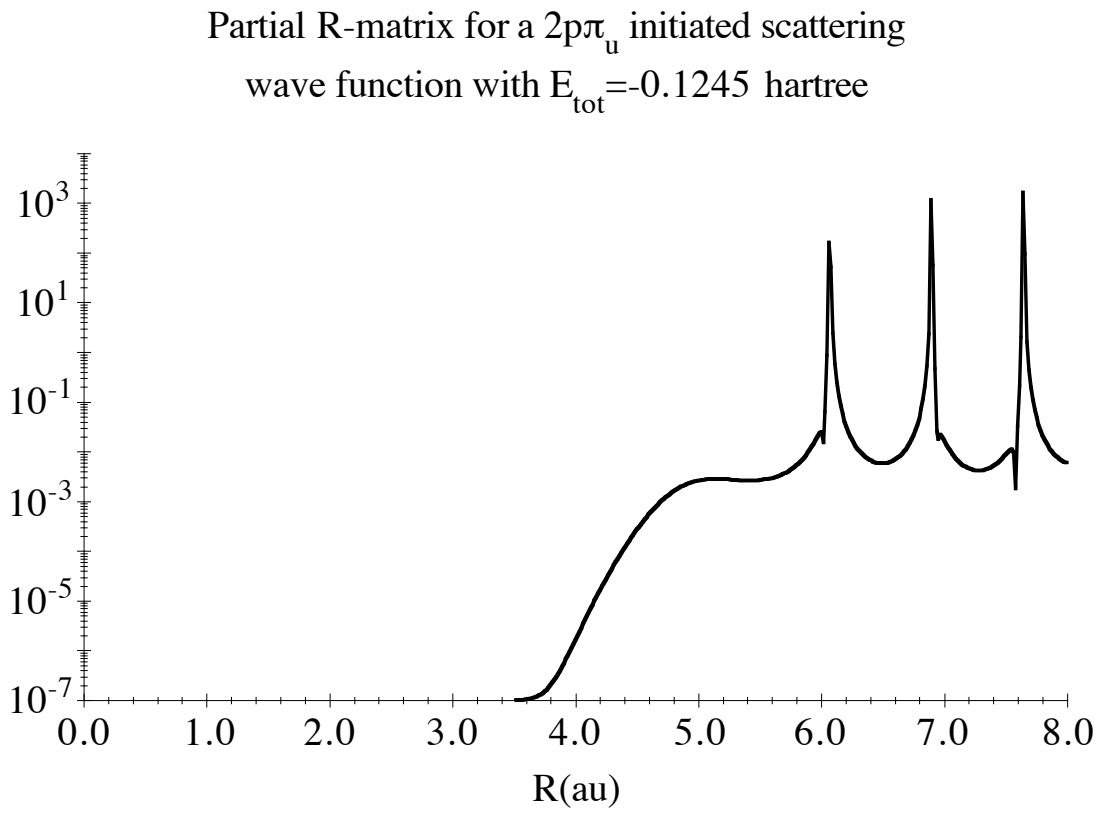

Figure 40 Plot of artial R-matrix for $\mathbf{C(2p\pi_u)}$

Figure 41 Color plot of $\mathbf{C}\left(\mathbf{1s}\sigma_{\mathbf{g}}\right)$

Figure 42 Color plot of $\mathbf{C}\left(\mathbf{2p}\sigma_{\mathbf{u}}\right)$

6.4 Conclusion

I have demonstrated a new approach to the full quantum mechanical three body problem of the hydrogen molecular ion, using a variational R-matrix method on proton hydrogen scattering. So far this approach has proven to be very versatile and promising, but as emphasized previously a conclusive evaluation in terms of comparison with experimental results, still can not be made. However it should be clear from the interim results presented in the previous section that nothing so far indicates that the model suffer from neither numerical instabilities nor subsequent problems with convergence. Actually all the computed wave functions seems to be in excellent agreement with the intuitively expected results using semi-classical arguments. Especially a justification or rather motivation for the Born-Oppenheimer approximation emerge from my calculations. Of the more practical aspects of this project, I would like to stress that it has been a very computationally intensive task to solve this quantum mechanical three body problem, and as such it is not surprising that it has never been attempted before - at least not in this sort of formulation. Besides the fact that the implementation of the variational R-matrix algorithm appears to give correct results, the numerically most exciting aspect of the project was certainly that I obtained exact eigenvalues down to the floating point precision of the computer, for at least the two lowest electronic states of H_2^+. Thus the developed DVR-scheme has definitely proved practicable and possibly even advantageous to the other numerical schemes used for solving the Born-Oppenheimer approximate states of the hydrogen molecular ion.

As have been pointed out several time before, the project is not yet completed in terms of obtaining the desires absorption coefficients for H_2^+. Next I have to compute transition dipole moments as outlined in section 5.9, and from these data the absorption spectra for the hydrogen molecular ion should be generated. Also the development of the non-adiabatic model itself is far from over. Future steps involve inclusion the non-adiabatic angular momentum coupling terms in Eq. (5.6.12,13). This will introduce coupling between wave functions with difference of unity in the m quantum number, such that states with different parity couples. Consequently many more channels will be open, and the DVR scheme will be complicate by the fact that we must define a new DVR/FBR for every value of m. However using the same sort of technique as outlined in the end of section 5.9 and discussed in reference [65], this problem can be dealt with most efficiently.

Concluding a project that has been going on for more than to years, brought me to Aarhus, Copenhagen and Paris, and still “not produced concrete decisive results” is not an easy thing. However one conclusion can be drawn from this project without any hesitation at all: I have learned a lot about many different aspects of quantum mechanics and general numerical methods in the past two years. Still this must be the primary and central object for such a project, for as Blaise Pascal (1623–1662) has put it “since we cannot know all that is to be known of everything, we ought to know a little about everything”.

A The mass-weighted Jacobi-coordinates

In this appendix we are going to present a general scheme for the construction of mass-weighted Jacobi-coordinates for the N-particle system. Let

$$\vec{\vec{\alpha}} \equiv \left[\vec{R}_1, \vec{R}_2, ..., \vec{R}_N\right] \tag{A.1}$$

collectively denote the coordinates of the particles in the laboratory-fixed frame of reference. The corresponding kinetic energy density $\mathbf{T}\left[\Psi\left(\vec{\vec{\alpha}}\right)\right]$ now reads as

$$\mathbf{T}\left[\Psi\left(\vec{\vec{\alpha}}\right)\right] = \sum_{j=1}^{N} \frac{1}{2m_j} \left| -i\hbar \vec{\nabla}_j \Psi\left(\vec{\vec{\alpha}}\right)\right|^2 \tag{A.2}$$

where m_j refers to the mass of particle j. To obtain the desired canonical form for the kinetic energy density

$$\mathbf{T}\left[\Psi\left(\vec{\vec{\beta}}\right)\right] = \frac{1}{2M} \sum_{j=1}^{N} \left| -i\hbar \vec{\nabla}'_j \Psi\left(\vec{\vec{\beta}}\right)\right|^2 \tag{A.3}$$

where M is the total mass of the system and $\vec{\vec{\beta}}$ collectively denotes a new set of coordinates

$$\vec{\vec{\beta}} = \left[\vec{R}'_1, \vec{R}'_2, ..., \vec{R}'_N\right] \tag{A.4}$$

clearly from Eq. (A.2) and Eq. (A.3) $\vec{\nabla}_j \Psi\left(\vec{\vec{\alpha}}\right)$ should then transform as

$$\vec{\nabla}_j \Psi\left(\vec{\vec{\alpha}}\right) \rightarrow \sqrt{\frac{m_j}{M}} \vec{\nabla}'_j \Psi\left(\vec{\vec{\beta}}\right) \tag{A.5}$$

which is easily obtained if the coordinates $\vec{\vec{\alpha}}$ transform into the new coordinates $\vec{\vec{\beta}}$ in the following way

$$\vec{R}_j \rightarrow \sqrt{\frac{m_j}{M}} \vec{R}'_j \tag{A.6}$$

In a matrix notation this transformation then reads as

$$\begin{aligned} \vec{\vec{\beta}} \equiv \left[\vec{R}'_1, \vec{R}'_2, ..., \vec{R}'_N\right] &= \left[\vec{R}_1, \vec{R}_2, ..., \vec{R}_N\right] \begin{bmatrix} \sqrt{\beta_1} & 0 & \cdots & 0 \\ 0 & \sqrt{\beta_2} & 0 & \vdots \\ \vdots & 0 & \ddots & 0 \\ 0 & \cdots & 0 & \sqrt{\beta_N} \end{bmatrix} \\ &= \left[\sqrt{\beta_1}\vec{R}_1, \sqrt{\beta_2}\vec{R}_2, ..., \sqrt{\beta_N}\vec{R}_N\right] \end{aligned} \tag{A.7}$$

where we have defined the constants $\beta_j = m_j/M$, that should not be confused with $\vec{\vec{\beta}}$ defined in Eq. (A.4). This new set of N coordinates $\vec{\vec{\beta}}$ is clearly not translationally invariant as desired. To obtain such a set of N-1 translationally invariant coordinates, $\vec{\vec{\gamma}}$, that leaves the kinetic energy density in the canonical form depicted in Eq. (A.3), we have to construct an orthogonal matrix $\overline{\overline{C}}$ that when multiplied on $\vec{\vec{\beta}}$ generates the center of mass coordinates as one of the new vectors, say at position N in the array $\vec{\vec{\gamma}}$. That is

$$\vec{\vec{\gamma}} \equiv \left[\vec{r}_1, \vec{r}_2, ... \vec{r}_{N-1}, \vec{R}_G\right] = \left[\vec{R}'_1, \vec{R}'_2, ..., \vec{R}'_N\right]\overline{\overline{C}} = \vec{\vec{\beta}}\overline{\overline{C}} \tag{A.8}$$

Hence the last column of $\overline{\overline{C}}$ should read as $\sqrt{\beta_1}, \sqrt{\beta_2}, ..., \sqrt{\beta_N}$, i.e. $C_{iN} = \sqrt{\beta_i}$. We now initiate our scheme choosing only the first two elements of the first column to be different from zero, as this is the simplest possible choice. From the constraint that $\overline{\overline{C}}$ should be orthogonal it follows that

$$\left.\begin{aligned} C_{11}^2 + C_{21}^2 &= 1 \\ \sqrt{\beta_1}C_{11} + \sqrt{\beta_2}C_{21} &= 0 \end{aligned}\right\} \Rightarrow \begin{cases} C_{11} = \sqrt{\mu_{12}/m_1} \\ C_{21} = -\sqrt{\mu_{12}/m_2} \end{cases} \tag{A.9}$$

where $1/\mu_{12} \equiv 1/m_1 + 1/m_2$ is the inverse of the reduced mass of particle 1 and 2. In the second column we choose the three first elements to be different from zero, and it then follows that

$$\left.\begin{aligned} C_{12}^2 + C_{22}^2 + C_{32}^2 &= 1 \\ C_{12}\sqrt{\mu_{12}/m_1} - C_{22}\sqrt{\mu_{12}/m_2} &= 0 \\ \sqrt{\beta_1}C_{12} + \sqrt{\beta_2}C_{22} + \sqrt{\beta_3}C_{32} &= 0 \end{aligned}\right\} \Rightarrow \begin{cases} C_{12} = \sqrt{\mu_{12,3}m_1}\big/\left(m_1 + m_2\right) \\ C_{22} = \sqrt{\mu_{12,3}m_2}\big/\left(m_1 + m_2\right) \\ C_{32} = -\sqrt{\mu_{12,3}/m_3} \end{cases} \tag{A.10}$$

where we have defined the inverse three particle reduced mass as $1/\mu_{12,3} \equiv 1/\left(m_1 + m_2\right) + 1/m_3$. We could now proceed in this way for the rest of the N-3 columns, and for each column j we would have the following j+1 working equations

$$\begin{aligned} &\sum_{i=1}^{N} \sqrt{\beta_i}C_{ij} = 0, \quad \text{for} \quad 1 \le j \le N-1 \\ &\sum_{i=1}^{N} C_{ik}C_{ij} = \delta_{jk} \end{aligned} \tag{A.11}$$

In a matrix notation we have

$$\left[\vec{r}_1,\vec{r}_2,\ldots,\vec{r}_{N-1},\vec{R}_G\right]=\left[\sqrt{\beta_1}\vec{R}_1,\sqrt{\beta_2}\vec{R}_2,\ldots..,\sqrt{\beta_N}\vec{R}_N\right]\begin{bmatrix}\sqrt{\frac{\mu_{12}}{m_1}} & \frac{\sqrt{\mu_{12,3}m_1}}{m_1+m_2} & \vdots & \sqrt{\beta_1}\\ -\sqrt{\frac{\mu_{12}}{m_2}} & \frac{\sqrt{\mu_{12,3}m_2}}{m_1+m_2} & \vdots & \sqrt{\beta_2}\\ 0 & -\sqrt{\frac{\mu_{12,3}}{m_3}} & \vdots & \sqrt{\beta_3}\\ 0 & 0 & \vdots & \sqrt{\beta_4}\\ \vdots & \vdots & \vdots & \vdots\\ 0 & 0 & \vdots & \sqrt{\beta_N}\end{bmatrix} \tag{A.12}$$

and rewriting this in terms of the coordinate set $\vec{\vec{\alpha}}$, using Eq. (A.7), we find

$$\vec{\vec{\gamma}}=\left[\vec{R}_1,\vec{R}_2,\ldots..,\vec{R}_N\right]\begin{bmatrix}\sqrt{\frac{\mu_{12}\beta_1}{m_1}} & \frac{\sqrt{\mu_{12,3}\beta_1 m_1}}{m_1+m_2} & \vdots & \beta_1\\ -\sqrt{\frac{\mu_{12}\beta_1}{m_2}} & \frac{\sqrt{\mu_{12,3}\beta_2 m_2}}{m_1+m_2} & \vdots & \beta_2\\ 0 & -\sqrt{\frac{\mu_{12,3}\beta_3}{m_3}} & \vdots & \beta_3\\ 0 & 0 & \vdots & \beta_4\\ \vdots & \vdots & \vdots & \vdots\\ 0 & 0 & \vdots & \beta_N\end{bmatrix}=\vec{\vec{\alpha}}\,\overline{\overline{V}} \tag{A.13}$$

Hence

$$\begin{aligned}\vec{r}_1&=\sqrt{\frac{\mu_{12}}{M}}\left(\vec{R}_1-\vec{R}_2\right)\\ \vec{r}_2&=\sqrt{\frac{\mu_{12,3}}{M}}\left(\frac{m_1\vec{R}_1+m_2\vec{R}_2}{m_1+m_2}-\vec{R}_3\right)\end{aligned} \tag{A.14}$$

which correspond to $\vec{r}_a$ and $\vec{R}_a$ mentioned in chapter 1 section 2. The first N-1 coordinates in the new coordinate set $\vec{\vec{\gamma}}$ are now referred to as *mass weighted Jacobi coordinates*. It is important at this stage to emphasize that the matrix $\overline{\overline{C}}$, and hence also $\overline{\overline{V}}$, can of course be constructed in a number of different ways corresponding to different choices of Jacobi coordinates. Since the sum of all the elements in each column of $\overline{\overline{V}}$ vanish, by virtue of the definition of $\overline{\overline{C}}$ as an orthonormal matrix (A.11), we observe that the defined Jacobi coordinates are translationally invariant as expected - that is

$$\left[\vec{r}_1,\vec{r}_2,\ldots..,\vec{r}_{N-1},\vec{R}_G\right]\xrightarrow{\text{Translation by }\vec{K}}\left[\vec{R}_1+\vec{K},\vec{R}_2+\vec{K},\ldots..,\vec{R}_N+\vec{K}\right]\overline{\overline{V}}=\left[\vec{r}_1,\vec{r}_2,\ldots..,\vec{r}_{N-1},\vec{R}_G+\vec{K}\right] \tag{A.15}$$

Also from the chain-rule

$$\vec{\nabla}_i^{\alpha}\Psi = \sum_{j=1}^{N} \frac{\partial \vec{r}_j^{\,\gamma}}{\partial \vec{r}_i^{\,\alpha}} \vec{\nabla}_j^{\gamma}\Psi = \sqrt{\beta_i} \sum_{i=1}^{N} C_{ij} \vec{\nabla}_j^{\gamma}\Psi \quad ,i = 1,2,\ldots N \tag{A.16}$$

we conclude that the canonical form Eq. (A.3) is maintained for the mass weighted Jacobi coordinates

$$\begin{aligned} \mathbf{T}[\Psi] &= \sum_{i=1}^{N} \left\{ \frac{1}{2m_i} \left| -i\hbar \vec{\nabla}_i^{\alpha}\Psi \right|^2 \right\} = \sum_{i=1}^{N} \left\{ \frac{\beta_i}{2m_i} \left| -i\hbar \sum_{j=1}^{N} C_{ij} \vec{\nabla}_j^{\gamma}\Psi \right|^2 \right\} \\ &= \frac{\hbar^2}{2M} \sum_{j=1}^{N} \vec{\nabla}_j^{\gamma *}\Psi \sum_{k=1}^{N} \vec{\nabla}_k^{\gamma}\Psi \sum_{i=1}^{N} C_{ik}C_{ij} = \frac{1}{2M} \sum_{j=1}^{N} \left| -i\hbar \vec{\nabla}_j^{\gamma}\Psi \right|^2 \end{aligned} \tag{A.17}$$

where we have used the orthogonality relation Eq.(A.11).

B Reduction of the total kinetic energy density

The total kinetic energy density of a N particle system, in the laboratory-fixed frame of reference

$$\mathbf{T}[\Psi] = \sum_{j=1}^{N} \frac{1}{2m_j} \left| -i\hbar \vec{\nabla}'_j \Psi \right|^2 \tag{B.1}$$

where the labels 1 through g refer to nuclei and the remainder to electrons, is transformed into a space-fixed frame of reference whose origin is the *nuclear center of mass* according to Eq. (2.1.5),Eq. (2.1.6), Eq. (2.1.7) and Eq. (2.1.8). Using the well known chain rule it follows that the gradient transforms as

$$\begin{aligned}
\vec{\nabla}'_j \Psi &= \sum_{i=1}^{N} \left\{ \vec{\nabla}_i \Psi \frac{\partial \vec{r}_i}{\partial \vec{r}'_j} \right\} + \vec{\nabla}_G \Psi \frac{\partial \vec{r}_G}{\partial \vec{r}'_j} \\
&= \sum_{i=1}^{N} \left\{ \vec{\nabla}_i \Psi \frac{\partial}{\partial \vec{r}'_j} \left[\vec{r}'_i - \sum_{k=1}^{N} \beta_k \vec{r}'_k \right] \right\} + \vec{\nabla}_G \Psi \frac{\partial}{\partial \vec{r}'_j} \left[\sum_{i=1}^{N} \mu_i \vec{r}'_i \right] \\
&= \vec{\nabla}_j \Psi - \beta_j \sum_{i=1}^{N} \vec{\nabla}_i \Psi + \mu_j \vec{\nabla}_G \Psi
\end{aligned} \tag{B.2}$$

and inserting this into Eq. (B.1) gives

$$\begin{aligned}
\mathbf{T}[\Psi] \rightarrow \sum_{j=1}^{N} \Bigg[& \frac{1}{2m_j} \left| -i\hbar \vec{\nabla}_j \Psi \right|^2 + \frac{\mu_j^2}{2m_j} \left| -i\hbar \vec{\nabla}_G \Psi \right|^2 \\
& + \frac{\beta_j^2}{2m} \left| \sum_{k=1}^{N} -i\hbar \vec{\nabla}_k \Psi \right|^2 - \frac{\hbar^2 \beta_j}{2m_j} \vec{\nabla}_j^* \Psi \sum_{k=1}^{N} \vec{\nabla}_k \Psi - \text{C.C.} \\
& + \frac{\hbar^2 \mu_j}{2m_j} \vec{\nabla}_j^* \Psi \vec{\nabla}_G \Psi + \text{C.C.} - \frac{\hbar^2 \beta_j \mu_j}{2m_j} \left(\sum_{k=1}^{N} \vec{\nabla}_k^* \Psi \right) \vec{\nabla}_G \Psi - \text{C.C.} \Bigg]
\end{aligned} \tag{B.3}$$

where C.C. denotes the complex conjugated of the term before. Using that

$$\frac{\mu_j}{2m_j} = \frac{m_j}{M_G} \frac{1}{2m_j} = \frac{1}{2M_G} \tag{B.4}$$

the last four cross terms in Eq. (B.3) reduce to

$$\begin{aligned}
& \vec{\nabla}_G \left[\sum_{j=1}^{N} \frac{\hbar^2 \mu_j}{2m_j} \vec{\nabla}_j^* \Psi - \left(\sum_{k=1}^{N} \frac{\hbar^2 \beta_k \mu_k}{2m_k} \right) \sum_{j=1}^{N} \vec{\nabla}_j^* \Psi \right] + \text{C.C.} \\
& = \frac{\hbar^2}{2M_G} \vec{\nabla}_G \Psi \left[\sum_{j=1}^{N} \vec{\nabla}_j^* \Psi - \left(\sum_{k=1}^{N} \beta_k \right) \sum_{j=1}^{N} \vec{\nabla}_j^* \Psi \right] + \text{C.C.}
\end{aligned} \tag{B.5}$$

and noting that

$$\sum_{j=1}^{N}\beta_j = \sum_{j=1}^{g}\frac{m_j}{M} = 1 \tag{B.6}$$

it is clear from Eq. (B.5) that these four cross terms involving $\vec{\nabla}_G$ all cancel out. We proceed with a partitioning of the third, forth and fifth term in Eq. (B.3) into a nuclear and a electronic part, using

$$\left.\begin{aligned}&\frac{\beta_j}{2m_j} = \frac{m_j}{M}\frac{1}{2m_j} = \frac{1}{2M}, \quad \text{for} \quad j = 1,....,g\\ &\frac{\beta_j}{2m_j} = 0, \quad \text{for} \quad j = g+1,....,N\end{aligned}\right\} \Rightarrow \sum_{j=1}^{N}\frac{\beta_j^2}{2m_j} = \frac{1}{2M}\sum_{j=1}^{g}\beta_j = \frac{1}{2M} \tag{B.7}$$

We further choose to eliminate the vector $\vec{r}_g$ (i.e. $\vec{\nabla}_g\Psi = \vec{0}$) as argued in Eq. (2.1.8). We then have

$$\begin{aligned}&\sum_{j=1}^{N}\left[\frac{\beta_j^2}{2m}\left|\sum_{k=1}^{N}-i\hbar\vec{\nabla}_k\Psi\right|^2 - \frac{\hbar^2\beta_j}{2m_j}\vec{\nabla}_j^*\Psi\sum_{k=1}^{N}\vec{\nabla}_k\Psi - C.C.\right]\\ &= \frac{1}{2M}\left[\left|\sum_{k=1}^{N}-i\hbar\vec{\nabla}_k\Psi\right|^2 - \hbar^2\sum_{j=1}^{g}\vec{\nabla}_j^*\Psi\sum_{k=1}^{N}\vec{\nabla}_k\Psi - C.C.\right]\end{aligned} \tag{B.8}$$

The first term in (B.8) can be rewritten as

$$\frac{1}{2M}\left|\sum_{k=1}^{g-1}-i\hbar\vec{\nabla}_k\Psi\right|^2 + \frac{1}{2M}\left|\sum_{k=g+1}^{N}-i\hbar\vec{\nabla}_k\Psi\right|^2 + \frac{\hbar^2}{2M}\sum_{j=1}^{g-1}\vec{\nabla}_j^*\Psi\sum_{k=g+1}^{N}\vec{\nabla}_k\Psi + C.C. \tag{B.9}$$

The last two terms of Eq. (B.8) can equally be rewritten as

$$\begin{aligned}&-\frac{\hbar^2}{2M}\sum_{j=1}^{g-1}\vec{\nabla}_j^*\Psi\left[\sum_{k=1}^{g-1}\vec{\nabla}_k\Psi + \sum_{k=g+1}^{N}\vec{\nabla}_k\Psi\right] - C.C.\\ &= -\frac{2}{2M}\left|\sum_{k=1}^{g-1}-i\hbar\vec{\nabla}_k\Psi\right|^2 - \frac{\hbar^2}{2M}\sum_{j=1}^{g-1}\vec{\nabla}_j^*\Psi\sum_{k=g+1}^{N}\vec{\nabla}_k\Psi - C.C.\end{aligned} \tag{B.10}$$

and adding Eq. (B.9) and Eq. (B.10) we see that Eq. (B.8) reduces to

$$-\frac{1}{2m_j}\left|\sum_{j=1}^{g+1}\vec{\nabla}_j\Psi\right|^2 + \frac{1}{2M}\left|\sum_{j=g+1}^{N}\vec{\nabla}_j\Psi\right|^2 \tag{B.11}$$

All in all we now conclude that under the transformation described in Eq. (2.1.5-8) the kinetic energy density Eq. (B.1) can be written as

$$\mathbf{T}(\Psi) = \mathbf{T}_N(\Psi) + \mathbf{T}_E(\Psi) + \mathbf{T}_G(\Psi) \tag{B.12}$$

where we have defined the nuclear, electronic and center-of-mass terms

$$\begin{aligned}
\mathbf{T}_N(\Psi) &= \sum_{j=1}^{g-1}\left\{\frac{1}{2m_j}\left|-i\hbar\vec{\nabla}_j\Psi\right|^2\right\} - \frac{1}{2M}\left|\sum_{j=1}^{g-1}\left\{-i\hbar\vec{\nabla}_j\Psi\right\}\right|^2 \\
\mathbf{T}_E(\Psi) &= \sum_{j=g+1}^{N}\left\{\frac{1}{2m_j}\left|-i\hbar\vec{\nabla}_j\Psi\right|^2\right\} + \frac{1}{2M}\left|\sum_{j=g+1}^{N}\left\{-i\hbar\vec{\nabla}_j\Psi\right\}\right|^2 \\
\mathbf{T}_G(\Psi) &= \frac{1}{2M_G}\left|-i\hbar\vec{\nabla}_G\Psi\right|^2
\end{aligned} \tag{B.13}$$

C The third degree Hermite type functions

The simple linear basis functions defined in chapter 3 belong to C^0, and operators represented in this basis will be simple tridiagonal matrices. The price on the other hand for this simplicity is that one will have to include a large number of these linear basis function in order to obtain convergence, and for a fixed grid interval this is equivalent to using a dense grid. Alternatively one can use polynomials of a higher degree in each element of the grid, at the price of less sparse matrices. As this was also one of the techniques used in the study of H_2^+ we introduce the so-called third degree Hermite type functions defined from the third degree Bézier polynomials (Eq. (3.2.3) with N=3) as

$$\left[\left\langle \mathcal{B}_i^3 \middle| H_j^3 \right\rangle\right] = \begin{array}{c} \\ \mathcal{B}_0^3 \\ \mathcal{B}_1^3 \\ \mathcal{B}_2^3 \\ \mathcal{B}_3^3 \end{array} \begin{array}{c} \begin{array}{cccc} H_0^3 & H_1^3 & H_2^3 & H_3^3 \end{array} \\ \begin{bmatrix} 1 & 0 & 0 & 0 \\ 3 & h & 0 & 0 \\ 0 & 0 & 3 & -h \\ 0 & 0 & 1 & 0 \end{bmatrix} \end{array}, \quad h \equiv b - a \tag{C.1}$$

In reference [50] Linderberg uses a different notation for these third degree Hermite type functions

$$ha \equiv H_0^3, \quad da \equiv H_1^3, \quad hb \equiv H_2^3, \quad db \equiv H_3^3 \tag{C.2}$$

for reasons that shall soon become obvious. In figure (C.1), below, the four basis functions are shown for the interval $a = -1$ and $b = 1$.

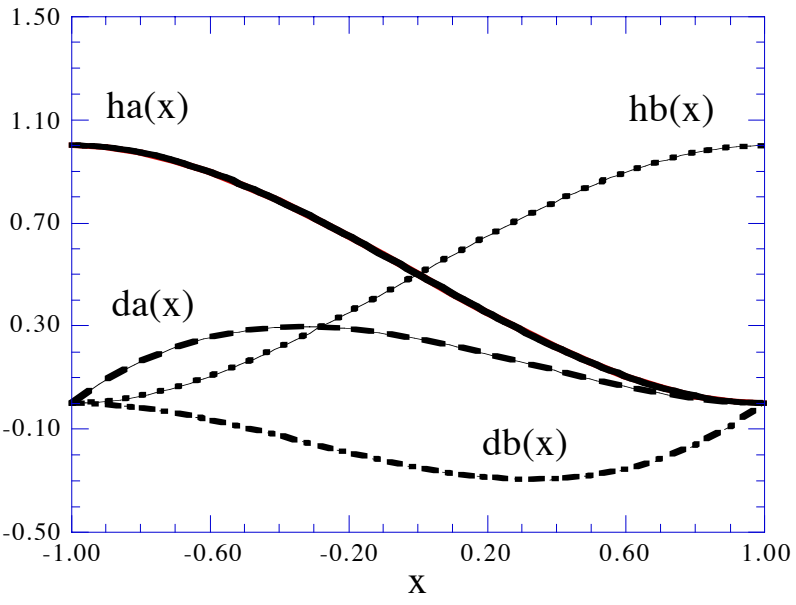

Figure (C.1) Third degree Hermite type functions

From the definition given in Eq. (C.1) it follows that $ha(x)$ has unit amplitude at $x = a$, zero derivative at $x = a$ and $x = b$ and zero amplitude at $x = b$, while $da(x)$ is a function that has zero amplitude at both a and b, unit derivative at a and zero derivative at b. The functions $hb(x)$ and $db(x)$ have analog relations, just where a and b has been interchanged. A Hermite type interpolation of a function $f(x)$ in the interval from a to b then reads as

$$f(x) \approx f(a)ha(x) + f(b)hb(x) + f'(a)da(x) + f'(b)db(x) \tag{C.3}$$

For these functions, $H_k^3(x)$, we have the following expression for the x-derivative

$$\frac{d}{dx}H_k^3(x) = \langle x|\mathbf{P}|H_k^3\rangle = \langle x|\mathbf{P}\left\{\sum_{i=0}^{3}|B_i^3\rangle\langle\tilde{B}_i^3|\right\}|H_k^3\rangle = \sum_{i=0}^{3}\langle x|\mathbf{P}|B_i^3\rangle\langle\tilde{B}_i^3|H_k^3\rangle \tag{C.4}$$

where we have introduced the third degree Bézier functions $B_i^3(x)$ and their biorthogonal functions $\tilde{B}_i^3(x)$ as described in chapter 3. Inserting Eq. (3.2.5) into Eq. (C.4) give us

$$\frac{d}{dx}H_k^3(x) = \sum_{i,j=0}^{3}\langle\tilde{B}_j^3|H_k^3\rangle\langle\tilde{B}_j^3|\mathbf{P}|B_i^3\rangle\langle x|B_i^3\rangle = \sum_{i=0}^{3}\langle\tilde{B}_i^3|\mathbf{P}|H_k^3\rangle\langle x|B_i^3\rangle \tag{C.5}$$

which expresses that the matrix $\left[\overline{\langle\tilde{B}_i^3|\mathbf{P}|H_j^3\rangle}\right]$ is readily obtained by multiplying $\left[\overline{\langle\tilde{B}_i^3|\mathbf{P}|B_j^3\rangle}\right]$ (from Eq. (3.6)) by $\left[\overline{\langle\tilde{B}_i^3|H_j^3\rangle}\right]$ (from Eq. (C.1)) to give

$$\left[\langle\tilde{B}_i^3|\mathbf{P}|H_j^3\rangle\right] = \begin{array}{c} \\ \tilde{B}_0^3 \\ \tilde{B}_1^3 \\ \tilde{B}_2^3 \\ \tilde{B}_3^3 \end{array}\begin{array}{c} \begin{array}{cccc} \mathbf{P} & H_0^3 & H_1^3 & H_2^3 & H_3^3 \end{array} \\ \begin{bmatrix} 0 & 1 & 0 & 0 \\ -6h & -1 & 6h & -2 \\ -6h & -2 & 6h & -1 \\ 0 & 0 & 0 & 1 \end{bmatrix} \end{array} \tag{C.6}$$

Higher order x-derivatives are now simply obtained by using Eq. (3.7) in Eq. (C.4). In order to fulfill the continuity criterion $F_i(x) \in C^0$ for the overall basis functions or elements $F_i(x)$ defined in this FEM scheme, we construct the basis functions as shown in figure (C.2) (where we have assumed for simplicity that the grid consists of only 3 grid points). We note that in this way we have 2N elements F_i defining the FEM scheme, where N denotes the number of grid points, and that $F_i \in C^1$ for $3 \le i \le 2N - 2$.

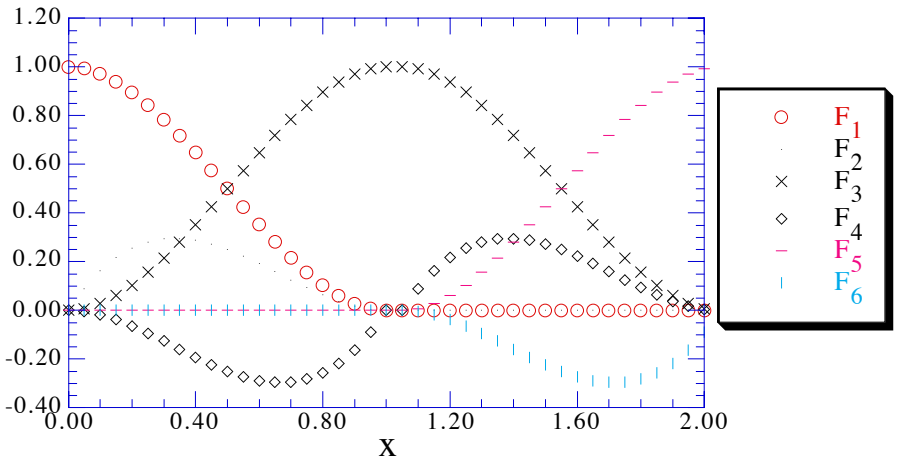

Figure (C.2) Hermite type FEM functions

A matrix representation of an operator in this FEM basis results in a sparse matrix with a simple block structure as illustrated in figure (C.3), where the type of overlap integrals has been indicated using a prime for integrals involving Hermite type functions defined in the second grid interval (from 1 to 2 in figure (C.2)) and no labels for functions defined in the first interval (from 0 to 1 in figure (C.2)).

$$\begin{bmatrix}
\langle ha|\mathbf{o}|ha\rangle & \langle ha|\mathbf{o}|da\rangle & \langle ha|\mathbf{o}|hb\rangle & \langle ha|\mathbf{o}|db\rangle & 0 & 0 \\
\langle da|\mathbf{o}|ha\rangle & \langle da|\mathbf{o}|da\rangle & \langle da|\mathbf{o}|hb\rangle & \langle da|\mathbf{o}|db\rangle & 0 & 0 \\
\langle hb|\mathbf{o}|ha\rangle & \langle hb|\mathbf{o}|da\rangle & \langle hb|\mathbf{o}|hb\rangle + \langle ha|\mathbf{o}|ha\rangle' & \langle hb|\mathbf{o}|db\rangle + \langle ha|\mathbf{o}|da\rangle' & \langle ha|\mathbf{o}|hb\rangle' & \langle ha|\mathbf{o}|db\rangle' \\
\langle db|\mathbf{o}|ha\rangle & \langle db|\mathbf{o}|da\rangle & \langle db|\mathbf{o}|hb\rangle + \langle da|\mathbf{o}|ha\rangle' & \langle db|\mathbf{o}|db\rangle + \langle da|\mathbf{o}|da\rangle' & \langle da|\mathbf{o}|hb\rangle' & \langle da|\mathbf{o}|db\rangle' \\
0 & 0 & \langle hb|\mathbf{o}|ha\rangle' & \langle hb|\mathbf{o}|da\rangle' & \langle hb|\mathbf{o}|hb\rangle' & \langle hb|\mathbf{o}|db\rangle' \\
0 & 0 & \langle db|\mathbf{o}|ha\rangle' & \langle db|\mathbf{o}|da\rangle' & \langle db|\mathbf{o}|hb\rangle' & \langle db|\mathbf{o}|db\rangle'
\end{bmatrix}$$

Figure (C.3) Structure of matrix expressed in Hermite functions

D Representation of derivatives in the FD method

An analytic function, $\Psi(x)$, at a grid point x_p can be expanded in a Taylor series around some other grid point x_0.

$$\begin{aligned}\Psi(x_p) = \Psi(x_0 + p\Delta x) &= \sum_{n=0}^{\infty} \frac{(p\Delta x)^n}{n!} \frac{d^n}{dx^n}\left[\Psi(x)\right]_{x_0} \\ &\approx \sum_{n=0}^{2D} \frac{(p\Delta x)^n}{n!} \Psi^n(x_0), \quad \text{where } p = -D, -D+1, \ldots, D\end{aligned} \tag{D.1}$$

This set of $2D+1$ equations can be written in the following matrix notation,

$$\overline{\Psi} \equiv \begin{bmatrix} \Psi(x_{-D}) \\ \vdots \\ \Psi(x_D) \end{bmatrix} = \begin{bmatrix} 1 & \cdots & \frac{(-D\Delta x)^{2D}}{(2D)!} \\ \vdots & A_{pn} = \frac{(p\Delta x)^n}{n!} & \vdots \\ 1 & \cdots & \frac{(D\Delta x)^{2D}}{(2D)!} \end{bmatrix} \times \begin{bmatrix} \Psi^0(x_0) \\ \vdots \\ \Psi^{2D}(x_0) \end{bmatrix} \equiv \overline{\overline{A}}\,\overline{\Psi}' \tag{D.2}$$

and inverting this linear equation result in

$$\overline{\Psi}' \equiv \begin{bmatrix} \Psi^0(x_0) \\ \vdots \\ \Psi^{2D}(x_0) \end{bmatrix} = \begin{bmatrix} 1 & \cdots & \frac{(-D\Delta x)^{2D}}{(2D)!} \\ \vdots & A_{pn} = \frac{(p\Delta x)^n}{n!} & \vdots \\ 1 & \cdots & \frac{(D\Delta x)^{2D}}{(2D)!} \end{bmatrix}^{-1} \times \begin{bmatrix} \Psi(x_{-D}) \\ \vdots \\ \Psi(x_D) \end{bmatrix} = \overline{\overline{A}}^{-1}\overline{\Psi} \tag{D.3}$$

Since $\overline{\overline{A}}$ obviously can be written as

$$\overline{\overline{A}} = \begin{bmatrix} 1 & \cdots & \frac{(-D)^{2D}}{(2D)!} \\ \vdots & \frac{p^n}{n!} & \vdots \\ 1 & \cdots & \frac{D^{2D}}{(2D)!} \end{bmatrix} \times \begin{bmatrix} 1 & 0 & \cdots & 0 \\ 0 & \Delta x & 0 & \cdots \\ \vdots & 0 & \ddots & 0 \\ 0 & \vdots & 0 & (\Delta x)^{2D} \end{bmatrix} \tag{D.4}$$

if follows that

$$\overline{\overline{A}}^{-1} = \begin{bmatrix} 1 & 0 & \cdots & 0 \\ 0 & \Delta x^{-1} & 0 & \cdots \\ \vdots & 0 & \ddots & 0 \\ 0 & \vdots & 0 & (\Delta x)^{-2D} \end{bmatrix} \times \begin{bmatrix} 1 & \cdots & \dfrac{(-D)^{2D}}{(2D)!} \\ \vdots & \dfrac{p^n}{n!} & \vdots \\ 1 & \cdots & \dfrac{D^{2D}}{(2D)!} \end{bmatrix}^{-1} \tag{D.5}$$

and combining Eq. (D.3) and Eq. (D.5) we write

$$\begin{bmatrix} \Psi^0(x_0) \\ \vdots \\ \Psi^{2D}(x_0) \end{bmatrix} = \begin{bmatrix} 1 & 0 & \cdots & 0 \\ 0 & \Delta x^{-1} & 0 & \cdots \\ \vdots & 0 & \ddots & 0 \\ 0 & \vdots & 0 & (\Delta x)^{-2D} \end{bmatrix} \times \begin{bmatrix} 1 & \cdots & \dfrac{(-D)^{2D}}{(2D)!} \\ \vdots & \dfrac{p^n}{n!} & \vdots \\ 1 & \cdots & \dfrac{D^{2D}}{(2D)!} \end{bmatrix}^{-1} \times \begin{bmatrix} \Psi(x_{-D}) \\ \vdots \\ \Psi(x_D) \end{bmatrix} \tag{D.6}$$

We finally obtain the expression

$$\Psi^n(x_0) \approx (\Delta x)^{-n} \sum_{p=-D}^{D} C_p^{(D)} \Psi(x_p) \tag{D.7}$$

where we have introduced the coefficients $C_p^{(D)}$, and just note that it is actually possible to derive an explicit expression for these coefficients using the solution for a so-called Vadermonde's determinant. However we will demonstrate that for (very) small meshes it is equally possible to determine the coefficients $C_p^{(D)}$ analytically in a more straightforward way, but it should be emphasized that this approach is generally poor for larger meshes. Let us consider the trivial situation for which $D = 2$. Eq. (D.2) then reads as

$$\begin{aligned} \begin{bmatrix} \Psi(x_{-2}) \\ \Psi(x_{-1}) \\ \Psi(x_0) \\ \Psi(x_1) \\ \Psi(x_2) \end{bmatrix} &= \begin{bmatrix} (-2\Delta x)^0 & (-2\Delta x)^1 & \frac{1}{2}(-2\Delta x)^2 & \frac{1}{6}(-2\Delta x)^3 & \frac{1}{24}(-2\Delta x)^4 \\ (-1\Delta x)^0 & (-1\Delta x)^1 & \frac{1}{2}(-1\Delta x)^2 & \frac{1}{6}(-1\Delta x)^3 & \frac{1}{24}(-1\Delta x)^4 \\ (0\Delta x)^0 & (0\Delta x)^1 & \frac{1}{2}(0\Delta x)^2 & \frac{1}{6}(0\Delta x)^3 & \frac{1}{24}(0\Delta x)^4 \\ (1\Delta x)^0 & (1\Delta x)^1 & \frac{1}{2}(1\Delta x)^2 & \frac{1}{6}(1\Delta x)^3 & \frac{1}{24}(1\Delta x)^4 \\ (2\Delta x)^0 & (2\Delta x)^1 & \frac{1}{2}(2\Delta x)^2 & \frac{1}{6}(2\Delta x)^3 & \frac{1}{24}(2\Delta x)^4 \end{bmatrix} \times \begin{bmatrix} \Psi^0(x_0) \\ \Psi^1(x_0) \\ \Psi^2(x_0) \\ \Psi^3(x_0) \\ \Psi^4(x_0) \end{bmatrix} \\ &= \begin{bmatrix} 1 & -2 & 2 & -\frac{4}{3} & \frac{2}{3} \\ 1 & -1 & \frac{1}{2} & -\frac{1}{6} & \frac{1}{24} \\ 1 & 0 & 0 & 0 & 0 \\ 1 & 1 & \frac{1}{2} & \frac{1}{6} & \frac{1}{24} \\ 1 & 2 & 2 & \frac{4}{3} & \frac{2}{3} \end{bmatrix} \times \begin{bmatrix} 1 & 0 & 0 & 0 \\ 0 & \Delta x & 0 & 0 \\ 0 & 0 & \Delta x^3 & 0 \\ 0 & 0 & 0 & \Delta x^4 \end{bmatrix} \times \begin{bmatrix} \Psi^0(x_0) \\ \Psi^1(x_0) \\ \Psi^2(x_0) \\ \Psi^3(x_0) \\ \Psi^4(x_0) \end{bmatrix} \end{aligned} \tag{D.8}$$

We now invert this matrix equation to give

$$\begin{bmatrix} \Psi^0(x_0) \\ \Psi^1(x_0) \\ \Psi^2(x_0) \\ \Psi^3(x_0) \\ \Psi^4(x_0) \end{bmatrix} = \begin{bmatrix} 1 & 0 & 0 & 0 \\ 0 & \Delta x^{-1} & 0 & 0 \\ 0 & 0 & \Delta x^{-3} & 0 \\ 0 & 0 & 0 & \Delta x^{-4} \end{bmatrix} \times \begin{bmatrix} 0 & 0 & 1 & 0 & 0 \\ \frac{1}{12} & -\frac{2}{3} & 0 & \frac{2}{3} & -\frac{1}{12} \\ -\frac{1}{12} & \frac{4}{3} & -\frac{5}{2} & \frac{4}{3} & -\frac{1}{12} \\ -\frac{1}{2} & 1 & 0 & -1 & \frac{1}{2} \\ 1 & -4 & 6 & -4 & 1 \end{bmatrix} \times \begin{bmatrix} \Psi(x_{-2}) \\ \Psi(x_{-1}) \\ \Psi(x_0) \\ \Psi(x_1) \\ \Psi(x_2) \end{bmatrix} \tag{D.9}$$

Taking the second derivative as an example, we conclude from the above derivations that

$$\left.\frac{d^2}{dx^2}\Psi(x)\right|_{x_0} \approx \Delta x^{-2}\left\{-\frac{1}{12}\Psi(x_{-2}) + \frac{4}{3}\Psi(x_{-1}) - \frac{5}{2}\Psi(x_0) + \frac{4}{3}\Psi(x_1) - \frac{1}{12}\Psi(x_2)\right\} \tag{D.10}$$

Hence the matrix representation $\overline{\overline{T}}$ of the one dimensional kinetic energy operator $\mathbf{T}$

$$\mathbf{T}\Psi(x) = -\frac{\hbar^2}{2m}\frac{d^2}{dx^2}\Psi(x) \tag{D.11}$$

in a five point finite difference scheme reads as

$$\overline{\overline{T}}\overline{\Psi}_p = -\frac{\hbar^2}{2m}\overline{\Psi}_p'' = -\frac{\hbar^2}{2m}\begin{bmatrix} \Psi''(x_2) \\ \Psi''(x_1) \\ \Psi''(x_0) \\ \Psi''(x_{-1}) \\ \Psi''(x_{-2}) \end{bmatrix} = -\frac{\hbar^2}{2m}\frac{1}{\Delta x^2}\begin{bmatrix} -\frac{5}{2} & \frac{4}{3} & -\frac{1}{12} & 0 & 0 \\ \frac{4}{3} & -\frac{5}{2} & \frac{4}{3} & -\frac{1}{12} & 0 \\ -\frac{1}{12} & \frac{4}{3} & -\frac{5}{2} & \frac{4}{3} & -\frac{1}{12} \\ 0 & -\frac{1}{12} & \frac{4}{3} & -\frac{5}{2} & \frac{4}{3} \\ 0 & 0 & -\frac{1}{12} & \frac{4}{3} & -\frac{5}{2} \end{bmatrix} \times \begin{bmatrix} \Psi(x_2) \\ \Psi(x_1) \\ \Psi(x_0) \\ \Psi(x_{-1}) \\ \Psi(x_{-2}) \end{bmatrix} \tag{D.12}$$

E Volume-elements and the Jacobian-determinant

For the transformation of general coordinates $\vec{x} = \{x_i, i = 1, .., N\}$ to the coordinates $\vec{y} = \{y_i, i = 1, .., N\}$ we define the *Jacobian matrix*, $\overline{\overline{J}}$, as

$$\overline{\overline{J}} \equiv \frac{\partial \vec{y}}{\partial \vec{x}} = \begin{bmatrix} \frac{\partial y_1}{\partial x_1} & \frac{\partial y_2}{\partial x_1} & \cdots & \frac{\partial y_N}{\partial x_1} \\ \frac{\partial y_1}{\partial x_2} & \frac{\partial y_2}{\partial x_2} & \cdots & \frac{\partial y_N}{\partial x_2} \\ \cdots & \cdots & \cdots & \cdots \\ \frac{\partial y_1}{\partial x_N} & \frac{\partial y_2}{\partial x_N} & \cdots & \frac{\partial y_N}{\partial x_N} \end{bmatrix} \tag{E.1}$$

For this transformation it can be shown[98] that the corresponding change of the volume-element in an N-fold integral reads as

$$dx_1 dx_2 \cdots dx_N = \left| \det\left[\frac{\partial \vec{x}}{\partial \vec{y}} \right] \right| dy_1 dy_2 \cdots dy_N = \left| \det\left[\overline{\overline{J}}^{-1} \right] \right| dy_1 dy_2 \cdots dy_N = \frac{dy_1 dy_2 \cdots dy_N}{\left| \det\left[\overline{\overline{J}} \right] \right|} \tag{E.2}$$

If the transformation from the coordinates $\vec{x} = \{x_i, i = 1, .., N\}$ to $\vec{y} = \{y_i, i = 1, .., N\}$ is a simple *linear transformation* (i.e. $\overline{Y} = \overline{X}\overline{\overline{T}}$, where $\overline{X}$ and $\overline{Y}$ are row vectors), we simply have $\overline{\overline{J}} = \overline{\overline{T}}$. Thus if the linear transformation is unitary (i.e. $\overline{\overline{T}}^{-1} = \overline{\overline{T}}^{+} \Rightarrow \left| \det\left[\overline{\overline{T}} \right] \right| = 1$) or just unimodular (i.e. $\left| \det\left[\overline{\overline{T}} \right] \right| = 1$), we have the trivial result

$$dx_1 dx_2 \cdots dx_N = dy_1 dy_2 \cdots dy_N \tag{E.3}$$

In other words *there is no contribution from the Jacobian determinant to the volume-element for unitary or unimodular linear transformations*. In the special case of a three dimensional transformation of Cartesian coordinates we have the result[99]

$$\overline{\overline{J}} \equiv \frac{\partial \vec{y}}{\partial \vec{x}} = \begin{bmatrix} \frac{\partial y_1}{\partial x_1} & \frac{\partial y_2}{\partial x_1} & \frac{\partial y_3}{\partial x_1} \\ \frac{\partial y_1}{\partial x_2} & \frac{\partial y_2}{\partial x_2} & \frac{\partial y_3}{\partial x_2} \\ \frac{\partial y_1}{\partial x_3} & \frac{\partial y_2}{\partial x_3} & \frac{\partial y_3}{\partial x_3} \end{bmatrix} = \overline{\nabla}_x y_1 \bullet \left(\overline{\nabla}_x y_2 \times \overline{\nabla}_x y_3 \right) \tag{E.4}$$

and consequently we write

---

98 In the simple two-dimensional case this is shown in reference [73] p. 798-800. This procedure can then easily be generalized to an N-fold integral as discussed above.

99 We recall that $\overline{y}_1 \bullet \left(\overline{y}_2 \times \overline{y}_3 \right)$ exactly denotes the volume of the polygon spanned by the three vectors $\overline{y}_1, \overline{y}_2$ and $\overline{y}_3$, and hence we can designate the name "differential *volume*-element" to the term $\overline{\nabla}_x y_1 \bullet \left(\overline{\nabla}_x y_2 \times \overline{\nabla}_x y_3 \right)$ in Eq. (E.5).

$$dx_1 dx_2 dx_3 = \left|\overline{\nabla}_x y_1 \bullet \left(\overline{\nabla}_x y_2 \times \overline{\nabla}_x y_3\right)\right|^{-1} dy_1 dy_2 dy_3 \tag{E.5}$$

We are now in the position to transform the volume-element entering the A-term of the J-functional, Eq. (5.2.1), from the lab-fixed coordinates to the body-fixed coordinates as outlined in chapter five. The space-fixed coordinates, $\vec{r}'$, $\vec{R}'$ and $\vec{R}_G'$, were obtained from the lab-fixed coordinates, $\vec{r}_a$, $\vec{r}_b$ and $\vec{r}_e$, by a simple linear transformation, Eq. (5.3.2), of the latter. Consequently the Jacobian of this transformation simply reads as

$$\overline{\overline{J}} \equiv \begin{bmatrix} \frac{\partial \vec{r}'}{\partial \vec{r}_a} & \frac{\partial \vec{R}'}{\partial \vec{r}_a} & \frac{\partial \vec{R}_G'}{\partial \vec{r}_a} \\ \frac{\partial \vec{r}'}{\partial \vec{r}_b} & \frac{\partial \vec{R}'}{\partial \vec{r}_b} & \frac{\partial \vec{R}_G'}{\partial \vec{r}_b} \\ \frac{\partial \vec{r}'}{\partial \vec{r}_e} & \frac{\partial \vec{R}'}{\partial \vec{r}_e} & \frac{\partial \vec{R}_G'}{\partial \vec{r}_e} \end{bmatrix} = \overline{\overline{V}} = \begin{bmatrix} -\frac{m_a}{m_a + m_b} & 1 & \frac{m_a}{M} \\ -\frac{m_b}{m_a + m_b} & -1 & \frac{m_b}{M} \\ 1 & 0 & \frac{m_e}{M} \end{bmatrix} \tag{E.6}$$

such that the Jacobian is easily shown to be unimodular

$$\left|\det\left[\overline{\overline{J}}\right]\right| = \left|\frac{m_a}{M} + \frac{m_b}{M} + \frac{m_a m_e}{(m_a + m_b)M} + \frac{m_b m_e}{(m_a + m_b)M}\right| = 1 \tag{E.7}$$

Hence for the transformation from lab-fixed to space-fixed coordinates we write the corresponding volume-element as

$$d\vec{r}_a d\vec{r}_b d\vec{r}_e = d\vec{r}' d\vec{R}' d\vec{R}_G' \tag{E.8}$$

Next we transform the space-fixed coordinates, $\vec{r}', \vec{R}'$ and $\vec{R}_G'$, into the body-fixed coordinates, $\vec{r}, \vec{R}$ and $\vec{R}_G$, using the definition Eq. (5.4.2) - that is

$$\left[\vec{r}, \vec{R}, \vec{R}_G\right] = \left[\vec{r}', \vec{R}', \vec{R}_G'\right]\overline{\overline{R}}(\alpha, \beta, 0) \tag{E.9}$$

where $\overline{\overline{R}}(\alpha, \beta, 0)$ is the real *unitary* matrix, Eq. (4.3.3), representing the rotation of the space-fixed frame of reference into body-fixed frame of reference. Thus it follows from Eq. (E.3) that

$$d\vec{r}' d\vec{R}' d\vec{R}_G' = d\vec{r} d\vec{R} d\vec{R}_G \tag{E.10}$$

With the introduction of body-fixed coordinates, as described in chapter 5 section 4, the inter-nuclear coordinate vector $\vec{R}$, can be parametrized in terms of the two Euler angles α and β, needed to rotate the space-fixed frame of reference into the body-fixed frame of reference, and the inter-nuclear separation R. From the explicit expression of this rotation, Eq. (5.4.4), it follows that

$$\overline{\mathrm{R}} = \begin{bmatrix} \mathrm{R}_1 \\ \mathrm{R}_2 \\ \mathrm{R}_3 \end{bmatrix} = \overline{\overline{\mathrm{R}}}(\alpha,\beta,0) \begin{bmatrix} 0 \\ 0 \\ \mathrm{R} \end{bmatrix} = \begin{bmatrix} \cos\alpha\cos\beta & -\sin\alpha & \cos\alpha\sin\beta \\ \sin\alpha\cos\beta & \cos\alpha & \sin\alpha\sin\beta \\ -\sin\beta & 0 & \cos\beta \end{bmatrix} \begin{bmatrix} 0 \\ 0 \\ \mathrm{R} \end{bmatrix} = \begin{bmatrix} \mathrm{R}\cos\alpha\sin\beta \\ \mathrm{R}\sin\alpha\sin\beta \\ \mathrm{R}\cos\beta \end{bmatrix} \tag{E.11}$$

Clearly the transformation from the coordinates $\{\mathrm{R}_1, \mathrm{R}_2, \mathrm{R}_3\}$ to $\{\alpha, \beta, \mathrm{R}\}$ is not linear, and so we use the definition of the Jacobian, Eq. (E.1), to determine the change in the volume-element caused by this change of variables.

$$\overline{\overline{\mathrm{J}}}^{-1} = \frac{\partial\{\mathrm{R}_1, \mathrm{R}_2, \mathrm{R}_3\}}{\partial\{\alpha, \beta, \mathrm{R}\}} = \begin{bmatrix} \frac{\partial \mathrm{R}_1}{\partial\alpha} & \frac{\partial \mathrm{R}_2}{\partial\alpha} & \frac{\partial \mathrm{R}_3}{\partial\alpha} \\ \frac{\partial \mathrm{R}_1}{\partial\beta} & \frac{\partial \mathrm{R}_2}{\partial\beta} & \frac{\partial \mathrm{R}_3}{\partial\beta} \\ \frac{\partial \mathrm{R}_1}{\partial \mathrm{R}} & \frac{\partial \mathrm{R}_2}{\partial \mathrm{R}} & \frac{\partial \mathrm{R}_3}{\partial \mathrm{R}} \end{bmatrix} = \begin{bmatrix} -\mathrm{R}\sin\alpha\sin\beta & \mathrm{R}\cos\alpha\sin\beta & 0 \\ -\mathrm{R}\cos\alpha\cos\beta & \mathrm{R}\sin\alpha\cos\beta & -\mathrm{R}\sin\beta \\ \cos\alpha\sin\beta & \sin\alpha\sin\beta & \cos\beta \end{bmatrix} \tag{E.12}$$

such that

$$\left|\det\left[\overline{\overline{\mathrm{J}}}^{-1}\right]\right| = \left|-\mathrm{R}^2\sin\beta\right| = \mathrm{R}^2\sin\beta \tag{E.13}$$

and

$$\mathrm{d}\vec{\mathrm{R}} = \mathrm{dR}_1\mathrm{dR}_2\mathrm{dR}_3 = \mathrm{R}^2\sin\beta\mathrm{d}\alpha\mathrm{d}\beta\mathrm{dR} \tag{E.14}$$

Finally we combine Eq. (E.8), Eq. (E.10) and Eq. (E.14), and conclude in a somewhat vague notation

$$\int \mathrm{d}\vec{\mathrm{r}}_a \mathrm{d}\vec{\mathrm{r}}_b \mathrm{d}\vec{\mathrm{r}}_e = \int \mathrm{d}\vec{\mathrm{r}}' \mathrm{d}\vec{\mathrm{R}}' \mathrm{d}\vec{\mathrm{R}}'_G = \int \mathrm{d}\vec{\mathrm{r}} \mathrm{d}\vec{\mathrm{R}} \mathrm{d}\vec{\mathrm{R}}_G = \int \mathrm{d}\vec{\mathrm{r}} \left\{\sin\beta \mathrm{R}^2\right\} \mathrm{d}\alpha\mathrm{d}\beta\mathrm{dR}\mathrm{d}\vec{\mathrm{R}}_G \tag{E.15}$$

Subject index

References

1. M. Born, J. R. Oppenheimer, *Ann. Phys.* **84**, 457-484 (1927).

2. E. P. Wigner, L. Eisenbud, "Higher Angular and Long Range Interaction in Resonance Reactions", *Phys. Rev.* **72**, 29-41 (1947).

3. J. Linderberg, B. Vessel, "Reactive Scattering in Hyperspherical Coordinates", *Int. J. Quant. Chem.* **31**, 65-71 (1987).

4. R. T. Pack, J. O. Hirschfelder, "Separation of Rotational Coordinates from the N-Electron Diatomic Schrödinger Equation", *J. Chem. Phys.* **49**, 4009-4020 (1968).

5. J. Linderberg, "An Algorithm for R Matrix Calculations for Atom-Diatom Reactive Scattering", *Int. J. Quant. Chem.* **35**, 801-811 (1989).

6. J. Avery, D. R. Herschbach, "Hyperspherical Sturmian Basis Functions", *Int. J. Quant. Chem.* **41**, 673-686 (1992).

7. C. Leforestier, Université Paris-Sud, Orsay, France, private communication (1992)

8. M. Baranger, "Simplified quantum-mechanical theory of pressure broadening", *Phys. Rev.* **111**, 481-493 (1958).

9. N. Allard, J. Kielkopf, "Temperature and density dependence of the Lyman α line wing in hydrogen-rich white dwarf atmospheres", *Astron. Astrophys.* **242**, 133-141 (1991).

10. P. Thejll, NORDITA, Niels Bohr Institute, University of Copenhagen, private communication (1992)

11. W. Pauli, *Ann. Phys.* **68**, 177 (1922).

12. O. Burrau, *Kgl. Danske Vid. Selsk. Math.-fys. Medd.* **7**, Nr. 14 (1927).

13. E. A. Hylleraas, *Z. Phys.* **71**, 739 (1931).

14. G. Jaffé, "Zur Theorie des Wasserstoffmolekülions", *Z. Phys.* **87**, 535-544 (1934).

15. I. Sandman, *Proc. Roy. Soc. Edinb.* **55**, 72 (1935).

16. P. A. Thejll, *Molecules in the Stellar Environment*., U. G. Jørgensen, ed. (Springer Verlag, p.x., 1993).

17. D. R. Bates, "Rate of formation of molecules by radiative association", *M. N. R. A. S.* **III**, 303-314 (1951).

18. D. R. Bates, "Absorption of radiation by an atmosphere of H, H^+ and H_2^+ - semi-classical treatment", *M. N. R. A. S.* **112**, 40-44 (1952).

19. B. R. Johnson, *J. Chem. Phys.* **73**, 5051 (1980).

20. L. M. Delvers, *Nucl. Phys.* **9**, 391 (1959).

21. L. M. Delvers, *Nucl. Phys.* **20**, 275 (1960).

22. C. A. Mead, *J. Chem. Phys.* **72**, 3839 (1980).

23. J. Linderberg, "Basis for Coupled Channel Approach to Reactive Scattering", *Int. J. Quant. Chem.* **19**, 467-476 (1986).

24. Y. Öhrn, J. Linderberg, "Hyperspherical coordinates in four particle systems", *Mol. Phys.* **49**, 53-64 (1983).

25. K. L. Bak, Masters thesis, Born-Oppenheimer approksimationens vanskeligheder, University of Aarhus, Denmark (1989).

26. M. Born, K. Huang, *Dynamical Theory of Crystal Lattices*. (U. P., Oxford, 1955), vol. Appendix 8.

27. B. T. Sutcliffe, The Born-Oppenheimer Approximation, Advanced NATO study institute. Methods in Computational Molecular Physics. (Bad Windsheim, Germany, 1991)

28. L. Hulthén, *Kgl. Fysiogr. Sällsk. Lund Förh.* **14**, No. 21 (1944).

29. L. Hulthén, *Arkiv Mat. Astron. Fysik* **35A**, No. 25 (1948).

30. W. Kohn, "Variational Methods in Nuclear Collision Problems", *Phys. Rev.* **74**, 1763-1772 (1948).

31. R. K. Nesbet, *Variational Methods in Electron-Atom Scattering Theory*. (Plenum, New York, 1980).

32. J. Z. H. Zhang, S. Chu, W. H. Miller, "Quantum scattering via the S-matrix version of the Kohn variational principle", *J. Chem. Phys.* **88**, 6233-6239 (1988).

33. G. W. Kellner, *Z. Phys.* **44**, 91 (1927).

34. E. A. Hylleraas, *Z. Phys.* **48**, 469 (1928).

35. E. A. Hylleraas, *Z. Phys.* **54**, 347 (1929).

36. J. Schwinger, *Phys. Rev.* **72**, 1763 (1947).

37. R. G. Newton, *Scattering Theory of Particles and Waves*. (Plenum, New York, 1982).

38. T. Kato, "Variational Methods in Collision Problems", *Phys. Rev.* **80**, 475 (1950).

39. C. Schwartz, "Electron Scattering from Hydrogen", *Phys. Rev.* **124**, 1468-1471 (1961).

40. C. Winstead, V. McKoy, *Phys. Rev.* **A 41**, 49 (1990).

41. D. W. Schwenke, et al., *J. Chem. Phys.* **92**, 3202 (1988).

42. X. Wu, B. Ramachandran, R. E. Wyatt, "A single arrangement variational method for total reaction probabilities", *Chem. Phys. Letters* **214, I**, 118-124 (1993).

43. A. J. F. Siegert, *Phys. Rev.* **56**, 750 (1939).

44. A. M. Lane, R. G. Thomas, "R-matrix Theory of Nuclear Reactions", *Rev. Mod. Phys.* **30**, 257-353 (1958).

45. D. M. Hirst, *A Computational Approach to Chemistry.* (Blackwell Scientific Publications, Oxford, 1990).

46. J. Linderberg, S. B. Padkjær, "Numerical implementation of reactive scattering theory", *J. Chem. Phys.* **90**, 6254-6264 (1989).

47. A. Szabo, N. S. Ostlund, *Modern quantum chemistry*. (McGraw-Hill Publishing co., New York, 1989).

48. D. P. Craig, T. Thirunamachandran, *Molecular Quantum Electrodynamics*., Theoretical Chemistry (Academic Press, London, 1984).

49. P. Jørgensen, Calculation of geometrical derivatives in molecular electronic structure theory, Advanced NATO study institute. Methods in Computational Molecular Physics. (Bad Windsheim, Germany, 1991)

50. J. Linderberg, "Finite Element Method in Quantum Mechanics", *Comp. Phys. Rep.* **6**, 209-242 (1987).

51. D. R. Hartree, "The wave mechanics of an atom with a noncoulombic central field", *Proc. Camp. Phil. Soc.* **24**, 111 (1928).

52. M. Abramowitz, I. A. Stegun, ed., *Handbook of Mathematical Functions* (Dover Publications, Inc., New York, 1968).

53. W. H. Press, B. P. Flannery, S. A. Teukolsky, W. T. Vetterling, *Numerical Recipes, The Art of Scientific Computing (FORTRAN Version)*. (Cambridge University Press, Cambridge, 1989).

54. L. C. Biedenharn, J. D. Louck, *Angular momentum in quantum physics: Theory and Applications*., G.-C. Rota, ed. , Encyclopedia of Mathematics and its Applications (Cambridge University, New York, 1981), vol. 8.

55. D. M. Brink, G. R. Satchler, *Angular Momentum*. (Oxford University Press, 1968).

56. B. R. Judd, *Angular Momentum Theory for Diatomic Molecules*. (Academic Press, Inc., New York, 1975).

57. M. E. Rose, *Elementary Theory of Angular Momentum*. (Wiley, New York, 1957).

58. M. Tinkham, *Group Theory and Quantum Mechanics*. (McGraw-Hill Book Company, 1964).

59. R. T. Pack, "Quantum reactive scattering in three dimensions using hyperspherical (APH) coordinates. Theory", *J. Chem. Phys.* **87**, 3888-3921 (1987).

60. R. C. Weast, ed., *Handbook of Chemistry and Physics* (CRC press, Inc., Boca Raton, Florida, 1984).

61. I. N. Levine, *Quantum Chemistry*. (Allyn and Bacon, Inc., 1983).

62. M. Rotenberg, *Adv. At. Mol. Phys.* **6**, 233 (1970).

63. J. D. Power, *Phil. Trans. R. Soc. London* **A 274**, 663 (1974).

64. E. U. Condon, G. H. Shortley, *The Theory of Atomic Spectra.* (Cambridge University Press, London, 1935).

65. C. Leforestier, "Grid representation of rotating triatomics", *J. Chem. Phys.* **94**, 6388-6397 (1991).

66. T. Ericsson, A. Ruhe, "STLM, A Software Package for the Spectral Transform Lanczos Method", *Math. of Comp.* **35-152**, 1251 (1980).

67. B. S. Garbow, . Applied Mathematics Division, Argonne National Laboratory,

68. Moler, Stewart, *SIAM J. Numer. Anal.* **10**, 241-256 (1973).

69. D. R. Bates, K. Ledsham, A. L. Stewart, "Wave Functions of the Hydrogen Molecular Ion", *Phil. Trans. R. Soc. London* **A 246**, 215-240 (1953).

70. J. M. Peek, "Eigenparameters for the $1s\sigma_g$ and $2p\sigma_u$ Orbitals of H_2^+", *J. Chem. Phys.* **43**, 3004-3006 (1965).

71. H. E. Montgomery Jr., "One-electron Wavefunctions. Accurate Expectation Values", *Chem. Phys. Letters* **50**, 455-458 (1977).

72. K. Way, ed., *Atomic Data and Nuclear Data Tables* , vol. 14 (Academic Press, Inc., New York, 1974).

73. J. Irving, N. Mullineux, *Mathematics in Physics and Engineering*. (Academic Press, London, 1959).